UNIVERSIDADE FEDERAL DE MINAS GERAIS
Instituto de Ciências Biológicas
Programa de pós-graduação em Bioquímica e Imunologia

KATHOLIEKE UNIVERSITEIT LEUVEN
Rega Institute for Medical Research
Postgraduate Program in Biomedical Sciences

Vivian Louise Soares de Oliveira

DIFFERENT APPROACHES TO UNDERSTAND THE ROLE OF CHEMOKINES IN MURINE MODELS OF LUNG INFLAMMATION

Belo Horizonte
2022

Vivian Louise Soares de Oliveira

DIFFERENT APPROACHES TO UNDERSTAND THE ROLE OF CHEMOKINES IN MURINE MODELS OF LUNG INFLAMMATION

Tese apresentada ao Programa de Pós-graduação da Universidade Federal de Minas Gerais como requisito parcial para a obtenção do titulo de Doutora em Imunologia e ao Programa de Pós-graduação em Ciências Biomédicas da Universidade Católica de Leuven para a obtenção do titulo de Doutora em Ciências Biomédicas (regime de cotutela).

Orientadores: Prof. Dr. Flavio Almeida Amaral
Profa. Dra. Sofie Struyf

Coorientadores: Prof. Dr. Mauro Martins Teixeira
Prof. Dr. Paul Proost

Belo Horizonte

2022

043 Oliveira, Vivian Louise Soares de.
Different approaches to understand the role of chemokines in murine models of lung inflammation [manuscrito] / Vivian Louise Soares de Oliveira. – 2022.
194 f. : il. ; 29,5 cm.

Orientadores: Prof. Dr. Flavio Almeida Amaral; Profa. Dra. Sofie Struyf. Coorientadores: Prof. Dr. Mauro Martins Teixeira; Prof. Dr. Paul Proost.
Tese (doutorado) – Universidade Federal de Minas Gerais, Instituto de Ciências Biológicas. Programa de Pós-Graduação em Bioquímica e Imunologia. Universidade Católica de Leuven. Programa de Pós-graduação em Ciências Biomédicas.

1. Bioquímica e imunologia. 2. Pneumopatias. 3. Síndrome do Desconforto Respiratório. 4. Pneumonia Estafilocócica. 5. SARS-CoV-2. 6. Quimiocinas. I. Amaral, Flavio Almeida. II. Struyf, Sofie. III. Teixeira, Mauro Martins. IV. Proost, Paul. V. Universidade Federal de Minas Gerais. Instituto de Ciências Biológicas. VI. Título.

CDU: 577.1

Ficha catalografica elaborada pela bibliotecária Fabiane C M Reis - CRB 6 2680

Universidade Federal de Minas Gerais
Curso de Pós-Graduação em Bioquímica e Imunologia ICB/UFMG
Av. Antônio Carlos, 6627 – Pampulha
31270-901 – Belo Horizonte – MG
e-mail: pg-biq@icb.ufmg.br (31)3409-2615

ATA DA DEFESA DA TESE DE DOUTORADO DE VIVIAN LOUISE SOARES DE OLIVEIRA. Aos treze dias do mês de dezembro de 2022 às 10:00 horas, reuniu-se de forma "on line" utilizando a plataforma "Teams", no Instituto de Ciências Biológicas da Universidade Federal de Minas Gerais, a Comissão Examinadora da tese de Doutorado, indicada *ad referendum* do Colegiado do Curso, para julgar, em exame final, o trabalho intitulado "Different approaches to understand the role of Chemokines in murine models of Lung Inflammation", requisito final para a obtenção do grau de Doutor em Ciências: Imunologia. Abrindo a sessão, o Presidente da Comissão, Prof. Flávio Almeida Amaral, da Universidade Federal de Minas Gerais, após dar a conhecer aos presentes o teor das Normas Regulamentares do Trabalho Final, passou a palavra à candidata para apresentação de seu trabalho. Seguiu-se a arguição pelos examinadores, com a respectiva defesa da candidata. Logo após a Comissão se reuniu, sem a presença da candidata e do público, para julgamento e expedição do resultado final. Foram atribuídas as seguintes indicações: Dr. Philippe Van den Steen (KU Leuven), aprovada; Dra. Patrícia Silva Martins (Instituto Oswaldo Cruz - Fiocruz-RJ), aprovada; Dr. Thiago Mattar Cunha (Universidade de São Paulo), aprovada; Dra. Angélica Thomaz Vieira (Universidade Federal de Minas Gerais), aprovada; Dr. Helton da Costa Santiago (Universidade Federal de Minas Gerais), aprovada; Dr. Mauro Martins Teixeira - Coorientador (Universidade Federal de Minas Gerais), aprovada; Dr. Paul Proost - Coorientador (KU Leuven), aprovada; Dr. Sofie Struyf – Orientador (KU Leuven), aprovada; Dr. Flávio Almeida Amaral - Orientador (Universidade Federal de Minas Gerais), aprovada. Pelas indicações a candidata foi considerada:

(X) APROVADA
( ) REPROVADA

O resultado final foi comunicado publicamente à candidata pelo Presidente da Comissão. Nada mais havendo a tratar, o Presidente da Comissão encerrou a reunião e lavrou a presente Ata que será assinada por todos os membros participantes da Comissão Examinadora. Belo Horizonte, 13 de dezembro de 2022.

Dr. Philippe Van den Steen (KU Leuven)

Dra. Patrícia Silva Martins (Instituto Oswaldo Cruz - Fiocruz-RJ)

gov.br Documento assinado digitalmente PATRICIA MACHADO RODRIGUES E SILVA M Data: 19/12/2022 17:02:45-0300 Verifique em https://verificador.iti.br

Dr. Thiago Mattar Cunha (Universidade de São Paulo)

gov.br Documento assinado digitalmente ANGELICA THOMAZ VIEIRA Data: 19/12/2022 10:09:45-0300 Verifique em https://verificador.iti.br

Dra. Angélica Thomaz Vieira (UFMG)

Dr. Helton da Costa Santiago (UFMG)

gov.br Documento assinado digitalmente HELTON DA COSTA SANTIAGO Data: 16/12/2022 23:48:24-0300 Verifique em https://verificador.iti.br

gov.br Documento assinado digitalmente THIAGO MATTAR CUNHA Data: 20/12/2022 09:28:50-0300 Verifique em https://verificador.iti.br

Dr. Mauro Martins Teixeira - Coorientador (UFMG)

MAURO MARTINS TEIXEIRA:69525188604 Assinado de forma digital por MAURO MARTINS TEIXEIRA:69525188604 Dados: 2022.12.19 21:25:27 -03'00'

Dr. Paul Proost - Coorientador Co-tutela (KU Leuven)

Dr Sofie Struyf - Orientador Co-tutela (KU Leuven)

Dr. Flávio Almeida Amaral - Orientador (UFMG)

gov.br Documento assinado digitalmente FLAVIO ALMEIDA AMARAL Data: 16/12/2022 12:07:27-0300 Verifique em https://verificador.iti.br

Acknowledgments (Agradecimentos)

Words cannot express my gratitude to everyone that helped me in my PhD. I could not have undertaken this journey without Prof Flávio Amaral and Prof Sofie Struyf. *Flávio, obrigada por abrir as portas do seu laboratório para mim lá em 2011 e por me conduzir durante todo esse tempo. Por onde eu caminhar, com certeza vou sempre me lembrar dos primeiros passos que dei ao seu lado e do tanto que aprendi e amadureci no laboratório.* Sofie, after many years being supervised by the same advisor, I had a delightful surprise with you. All your trust and your support gave me a lot of what I needed, especially in the end of my PhD. I am happy to say that I had two wonderful supervisors that guided me through good and difficult moments and kept me motivated until now. I need to extend this gratitude to my co-supervisors, Prof Paul Proost and Prof Mauro Teixeira. In special, I want to thank Paul and Sofie for all the support while I was in Leuven. I went abroad in the middle of COVID crisis, and I would not change anything, because of how welcoming you were.

I would like to express my deepest gratitude to the funding agencies and doctoral schools from both Brazil and Belgium. This study was financed in part by the Coordenação de Aperfeiçoamento de Pessoal de Nível Superior – Brasil (CAPES) – Finance Code 001 – to whom I am very grateful. Additionally, I want to thank all the staff from the Rega Institute, especially from the secretary and the animalium. I also could not have undertaken this journey without my defense committee, who generously agreed to share their knowledge and experience with us. Among them, I would like to thank Prof Philippe Van den Steen and his team for providing the knockout mice and their expertise.

To my dear friends from the Immunity and Inflammation research group, I am so happy I got to know you. Eva, Noemie, Alexandra, Nele, Mieke, Helena, Lotte, Sarah, Karen, Marfa, Seppe, Sara, Luna, Emily, Delphine, Matheus, Estefi (with Luca, off course) and other colleagues: thank you for being my home away from home. Thank you for all the lunches, drinks, experiments, etc. I need to specially thank Mirre, Sofie, Pedro and Rafa for embracing me like a family member, I miss you daily. Bedankt!

Aos amigos que fiz no Laboratório de Imunofarmacologia, vocês também são partes desta história. Obrigada por toda a paciência, todo momento de risadas, todos os cafés, todas as lágrimas, todos os grupos de Whatsapp etc. que compartilhamos. Em

especial, gostaria de agradecer à Amanda, Izabela, Eliza, Ilma, Daiane, Paula, Rebeca, Juliana, aos amigos do Salsicha e aos amigos do Reumatexp que tanto me ensinaram e me ajudaram na última década. Lidar com a pressão do doutorado, a ansiedade de sair do país e o abatimento de voltar ao Brasil seria impossível sem vocês.

Aos amigos do CETAP, do CEFET e da FaFar, obrigada por me acompanharem desde sempre e serem tão pacientes, torcendo tanto por mim nessa minha jornada acadêmica. Feza, Thaís e Mari: vocês são as melhores amigas que eu poderia desejar. À Yasmin, talvez a pessoa que me conhece de maneira mais profunda, obrigada por me ouvir falando a mesma coisa toda semana por mais de 4 anos e sempre me fazer acreditar nesse doutorado e em mim mesma.

A minha querida família, incluindo a família do Anderson, obrigada pelo imenso suporte. Aos meus pais, Cláudia e Vinicius, obrigada pelo amor incondicional. Todo apoio e todo incentivo que vocês me deram foi essencial para concluir mais essa etapa. Aos meus irmãos, Lilian e Hugo, obrigada pelo companheirismo irrestrito. Vocês são a minha maior certeza de que nunca estarei só, pois, aconteça o que acontecer, esse laço jamais será quebrado. Aos meus sobrinhos, Otávio e Melissa, vocês são o meu amor mais puro e minha maior força para tentar mudar o mundo, não tenho palavras para agradecer pelo carinho ou pelo simples sorriso que enchem meu coração.

Ao Anderson, meu maior companheiro, eu sou inteiramente grata pelo amor que você me dá diariamente, sem pedir nada em troca. Nos conhecemos no mesmo período que entrei no laboratório e não sei como eu trilharia esse caminho tão duro sem você. Obrigada por acreditar tanto nos meus sonhos e topar viver essa aventura do meu lado, mesmo que fisicamente distante.

O meu muito obrigada a todos que me ajudaram nesse processo, vocês são muito especiais e sempre serei grata.

Resumo

As doenças pulmonares representam um fardo significativo para os pacientes e para o sistema de saúde, sendo uma das principais causas de mortalidade no mundo. Em especial, a síndrome do desconforto respiratório agudo (SDRA) é uma condição inflamatória pulmonar aguda e difusa, causada pelo enfraquecimento das barreiras epitelial e endotelial, o que leva ao acúmulo de líquido nos alvéolos e compromete a troca gasosa adequada. A pneumonia, por sua vez, é uma infecção dos alvéolos e do tecido pulmonar, podendo ser causada por diferentes agentes, como Staphylococcus aureus e o coronavírus da síndrome respiratória aguda grave 2 (SARS-CoV-2). O recrutamento maciço de leucócitos para o tecido pulmonar e os alvéolos é uma característica marcante da SDRA e é necessário para lidar adequadamente com a lesão pulmonar, embora esteja associado à inflamação e à progressão da doença.

Neste estudo, investigamos a contribuição do sistema de quimiocinas durante a migração e ativação de leucócitos em diferentes modelos murinos de inflamação pulmonar. Usando um modelo agudo e autolimitado de inflamação pulmonar induzida por LPS, observamos um acúmulo crescente de linfócitos do meio para o final da inflamação, e muitos dos linfócitos presentes no espaço alveolar expressavam CXCR3 e CXCR6. Embora a ausência de linfócitos T e B maduros não pareça prejudicar a resolução adequada da inflamação, os pulmões de camundongos deficientes em RAG2 apresentam enriquecimento em linfócitos inatos na fase final da inflamação, os quais também podem contribuir para o controle inflamatório.

Nesse mesmo modelo, observamos que CCR2 é essencial para o recrutamento de algumas populações de monócitos/macrófagos, e sua deficiência altera o perfil celular acumulado nos pulmões sem impactar significativamente a resolução da inflamação. Em camundongos deficientes em CCR2, há maior proliferação de macrófagos alveolares com perfil M2 pronunciado, sugerindo um mecanismo compensatório para a resolução da inflamação pulmonar devido à ausência de monócitos/macrófagos recrutados.

Por fim, utilizamos o fragmento de quimiocina ligante de glicosaminoglicanos CXCL9(74-103) para tratar a pneumonia causada por S. aureus ou pelo betacoronavírus murino MHV-3. Em ambos os modelos, o tratamento com CXCL9(74-103) reduziu o

acúmulo de neutrófilos no espaço alveolar e melhorou alguns parâmetros da disfunção pulmonar, especialmente a perda da elasticidade pulmonar. No modelo com MHV-3, o tratamento levou a um resultado bastante positivo, prevenindo inclusive a lesão pulmonar.

Em conclusão, o presente estudo oferece insights valiosos sobre como o sistema de quimiocinas regula a inflamação pulmonar e sugere possíveis estratégias terapêuticas nessas condições.

Palavras-chave: Bioquímica e imunologia; Pneumopatias; Síndrome do Desconforto Respiratório; Pneumonia Estafilocócica; SARS-CoV-2. 6; Quimiocinas.

Abstract

Pulmonary diseases represent a significant burden to patients and the healthcare system and are one of the leading causes of mortality worldwide. Particularly, the acute respiratory distress syndrome (ARDS) is an acute, diffuse, pulmonary inflammatory condition caused by the weakening of epithelial and endothelial barriers, which leads to the filling of the alveolar sacs with fluid, impairing the proper gas exchange. In turn, pneumonia is an infection of the alveoli and lung tissue and can be caused by different agents, such as *Staphylococcus aureus* and severe acute respiratory syndrome coronavirus (SARS-CoV)-2. The massive recruitment of leukocytes to lung tissue and alveoli is a hallmark factor in ARDS and necessary to properly deal with the lung insult, while it is associated with lung inflammation and disease. Here, we investigated the contribution of the chemokine system during leukocyte migration and activation in different murine models of lung inflammation. Using an acute and self-resolving model of LPS-induced lung inflammation, we observed a crescent accumulation of lymphocytes from the middle to the final phase of inflammation and many of the lymphocytes present in the alveolar space expressed CXCR3 and CXCR6. Although the absence of mature T and B cells does not seem to impair the proper resolution of inflammation, the lungs of RAG2-deficient mice are enriched with innate lymphocytes in the later phase of inflammation, which may also contribute to the control of inflammation. In the same model, we observed that CCR2 is essential for the recruitment of some populations of monocytes/macrophages and its deficiency changes the profile of cells accumulating in the lungs without significantly affecting the resolution of inflammation. In CCR2-deficient mice, there is higher proliferation of alveolar macrophages with pronounced M2 profile, suggesting a compensatory mechanism for the resolution of ARDS inflammation due to the lack of migrated monocytes/macrophages. Lastly, we used the glycosaminoglycan-binding chemokine fragment CXCL9(74-103) to treat pneumonia caused by *S. aureus* or murine betacoronavirus murine hepatitis coronavirus 3 (MHV-3). In both models, CXCL9(74-103) treatment decreased the accumulation of neutrophils to the alveolar space and improved some parameters of lung dysfunction, mainly lung elasticity loss. In the MHV-3 model, CXCL9(74-103) led to a very positive outcome given that it also prevented lung injury. In conclusion, the present study provides valuable insights into how

the chemokine system regulates lung inflammation and suggests possible therapeutic options in these circumstances.

Keywords: Biochemistry and immunology; Pulmonary diseases; Acute respiratory distress syndrome; Staphylococcal pneumonia; SARS-CoV-2; Chemokines.

Samenvatting

Longziekten vormen een aanzienlijke belasting voor patiënten en de gezondheidszorg en zijn wereldwijd één van de belangrijkste doodsoorzaken. Met name het acute ademnoodsyndroom (ARDS is een acute, diffuse ontsteking van de longen die wordt veroorzaakt door de verzwakking van de epitheliale en endotheelbarrières, waardoor de alveolaire zakjes zich met vocht vullen en een goede gasuitwisseling wordt belemmerd. ARDS kan het gevolg zijn van een infectie, maar evengoed van een andere systemische aandoening. Infectueuze longontstekingen kunnen worden veroorzaakt door verschillende pathogenen, zoals *Staphylococcus aureus* en het severe acute respiratory syndrome coronavirus (SARS-CoV)-2. De massale rekrutering van leukocyten naar longweefsel en alveoli is een kenmerkende factor bij ARDS en is een noodzakelijk antwoord op het longinsult, maar is terwijl ook de oorzaak van mogelijks onherstelbare schade aan het longweefsel. Hier onderzochten wij de bijdrage van het chemokinesysteem aan de migratie en activatie van leukocyten in verschillende muismodellen van longontsteking. In een acuut en zelfherstellend model van LPS-geïnduceerde longontsteking observeerden we een gestaag toenemende accumulatie van lymfocyten vanaf de middelste tot de laatste fase van de ontsteking, waarbij de meerderheid van de lymfocytenpopulatie in de alveolaire ruimte CXCR3 en CXCR6 exprimeerden . Hoewel de afwezigheid van rijpe T- en B-cellen de goede resolutie van de ontsteking niet lijkt te belemmeren, bevatten de longen van RAG2-deficiënte muizen meer aangeboren lymfocyten in de latere fase van de ontsteking. Deze cellen kunnen ook bijdragen aan de beheersing van de ontsteking. In hetzelfde model hebben wij geconstateerd dat CCR2 essentieel is voor de rekrutering van bepaalde populaties van monocyt/macrofagen en dat deficiëntie ervan het profiel van de in de longen geaccumuleerde cellen verandert zonder significante gevolgen voor de resolutie van inflammatie. In CCR2-deficiënte muizen is er een sterkere proliferatie van alveolaire macrofagen met een uitgesproken M2 profiel, wat wijst op een compensatiemechanisme voor het herstel van ARDS ontsteking bij een gebrek aan monocyten/macrofagen die kunnen worden gerecruteerd. Tenslotte gebruikten wij het glycosaminoglycaan-bindende chemokinefragment CXCL9(74-103) om longontsteking veroorzaakt door *S. aureus* of murien betacoronavirus murine hepatitis coronavirus 3 (MHV-3) te behandelen. In beide

modellen verminderde de behandeling met CXCL9(74-103) de accumulatie van neutrofielen in de alveolaire ruimte en verbeterden sommige parameters van longdysfunctie, voornamelijk het verlies van longelasticiteit. In het MHV-3 model leidde behandeling met CXCL9(74-103) tot een zeer positief resultaat, aangezien deze ook longschade verhinderde. De conclusie is dat deze studie waardevolle inzichten verschaft in de wijze waarop het chemokinesysteem longontstekingen regelt en mogelijke therapeutische opties aanrijkt voor zulke omstandigheden .

Trefwoorden: Biochemie en immunologie; Longziekten; Acuut respiratoir distresssyndroom; Stafylokokkenpneumonie; SARS-CoV-2; Chemokinen.

List of figures

List of abbreviations

ACE2	Angiotensin-converting enzyme 2
ACKR	Atypical chemokine receptors
ALI	Acute lung injury
AM	Alveolar macrophages
ARDS	Acute respiratory distress syndrome
BALF	Bronchoalveolar lavage fluid
BHI	Brain heart infusion
BPI	Bactericidal/permeability-increasing protein
BrdU	5-Bromo-2'-deoxyuridine
B_{regs}	Regulatory B lymphocytes
CAP	Community-acquired pneumonia
Cdyn	Dynamic compliance
CEACAM1a	Carcinoembryonic antigen-related cell adhesion molecule 1a
CFU	Colony forming units
COPD	Chronic obstructive pulmonary disease
CpG-DNA	DNA containing non-methylated cpg motifs
Cpk	Peak of compliance
DC	Dendritic cells
DMEM	Dulbecco's modified eagle's medium
ELISA	Enzyme immunosorbent assay
FEV	Forced expiratory volume
fMLP	Formylated methionyl-leucyl-phenylalanine
Fmoc	Fluorenyl methoxycarbonyl
FPR2	N-formyl peptide receptor 2
FVC	Forced vital capacity
GAGs	Glycosaminoglycans

GM-CSF	Granulocyte-macrophage colony-stimulating factor
GPCR	G-protein-coupled receptors
HAP	Hospital-acquired pneumonia
IC	Inspiratory capacity
IFN-γ	Interferon gamma
ILCs	Include innate lymphoid cells
IM	Interstitial macrophages
LPS	Lipopolysaccharide
M-CSF	Macrophage colony-stimulating factor
MERS-CoV	And Middle East respiratory syndrome coronavirus
MHV	Mouse hepatitis virus
MMP	Matrix metallopeptidase
MPO	Myeloperoxidase
Mrc1	Mannose receptor type 1
MRSA	Methicillin-resistant *S. Aureus*
MV	Volume per minute
NADPH	Nicotinamide adenine dinucleotide phosphate
NGAL	Neutrophil gelatinase-associated lipocalin
NLR	NOD-type receptors
NLR	Ratio of neutrophils and lymphocytes
PAMPs	Pathogen-associated molecular patterns
PD-1	Programmed cell death protein 1
PFU	Plaque-forming units
PGN	Peptidoglycan
PMNs	Polymorphonuclear cells
PRRs	Pattern recognition receptors
RI	Lung resistance
RLRs	Retinoic acid-inducible gene-I-like receptors

ROS	Reactive oxygen species
RV	Residual volume
SARS-CoV	Severe acute respiratory syndrome coronavirus
TFA	Trifluoroacetic acid
TLC	Total lung capacity
TLR	Toll-type receptors
TNF-α	Tumor necrosis factor alpha
T_{regs}	Regulatory T lymphocytes
TV	Tidal volume
VAP	Ventilator-associated pneumonia

Table of Contents

1

Literature review and research objetives

1. INTRODUCTION

Respiratory diseases are among the leading causes of death worldwide. In 2016, chronic obstructive pulmonary disease (COPD) was the third leading cause of death, while lower respiratory tract infections were the fourth (1). According to the 2017 Global Burden Disease study, respiratory infections, such as tuberculosis, pneumonia, cancer of the trachea, bronchi, and lung, and chronic respiratory diseases are responsible for more than 9.5 million deaths each year, which means more than 15% of total deaths (2). Additionally, these diseases have high rates of morbidity and disable millions of people every year (3,4). The group of respiratory diseases is broad and diverse, encompassing diseases caused by sterile agents such as COPD, infectious agents such as pneumonia and tuberculosis, and multifactorial conditions, such as ARDS (5–7).

1.1. PULMONARY PHYSIOLOGY

Before understanding the physiology of lung diseases, it is necessary to understand the anatomy of a healthy lung. It is well established that the function of the lung is gas exchange. The right and left sides of the lung are similar but asymmetrical, with the first divided into three lobes and the second divided into two. The lobes are subdivided into segments that are associated with the bronchi, a subdivision of the trachea. The main bronchi divide into lobar or secondary bronchi within each lung. In turn, the lobar bronchi give rise to the segmental or tertiary bronchi that precede the bronchioles, forming a bronchial tree in which the trunks become thinner and more numerous as they go deeper into the lung until they end up into the alveoli, the structural and functional unit of the respiratory system (Figure 1) (8–10).

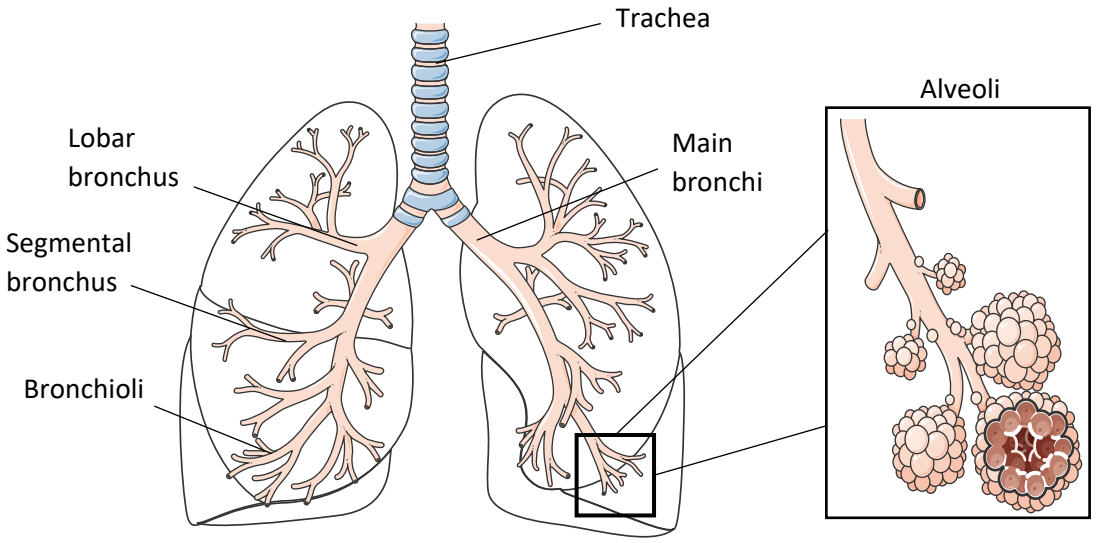

Figure 1 – Schematic of the lung and airways. The following are highlighted: trachea, main bronchi, lobar bronchi, segmental bronchi, bronchioles, and alveoli (8-10).

Alveoli are air pockets specialized in the exchange of oxygen and carbon dioxide. There are approximately 300 million alveoli in the lungs. The average diameter of the alveoli is around 200 µm, thus providing more than 100 m² of surface for hematosis (11). Two types of cells form a continuous lining around each alveolus. They are type I pneumocytes, which form most of the alveolar epithelium, forming a thin air-blood diffusion barrier, and type II pneumocytes, which are responsible for the production of surfactant, a substance capable of reducing the surface tension of the alveoli, preventing alveolar collapse, and decreasing respiratory effort (11,12) (Figure 2). Hematosis is performed at the contact between the alveolus wall and the capillary wall, a connection known as the alveolus-capillary membrane. Through this membrane, oxygen is transferred from the lungs to the bloodstream, while carbon dioxide passes from the blood to the lungs. Subsequently, the oxygenated blood proceeds through the capillary towards the venules and pulmonary veins to the heart where it is pumped throughout the body (8,11,13).

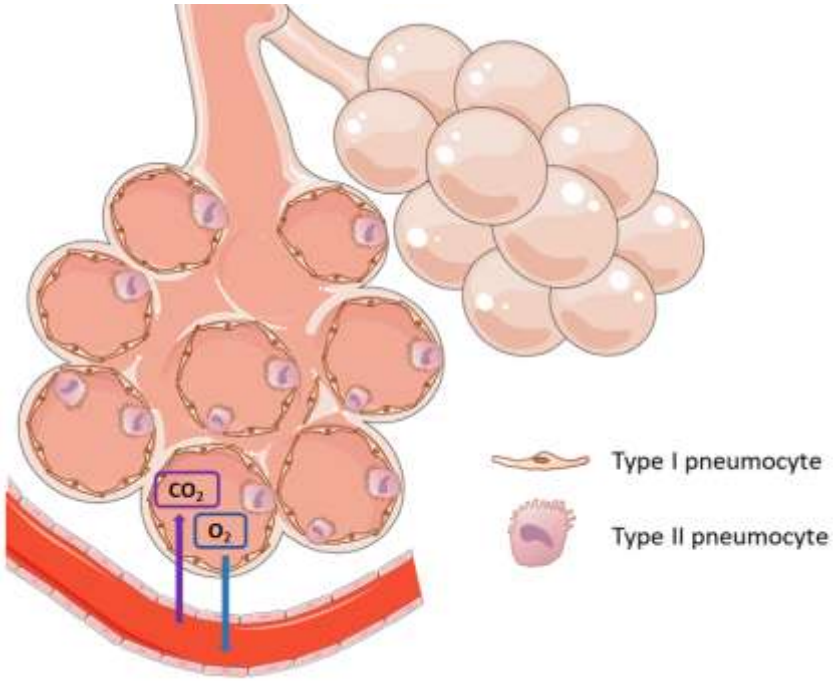

Figure 2 – Representation of an alveolus. Lined by type I and II pneumocytes, the alveoli are tiny air sacs at the end of the bronchioles. They are where the lungs and the blood exchange oxygen and carbon dioxide during the process of breathing in and breathing out (11, 12).

The cells that form the respiratory epithelium vary in terms of morphology and function according to the part of the respiratory tract in which they are found. Before reaching the alveolus, the central point of gas exchange, some lining cells are very important in protecting the upper, conducting, and respiratory airways due to the production of mucus and the rhythmic waving motion that entrap and clear inhaled particles and pathogens. The mucociliary clearance is composed of (1) ciliated cells, which have hairlike motile cilia, and (2) goblet cells and submucosal glands, which secrete mucus (14). This mechanism of clearance is the initial barrier to preventing lung infection and inflammation (15–17). Additionally, several cells participate more actively in host defense and deal with particles and microorganisms that have managed to pass the initial barrier and can cause serious damage to lung tissue. These cells include alveolar macrophages (AM), neutrophils, dendritic cells, and lymphocytes (12,14).

1.2. PULMONARY DISEASES

1.2.1. PNEUMONIA

Pneumonia is an infection of the lung parenchyma that leads to inflammation of the alveolar sacs, filling them with fluid, hindering gas exchange, and, consequently, blood

oxygenation. Symptoms of the disease include cough, fever, back and chest pain, chills, fatigue, and difficulty breathing (4,18–20). The severity of the symptoms varies according to the health and age of the individual, and the microorganism causing the infection. Risk factors for the incidence and severity of the disease include age, as children and elderly are more susceptible and have a higher risk of death; comorbidities such as chronic respiratory, cardiovascular, and renal diseases; and lifestyle-related, such as smoking, alcoholism, malnutrition, and poor dental hygiene (20–22). Bacteria, viruses, and fungi can cause pneumonia, but the most common are *Streptococcus pneumoniae* and *Haemophilus influenzae* type b; respiratory syncytial virus, influenza virus, and coronaviruses; and *Pneumocystis jirovecii*, mainly in immunocompromised patients (19,23). It is also important to consider the high incidence of co-infections, where the patient with a recent history of viral pneumonia, usually caused by the influenza virus, acquires bacterial pneumonia, commonly caused by *Streptococcus pneumoniae* or *Staphylococcus aureus* (24,25). This condition is severe and can lead to death if not treated properly and quickly with specific medicines (26,27).

It is possible to classify pneumonia according to the way the patient is infected, being categorized as (1) community-acquired (CAP), (2) hospital-acquired (HAP), or (3) associated with mechanical ventilation (VAP). HAP and VAP are hospital-acquired diseases, the first occurring when the patient is infected after a minimum of 48 h of hospitalization and the second when the patient is infected after a minimum of 48 h under mechanical ventilation (28,29). Hospital-acquired cases of pneumonia receive special attention due to the high risk of being caused by microorganisms related with the hospital environment, such as *Staphylococcus aureus*, *Pseudomonas aeruginosae*, *Acinetobacter spp*., and *Enterobacteriaceae*, which are able to cause a more serious infection and might be harder to treat due to antimicrobial resistance (30–32). In addition, hospitalized patients are generally more vulnerable, immunocompromised, and have comorbidities, which results in more severe cases of pneumonia, with mortality rates above 30% (29,33).

1.2.1.1. PNEUMONIA INDUCED BY *STAPHYLOCOCCUS AUREUS*

A relevant bacterium in the context of pneumonia is *S. aureus*. From the group of Gram-positive cocci, this bacterium is responsible for less than 5% of CAP cases but can

cause almost 50% of HAP and VAP cases (34–36). In addition to affecting mainly hospitalized patients, *S. aureus* has numerous virulence factors and a high degree of antimicrobial resistance, which makes it difficult to eliminate the microorganism and treat the disease (37–39). The rise of resistant strains of *S. aureus* associated with the shortage of new and more efficient antimicrobials has become a major public health problem and a challenge in the treatment of infections, with about 50% of staphylococcal pneumonia being caused by methicillin-resistant strains of *S. aureus* (MRSA) (39,40).

After crossing the lung initial barriers, *S. aureus* induces a response from the innate and adaptive immune system. It is important to emphasize that this answer must be complex and redundant, since *S. aureus* has evasion mechanisms and virulence factors, such as toxins, which evade the immune system and make it difficult to eliminate the bacteria (41–44). Once the microorganism enters the lung, pathogen-associated molecular patterns (PAMPs), such as peptidoglycan and lipoteichoic acid, are recognized by pattern recognition receptors (PRRs), such as toll-type receptors (TLR) and NOD-type receptors (NLR). These receptors are expressed on the alveolar endothelium and by resident cells, such as AM. In the case of the response against *S. aureus*, TLR2 is crucial (45–47). After the recognition of molecular patterns, the production of molecules such as chemokines, prostanoids, and cytokines begins, which are able to attract, prime, and activate polymorphonuclear cells (PMN), mainly neutrophils (48), and other cells such as macrophages, dendritic cells and T lymphocytes (17), triggering the inflammatory response.

Pneumonia and other diseases caused by *S. aureus* are intensively studied due to their severity and the need for more adequate treatments to control the bacteria and the immune response (37,49,50). Currently, the treatment of *S. aureus* pneumonia varies according to the bacteria's resistance to antimicrobials, the type of infection (acquired in the community or the hospital), and the patient's risk factors. The identification of *S. aureus* from blood cultures and the analysis of the most adequate antimicrobial might take a long time, thus it is recommended to start the treatment empirically, following pre-defined protocols, with subsequent adjustments (28,51). Since it is a condition of intense inflammation, treatment can also include steroidal anti-inflammatory drugs, such as prednisone (52,53). The use of antimicrobials must be effectively monitored regarding

their efficacy, safety, and duration to avoid the aggravation of the disease and the selection of multidrug-resistant strains. Multidrug-resistant strains are increasingly common and are of great concern, highlighting the need to develop new antimicrobials (54–56).

1.2.1.2. PNEUMONIA INDUCED BY SARS-COV-2

SARS-CoV-2 is a novel virus that causes a severe and highly contagious disease called COVID-19. This virus belongs to the order *Nidovirales*, the family *Coronaviridae* and the genus *Betacoronavirus*, which can be divided into 4 subgenera. The subgenus *Embecovirus* contains the mouse hepatitis virus (MHV) and the subgenus *Sarbecovirus* includes SARS-CoV and SARS-CoV-2. These viruses are pleomorphic or spherical, 80-220 nm in diameter, enveloped, and have large club-shaped spikes. The genome consists of a single molecule of linear positive-sense, single-stranded RNA, which is around 30 kb in size. Usually, they contain four structural proteins, which are a major spike glycoprotein (S), an envelope protein (E), a membrane protein (M), and a nucleoprotein (N) (57). Coronaviruses have a vast genetic diversity due to point mutations by polymerase errors. Furthermore, genetic recombination occurs frequently between the genomes of different but related coronaviruses. These mechanisms allow the constant generation of new viruses with novel phenotypes and can be a threat in the virus spread control (58).

The first reports of COVID-19 were in December 2019, and, in March 2020, it was considered by the World Health Organization as a pandemic due to the intercontinental spread (59,60). Up to this date, more than 600 million cases of COVID-19 were confirmed, with almost 7 million deaths worldwide (61), therefore SARS-CoV-2 is a major concern and a public health emergency. Compared to SARS-CoV and Middle East respiratory syndrome coronavirus (MERS-CoV), SARS-CoV-2 is considerably more transmissible, although not so lethal (62). The virus is mainly transmitted through respiratory droplets, but aerosol, direct contact with contaminated surfaces, and fecal-oral transmissions were also reported (60,63–65). COVID-19 symptoms might range from minor to extreme according to many factors such as age and underlying conditions. The most common symptoms are fever, cough, and myalgia or fatigue, while the less common symptoms are sputum production, headache, hemoptysis, and diarrhea (66). In some cases, the disease

can progress to pneumonia, ARDS, systemic inflammation, multiorgan failure, and death (62).

Similar to SARS-CoV, SARS-CoV-2 enters the cells via angiotensin-converting enzyme 2 (ACE2) on the cell surface, inducing endocytosis (67). The infection of epithelial cells induces the release of several pro-inflammatory cytokines and chemokines, leading to the recruitment of innate immune cells, such as neutrophils and macrophages (68). In addition to detection by virus specific PRRs of epithelial cells, sentinel immune cells (macrophages, mast cells, dendritic cells) in the underlying lung tissue sense the presence of viral intruders and respond similarly. The uptake of viral antigen by dendritic cells that subsequently migrate to the draining lymph node to present the pathogenic peptides to $CD4^+$ and $CD8^+$ T cells leads to the formation of effector T cells and antibody-producing B cells. Importantly, the prolonged release of pro-inflammatory mediators, if the virus is not fast and adequately cleared, may lead to very characteristic features of COVID-19: cytokine storm and, consequently, hyperinflammation. Briefly, cytokine storm is a sudden increase in systemic levels of pro-inflammatory cytokines such as interleukin (IL)-1, IL-6, IL-8, tumor necrosis factor alpha (TNF-α), interferon gamma (IFN-γ), and CCL2 (69,70), which leads to the recruitment of more cells and a dramatic amplification of the inflammation. Eventually, the cytokine storm might cause endothelial dysfunction, vascular damage, and metabolic dysregulation, damaging multiple organ systems (71).

There are multiple potential options for COVID-19 treatment, such as lopinavir, remdesivir, immunomodulatory drugs, corticosteroids, antimicrobials, plasma and hyperimmune immunoglobulins, and inflammation inhibitors. However, to date, there is not a completely effective drug to treat COVID-19 (72–74). Despite the vaccines' success and the great reduction of SARS-CoV-2 spread, studies are needed to find better treatment options and to understand the disease pathogenesis (75). To do that, mouse models are essential. Different animal models have been tested to study the pathogenesis of SARS-CoV-2, but wild-type mice are resistant to SARS-CoV-2 infection due to differences between human ACE2 (the enzyme that allows virus entry) and its mouse orthologue (76). Therefore, the research is impaired by interspecies differences and other models using murine viruses should be applied (77).

1.2.1.3. MURINE HEPATITIS VIRUS

MHV belongs to the family *Coronaviridae*, sub-family *Orthocoronavirinae*, genus *Betacoronavirus*, and subgenus *Embecovirus*. Like the other *Coronaviridae* viruses, it is characterized by an enveloped positive-sense single-stranded ribonucleic acid of 25 to 31 kb (78). First isolated in 1949 (79) and with *Mus musculus* as its main host, MHV includes a set of well-described more virulent (MHV-2, MHV-3, MHV-A59, and MHV-JHM) and less virulent (MHV-1, MHV-S, MHV-Y, and MHV-Nu) strains. Besides the virulence, the MHV strains differ in organotropism and pathogenicity (58). Over time, MHV has been used as a model to study hepatitis (80) and demyelinating diseases (81) in humans. Since it shares the same genus (*Betacoronavirus*) as SARS-CoV-2, MHV together with murine models could offer, through a translational approach, mechanistic insight into SARS-CoV-2 biology, pathogenesis, and the development of new therapies (57).

Differently from SARS-CoV-2, the S protein of the murine virus uses the hosts' carcinoembryonic antigen-related cell adhesion molecule 1a (CEACAM1a) receptor to enter the host cells instead of ACE2 (82). After intranasal inoculation, MHV starts its replication in the respiratory epithelium of the nose and lungs, followed by dissemination via the lymphatic system and blood vessels, together with a prolonged and uncontrolled inflammatory response. Subsequently, it is possible to observe a secondary infection of the vascular endothelium in the liver, brain, and other sites. Additionally, syncytia are found as a sign of infection in multiple tissues such as lungs and lymph nodes (77,83).

1.2.2. ARDS

ARDS is another clinically important lung condition, which consists of an acute, uncontrolled pulmonary inflammation that leads to the rupture of the endothelial and epithelial barriers of the lung, culminating in hypoxemia and reduced lung compliance (7,84). ARDS develops after pulmonary or systemic diseases and has almost 40% mortality in the most severe conditions. Morbidity rates are also significant, and patients are often burdened with severe physical disabilities, requiring long-term therapeutic care (85). Various stimuli, pulmonary or not, can predispose and/or trigger ARDS, such as pneumonia and COVID-19, as well as sepsis, trauma, gastric aspiration, pancreatitis, blood transfusion, inhalation of toxic gases, or smoking (86,87).

From a molecular point of view, ARDS starts with the loss of integrity of the alveolar-capillary membrane that allows the passage of proteins and cells. The increase in permeability leads to protein-rich alveolar edema and a vast accumulation of PMNs, such as neutrophils (88). These cells, together with resident cells, produce several pro-inflammatory and chemoattractant molecules, such as cytokines and chemokines, which induce an increased expression of adhesion molecules in PMNs and vascular endothelium. Other mediators produced are proteases, prostanoids, leukotrienes, and oxygen radicals. This set of molecules is capable of degrading alveolar structures and attracting more PMN, cells responsible for containing the initial injury, but with the potential to cause extensive tissue damage (88). The accumulation of cells and the inflammatory process in the lung interstitium and alveolar sacs impair their functionality and impair gas exchange (85). This acute pulmonary dysfunction manifests as tachypnea with respiratory distress, drop in blood pressure and oxygen saturation, and chest radiographs or CT scans showing bilateral infiltrates (86,87).

Despite being a known disease, the pathophysiology of ARDS is complex and involves many different cells and mediators, so many gaps still need to be filled. A better understanding of the molecular and cellular aspects of this disease would open the door to new, more specific, and effective treatments. Currently, treatment is limited to supportive care and lung protection ventilation, in addition to the use of pharmacological measures such as steroid anti-inflammatory drugs and β2 agonists, although the use of the latter one is still controversial (86,89,90).

Experimentally, translational research of human ARDS is performed in murine “acute lung injury (ALI)” models, as those models quite accurately mimic human clinical manifestations. Despite ARDS being a disease of diffuse cause, it is possible to partially reproduce it with the use of lipopolysaccharide (LPS) from the bacterium *E. coli* (91). It is observed that intratracheal administration of LPS causes an increase in the permeability of the alveolar wall, edema, and inflammatory infiltrates in the interstitium and alveolus and the production of mediators similar to those seen in patients with ARDS (92,93). In the LPS-induced ALI/ARDS model, it is possible to observe an intense accumulation of neutrophils recruited by synergizing chemokines (94). In addition to chemokines, cytokines are also important mediators of the disease, especially TNF-α (95), IL-17, IL-6,

and IL-1β (84,96–99). Anti-inflammatory cytokines, such as IL-10, are also important in ALI/ARDS as they control inflammation, preventing the exacerbation of tissue damage (100,101).

1.3. THE CHEMOKINE SYSTEM

Chemokines, or chemotactic cytokines, are a family of relatively small signaling proteins with a molecular mass of approximately 10 kDa, structurally characterized by the presence of four conserved cysteine residues (102). The hallmark function of chemokines is to induce and guide the movement of cells, especially leukocytes. Additionally, chemokines trigger effector functions in the target cells, e.g., the release of granules by PMN. Therefore, chemokines are important in inflammation, but they also act in homeostasis, angiogenesis, and embryogenesis (103–105). Based on the position of the cysteine residues in the N terminal portion, chemokines are classified into 4 subfamilies: (1) CC chemokines have two adjacent N-terminal cysteines, (2) CXC chemokines present one amino acid between the two first cysteines, (3) the CX3C chemokine has 3 amino acids between the cysteines, and (4) C chemokines have only one N-terminal cysteine and one cysteine downstream (106). The CXC chemokine subfamily can be further subclassified into Glu-Leu-Arg $(ELR)^{+}$ and ELR^{-} CXC chemokines. The ELR^{+} CXC chemokines are associated with neutrophil recruitment and include CXCL1, 2, 3, 5, 6, 7, and 8 (107,108).

1.3.1. CHEMOKINE RECEPTORS

Chemokines can bind to G-protein-coupled receptors (GPCR) and atypical chemokine receptors (ACKR). Chemokine-binding GPCRs are classified as CCR, CXCR, CX3CR, and XCR according to the cysteine motif in their ligands (109). Interestingly, one chemokine can bind to different receptors and one receptor may transduce signals for distinct ligands. These interactions elucidate the bias of the chemokine system, which allows us to understand how one chemokine might promote different responses in different contexts (110,111). A GPCR is a single polypeptide that is folded into a globular shape and anchored in the cell's membrane. This receptor has seven transmembrane helices and six loops, three extra and three intra-cellularly. The extracellular loops form

part of the pockets wherein chemokines bind, inducing intracellular signaling by second messengers such as calcium, cyclic adenosine monophosphate, and GTPases (112,113).

Currently, there are 20 conventional chemokine receptors, and they are widely expressed in leukocytes (Figure 3) (114,115). During inflammation, the fundamental role of chemokines is cellular recruitment to the inflammation site. As previously mentioned, chemokines and their receptors might have different functions or bind differently according to the context, thus it is important to notice that they can recruit other cells and can be involved in different processes (116).

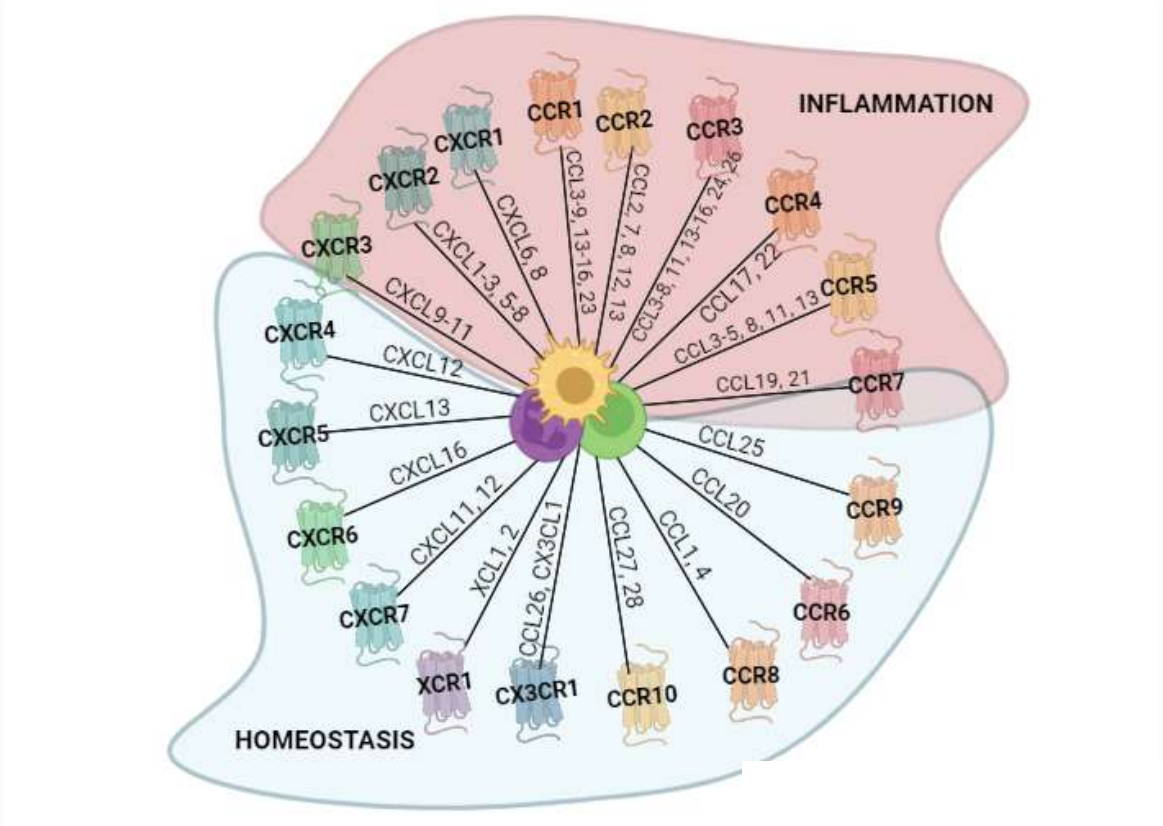

Figure 3 - Chemokine receptors and their ligands. The outer ring of the wheel is composed of representations of the known chemokine receptors from each of the chemokine families (C, CC, CXC, and CX3C), with the chemokine ligands along the wheel spokes (114,115). In the center, there are some cells that express chemokine receptors. Chemokines have roles in different contexts. As pointed out in the picture, some of them are mainly connected with homeostasis, therefore being important for the homing of the cells and contributing for the proper composition of resident cells in the different tissues. In contrast, during inflammation the chemokines respond to inflammatory stimuli and aim to eliminate the invaders.

1.3.2. GLYCOSAMINOGLYCANS

Glycosaminoglycans (GAGs) are negatively charged, linear carbohydrate structures composed of a repeating disaccharide unit consisting of a hexuronic acid linked to an N-acetyl-hexosamine that can be sulfated at various positions. They are classified into 6 categories: heparan sulfate, heparin, chondroitin sulfate, dermatan sulfate, keratan sulfate, and hyaluronic acid. These sugar units can bind to the protein cores of proteoglycans and can also be found in the extracellular matrix (117). Due to their conjugation with various proteins, such as proteases, growth factors, cytokines, chemokines, extracellular matrix proteins, and membrane receptors, GAGs play important roles in a variety of bioactivities such as cell recruitment and proliferation, angiogenesis, tumor progression, embryogenesis, and wound healing, as well as in the maintenance of homeostasis (118). GAGs ensure that their protein ligands mediating specific functions are presented at the correct site and time, besides directly inducing signaling or biologic activities (119).

For instance, the interaction between chemokines and GAGs is crucial for *in vivo* cell migration, because it creates a concentration gradient of chemokines, leading to the recruitment of cells (120). Due to the presence of several Arg, Lys, or His residues in chemokines, chemokines are very often basic, have a pI of 10 or higher, and have positive charges, allowing them to bind to GAGs, which are negatively charged. The GAG-binding motifs in chemokines are called BBXB and BBBXXB, where B represents a basic amino acid (118). GAGs are a diverse group with variable affinities for specific chemokines, allowing the control of chemokine activity during inflammation in time, space, and intensity (120). It is known that chemokines might act as monomers or as oligomers, (dimers, tetramers, or polymers) (117). Oligomerization increases the number of epitopes that bind to GAGs and, subsequently, the affinity of chemokines for GAGs through an avidity effect. Therefore, chemokine oligomerization may have a remarkable effect on GAG affinity and specificity (121).

1.3.3. CHEMOKINES AS THERAPEUTIC TARGETS

The importance of chemokines and their receptors in the inflammation process is undeniable. Hence, they have been extensively studied as therapeutic targets by different

approaches. One of these is the inhibition of chemokine and chemokine receptor expression by immunosuppressors, like ML3000, a molecule that downregulates CCR3 ligand levels in rheumatoid arthritis synovial fibroblasts (122). The use of knockout mice lacking chemokine receptors is also an important tool to clarify their relevance in certain diseases and to better elucidate the role of some cells in different types of inflammation (123,124). Another example is the blockade of CCR2, CCR5, and CXCR3 by a non-peptide antagonist protecting mice from colitis (125). Similarly, modified chemokines are also used as a therapeutic strategy. It has been demonstrated that the truncation of chemokines, such as CCL2, potentially produces antagonists for the respective chemokine receptor (126–128). This last approach might be promising to reduce the function of chemokines during excessive inflammatory responses. As published by our group, different isoforms of chemokines and chemokine-derived peptides compete with intact chemokines for GAG binding, thereby reducing the chemokine activity (120,129–131). For instance, CXCL9 consists of 103 amino acids and attracts activated T lymphocytes and NK cells after binding to CXCR3 (132). Nevertheless, a COOH-terminal fragment of CXCL9 [CXCL9(74-103)] competes for GAG binding and reduces neutrophil recruitment leading to a reduction in inflammation in different animal models (129–131).

1.4. RECRUITED CELLS AND THEIR IMMUNOLOGIC RESPONSE

Recruitment of immune cells is essential for survival. Leukocytes must leave the bloodstream to reach areas of infection or injury in peripheral tissues in order to perform their roles in surveillance and immunological responses (133). Leukocyte diapedesis can be divided into the following steps: tethering, rolling, adhesion, crawling on the endothelial cell surface, and, finally, transmigration (134). This process is highly dependent on interactions between endothelial cells and leukocytes (135). Endothelial cells can be activated via PAMPs binding to PRR, leading to the exposure of adhesion molecules on their surface and allowing the generation of chemotactic gradients (136). Selectins are expressed on the endothelial cells and bind to their counter-receptors on the leukocytes, leading to the capture of the leukocyte (tethering) from the bloodstream (137). After the capture, rapid adhesive bonds between leukocytes and endothelial cells are observed.

The rolling of neutrophils facilitates their contact with GAG-bound chemokines on the endothelium to result in tight adhesion and activation. Leukocyte activation is usually a two-step process induced by pro-inflammatory cytokines, PAMPs, chemoattractants, or growth factors (138,139). After its activation, the leukocyte is ready for transmigration. Due to strong bonds between integrins and their counter-receptors leukocytes start their extravasation from the vessels to the tissue, which can be paracellularly or transcellularly. Next, leukocytes migrate towards the infectious/inflammatory focus in the tissue (140,141). Many cell types undergo this multistep cascade of extravasation, but the present work is focused on the most abundant cells taking part in pulmonary inflammation: neutrophils, lymphocytes, and monocytes/macrophages.

1.4.1. NEUTROPHILS

Neutrophils are the most abundant circulating leukocyte in humans and a very relevant cell population in mice models. They are continuously generated in the bone marrow, and, when mature, are characterized by their segmented nucleus and granules and secretory vesicles in the cytoplasm (134). Neutrophils have always been considered short-lived immune cells with a circulating half-life of approximately 1.5 in mice and 8 h in humans (142,143). Interestingly, a new study shows a notable neutrophil lifespan of 18 h for mice and 5.4 days for humans (144). There are some criticisms regarding this study, but it shows the importance of new research and the remarkable plasticity of neutrophils (145,146).

Usually, neutrophils are the first recruited cells at the beginning of inflammation and infections. As previously mentioned, chemokines are important chemotactic agents, but they are not the only ones. Additional G protein-coupled receptor agonists, including bacterial peptides, such as formylated methionyl-leucyl-phenylalanine (fMLP) (147), products of complement activation, such as C5a (148), extracellular-matrix degradation products, such as laminin-derived peptides (149), and lipid mediators, such as leukotriene B4 (150). During the migration process, neutrophils can unzip the endothelial tight junctions and squeeze themselves between the endothelial cells, leading to paracellular transmigration. For transcellular migration, neutrophils pass through an endothelial cell without mixing their cytoplasmic contents (140,141). After arriving at the site of

inflammation, neutrophils have several mechanisms to eliminate the intruder, especially bacteria. They can phagocytose, secrete the content of their granules, such as enzymes and antimicrobial peptides, produce reactive oxygen species (ROS), and release neutrophil extracellular traps (NETs) (151,152). Once activated, neutrophils have a prolonged lifespan and phagocytose the microorganism. Opsonins and evolutionarily conserved structures from bacteria, such as LPS, lipoproteins, and peptidoglycan (PGN), are recognized by PRRs and opsonic receptors, respectively, expressed on the neutrophils (153,154). After the recognition, neutrophils project pseudopod extensions around the attached particle and engulf it, leading to the formation of a phagosome, which is an outside-in compartment inside the cell. Subsequently, the phagosome is mobilized and fused with different granules, resulting in the killing of the microorganism (155,156). There are different types of granules: primary or azurophilic, secondary or specific, tertiary, or gelatinase-containing granules, ficolin-1-rich granules, and secretory vesicles (157). Primary granules contain myeloperoxidase (MPO), defensins, lysozyme, bactericidal/permeability-increasing protein (BPI), and several serine proteases, such as neutrophil elastase, proteinase 3 and cathepsin G (105). Secondary granules contain the glycoprotein lactoferrin and antimicrobial compounds including neutrophil gelatinase-associated lipocalin and lysozyme (106). Tertiary granules contain few antimicrobials but serve as storage for several metalloproteases, such as gelatinase. The ficolin-1-rich granules are more recently described and contain human serum albumin, CR1, actin, and several cytoskeleton-binding proteins. Lastly, secretory vesicles are not always considered proper granules, but they constitute a reservoir of membrane-associated receptors, actin, actin-binding proteins, and alkaline phosphatase that are required at the earliest phases of neutrophil-mediated inflammatory responses (158,159). Additionally, phagocytosis induces the production and release of ROS. The whole phagocytosis process triggers a series of molecular signals that modulate the cell functions, and the regulation of inflammation via cytokine production, which eventually leads to the recruitment of more leukocytes, including more neutrophils (160)

Differently from bacterial and fungal infections, clearance of viral particles is not normally associated with neutrophils (161). Nevertheless, neutrophils are usually the first responders and are very abundant at sites of viral infections, such as infections caused

by varicella zoster, West Nile virus, herpes simplex virus, COVID-19, H5N1, and more (162–165). The antiviral activity of neutrophils is much less studied, but it is known that these cells can (1) phagocytose viruses (166), (2) amplify inflammation via the production of pro-inflammatory mediators and antimicrobial molecules (161), (3) initiate, enlarge, and/or repress adaptive immune response (167), and (4) release NETs (168,169). Therefore, due to their predominance and the different effector mechanisms, neutrophils are also relevant for viral infection and might be an important link between the innate and adaptive immune response (170).

Although very important for infection control, the mechanisms for pathogen elimination can cause tissue injury (171,172). Hence, neutrophil recruitment must be tightly controlled, and neutrophils must be removed before they cause serious harm to host tissues. After the microorganism clearance, neutrophils normally undergo apoptosis. Moreover, this programmed cell death not only reduces the number of neutrophils but also produces signals that prevent further neutrophil recruitment (173,174).

1.4.2. LYMPHOCYTES

Lymphocytes are bone marrow-derived cells arising from a common lymphoid progenitor. In general, lymphocytes can be classified by cell surface receptors and by the specific immune functions attributed to each cell type. Lymphocytes can be divided into innate and adaptive cells. Innate lymphocytes consist of innate lymphoid cells (ILCs), including NK cells, while adaptive lymphocytes comprise NKT cells, T, and B lymphocytes (175,176). The main effector cells of the adaptive immune response are T and B lymphocytes, these lymphocytes generate remarkably specific responses and immunological memory.

Lymphocytes are extremely mobile. After developing in the primary lymphoid organs (thymus and bone marrow), they migrate to secondary lymphoid organs, such as lymph nodes and the spleen, where they search for their corresponding antigen, which might be derived from lymph or blood, respectively. Lastly, effector lymphocytes can also migrate to inflammation sites, where they can produce more cytokines or interact directly with other cells (177,178). Several chemotactic molecules and chemokine receptors

regulate this trafficking and should be thoroughly studied to characterize the different subpopulations of lymphocytes and their role in lung inflammation, such as ARDS.

In bacterial infections, $CD4^+$ T lymphocytes and plasma cells are crucial as producers of cytokines, important for propagation of the inflammation, and immunoglobulins, which neutralize particles and have a role in opsonization and cell activation, respectively (179). Studies show that Th1 and Th17 responses, together with immunoglobulins, induce protective immunity against infections, and are important for clearance of the microorganisms (180–182). However, the role of lymphocytes in this group of diseases is ambiguous, since they can be unessential (183) and even harmful, increasing tissue damage. In contrast, the role of lymphocytes in viral infections is commonly addressed, mostly because of the cytotoxicity of $CD8^+$ T cells and NK cells, and the release of neutralizing immunoglobulins by plasma cells (184). Cytolytic lymphocytes kill target host cells through a contact-dependent mechanism. This process occurs when host cells present foreign cytosolic peptides to the $CD8^+$ lymphocyte, leading to the formation of an immunologic synapse. Subsequently, lymphocyte granules are rapidly mobilized to the synapse, followed by granule membrane fusion with the target cell plasma membrane and exocytosis of granule contents such as granzymes and perforin. Lymphocyte activation also causes the surface expression of Fas ligand, which binds to Fas on the target cell membrane, also triggering apoptosis (176). The role of lymphocytes in the pathogenesis of ARDS is dependent on the syndrome's cause. As mentioned, after the recognition of bacterial molecules, such as LPS, innate immune cells are activated, and this eventually leads to the activation and recruitment of different types and subtypes of lymphocytes. Nevertheless, the only lymphocyte characterized and often studied in ARDS is the regulatory T cell, which is very important for the resolution of inflammation and can help to restore lung homeostasis in these diseases (185,186).

1.4.3. MACROPHAGES (THE FOLLOWING TOPIC IS ADAPTED FROM A REVIEW PUBLISHED BY THE AUTHOR – ANNEX I)

Pulmonary homeostasis is maintained by tissue-resident cells that protect the lung from a broad range of antigens during respiration (187). Macrophages are the primary immune sentinels and protect the lung by phagocytosing inhaled particulates, pathogens,

surfactants, apoptotic cells, and cell debris (187). In addition to the phagocytic activity, macrophages have an important role in keeping the balance between immune cell defense against invaders and tolerance to non-inflammatory stimuli and are crucial for the maintenance of lung homeostasis and tissue repair. As a first line of defense, macrophages have an important role in the recognition of pathogens and molecules associated with damage. Upon encounter with such a trigger, macrophages initiate the inflammation, for instance by producing pro-inflammatory cytokines and chemokines that attract additional leukocytes, but, on the other hand, macrophages are also central in the resolution of inflammation by producing anti-inflammatory cytokines and engulfing apoptotic cells (188,189).

1.4.3.1. MACROPHAGE RESPONSE DURING NON-INFECTIOUS INFLAMMATION

Several diseases can result from non-infectious stimuli, such as COPD (188,189), asthma, silicosis, and asbestosis (190). AM are the first line of defense against xenobiotics, and particles, they can recognize and phagocytose them, and secrete a myriad of mediators to recruit and activate other cells such as neutrophils and monocytes.

In silicosis, for instance, the silica particles are engulfed by the AM through a class A scavenger receptor (191). However, the phagocytosed particles are indigestible hence causing lysosomal membrane damage and allowing the leaking of enzymes in the cytoplasm, which leads to the apoptosis of AM and further propagation of the inflammation. In summary, the phagocytosis of silica particles results in the release of several mediators that induces a strong inflammatory response (192,193). Excessive inflammation and cell death lead to tissue damage and repair, eventually inducing pulmonary fibrosis (194–196). It is important to highlight that macrophages contribute to fibrosis through all phases of tissue injury and repair and support either fibrogenesis or fibrolysis depending on the local tissue environment (197). Furthermore, the emphysema observed in cigarette smoke-induced COPD is also related with AM activity (198,199). They secrete metalloproteases such as matrix metallopeptidase (MMP)-9 and MMP-12, leading to the destruction of the lung parenchyma (200). MMP-12 is also important in the activation of elastin peptides that perpetuates inflammatory responses, particularly IL-17A-driven processes (201–203).

Interstitial macrophages (IM) are also important in lung inflammation. Despite producing IL-6 and TNF-α in human and mice, IM have remarkable regulatory properties due to the secretion of IL-10 in response to LPS and DNA containing non-methylated CpG motifs (CpG-DNA), for instance (204). In addition, the production of IL-10 by IM inhibits the maturation and migration of dendritic cells (DC) to the lung thereby reducing excessive endotoxin and antigen-induced airway allergic response in mice (205,206). Despite the current findings, the functions of IM are not yet completely covered and remain to be investigated (207).

Regarding the macrophage polarization, M1 macrophages release several pro-inflammatory mediators and activate the nicotinamide adenine dinucleotide phosphate (NADPH) oxidase system releasing high levels of ROS (208–212). M2 macrophages appear to be more important in fibrotic diseases, such as COPD. In fact, it is known that patients with severe forms of COPD have an increase of M2 in the lungs, suggesting that these cells are involved in COPD pathogenesis (213–215). In allergic diseases, such as asthma, eosinophils can induce the polarization of M2 that have an important role in the disease development (216,217). Although anti-inflammatory macrophages are extensively studied and correlated with allergic diseases, it is known that a specific population of pro-inflammatory macrophages ($IRF5^{+}$) is also relevant in the context of asthma (218).

1.4.3.2. MACROPHAGE RESPONSE DURING INFECTIONS

In the context of infectious lung diseases, AM sense the presence of fungi, viruses, parasites, and bacteria. They recognize pathogen components through PRRs (219) such as TLRs 2, 3, 4, 5, 7/8, and 9 and retinoic acid-inducible gene-I-like receptors (RLRs), among others (220,221). Such activation of AM results in increased concentrations of pro-inflammatory cytokines and chemokines, such as TNF-α, IL-1β, IL-6, IFN-γ, CXCL1/KC, and CCL2/MCP-1 associated with an M1 phenotype and antimicrobial response (222,223). During infection, AM can also polarize to an M2 phenotype with low antimicrobial activity and repress the inflammatory response through the secretion of large amounts of IL-10, CCL17, CCL22, CCL24, and low levels of IL-12 (224).

AM can play a dual role during bacterial pneumonia. AM are required to eliminate for example *Streptococcus pneumoniae, Staphylococcus aureus* and *Klebsiella pneumoniae* since the depletion of these cells in vivo increases lung bacterial load and enhances mortality (225,226). However, in infections with intracellular bacteria such as *Mycobacterium tuberculosis* and *Bordetella pertussis,* macrophages play a detrimental role. In these infections, AM polarize to an M2 phenotype and can provide a niche for bacterial growth (227,228). When it comes to viral infections, macrophages can recognize viral proteins and genomes triggering antiviral responses which can limit viral replication and spread. Influenza A infection induces an early interferon response and increased production of pro-inflammatory cytokines and chemokines by AM, despite their failure to release infectious viruses (229). Although AM do not recognize SARS-CoV-2 (230), macrophages recruited to the airways during SARS-CoV-2 infection exacerbate inflammation, which is associated with a cytokine storm and ARDS (231).

During fungal infections, e.g., caused by *Aspergillus fumigatus, Paracoccidioides brasiliensis* and *Cryptococcus neoformans*, AM and infiltrated macrophages are responsible to recognize, phagocytose and destroy those pathogens via enzymatic digestion and production of ROS and RNS (232–235). Despite the ability of the macrophages to eliminate infections, some fungi can adapt and resist immune responses through mechanisms that reduce chemotaxis, inhibit phagocytosis, resist the microbicide effect and escape from phagolysosomes (236).

Macrophages contribute to resistance and susceptibility to infections. Some pathogens have developed complex strategies to evade the host's immune response. Some general mechanisms shared between them include evasion of cell recognition by modification of surface components; modulation or suppression of macrophage function by evasion of phagocytosis; induction of changes in cell metabolism; induction or inhibition of apoptosis or direct killing of the macrophage (237–239).

1.5. RESOLUTION OF INFLAMMATION

The recruitment of different leukocytes is also a crucial event in the resolution phase of inflammation. This phase is an active and complex process that occurs when the inflammatory stimulus is controlled. In this case, the production of pro-inflammatory

mediators and the recruitment of PMN leukocytes are discontinued, and the PMN leukocytes accumulated in the tissue undergo a process of apoptosis and are engulfed by macrophages (efferocytosis), leading to the clearance of cells and cell debris, allowing tissue repair and return to homeostasis (240–243). In addition, events related to the resolution of inflammation in lung disease include reduction of edema, repopulation of the airway epithelium, and restoration of lung surfactants (243,244).

Among the cells involved in the resolution of inflammation, macrophages must be highlighted. The role of these cells in the resolution of inflammation is crucial because they produce pro-resolving molecules and are directly affected by them (245). It is known that macrophages can be polarized to an anti-inflammatory and resolving profile (M2), assuming functions classically related to the resolution of inflammation, being able to phagocytize apoptotic cells and promote inflammation control and tissue repair (246,247). Macrophage polarization is a central event in the resolution of inflammation and can be induced by cytokines, hormones, microbial components, and others. M2 are polarized in the presence and phagocytosis of apoptotic cells, and molecules such as IL-10, TGF-β, M-CSF, IL-4, IL-13 and other (248). After polarization, these cells express scavenger receptors, mannose and galactose receptors, and chemokine receptors different from those expressed by M1 macrophages (249).

In addition to macrophages, lymphocytes might also have a role in the resolution of inflammation because they are able to induce neutrophil and macrophage apoptosis through the expression of Fas ligand, which reduces the production of pro-inflammatory cytokines and mechanisms associated with tissue damage (250,251). Another important role of lymphocytes during resolution is played by T_{regs} lymphocytes, which secrete molecules capable of suppressing inflammation, inducing efferocytosis and promoting tissue repair (252–254). Nevertheless, lymphocytes are divided into several populations and many of them do not have well characterized functions in the resolution phase of inflammation, especially in infectious conditions.

1.6. RESEARCH OBJECTIVES

Lung diseases, such as pneumonia and ARDS, cause high rates of morbidity and mortality worldwide. Despite being very relevant and intensively investigated, a lot remains to be studied regarding molecular pathogenesis, and the development of new and more effective treatments for these diseases is still needed. On this basis, we had three major aims in the present work:

a) Many cells are involved in resolution, such as macrophages that are extensively studied and characterized. In contrast, there are not much published few papers describing the role of lymphocytes in the resolution of the inflammatory process (255,256). Unpublished data from our group show that lymphocytes are also present at the inflammatory site during the resolving phase of lung inflammation. Thus, we aimed to investigate whether populations of lymphocytes actively participate in the resolution of lung inflammation, and it is therefore necessary to **characterize the lymphocytes subpopulations and their chemokine receptors** to understand their recruitment and how they would participate in the control of lung inflammation in a model of ALI/ARDS induced by LPS.

b) Monocytes and macrophages are crucial cells to the development and resolution of inflammation. The recruitment of these cells is mainly linked with the expression of CCR2. Therefore, **we aimed to evaluate the role of CCR2 in a model of ALI/ARDS induced by LPS using CCR2 KO mice**.

c) As mentioned, leukocytes are key factors in the inflammation process. Therefore, the study of leukocyte recruitment is essential. In this context, the use of GAG-binding proteins that can interfere with the cell diapedesis is an important tool. In this study, **we aimed to assess the effect of CXCL9(74-103) treatment in the recruitment of cells, especially neutrophils, in murine models of pneumonia induced by *S. aureus* and MHV-3**.

1.7. PART I: ROLE OF LYMPHOCYTES IN A MURINE MODEL OF ARDS

Lymphoid cells participate in a broad spectrum of immune and inflammatory responses, including innate and adaptive cells. Among them, T and B cells are classically

responsible for the adaptive immune response, coordinating an antigen-specific production of antibodies or cytotoxicity (257). Lymphocytes have a well-defined role in the stimulation of inflammation and tissue damage, but there are subsets of regulatory T and B lymphocytes (T_{regs} and B_{regs}). These cells secrete molecules capable of suppressing inflammation (IL-10 and TGF-β), inducing efferocytosis, and promoting tissue repair (253,258). T_{regs} also produce IL-13, a Th2 cytokine, that leads to additional production of IL-10 by macrophages and, consequently, promote macrophage efferocytosis and further propagation of resolution of inflammation (259). Furthermore, T cells can also be relevant for the resolution of inflammation due to their ability to induce apoptosis of neutrophils and macrophages through the expression of the Fas ligand, which reduces the production of pro-inflammatory cytokines and mechanisms associated with tissue damage (250,251).

Preliminary studies showed that the resolving phase of neutrophilic and self-resolving models of inflammation is marked by an increase in the progressive accumulation of lymphocytes (data no shown). Interestingly, this is concomitant with the increase of M2 macrophages (data not shown), indicating a possible role of lymphocytes in the process of resolution. Notably, lymphocytes are divided into different populations and many of them do not have a well-characterized function in the resolution phase of inflammation.

Different subsets of $CD4^+$ T lymphocytes have been described based on their secretion of cytokines and specific functions. In addition, these subpopulations can also be characterized by the surface expression of chemokine receptors (260). Th1 cells expressed CXCR3 and CCR5, Th2 cells express CCR4 and CCR8, and Th17 express CCR4, CCR6, and CXCR3 (261). Based on that, we can explore the role of chemokine receptors and how they impact the recruitment of different types of lymphocytes. In addition, these receptors are also markers of cell activation and are important in the balance between naïve, effector and memory of $CD4^+$ T and $CD8^+$ T lymphocytes (262,263). Therefore, the characterization of chemokine receptors' expression in T lymphocytes might suggest the role and the activation status of these cells in our ARDS

1.8. PART II: ABSENCE OF CCR2 PROMOTES PROLIFERATION OF ALVEOLAR MACROPHAGES THAT CONTROL LUNG INFLAMMATION IN ACUTE RESPIRATORY DISTRESS SYNDROME IN MICE

The following topic is adapted from an original article published by the author (ANNEX II)

Int. J. Mol. Sci. **2022**, 23, 12920

Vivian Louise Soares de Oliveira [1,2], Emilie Pollenus [3], Nele Berghmans [2], Celso Martins Queiroz-Junior [4], Marfa Blanter [2], Matheus Silvério de Mattos [2], Mauro Martins Teixeira [1], Paul Proost [2], Philippe Van den Steen [3], Flavio Almeida Amaral [1,†] and Sofie Struyf [2,*,†]

1 – Laboratory of Immunopharmacology, Department of Biochemistry and Immunology, Institute of Biological Sciences, Federal University of Minas Gerais, Belo Horizonte MG 31270-901, Brazil;

2 – Laboratory of Molecular Immunology, Department of Microbiology, Immunology and Transplantation, Rega Institute for Medical Research, KU Leuven, 3000 Leuven, Belgium;

3 – Laboratory of Immunoparasitology, Department of Microbiology, Immunology and Transplantation,
Rega Institute for Medical Research, KU Leuven, 3000 Leuven, Belgium;

4 – Laboratory of Immunopharmacology, Department of Morphology, Institute of Biological Sciences, Federal University of Minas Gerais, Belo Horizonte MG 31270-901, Brazil;

† These authors contributed equally to this work and share senior authorship.

ARDS was first described in 1967 (306) and is defined as noncardiogenic pulmonary edema leading to a respiratory failure with diffuse bilateral pulmonary infiltrates and tissue injury, besides severe hypoxemia (87). The pathogenesis of ARDS includes the dysfunction of the alveolar-capillary membrane, leading to excessive transendothelial and transepithelial leukocyte migration and the influx of protein rich edema fluid into the alveolar space. The inflammation is worsened by the release of several pro-inflammatory mediators that can also be cytotoxic, increasing the destruction of the membrane and diffuse tissue damage (307–309). ARDS is caused by pulmonary or systemic inflammation following gastric aspiration, pneumonia, COVID-19, sepsis, and trauma (7). Due to the diverse causes and complex pathogenesis, ARDS treatment is also unspecific, poorly described, and considered an important unmet medical need (310,311). In addition to the high rates of morbidity and mortality, ARDS has a great impact on the quality of life

of patients requiring a better understanding of the disease and new treatment options (312,313).

The acute inflammatory response consists of an intricate but well-coordinated chain of actions that involves molecular, cellular, and physiological changes (242). The recognition of the initial insults by lung resident cells causes the production and release of a plethora of mediators that trigger several inflammatory events. Among the cells involved in the different phases of inflammation, the AM are crucial. Being the most abundant innate immune cell in the alveolar spaces of the lungs (314), AM are the first line of defense against infections and invaders, recognizing pathogen-associated molecular patterns, such as LPS from Gram-negative bacteria. They are able to phagocytose and eliminate these pathogens and release pro-inflammatory cytokines to induce immune cell recruitment and the development of inflammation (315). Additionally, AM are very important in the late stages of ARDS since the depletion of these cells has been linked with decreased efferocytosis and lowered control of inflammation (266,316).

The release of several chemotactic factors leads to broad recruitment of leukocytes to the lung parenchyma and alveolar space, including polymorphonuclear (PMNs) and mononuclear cells. CCR2 is an important chemokine receptor that plays a fundamental role in monocyte recruitment and activation by the recognition of its high-affinity ligand CCL2 (317,318). Initially, the early accumulation of monocytes, monocyte-derived macrophages, and PMNs in the lungs determine local inflammation. Moreover, the activation state and viability of these cells modulate the different phases of inflammation, from the beginning to its resolution. The resolution of inflammation is essential to restore the tissue to its physiological functioning after the damage caused by the foreign insult and the inflammatory response. Impairment of this process may lead to an unresolved inflammation, which lies beneath the pathogenesis of several chronic inflammatory disease processes (281). While recruited $CCR2^{+}$ monocytes have a crucial role in the onset of inflammation, their presence in the tissue together with the recruitment of non-phlogistic monocytes in later phases helps to control the inflammation. An important event that causes the shift to the resolution of inflammation is the apoptosis of PMNs and their subsequent engulfment by local macrophages. This phenomenon is called efferocytosis and drives the differentiation of macrophages and their polarization into a pro-resolving

profile, stimulating the production and release of pro-resolving mediators that suppress the progression of inflammation and promote tissue repair (244,319,320).

Various experimental models have been used to investigate the molecular mechanisms of ARDS, with LPS-induced ARDS as one of the most common models (321). An advantage of this model is the possibility to investigate the mechanisms inherent to the different phases of lung inflammation, from the early events to its resolution and tissue repair (84). Here, we explored in this model the impact on lung inflammation of the CCL2–CCR2 axis through the use of CCR2 knock-out mice, both at the early pro-inflammatory phase and during the resolution of inflammation.

1.9. PART III: EFFECT OF TREATMENT WITH THE GAG-BINDING CHEMOKINE FRAGMENT CXCL9(74–103) IN MURINE MODELS OF PNEUMONIA

The treatment of pneumonia is strictly dependable on the causative pathogen. In this context, *S. aureus*-induced pneumonia is a challenge due to the bacteria ability to acquire antibiotic resistance and the lack of efficient treatments that prevent excessive tissue damage caused by the infection and the inflammatory response (360). Therefore, the hunt for new antibiotics to tackle the increase in bacterial resistance continues. Previous studies have shown that neutrophils are responsible for *S. aureus* clearance during infection (361). To get rid of bacteria, neutrophils have a rather broad weaponry: phagocytosis, production of antimicrobial peptides and proteins, and release of ROS and NETs (362). Understandably, overactivation of these cells is also harmful for the host tissue. This implicates that a balanced response of neutrophils should be obtained, sufficient neutrophils should be recruited to clear the bacteria, but numbers and cellular activation need to be controlled to prevent excessive damage to the lung tissue (171,362). On the other hand, the immune response induced by Sars-CoV-2 is composed by different cells, such as lymphocytes, macrophages, and neutrophils, and the systemic inflammation is remarkable, leading to cytokine storms and multiple organs failure. COVID-19 is not fully uncovered, and more studies should be developed to explore its intricate pathophysiology and search for more therapeutic targets. Nevertheless, murine models cannot be done using Sars-CoV-2, since murine cells do not express the receptor used

by this virus for the intracellular infection. Thus, multiple models were developed using alternative mice or alternative viruses, such as MHV-3. Here, we used the model developed and fully described by Andrade et al. (77). In this model, mice are intranasally inoculated with MHV-3 and, after 3 days, develop transient inflammation-associated lung injury, which includes severe respiratory distress. Afterwards, the virus systemically spread, and the disease affects different organs, evolving to death around the 6th day after the infection.

As mentioned, the recruitment of cells and their chemoattraction molecules are crucial for the inflammation and might be an important therapeutic target for the prevention of lung injury associated with infections. A good strategy to explore the role of chemokines and chemokine receptors is the utilization of modified chemokines that can impair the function of the natural chemokine(s) during the inflammatory response, such as the COOH-terminal fragment of CXCL9 [CXCL9(74-103)]. It has been shown that this peptide competes with chemokines for GAG binding and reduces neutrophil recruitment, leading to a reduction in inflammation in several animal models of disease (130–132): antigen-induced arthritis (129), gout induced by monosodium urate crystals (323), dinitrofluorobenzene-induced contact hypersensitivity (130), renal fibrosis (363), and *Klebsiella pneumoniae*-induced pneumonia (364).

The therapeutic application of CXCL9(74-103) in diseases wherein excessive neutrophil accumulation causes tissue damage is quite promising. Nevertheless, more information on the potential of this peptide in infectious models is still needed. It is known that neutrophils are essential for the clearance of bacteria and have a key role in infection control (365). However, this process can lead to extensive tissue damage caused by the release of ROS and several enzymes, for instance, neutrophil elastase and Cathepsin G (171,366). Thus, it is crucial to understand how to manipulate the recruitment of leukocytes and ensure bacterial clearance, controlling both inflammation and infection.

2

MATERIALS AND METHODS

2. MATERIALS AND METHODS

2.1. PART I: ROLE OF LYMPHOCYTES IN A MURINE MODEL OF ARDS

2.1.1. MICE AND REAGENTS

Eight to ten weeks old, male C57BL/6 were acquired from the Janvier Labs (Le Genest-Saint-Isle, France) and kept in the animal facility at the Rega Institute for Medical Research, KU Leuven. For the RAG2 experiments, eight to ten weeks old $RAG2^{-/-}$ and $RAG2^{+/+}$ were bred in the animal facility at the Rega Institute for Medical Research, KU Leuven. Previously, $RAG2^{-/-}$ mice (C57BL/6N-Rag2Tm1/CipheR) and $RAG2^{+/+}$ C57BL/6NRj mice were bought from the Janvier Labs. Knockout (KO) and wild-type (WT) mice were mated to generate F1 heterozygotes that were inter-crossed to create littermates. A SNP analysis was performed on tail or ear genomic DNA from original $RAG2^{-/-}$ mice and original C57BL/6 mice, and from $RAG2^{-/-}$ and $RAG2^{+/+}$ mice after the backcrossing (Mouse Genome Scanning panel of 2050 SNPs, Taconic, Rensselaer, NY, USA). This genotyping analysis showed that the genetic background of the $RAG2^{-/-}$ mice is >99.9% C57BL/6. All animals were maintained in a controlled environment, with *ad libitum* filtered water and food, and in a 12-h dark-light cycle. Experiments were performed **within** the norms of the European Union (directive 2010/63/EU) and the Belgian Royal Decree of 29/05/13 and the Brazilian Guideline for the Care and Use of Animals in Teaching or Scientific Research Activities. They were approved by the Animal Ethics Committees of KU Leuven (P101/2020). *E. coli* LPS (Sigma-Aldrich, Saint-Louis, MO, USA, 12.5 µg/mouse) was diluted in endotoxin-free phosphate-buffered saline (PBS - Lonza, Walkersville, MD, USA)

2.1.2. IN VIVO EXPERIMENTAL MODEL

Mice were anesthetized with a solution of ketamine (80 mg/kg) and xylazine (15 mg/kg), subcutaneously. For the induction of ARDS (91,264), bacterial LPS (Sigma-Aldrich, 12.5 µg/30 µL) was intranasally instilled. All the animals in the control group received the same volume of the vehicle (PBS) by the same route. For euthanasia, an overdose of anesthetic (ketamine and xylazine) was used. The doses and time points were based on the literature or preliminary experiments.

Body weight was measured daily, and the mice were euthanized at different time points after the instillation. For the dissection, mice received 100 µL of dolethal (Vetoquinol, Niel, Belgium; 200mg/mL). Bronchoalveolar lavage fluid (BALF) was obtained by the instillation of 500 µL of PBS through a catheter in the trachea. The fluid was withdrawn and instilled again two more times, PBS instillation was repeated three times, and the lavages were pooled. After perfusion, lungs were collected for analysis by flow cytometry and ELISA. The BALF was centrifuged (5 min, 300 × *g*, 4°C) and the supernatant was collected for the analysis of the cytokine levels by ELISA, and protein levels by BCA, whereas the cell pellet was combined or not with the cells isolated from the lungs for flow cytometry analysis. Furthermore, part of the resuspended cell pellet was used for cell counting.

2.1.3. ISOLATION OF SINGLE CELLS FROM THE LUNGS

During dissection, lungs were removed, cut into small pieces, and collected in RPMI medium [RPMI GlutaMAX (ThermoFisher, Waltham, MA, USA) + 5% fetal calf serum (FCS – Biowest, Nuaillé, France) + 1% penicillin/streptomycin (ThermoFisher)] at room temperature (RT). Lungs were then incubated for 30 min at 37 °C in RPMI medium with digestive enzymes [2 mg/mL collagenase D (Sigma-Aldrich) and 0.1 mg/mL DNase I (Sigma-Aldrich)]. The tissue was homogenized using a needle and syringe and fresh digestion medium was added for a second incubation at 37 °C for 15 min. After the second process of homogenization, the samples were centrifuged (5 min, 400 × *g*, RT), and the pellet was resuspended in 1 mL of 10 mM EDTA (Sigma-Aldrich) dissolved in PBS to stop the digestion. Cells were suspended in PBS + 2% FCS, centrifuged again, and treated with ACK lysing buffer (ThermoFisher) to lyse red blood cells. Subsequently, they were passed through a 70 µm cell strainer and resuspended in PBS + 2% FCS. To determine the number of live cells per mL, they were diluted in trypan blue solution and counted using a Bürker chamber. Cells from the lungs were combined or not with cells from the BALF for flow cytometry analysis.

2.1.4. ELISA

The measurement of cytokines and chemokines in lung tissue and bronchoalveolar lavage was performed using the enzyme immunosorbent assay (ELISA). A lung fragment

was weighed and suspended in a solution containing antiproteases and subjected to homogenization. The supernatant of the lung processing and the BALF were used for the assay. The ELISA kits were used according to the manufacturer's suggested procedures (R&D Systems, Abingdon, UK).

2.1.5. BALF PROTEIN CONCENTRATION

To assess the edema formation and the extend of the tissue damage, the concentration of protein in the BALF was measured using the Pierce BCA protein assay (ThermoFisher). Briefly, the BCA assay comprises mixing the BCA working reagent with BSA standards (Sigma-Aldrich) and samples followed by incubation for 30 minutes at 37ºC. The microplate is cooled to room temperature and the absorbance is read at 562 nm [PowerWave™ XS Microplate reader, with the Gen5 software – both from Biotek (Shoreline, WA, USA)].

2.1.6. STAINING AND FLOW CYTOMETRY

One million cells per sample were transferred to 96 well plates and washed with PBS. They were incubated for 15 min at RT in the dark with a viability dye, Zombie UV or Zombie Aqua (1/1,000; BioLegend, San Diego, CA, USA), and mouse Fc blocking reagent (MACS Miltenyi Biotec, Bergisch Gladbach, Germany). After the incubation time, the cells were washed with FACS buffer (PBS + 2% FCS + 2 mM EDTA) and stained with different panels of monoclonal antibodies (Supplementary Table S1) diluted in brilliant stain buffer (BD Biosciences; Erembodegem, Belgium) for 20 min at 4°C in the dark. The samples were washed with FACS buffer, fixed in 0.4% formaldehyde in PBS, and transferred to FACS tubes. The samples were read with an LSR Fortessa Flow cytometer (BD Biosciences), and 100,000 live single cells were acquired. For the analysis of the data, FlowJo V10 software (FlowJo, LLC – BD Biosciences) was used, and the gating strategies are described in Supplementary Figure S1.

2.1.7. STATISTICAL ANALYSIS

The data were analyzed using the GraphPad PRISM software (GraphPad, La Jolla, CA, USA, version 9.0.0). The one-way ANOVA test was performed followed by the Bonferroni correction. Significance was determined by comparing the different time points with the control, unchallenged group; between each condition for the WT and the KO mice

and between the WT and KO mice within each condition; and between control, treated, and non-treated (vehicle) groups. P-values were indicated as follows: * = p< 0.05 when compared to the corresponding control group and # = p<0.05 when comparing wild-type and knockout groups or when compared to the vehicle group.

2.2. PART II: ABSENCE OF CCR2 PROMOTES PROLIFERATION OF ALVEOLAR MACROPHAGES THAT CONTROL LUNG INFLAMMATION IN ACUTE RESPIRATORY DISTRESS SYNDROME IN MICE

The following topic is adapted from an original article published by the author (ANNEX II)

2.2.1. MICE

Eight to ten weeks old $CCR2^{-/-}$ and $CCR2^{+/+}$ were bred in the animal facility of the Rega Institute for Medical Research, KU Leuven. Previously, $CCR2^{-/-}$ mice were bought from The Jackson Laboratory (B6.129S4-Ccr2tm1Ifc/J; #004999; Bar Harbor, ME, USA) and $CCR2^{+/+}$ C57BL/6J mice from Charles River (JAX™ C57BL/6J SOPF Mice; #680; Ecully, France). Knockout and wild-type mice were mated to generate F1 heterozygotes that were inter-crossed to create littermates. A SNP analysis was performed on tail or ear genomic DNA from original $CCR2^{-/-}$ mice and original C57BL/6J mice, and from $CCR2^{-/-}$ and $CCR2^{+/+}$ mice after the backcrossing (Mouse Genome Scanning panel of 2050 SNPs, Taconic, Rensselaer, NY, USA). This genotyping analysis showed that the genetic background of the $CCR2^{-/-}$ mice is >99.9% C57BL/6J. All animals were maintained with ad libitum water and food (Ssniff Spezialdiäte, Soest, Germany), in a 12 h dark-light cycle and kept in a controlled environment. All the experiments were performed within the norms of the European Union (directive 2010/63/EU) and the Belgian Royal Decree of 29/05/13. They were approved by the Animal Ethics Committees of KU Leuven (P101/2020) and UFMG (420/2018).

2.2.2. ARDS MODEL

To induce ARDS, 30 µL of *Escherichia coli* LPS (12.5 µg/mouse) was administered intranasally to $CCR2^{-/-}$ and $CCR2^{+/+}$ mice. Control animals received the same amount of endotoxin-free PBS. Body weight was measured daily, and the mice were euthanized at

different time points after the instillation (1, 2, 3, 4, or 5 days). Before the dissection, mice were euthanized with an intraperitoneal (i.p.) injection of 100 µL of dolethal (200 mg/mL). BALF was obtained by the instillation of 500 µL of PBS through a catheter in the trachea. The fluid was withdrawn and instilled again two more times, PBS instillation was repeated three times, and the lavages were pooled. After perfusion with PBS, lungs were collected for analysis by flow cytometry or histopathological analysis. The small lungs were collected and immediately frozen for qPCR. The BALF was centrifuged (5 min, 300 × g, 4ºC) and the supernatant was collected for the analysis of the cytokine levels by ELISA and protein levels by BCA, whereas the cell pellet was combined with the cells isolated from the lungs for flow cytometry analysis.

2.2.3. BALF PROTEIN CONCENTRATION

To assess the edema formation and the extent of the tissue damage, the concentration of protein in the BALF was measured using the Pierce BCA protein assay. Briefly, this assay comprises mixing the BCA working reagent with protein standards and samples followed by incubation at 37ºC for 30 min. The microplate is cooled to room temperature and the absorbance is read at 562 nm.

2.2.4. ISOLATION OF SINGLE CELLS FROM THE LUNGS

During dissection, lungs were removed, the right lung is cut into small pieces, and collected in RPMI medium (RPMI GlutaMAX + 5% FCS + 1% penicillin/streptomycin) at room temperature (RT). Lungs were then incubated for 30 min at 37ºC in RPMI medium with digestive enzymes (2 mg/mL collagenase D and 0.1 mg/mL DNase I). The tissue was homogenized using a needle and syringe and fresh digestion medium was added for a second incubation at 37ºC C for 15 min. After a second process of homogenization, the samples were centrifuged (5 min, 400 × g, RT), and the pellet was resuspended in 1 mL of 10 mM EDTA dissolved in PBS to stop the digestion. *After the addition of 4 mL of* PBS + 2% FCS, *suspensions were* centrifuged again and treated with ACK lysing buffer to lyse red blood cells. Subsequently, they were passed through a 70 µm cell strainer and resuspended in PBS + 2% FCS. The number of live cells per mL was determined with trypan blue solution and a Bürker chamber. Cells from the lungs were combined or not with cells from the BALF for flow cytometry analysis.

2.2.5. STAINING AND FLOW CYTOMETRY

One million cells, 3 million in the case of intracellular staining, per sample were transferred to 96 well plates and washed with PBS. They were incubated for 15 min at RT in the dark with a viability dye, Zombie UV (1/1,000), and mouse Fc blocking reagent. After the incubation time, the cells were washed with FACS buffer (PBS + 2% FCS + 2mM EDTA) and stained with different panels of monoclonal antibodies (Supplementary Table S1) diluted in brilliant stain buffer for 20 min at 4ºC in the dark. The samples were washed with FACS buffer, fixed in 0.4% formaldehyde in PBS, and transferred to FACS tubes. For the intracellular staining, surface staining was performed and, instead of using formaldehyde, they were submitted to fixation and permeabilization using the fix/perm reagent for 45 min at RT in the dark, washed with the permeabilization buffer, incubated with the antibodies binding intracellular antigens (Supplementary Table S1) for 30 min at RT in the dark, and washed again with permeabilization buffer. The samples were analyzed with an LSR Fortessa Flow cytometer and 100,000 live single cells were acquired. For the analysis of the data, FlowJo V10 software was used, and the gating strategies are described in the Supplementary Materials (Supplementary Figure S1).

2.2.6. PROLIFERATION ASSAYS

2.2.6.1. Ki-67 Staining

Ki-67 is a nuclear protein expressed by proliferating cells and is very often used as a proliferation marker. After the isolation of single cells from the lungs, 3 million cells per sample were transferred to 96 well plates and the intracellular staining was performed as described above with the antibodies described in Supplementary Table S1.

2.2.6.2. BrdU Staining

Another method to evaluate cell proliferation is the use of 5-Bromo-2’-deoxyuridine (BrdU – Sigma-Aldrich). One day before the euthanasia, wild type and knockout mice received an i.p. injection of BrdU (1.5 mg/mouse). After the euthanasia and tissue processing, flow cytometry staining was performed as aforementioned. For the intracellular staining, the cells were permeabilized two extra times and treated with DNAse to expose incorporated BrdU before the staining with the anti-BrdU antibody (Supplementary Table S1).

2.2.7. QUANTITATION OF NEUTROPHIL PRODUCTS, GROWTH FACTORS, AND CYTOKINES IN BALF BY ELISA

Aliquots of cell-free BALF were used for the analysis of TNF-α, IFN-β, GM-CSF, M-CSF, NGAL, CCL2, CCL22, and CXCL1 by ELISA according to the manufacturer's instructions (R&D Systems). Absorbance was measured at 450 nm using a Biotek photometer and the Gen5 software (version 2.09, Biotek).

2.2.8. HISTOLOGY

Lungs for histopathological analysis were collected and inflated via the trachea with 4% formaldehyde (Sigma-Aldrich) in PBS. The samples were fixed overnight using the same solution, processed with different concentrations of ethanol (Sigma-Aldrich) and xylol (Sigma-Aldrich), embedded in paraffin (Synth, Diadema, São Paulo, Brazil), and sectioned (5 μm). Sections were stained with hematoxylin (Laborclin, Pinhais, Paraná, Brazil) and eosin (Laborclin) for the evaluation of the intensity and extension of polymorphonuclear infiltrates in different lung compartments, characterizing airway inflammation, vascular inflammation, and parenchymal inflammation, as described by Horvat et al (322). According to the histopathological score, the tissue damage was classified as absent, mild, moderate, intense, and severe. The analysis was performed by an independent pathologist that was blinded to the experimental conditions.

2.2.9. qPCR ANALYSIS

Following dissection, small lungs were removed from the mice and stored on dry ice until further use. Using the Qiagen RNeasy mini kit (cat #74106; Qiagen, Germantown, MD, USA), the lungs were subjected to homogenization and RNA extraction according to the manufacturer's instructions. Subsequently, the RNA was converted to cDNA using the high-capacity cDNA Reverse Transcriptase kit (cat #4368814; Applied Biosystems, San Francisco, CA, USA). IDT primers were used to analyze the gene expression of Siglec5 (Mm.PT.58.6685529), Mrc1 (Mm.PT.58.42560062), Nos2 (Mm.PT.58.43705194), Arg1 (Mm.PT.58.8651372), IL-1b (MM.PT.58.42940223) and IL-12b (Mm.PT.58.12409997). Ppia (Mm.PT.39a.2.gs) was used as the housekeeping gene. Per reaction, 10 ng cDNA was used. qPCR was performed using the TaqMan Gene Expression Mastermix (cat

#4369016, Applied Biosystems) and the 7500 Real-Time PCR system (Applied Biosystems). Relative gene expression was determined using the $2^{-\Delta DDCt}$ method.

2.2.10. DEPLETION OF AM USING CLODRONATE-LOADED LIPOSOMES

For depletion of AM, 0.5 mg of clodronate in 100 µL (Liposoma, Amsterdam, The Netherlands) was intranasally instilled in mice under anesthesia 48 and 24 h before the LPS challenge. The same volume of PBS-loaded liposomes was instilled in the control groups (323). Four days after the LPS challenge, mice were euthanized, and the dissection was conducted as described in topic 3.2.2.

2.2.11. STATISTICS

The data were analyzed using the GraphPad PRISM software (version 9.0.0, Graph-Pad). The data were checked for normality by Shapiro–Wilk test and Kolmogorov–Smirnov test. The data with normal distribution were submitted to the one-way ANOVA test followed by the Bonferroni correction. In case normality was not observed, Kruskal–Wallis with Dunn's multiple comparisons test was performed. If only two groups were to be compared, Mann–Whitney U test was performed. Significance was determined between each condition for the $CCR2^{+/+}$ and the $CCR2^{-/-}$ mice and between the $CCR2^{+/+}$ and $CCR2^{-/-}$ mice within each condition. Statistical differences are indicated with an asterisk above the individual data sets when compared to the corresponding control group and with horizontal lines with a hashtag on top in case of comparison between the indicated wild-type and knockout groups. p-values were indicated as follows: * = $p < 0.05$ when compared to the control group and # = $p < 0.05$ when comparing wild-type and knockout groups.

2.3. PART III: EFFECT OF TREATMENT WITH THE GAG-BINDING CHEMOKINE FRAGMENT CXCL9(74–103) IN MURINE MODELS OF PNEUMONIA

2.3.1. MICE AND REAGENTS

Six to eight weeks old, male C57BL/6 were acquired from the Central Animal House of UFMG and kept in the animal facility that belongs to the Laboratory of Immunopharmacology, ICB-UFMG, registered in the CTNBio. Animals were maintained

in a controlled environment, with *ad libitum* filtered water and food, and in a 12-h dark-light cycle. Experiments were made within the norms of the European Union (directive 2010/63/EU) and the Belgian Royal Decree of 29/05/13 and the Brazilian Guideline for the Care and Use of Animals in Teaching or Scientific Research Activities. They were approved by the Animal Ethics Committees of UFMG (420/2018).

S. aureus from American Type Culture Collection (ATCC) 6538 was provided by Professor Waldiceu Verri Jr from Universidade Estadual de Londrina (UEL, Brazil) and propagated in brain heart infusion (BHI) broth. The MHV-3 strain was provided and sequenced by Clarice Weis Arns and Ricardo Durães-Carvalho from the Universidade Estadual de Campinas (UNICAMP, Brazil), and propagated in L929 cells. The CXCL9(74-103) COOH-terminal peptide was chemically synthesized using fluorenyl methoxycarbonyl (Fmoc) chemistry using an Activo-P11 automated synthesizer (Activotec, Cambridge, UK), as previously described by Loos et al., 2009 (367). After synthesis, the peptides were dissolved in 0.1% trifluoroacetic acid (TFA – Sigma-Aldrich) and purified by RP-HPLC. Peptides were loaded on a 150×10 mm Proto 300 C18 column (Higgins Analytical Inc., Mountain View, CA, USA) in 0.1% TFA in water at a flow rate of 4 mL/min and eluted in an acetonitrile gradient in water containing 0.1% TFA. Eluted proteins were detected by splitting 0.7% of the volume of the column effluent to an ion trap mass spectrometer (Amazon SL, Bruker, Bremen, Germany).

2.3.2. IN VIVO EXPERIMENTAL MODELS

Mice were anesthetized with a solution of ketamine (80 mg/kg) and xylazine (15 mg/kg), subcutaneously. For the induction of pneumonia, *S. aureus* was grown in BHI agar (TM media, Rajhastan, India) supplemented with 5% of sheep blood (Newprov, Pinhais, Paraná, Brazil) for 24 h at 37°C (368). The bacterial solution was prepared in 0.9% sterile saline (Equiplex, Aparecida de Goiania, Goiás, Brazil) and intranasally instilled at a concentration of 10^8 CFU/30 uL and the animals were euthanized 12 to 48 h after the infection for the kinetics or 24 h after the infection for the CXCL9(74-103) experiments. Parallelly, for viral pneumonia, the suspension of MHV-3 was prepared in 0.9% sterile saline and intranasally instilled at a concentration of 10^3 PFU/mL (77) and the animals were euthanized 3 days after the infection. All the animals in the control group

received the same volume of the vehicle (0.9% sterile saline solution) by the same route. For euthanasia, an overdose of anesthetic (ketamine and xylazine) was used. The doses and time points were based on the literature or preliminary experiments.

Body weight was measured daily, and the mice were euthanized at different time points after the instillation. In the experiments with *S. aureus*, clinical score was performed according to the parameters described by Blättner et al, 2016 (369 – Table S2). For the dissection, mice received an overdose of anesthetic (ketamine and xylazine). BALF was obtained by the instillation of 500 µL of PBS through a catheter in the trachea. The fluid was withdrawn and instilled again two more times, PBS instillation was repeated three times, and the lavages were pooled. After perfusion, lungs were collected for analysis by flow cytometry, ELISA, bacterial/viral load, or histopathological analysis. The BALF was centrifuged (5 min, 300 × *g*, 4°C) and the supernatant was collected for the analysis of the cytokine levels by ELISA, protein levels by BCA, and bacterial load, for pneumonia. Furthermore, part of the resuspended cell pellet was used for cell counting.

For the CXCL9(74-103) experiments, the peptide was diluted in 0,9% sterile saline, and mice were intravenously treated with 100µL of CXCL9(74–103) 1 mg/mL or vehicle according to the timeline in Figure 4.

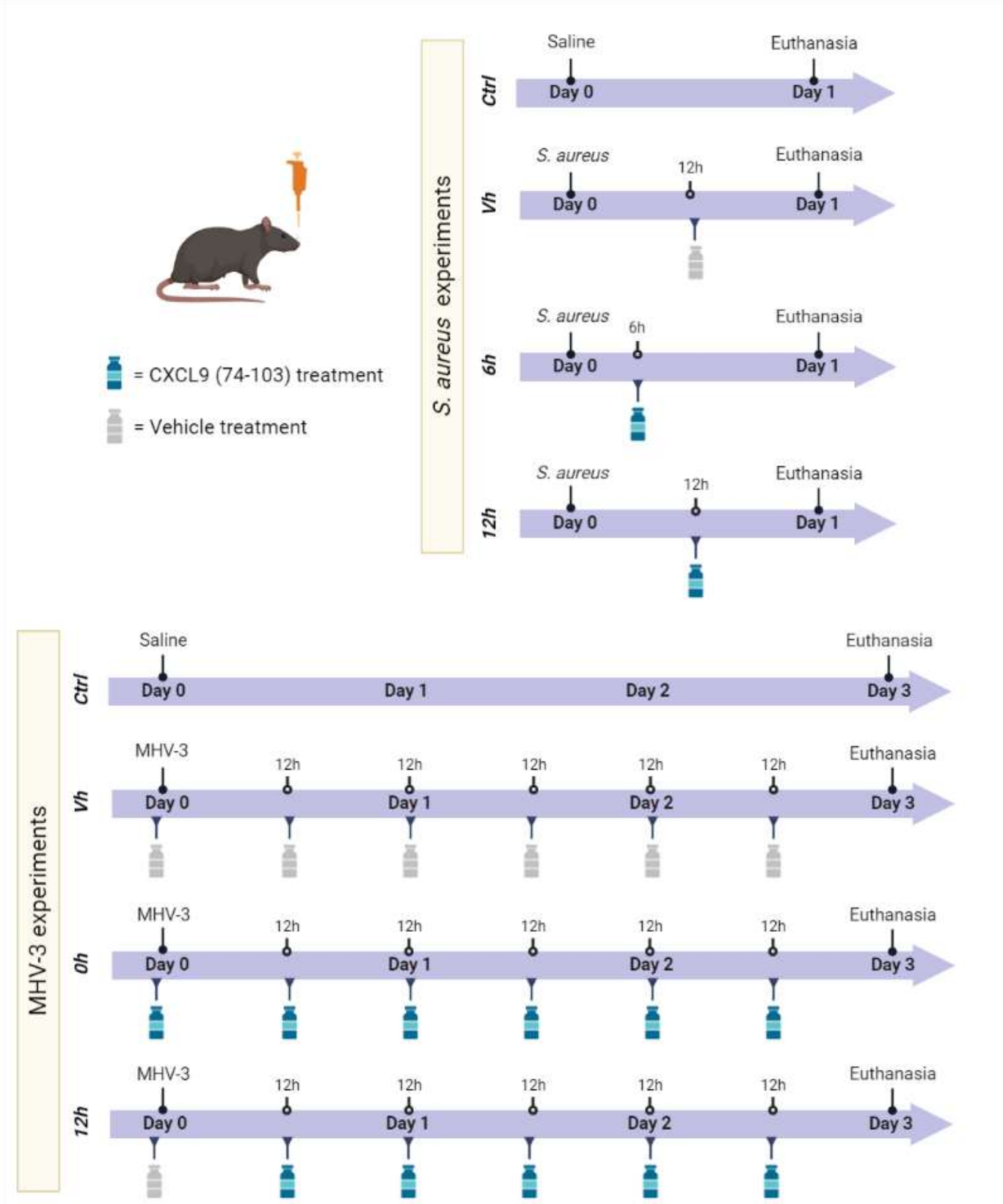

Figure 4 – Timeline of CXCL9(74-103) treatments in both models of pneumonia.

2.3.3. BACTERIAL/VIRAL LOAD

In the bacterial pneumonia experiments, the left lung was macerated and bronchoalveolar lavage was collected, both under sterile conditions, diluted, plated on BHI-blood agar, and incubated at 37°C. Colony forming units (CFU) were analyzed 24 h after plating and results are expressed as CFU per 50 mg of tissue or per mL. To determine the viral load in the MHV-3 experiments, a plaque assay was performed. Briefly, tissue homogenates were added onto a confluent monolayer of L929 cells in 24-well plates. The plates were incubated for 1 h and were gently agitated every 10 min to assure equal distribution of the sample. Subsequently, cultures were covered with the overlay medium [Dulbecco's Modified Eagle's Medium (DMEM – Cultilab, Campinas, São Paulo, Brazil) containing 0.8% carboxymethylcellulose (Sigma-Aldrich), 2% FCS (Cultilab)]. The plates were incubated for 2 days, at 37°C, and 5% CO_2. After incubation, cultures were fixed with 10% neutral buffered formalin for 1 h and stained with 0.1% crystal violet (Laborclin). Virus titers were determined by visual analysis of the plaques and expressed as plaque-forming units (PFU).

2.3.4. ELISA

The measurement of cytokines and chemokines in lung tissue and bronchoalveolar lavage was performed using ELISA. A lung fragment was weighed and suspended in a solution containing protease inhibitors and subjected to homogenization. Either the supernatant of the lung processing or the BALF were used for analyses. The ELISAs were performed according to the manufacturer's suggested procedures (R&D Systems).

2.3.5. BALF PROTEIN CONCENTRATION

To assess the edema formation and the extent of the tissue damage, the concentration of protein in the BALF was measured using Bradford assay (Bio-Rad, Hercules, California, USA). Briefly, the working reagent is diluted 5 times and mixed with the BSA standards and samples. After an incubation of 30 min at RT, the absorbance was measured at a wavelength of 595 nm (800 TS Absorbance Reader with the Gen5 software – both from Biotek)

2.3.6. ASSESSMENT OF RESPIRATORY MECHANIC DYSFUNCTION

Invasive forced spirometry was performed to evaluate lung function. As previously described by Russo et al. (370), mice were anesthetized with ketamine and xylazine, tracheostomized, placed in a body plethysmograph, and connected to a computer-controlled ventilator (Forced Pulmonary Maneuver System; Buxco Research Systems, Wilmington, NC, USA). Under mechanical respiration, the tidal volume (TV), volume per minute (MV), peak of compliance (Cpk), dynamic compliance (Cdyn), and lung resistance (RI) were determined by the resistance and compliance test. Next, a quasistatic Pressure-Volume maneuver was performed to obtain the total lung capacity (TLC), residual volume (RV), and inspiratory capacity (IC). This maneuver consists in inflating the lungs to +30 cm of H_2O and slowly exhaling until -30 cm of H_2O. Then, the lungs were inflated to +30 cm of H_2O and immediately connected to a highly negative pressure to enforce expiration till -30 cm of H_2O, to identify the fast-flow volume. The forced vital capacity (FVC) and forced expiratory volume at 20 or 50 ms (FEV 20 or FEV50) were measured during this last maneuver, and the Tiffeneau–Pinelliindex (FEV20/FVC or FEV50/FVC) was calculated using these two variables. Suboptimal maneuvers were rejected, and for each test in every single mouse, at least three acceptable maneuvers were conducted to obtain a reliable mean for all numeric parameters.

2.3.7. HISTOPATHOLOGICAL ANALYSIS

Lungs for histopathological analysis were collected and inflated via the trachea with 4% formaldehyde in PBS. The samples were fixed overnight using the same solution, processed with different concentrations of ethanol and xylol, embedded in paraffin, and sectioned (5 μm). Sections were stained with hematoxylin and eosin for the evaluation of airway inflammation, vascular inflammation, parenchymal inflammation, and polymorphonuclear infiltrates (322). The histological analysis was performed by an independent pathologist that was blinded to the experimental conditions.

2.3.8. STATISTICAL ANALYSIS

The data were analyzed using the GraphPad PRISM software (GraphPad, USA, version 9.0.0). The one-way ANOVA test was performed followed by the Bonferroni correction. Significance was determined by comparing the different time points with the

control, unchallenged group; between each condition for the WT and the KO mice and between the WT and KO mice within each condition; and between control, treated, and non-treated (vehicle) groups. P-values were indicated as follows: * = $p < 0.05$ when compared to the corresponding control group and # = $p<0.05$ when comparing wild-type and knockout groups or when compared to the vehicle group.

3

RESULTS

3. RESULTS

3.1. PART I: ROLE OF LYMPHOCYTES IN A MURINE MODEL OF ARDS

3.1.1. PROFILE OF CELLS, PULMONARY EDEMA, AND CYTOKINES IN A MURINE MODEL OF ARDS/ALI

The accumulation of leukocytes in the lungs is an essential part of the inflammation induced by LPS. Neutrophils and macrophages are the main cells recruited and have a well-studied role in the beginning and the resolution of the inflammation (265,266). In addition, other cell types can be part of this process, such as lymphocytes. To better understand our ARDS/ALI model and infer whether lymphocytes may be important in it, we evaluated the profile of cells recruited to the alveolar space by collecting BALF (Figure 5). In the first two days after the LPS challenge, we observed a massive influx of cells (Figure 5A), especially neutrophils (Figure 5B). After reaching its peak on day 2, the number of cells, as well as the number of neutrophils, decreased over time. In contrast, the accumulation of macrophages (Figure 5C) and lymphocytes (Figure 5D) in the alveolar space was significantly increased on day 3 and their numbers peak around day 5. The protein concentration was also measured in BALF to determine the extent of the tissue damage leading to protein leakage. We observed that, similar to the number of total cells and neutrophils, the peak of tissue damage was on day 2 and only basal levels of proteins were measured on day 5 and 7.

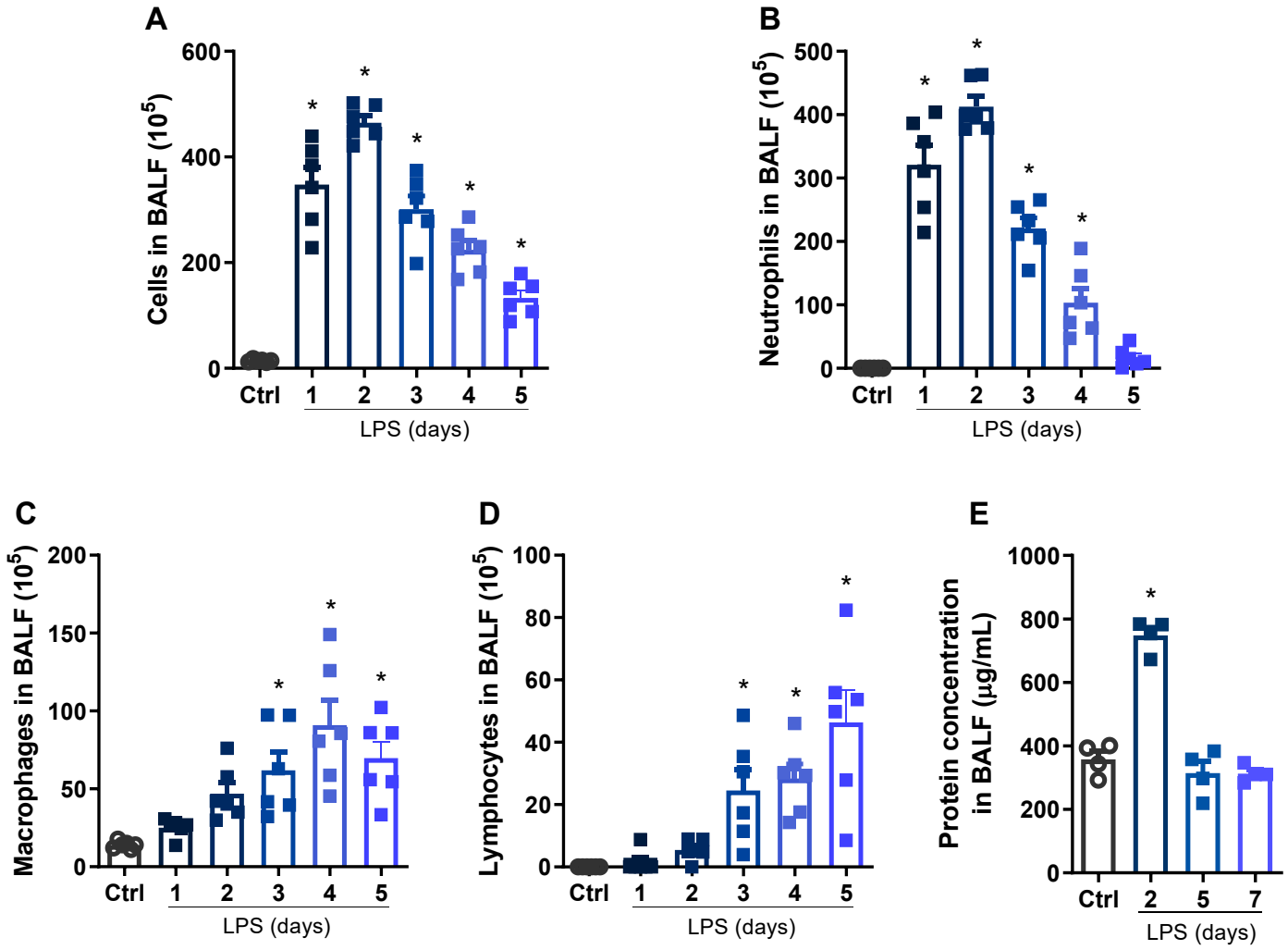

Figure 5 – Cell accumulation and protein concentration in the BALF in ARDS. C57BL/6 mice were challenged with LPS (12.5 µg/mouse) or PBS (Ctrl group) intranasally and dissected at the indicated days. Numbers of total leukocytes (A), neutrophils (B), macrophages (C), and lymphocytes (D) in BALF were counted in Bürker chambers. Pulmonary edema was quantified based on the protein concentration in the BALF (E). Graphs representative of two experiments. Data are shown as mean ± SEM. Each symbol represents data of an individual mouse. *p< 0.05 when compared with the healthy, unchallenged control group. ANOVA test followed by Bonferroni correction was used in the graphs with normal distribution. Otherwise, Kruskal-Wallis test was used. n=4-6

Cytokines are key molecules in the propagation and regulation of inflammation. Thus, we next measured some cytokines in BALF. TNF-α (Figure 6A) and IL-17 (Figure

6B) have well-established roles in promoting neutrophilic inflammation (267,268) and we observed increased levels of these cytokines at the beginning of inflammation, in agreement with the accumulation of neutrophils. The cytokines IL-10 and transforming growth factor beta (TGF-β) are classically related with anti-inflammatory events and, consequently, the proper resolution of inflammation (100,269,270). However, in our LPS-induced ARDS model, we were not able to detect significant alterations in the levels of these cytokines (Figure 6C, D), but there was a clear tendency of reduction on the first days of inflammation with increasing levels over the evaluated time.

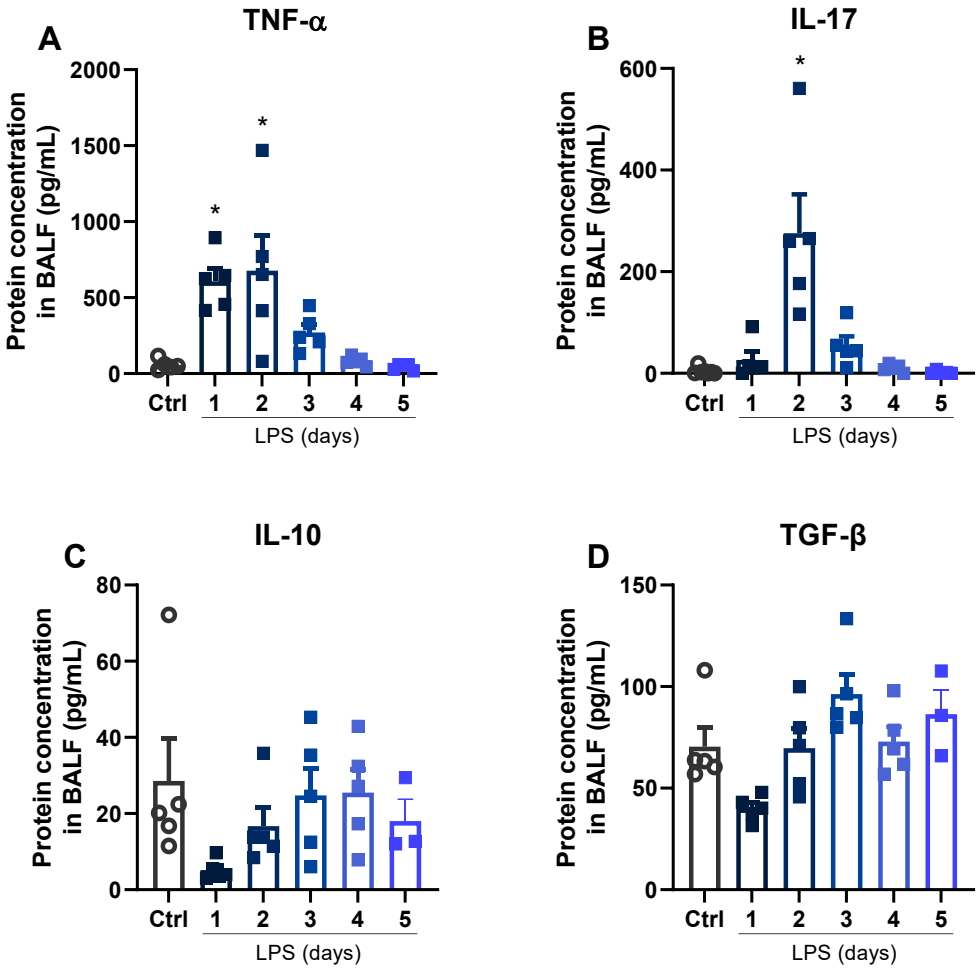

Figure 6 – BALF levels of cytokines in ARDS. C57BL/6 mice were challenged with LPS (12.5 μg/mouse) or PBS (Ctrl group) intranasally and dissected at the indicated days. Levels of TNF-α (A), IL-17 (B), IL-10 (C), and TGF-β (D) were measured in the BALF by ELISA. Graphs representative of two experiments. Data are shown as mean ± SEM. Each symbol represents data

of an individual mouse. *p< 0.05 when compared with the healthy, unchallenged control group. ANOVA test followed by Bonferroni correction was used in the graphs with normal distribution. Otherwise, Kruskal-Wallis test was used. n=5

To better elucidate the accumulation of cells in this model, we next evaluated the levels of chemokines related with mononuclear cells recruitment in the lung tissue. CCL2 and CCL3 target mainly monocytes and macrophages (271), respectively, and as observed in Figures 7A and B, their levels were increased from day 1 to 3 after the LPS challenge. In contrast, CCL5 has a broader target cell spectrum and can recruit T cells, dendritic cells, eosinophils, NK cells, mast cells, and basophils (272). This chemokine is increased during the whole period (Figure 7C) and might be relevant for lymphocyte recruitment at later time points. Lastly, we measured the levels of CXCL9 and CXCL10 (Figure 7D, E), chemokines important in the recruitment of lymphocytes, but also monocytes (132). Differently from expected, these chemokines were increased only at the beginning of inflammation, on day 1 for CXCL10 (Figure 7D) and days 1 and 2 for CXCL9 (Figure 7E).

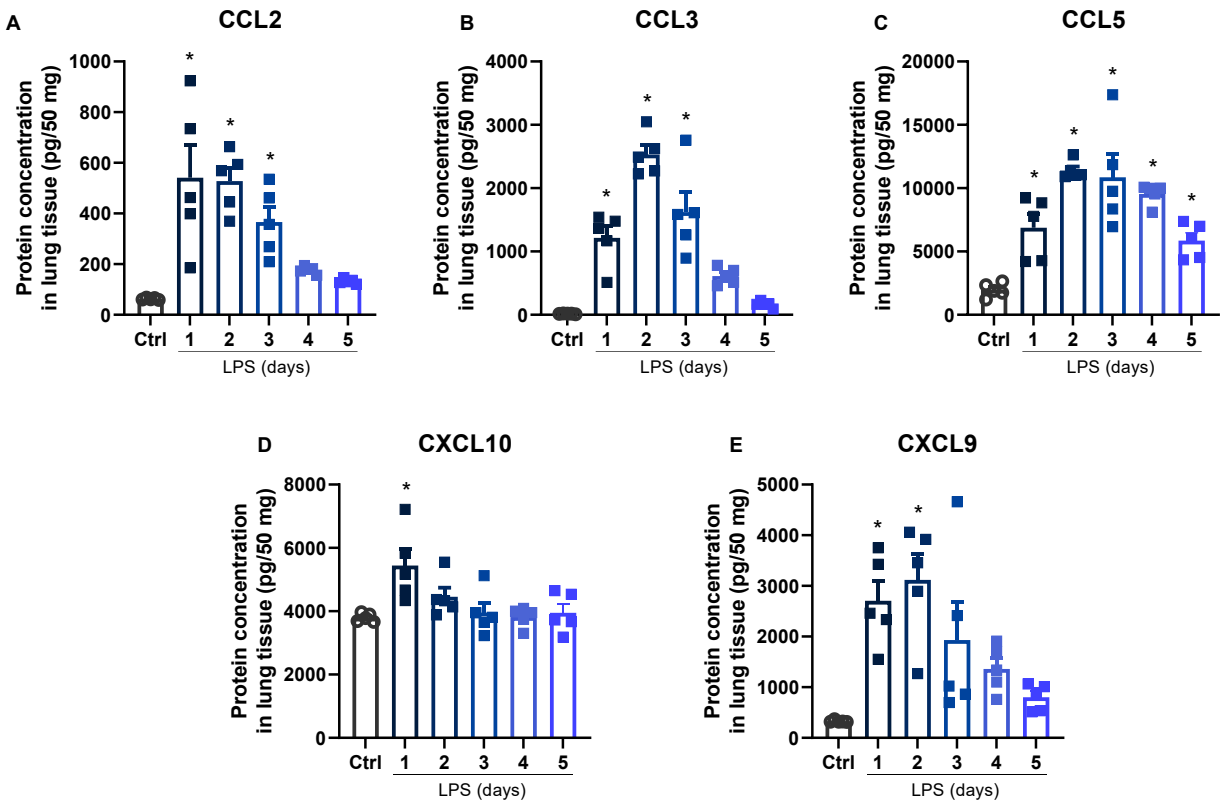

Figure 7 – Levels of chemokines in the lung tissue in the ARDS model. C57BL/6 mice were challenged with LPS (12.5 µg/mouse) or PBS (Ctrl group) intranasally and dissected at the indicated days. Levels of CCL2 (A), CCL3 (B), CCL5 (C), CXCL10 (D), and CXCL9 (E) were measured in the BALF by ELISA. Graphs representative of two experiments. Data are shown as mean ± SEM. Each symbol represents data of an individual mouse. *p< 0.05 when compared with the healthy, unchallenged control group. ANOVA test followed by Bonferroni correction was used in the graphs with normal distribution. Otherwise, Kruskal-Wallis test was used. n=5

3.1.2. THE INFLAMMATION INDUCED BY LPS INCREASES THE NUMBERS OF LYMPHOCYTES MAINLY IN THE ALVEOLAR SPACE (BALF) BUT ALSO IN THE LUNG TISSUE

Once we observed the increase of microscopically identified lymphocytes, we decided to evaluate the recruitment of different populations of lymphocytes ($CD4^+$ and $CD8^+$ T cells, B cells, and NK cells) in two lung compartments: the alveolar space hereby represented by the BALF and the pulmonary parenchyma, i.e., the lung tissue itself. As observed in Figure 8A-D, the percentages of adaptive lymphocytes increased 5 and 7

days after the challenge, opposite to the results obtained for $DX5^+$ NK cells. However, when we evaluated the absolute numbers of cells, T lymphocytes increased at all time points (Figure 8E, F). Since there was a massive influx of cells to the lungs and the alveolar space on day 2 (Figure 5A), it is reasonable that the numbers of cells increased in general, but the percentages of adaptive lymphocytes on days 5 and 7 are remarkably enhanced (for T cells from about 2% on day 2 to 10-30% on day 5) and may suggest an important role for these cells at later time points in ARDS. Despite the higher percentages of B cells at later time points, their total numbers are reduced on days 5 and 7. Hence, B cells are recruited to the alveolar space on day 2 but do not remain for a long period (Figure 8C, G). Interestingly, NK cell accumulation was increased at the peak of inflammation (day 2) and returned to basal levels on day 5 (absolute numbers) or day 7 (percentages) (Figure 8D, H).

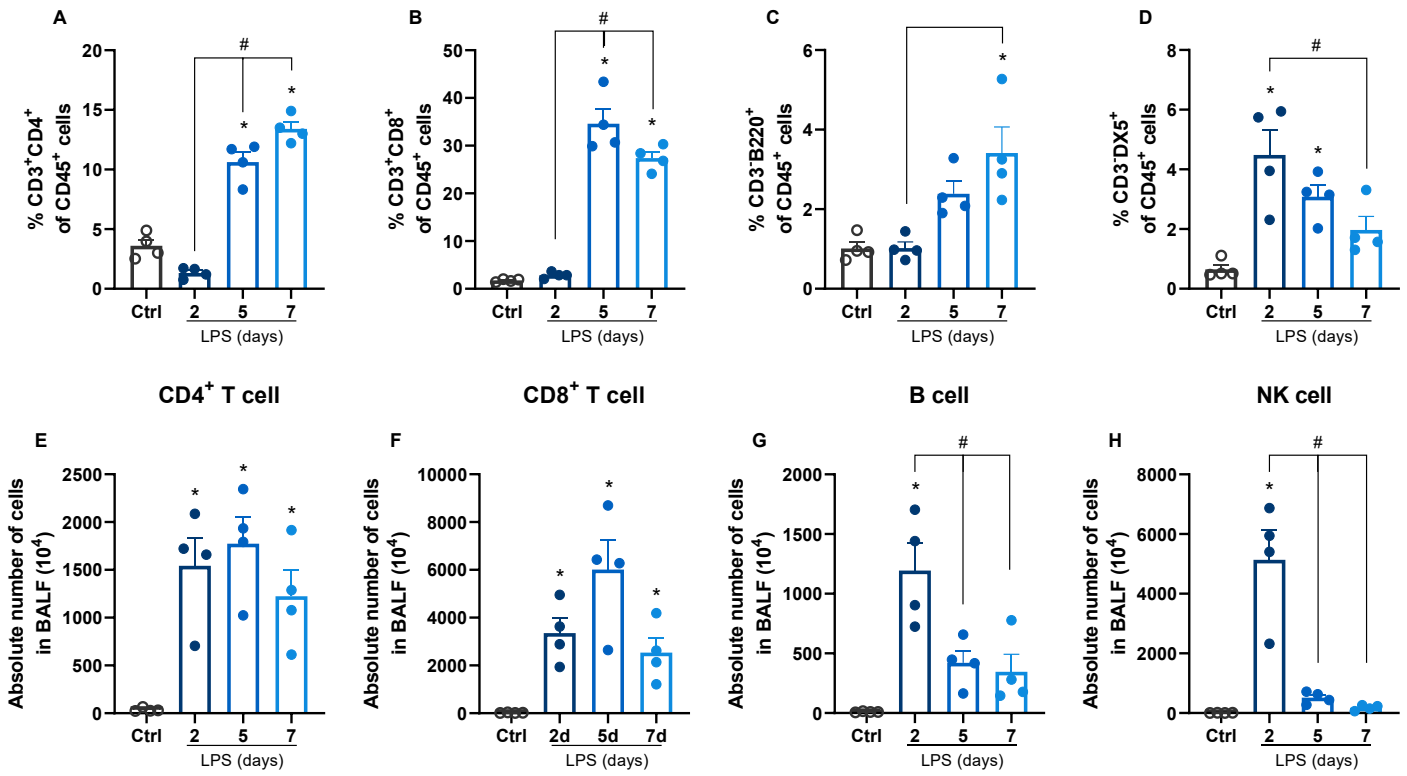

Figure 8 – Percentages and numbers of lymphocytes in BALF in the ARDS model. C57BL/6 mice were challenged with LPS (12.5 µg/mouse) or PBS (Ctrl group) intranasally and dissected at the indicated days. Percentages (A) and absolute numbers (E) of $CD4^+$ T lymphocytes ($CD45^+CD3^+CD4^+$ cells); (B and F) $CD8^+$ T lymphocytes ($CD45^+CD3^+CD8^+$ cells); (C and G) B lymphocytes ($CD45^+CD3^-CD19^+$ cells); and (D and H) NK cells ($CD45^+CD3^-NKp46^+$ cells) were quantified in BALF by flow cytometry. Graphs representative of two experiments. Data are shown as mean ± SEM. Each symbol represents data of an individual mouse. *p< 0.05 when compared with the healthy, unchallenged control group. #p<0.05 when comparing different time points with day 2. ANOVA test followed by Bonferroni correction was used in the graphs with normal distribution. Otherwise, Kruskal-Wallis test was used. n=4

Regarding the recruitment of cells to the tissue, we observed a decrease in all lymphocyte percentages on day 2 (Figure 9A-D), most likely because of the dominant recruitment of neutrophils and monocytes at the peak of inflammation. In contrast, the absolute numbers (Figure 9E-H) increased for CD8+ T cells on days 2 and 7; B cells on day 7; and NK cells on day 2. Interestingly, the differences in absolute numbers of cells

are not as dramatic as in the BALF (Figure 8), indicating that most of the cells are recruited to the alveolar space.

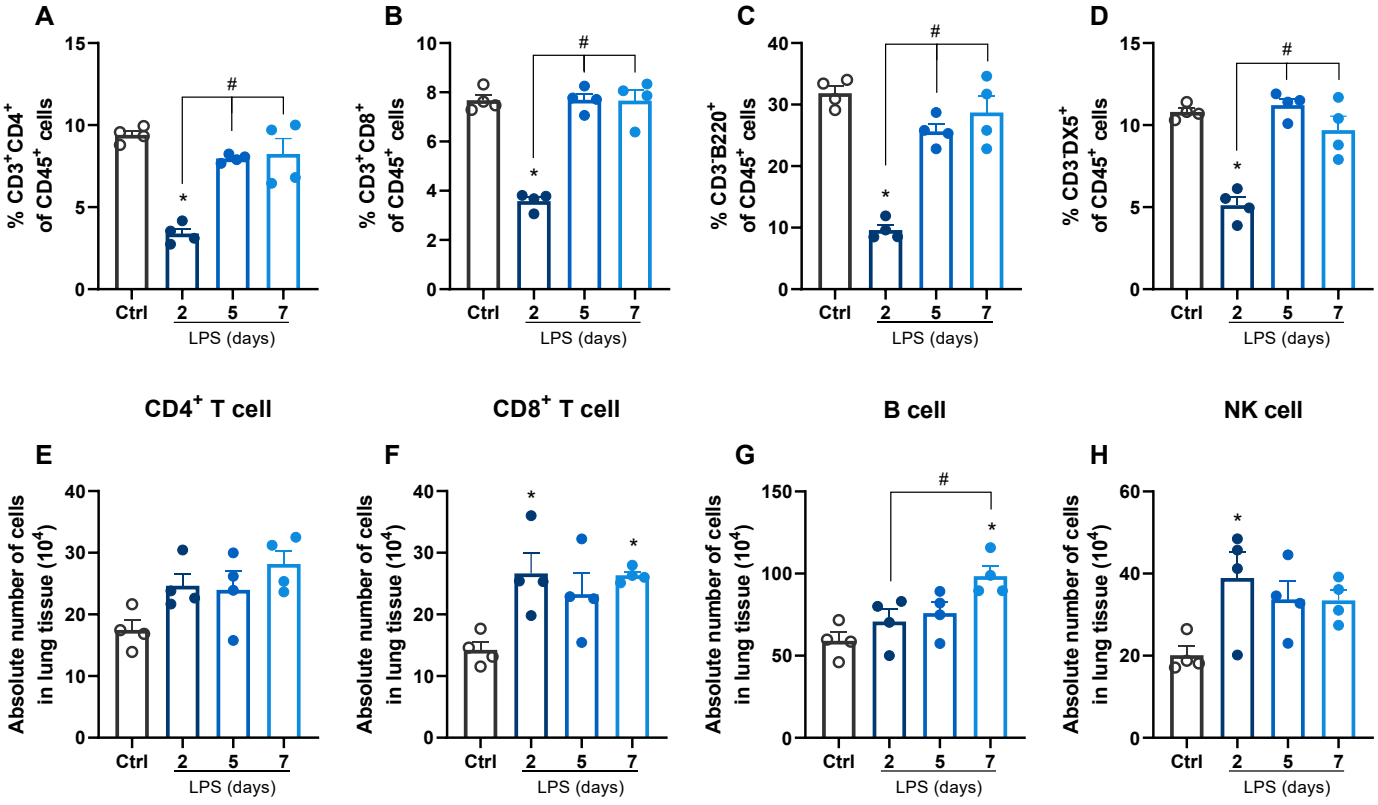

Figure 9 – Percentages and numbers of lymphocytes in the lungs in the ARDS model. C57BL/6 mice were challenged with LPS (12.5 µg/mouse) or PBS (Ctrl group) intranasally and dissected at the indicated days. Percentages (A) and absolute numbers (E) of $CD4^+$ T lymphocytes ($CD45^+CD3^+CD4^+$ cells); (B and F) $CD8^+$ T lymphocytes ($CD45^+CD3^+CD8^+$ cells); (C and G) B lymphocytes ($CD45^+CD3^-CD19^+$ cells); and (D and H) NK cells ($CD45^+CD3^-NKp46^+$ cells) were quantified in the lung tissue by flow cytometry. Graphs representative of two experiments. Data are shown as mean ± SEM. Each symbol represents data of an individual mouse. *p< 0.05 when compared with the healthy, unchallenged control group. #p<0.05 when comparing different time points with day 2. ANOVA test followed by Bonferroni correction was used in the graphs with normal distribution. Otherwise, Kruskal-Wallis test was used. n=4

3.1.3. LACK OF ADAPTIVE LYMPHOCYTES DOES NOT AFFECT THE INFLAMMATION NOR THE RESOLUTION OF ARDS

Since there was an increase of adaptive lymphocytes in the lungs, especially in the alveolar space in later time points after LPS challenge, we decided to further investigate their role in our model of LPS-induced ARDS using RAG2 knockout mice, that lack T and B lymphocytes. First, we evaluated some populations of lymphocytes to make sure that the RAG2 knockout mice did not have adaptive lymphocytes and to elucidate the impact of their absence on the numbers of NK cells. As expected, $CD4^+$ T, $CD8^+$, T, and B lymphocytes numbers were scarcely found at every timepoint in the $RAG2^{-/-}$ groups (Figure 10A-C). In contrast, under control conditions more NK cells were detected in $RAG2^{-/-}$ animals and their numbers were also significantly higher on day 4 in comparison to healthy mice and LPS-challenged WT mice. (Figure 10D).

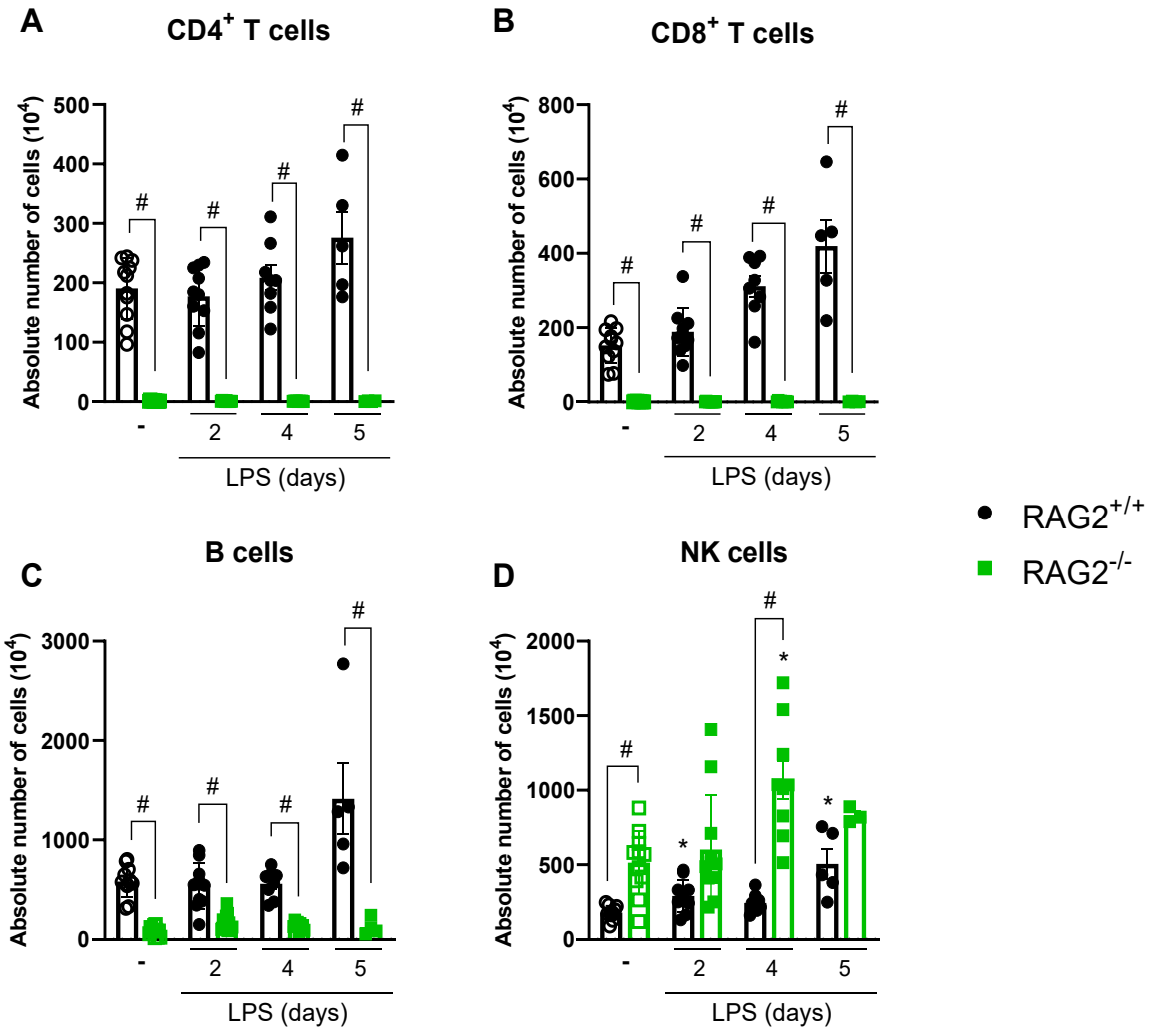

Figure 10 – RAG2 absence results in decreased accumulation of CD4 T lymphocytes, CD8 T lymphocytes, and B lymphocytes. In contrast, it increases the accumulation of NK cells. RAG2 WT and RAG2 KO C57BL/6 mice were challenged with LPS (12.5 µg/mouse) or PBS (Ctrl group; -) and dissected at the indicated days. Absolute numbers of $CD4^+$ T lymphocytes ($CD45^+CD3^+CD4^+$ cells) (A), $CD8^+$ T lymphocytes ($CD45^+CD3^+CD8^+$ cells) (B), B lymphocytes ($CD45^+CD3^-CD19^+$ cells) (C), and NK cells ($CD45^+CD3^-NKp46^+$ cells) present in the lung tissue combined with the BAL fluid were quantified by flow cytometry. Compilation of three experiments. Data are shown as mean ± SEM. Each symbol represents data of an individual mouse. *p< 0.05 when compared with the healthy, unchallenged control group. #p<0.05 when comparing wild type and knockout groups at the same time point. ANOVA test followed by Bonferroni correction was used in the graphs with normal distribution. Otherwise, Kruskal-Wallis test was used. n=4-11.

After observing the absence of adaptive lymphocytes and the increase of NK cell numbers, we evaluated the numbers of ILCs type 1, 2, and 3. Interestingly, all the subpopulations of ILC were enhanced in the absence of RAG2 on day 4 after the challenge (Figure 11).

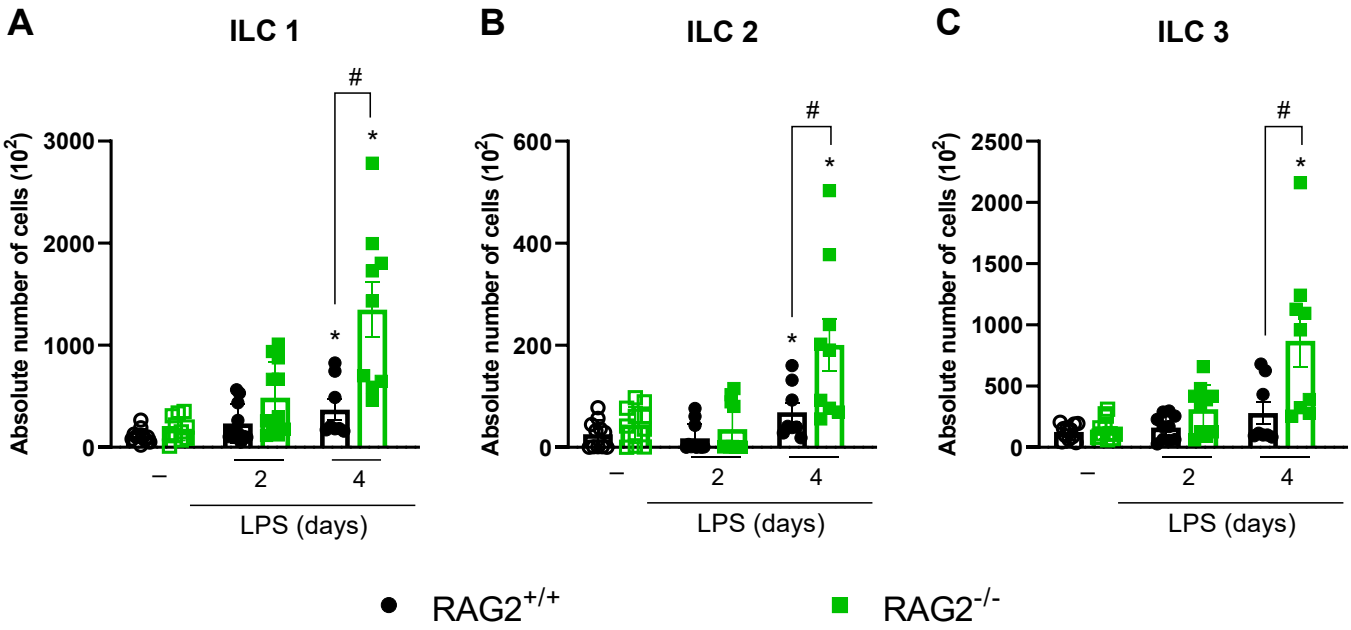

Figure 11 – The absence of RAG2 increases the number of ILC1, 2, and 3 on day 4 after the challenge. Rag2 WT and Rag2 KO C57BL/6 mice were challenged with LPS (12.5 µg/mouse) or PBS (Ctrl group; -) and dissected at the indicated days. Absolute numbers of ILC1 ($Lin^-CD3^-CD90.2^+T\text{-}bet^+$ cells) (A), ILC2 ($Lin^-CD3^-CD90.2^+GATA\text{-}3^+$ cells) (B), and ILC3 ($Lin^-CD3^-CD90.2^+ROR\text{-}\gamma t^+$ cells) (C) present in the lung tissue combined with the BAL fluid were quantified by flow cytometry. Compilation of two experiments. Data are shown as mean ± SEM. Each symbol represents data of an individual mouse. *p< 0.05 when compared with the healthy, unchallenged control group. #p<0.05 when comparing wild type and knockout groups at the same time point. ANOVA test followed by Bonferroni correction was used in the graphs with normal distribution. Otherwise, Kruskal-Wallis test was used. n=8-11.

Next, we evaluated some inflammation parameters. As observed in Figures 12A and B, the numbers of total cells and neutrophils in the $RAG2^{+/+}$ mice reached the peak on day 2 and were significantly reduced on days 4 (neutrophils) and 5 (neutrophils and total cells) after the challenge. Interestingly, the absence of RAG2 did not change the profile of cell accumulation in the lungs. Similarly, the pulmonary edema increased only

on day 2 and there were no significant differences between RAG2$^{+/+}$ and RAG2$^{-/-}$ (Figure 12C). Therefore, the recruitment of cells and tissue damage is not dependent on adaptive lymphocytes. To measure the systemic effects of ARDS, the animal body weight was monitored (Figure 12D), and we observed a dramatic weight loss already 1 day after the LPS challenge in both RAG2$^{+/+}$ and RAG2$^{-/-}$. On day 4, the RAG$^{+/+}$ animals recovered, but the RAG2$^{-/-}$ group had less bodyweight at that time point when compared to the RAG2$^{+/+}$ mice. On day 5, there was no differences between both LPS-stimulated groups.

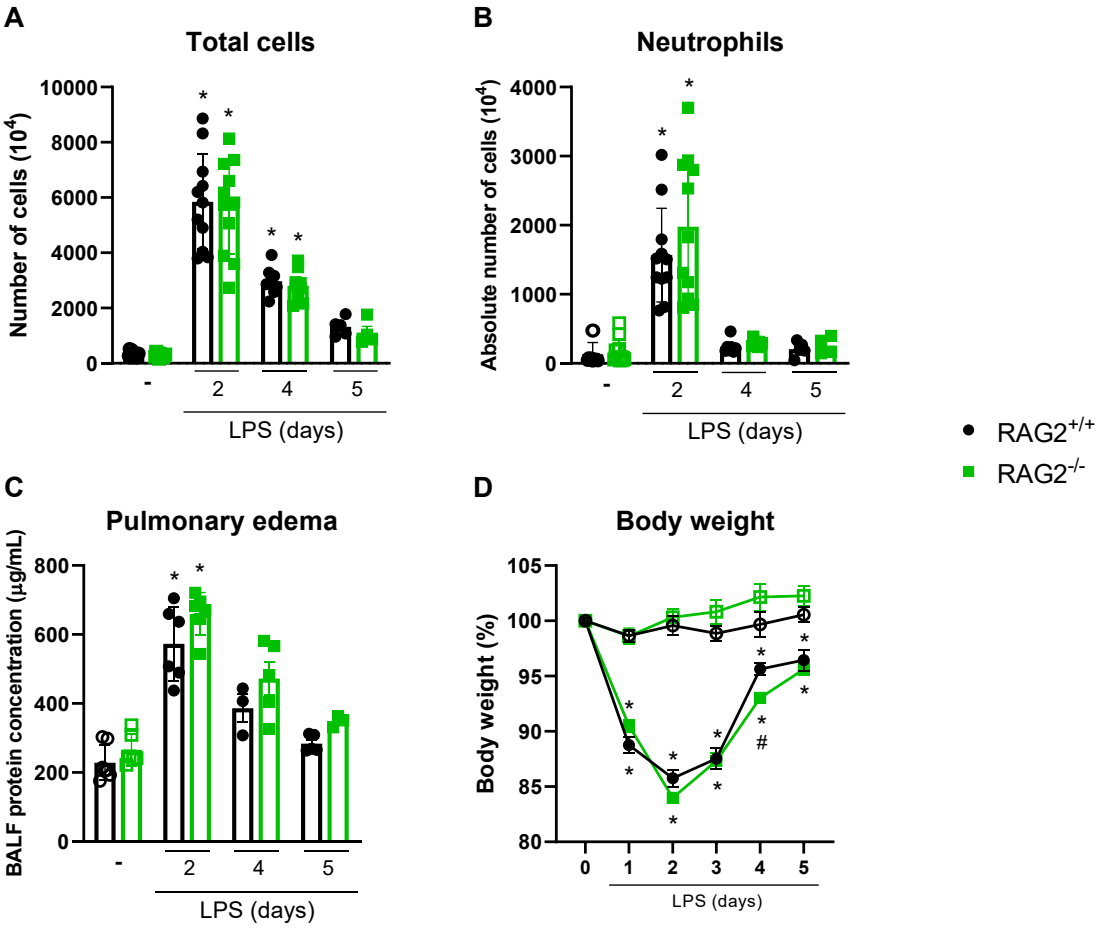

Figure 12 – RAG2 absence does not impact the accumulation of leukocytes, pulmonary edema, or weight loss. RAG2 WT and RAG2 KO C57BL/6 mice were challenged with LPS (12.5 µg/mouse) or PBS (Ctrl group; -) and dissected at the indicated days. Numbers of total leukocytes (A) were counted in Bürker chambers and neutrophils (B) were measured by flow cytometry. Both cells were analyzed in the lung tissue combined with the BAL fluid. Pulmonary edema was quantified based on the protein concentration in the BALF (C). Changes in body weight (D) were

calculated compared to day 0 (before infection). Compilation of three experiments. Data are shown as mean ± SEM. Each symbol represents data of an individual mouse, except for the weight loss. *p< 0.05 when compared with the healthy, unchallenged control group. #p<0.05 when comparing wild type and knockout groups at the same time point. ANOVA test followed by Bonferroni correction was used in the graphs with normal distribution. Otherwise, Kruskal-Wallis test was used. n=4-11.

In addition to the innate lymphocytes, we hypothesized that other cells could compensate for the lack of adaptive lymphocytes, such as monocytes and macrophages. Thus, we evaluated populations of monocyte-derived macrophages, AM, interstitial macrophages, Ly-6C^{+} monocytes, and Ly-6C^{-} monocytes. Curiously, compared to WT, the absence of RAG2 did not significantly alter the numbers of these populations (Figure 13).

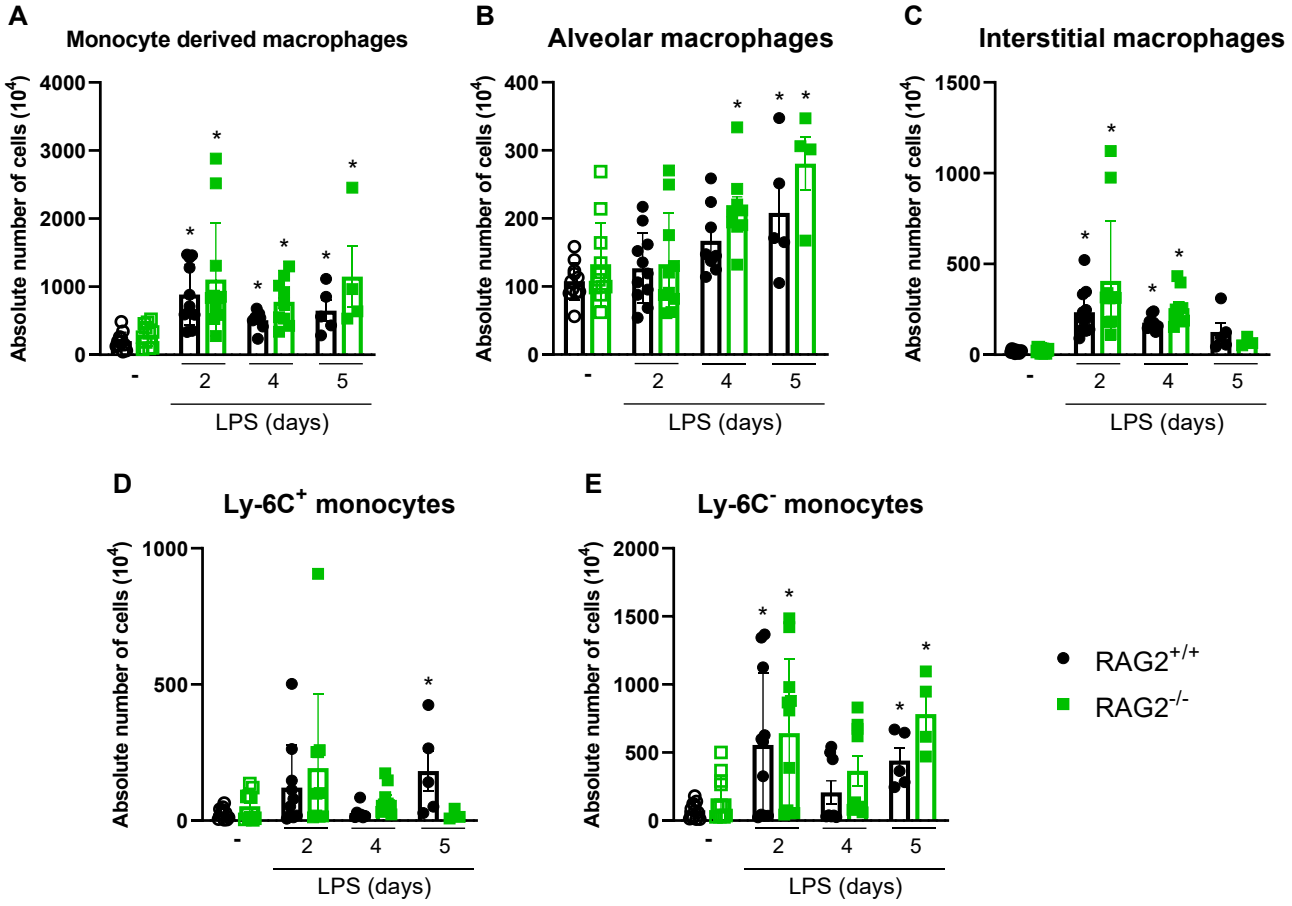

Figure 13 – RAG2 deficiency does not impact the number of monocytes or macrophages. Rag2 WT and Rag2 KO C57BL/6 mice were challenged with LPS (12.5 µg/mouse) or PBS (Ctrl group; -) and dissected at the indicated days. Absolute numbers of monocyte-derived macrophages ($CD45^+CD11b^+Ly6G^-CD3^-CD103^-SiglecF^-CD11c^-$ cells) (A), AM ($CD45^+SiglecF^+CD11c^+$ cells) (B), IM ($CD45^+CD11b^+SiglecF^-Ly6G^-Dump^-CD103^-CD64^+MHCII^+$ cells) (C), Ly-$6C^+$ monocytes ($CD45^+CD11b^+SiglecF^-Ly6G^-Dump^-CD103^-MHCII^-Ly6C^+$ cells) (D), and Ly-$6C^-$ monocytes ($CD45^+CD11b^+SiglecF^-Ly6G^-Dump^-CD103^-MHCII^-Ly6C^-$ cells) (E) were quantified by flow cytometry. Compilation of three experiments. Data are shown as mean ± SEM. Each symbol represents data of an individual mouse. *p< 0.05 when compared with the healthy, unchallenged control group. ANOVA test followed by Bonferroni correction was used in the graphs with normal distribution. Otherwise, Kruskal-Wallis test was used. n=4-11.

After evaluating the numbers of different leukocyte populations recruited to the lungs, we analyzed the levels of cytokines in the BALF. Levels of the inflammatory cytokines IL-6, TNF-α, and IFN-γ were significantly increased on day 2 in both $RAG2^{+/+}$

and RAG2$^{-/-}$ (Figure 14A-C). Remarkably, the increase in IFN-γ in the RAG2$^{-/-}$ was larger than in the RAG2$^{+/+}$ (Figure 14B), possibly because more NK cells were present. IL-13 and IL-10 were also measured, and a decrease was observed in mice lacking RAG2 at the peak of inflammation (day 2) (Figure 14D, E). In addition, there are no differences in the IL-10 and IL-13 levels between RAG2$^{+/+}$ and RAG2$^{-/-}$ mice. Lastly, TGF-β was increased on days 2 and 4, in the RAG2$^{+/+}$ group, while it was increased only on day 4 in the RAG2$^{-/-}$ group (Figure 14F). On day 4, the TGF-β level was lower in the absence of RAG2, suggesting that adaptive lymphocytes might have a role in the resolution of inflammation. In the absence of RAG2, the resolution is probably achieved through compensation by other cell populations.

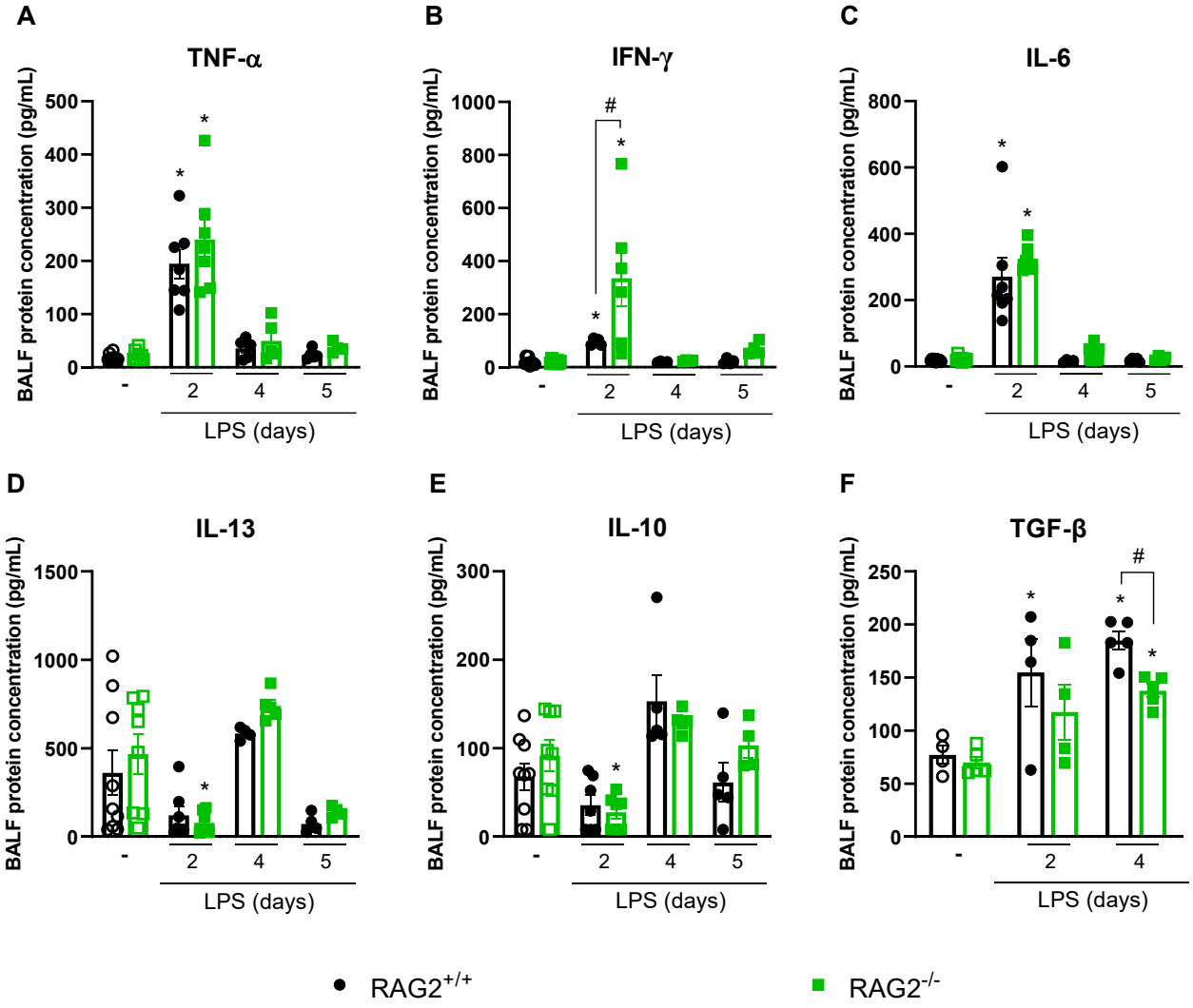

Figure 14 – RAG2 deficiency affects IFN-γ and TGF-β levels. Rag2 WT and Rag2 KO C57BL/6 mice were challenged with LPS (12.5 µg/mouse) or PBS (Ctrl group; -) and dissected at the indicated days. Levels of TNF-α (A), IFN-γ (B), IL-6 (C), IL-13 (D), IL-10 (E), and TGF-β (F) were measured in the BALF by ELISA. Compilation of two experiments in panels A-E and only one experiment in panel F. Data are shown as mean ± SEM. Each symbol represents data of an individual mouse. *p< 0.05 when compared with the healthy, unchallenged control group. #p<0.05 when comparing wild type and knockout groups at the same time point. ANOVA test followed by Bonferroni correction was used in the graphs with normal distribution. Otherwise, Kruskal-Wallis test was used. n=4-9.

3.1.4. LYMPHOCYTES FROM BALF AND LUNGS EXPRESS CXC RECEPTORS IN THE LATE TIME POINTS OF ARDS

Although the absence of total T and B lymphocytes did not affect the outcome of ARDS as expected, we decided to investigate the subpopulations of accumulated T cells according to their chemokine receptor expression profile. Thus, we tried to elucidate the role of specific cells, identified through the expression of particular chemokine receptors: CXCR3, CXCR6, CCR3, CCR4, and CCR5. In addition, we decided to explore the differences in the recruitment of T lymphocytes to different pulmonary compartments, the alveolar space (BALF), and the lung tissue (lungs), clarifying the importance of certain chemokine receptors to reach the alveolar space.

CXCR3, together with its IFN-γ induced ligands CXCL9, CXCL10, and CXCL11, has an important role in the activation and recruitment of T lymphocytes, especially T helper (Th) 1 (132). In our ARDS model, we observed that around 80% of the $CD4^+$ and $CD8^+$ T lymphocytes that reached the alveolar space on days 5 and 7 expressed CXCR3. Besides that, the median fluorescence intensity of CXCR3 also increased 5 and 7 days after the challenge, demonstrating the importance of this receptor for inflammation of the alveolar lumen (Figure 15A-D). In contrast, in the lung tissue, approximately 20% of the $CD4^+$ T lymphocytes and 25% of $CD8^+$ T lymphocytes expressed CXCR3 on days 5 and 7 (Figure 15E-H). It is important to notice that on day 2, the peak of inflammation, very few CXCR3+ lymphocytes were detected. The influx of CXCR3 nicely follows the upregulation of IFN-γ, and IFN-inducible chemokine ligands for CXCR3 that was detected on days 1 and/or 2 (Figures 15, 8).

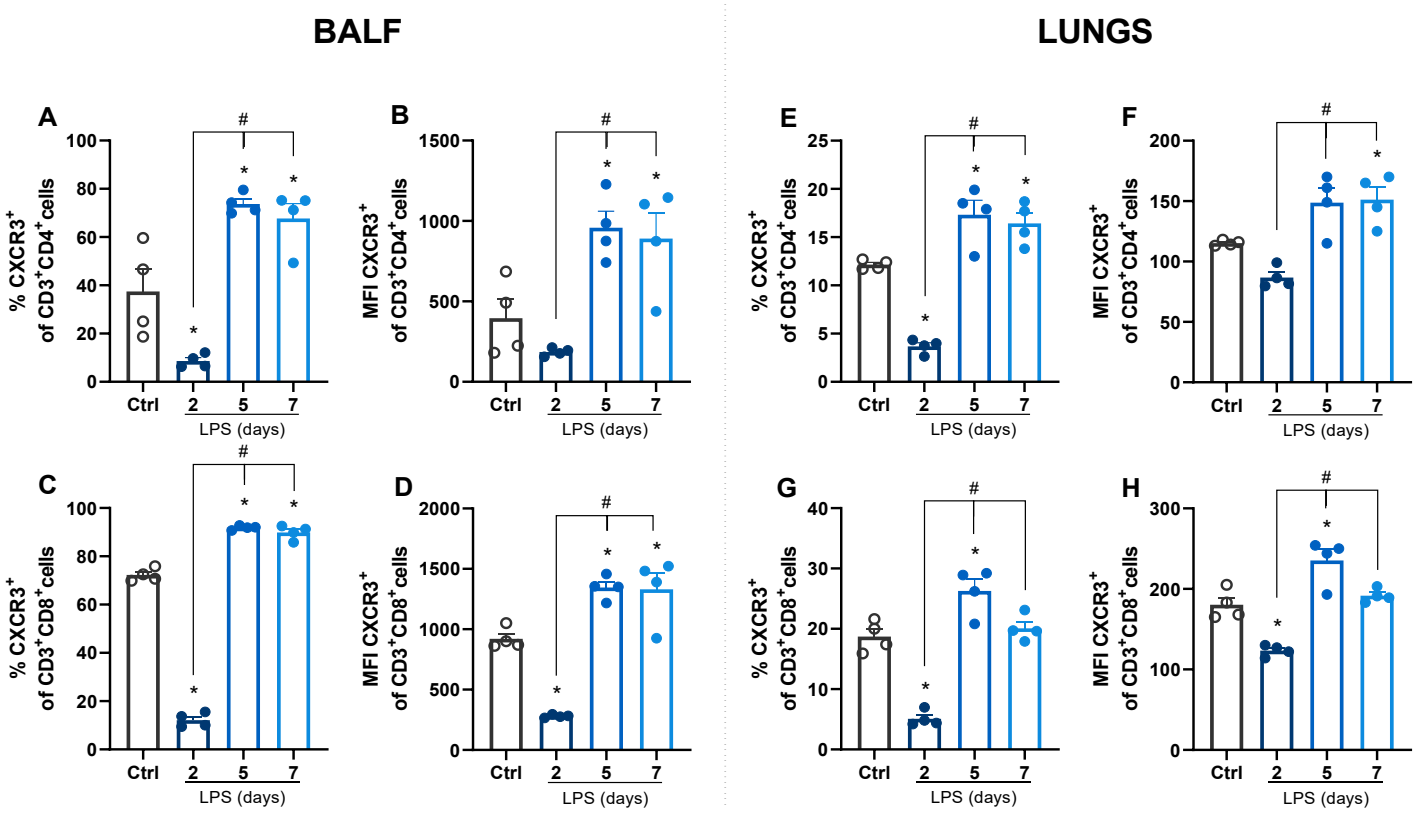

Figure 15 – Percentages and MFI of CXCR3 expression in lymphocytes in BALF and lungs in ARDS. C57BL/6 mice were challenged with LPS (12.5 µg/mouse) or PBS (Ctrl group) intranasally and dissected at the indicated days. Percentage (A) and MFI (B) of $CXCR3^+$ $CD4^+$ T lymphocytes ($CD45^+CD3^+CD4^+CXCR3^+$ cells); and (C and D) $CXCR3^+$ $CD8^+$ T lymphocytes ($CD45^+CD3^+CD8^+CXCR3^+$ cells) were quantified in BALF by flow cytometry. Additionally, the flow cytometric analysis was performed on lung tissue: percentage (E) and MFI (F) of $CXCR3^+$ $CD4^+$ T lymphocytes ($CD45^+CD3^+CD4^+CXCR3^+$ cells); and (G and H) $CXCR3^+$ $CD8^+$ T lymphocytes ($CD45^+CD3^+CD8^+CXCR3^+$ cells). Graphs representative of two experiments. Data are shown as mean ± SEM. Each symbol represents data of an individual mouse. *$p< 0.05$ when compared with the healthy, unchallenged control group. #$p<0.05$ when comparing different time points with day 2. ANOVA test followed by Bonferroni correction was used in the graphs with normal distribution. Otherwise, Kruskal-Wallis test was used. n=4

Next, we evaluated another receptor widely expressed by activated T lymphocytes: CXCR6. Its ligand, CXCL16, is constitutively produced by the alveolar epithelia, indicating a role of this receptor in T lymphocyte recruitment and retention in the alveolar space (273,274). As observed for CXCR3, the percentage of CXCR6-expressing $CD4^+$ T

lymphocytes in BALF was increased on days 5 and 7 after the LPS challenge (Figure 16A, B). However, for the other populations either no consistent results were obtained, or no differences were observed compared to the unchallenged control group (Figure 16C-H).

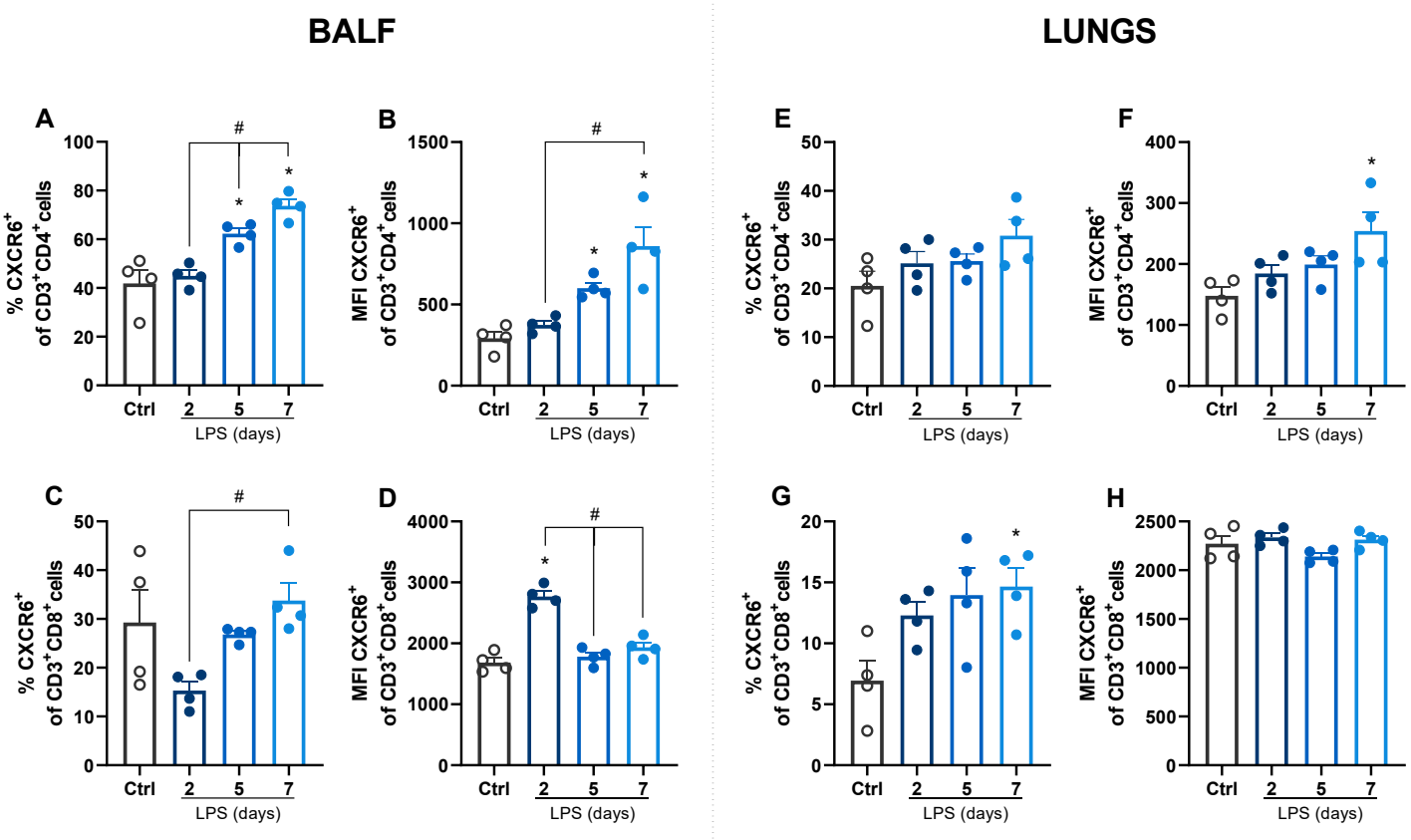

Figure 16 – Percentages and MFI of CXCR6 expression in lymphocytes in BALF and lungs in ARDS. C57BL/6 mice were challenged with LPS (12.5 µg/mouse) or PBS (Ctrl group) intranasally and dissected at the indicated days. Percentage (A) and MFI (B) of CXCR6$^+$ CD4$^+$ T lymphocytes (CD45$^+$CD3$^+$CD4$^+$CXCR6$^+$ cells); and (C and D) CXCR6$^+$ CD8$^+$ T lymphocytes (CD45$^+$CD3$^+$CD8$^+$CXCR6$^+$ cells) were quantified on BALF by flow cytometry. Additionally, the flow cytometric analysis was performed on lung tissue: percentage (E) and MFI (F) of CXCR6$^+$ CD4$^+$ T lymphocytes (CD45$^+$CD3$^+$CD4$^+$CXCR6$^+$ cells); and (G and H) CXCR6$^+$ CD8$^+$ T lymphocytes (CD45$^+$CD3$^+$CD8$^+$CXCR6$^+$ cells). Graphs representative of two experiments. Data are shown as mean ± SEM. Each symbol represents data of an individual mouse. *p< 0.05 when compared with the healthy, unchallenged control group. #p<0.05 when comparing different time points with day 2. ANOVA test followed by Bonferroni correction was used in the graphs with normal distribution. Otherwise, Kruskal-Wallis test was used. n=4

3.1.5. THE EXPRESSION OF CC RECEPTORS IN LYMPHOCYTES FROM BALF AND LUNGS IS NOT SO ABUNDANT AS CXC RECEPTORS

Receptors for inflammatory CC chemokines are expressed mainly by monocytes, macrophages, and lymphocytes, and are hence important factors for the recruitment of these cells. CCR3, CCR4, and CCR5 are expressed in different populations of lymphocytes. CCR3 is expressed by a subpopulation of Th2 lymphocytes reactive to eotaxin and predominantly related with allergic diseases (275,276). We observed that the expression of CCR3 is not so abundant in T and B lymphocytes in either BALF or lung tissue in our model (Figure 17). In fact, the population of $CD8^+$ T cells expressing CCR3 in the BALF was reduced when compared to the control group (Figure 16C, D). In contrast, $CD8^+$ and $CD4^+$ T cells expressing CCR3 in the lungs were increased on day 2, returning to basal levels at the later time points. Despite this increase, the percentage of $CCR3^+$ T lymphocytes did not reach 5% of the total T lymphocytes in the lungs.

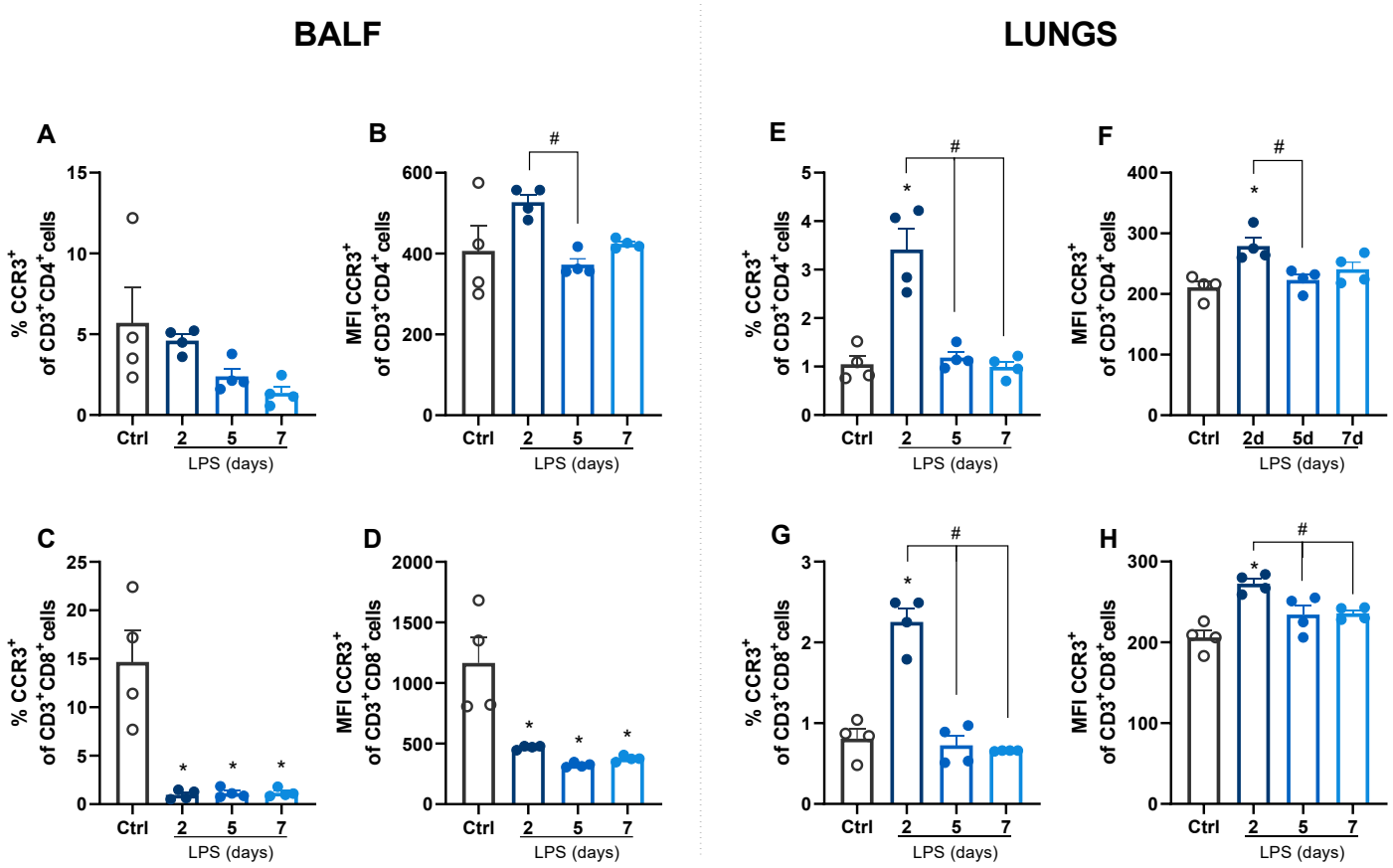

Figure 17 – Percentages and MFI of CCR3 expression in lymphocytes in BALF and lungs in ARDS. C57BL/6 mice were challenged with LPS (12.5 µg/mouse) or PBS (Ctrl group) intranasally and dissected at the indicated days. Percentage (A) and MFI (B) of $CCR3^+$ $CD4^+$ T lymphocytes ($CD45^+CD3^+CD4^+CCR3^+$ cells); and (C and D) $CCR3^+$ $CD8^+$ T lymphocytes ($CD45^+CD3^+CD8^+CCR3^+$ cells) were quantified on BALF by flow cytometry. Additionally, the flow cytometric analysis was performed on lung tissue: percentage (E) and MFI (F) of $CCR3^+$ $CD4^+$ T lymphocytes ($CD45^+CD3^+CD4^+CCR3^+$ cells); and (G and H) $CCR3^+$ $CD8^+$ T lymphocytes ($CD45^+CD3^+CD8^+CCR3^+$ cells). Graphs representative of two experiments. Data are shown as mean ± SEM. Each symbol represents data of an individual mouse. *$p< 0.05$ when compared with the healthy, unchallenged control group. #$p<0.05$ when comparing different time points with day 2. ANOVA test followed by Bonferroni correction was used in the graphs with normal distribution. Otherwise, Kruskal-Wallis test was used. n=4

Next, we assessed the expression of CCR4. This receptor is also related with Th2 cells, but its expression spectrum is broader than that of CCR3 (261,277). In addition,

CCR4 expression is linked with the reduction of IFN-γ production by CD8⁺ T cells (278). Despite the lack of differences between the control and the challenged groups, we observed relatively high percentages of CD8⁺ and CD4⁺ T cells expressing CCR4 in BALF and lungs (Figure 18). In the lungs, there was an increase in CD8⁺ CCR4⁺ T cell percentage and MFI on day 2, returning to basal levels afterwards (Figure 18G, H).

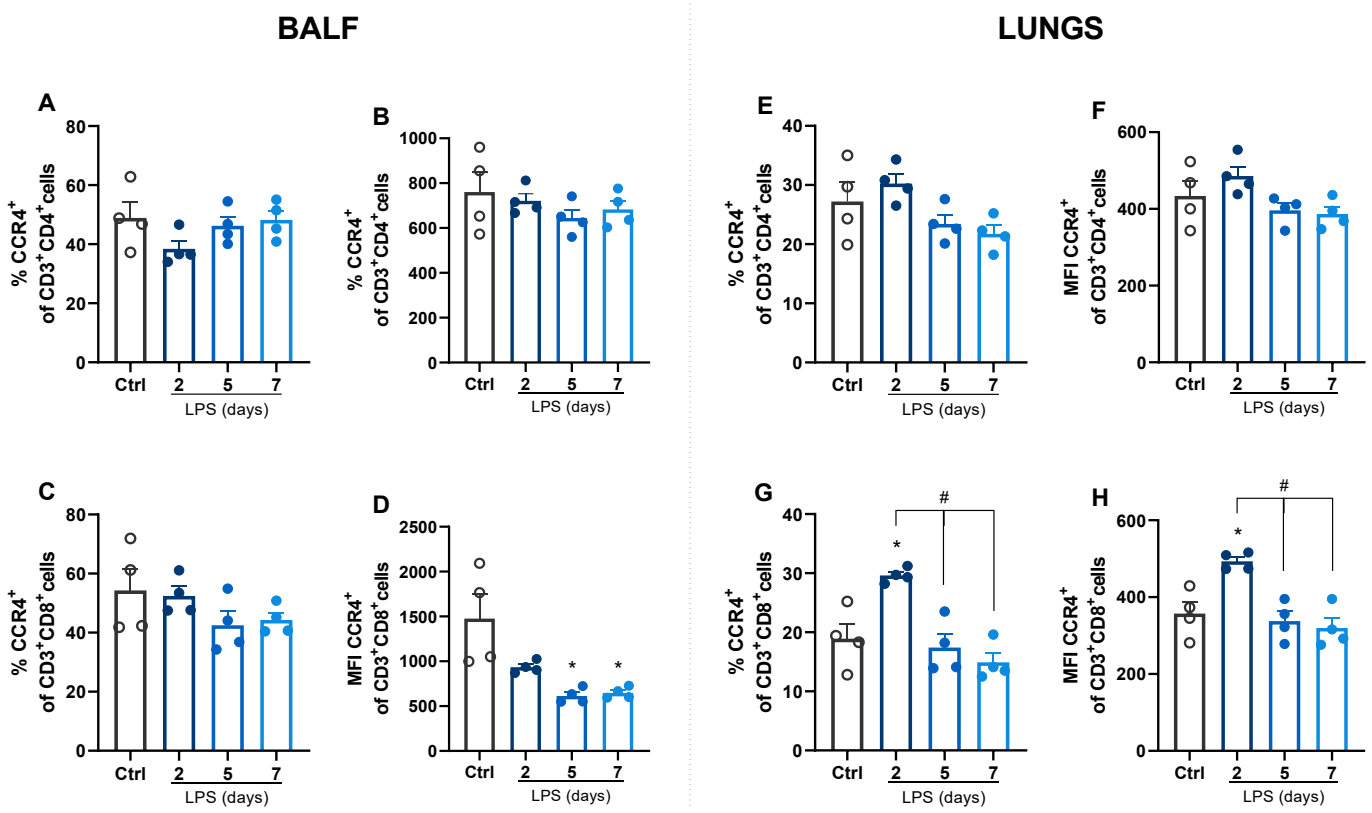

Figure 18 – Percentages and MFI of CCR4 expression in lymphocytes in BALF in ARDS. C57BL/6 mice were challenged with LPS (12.5 µg/mouse) or PBS (Ctrl group) intranasally and dissected at the indicated days. Percentage (A) and MFI (B) of CCR4⁺ CD4⁺ T lymphocytes (CD45⁺CD3⁺CD4⁺CCR4⁺ cells); and (C and D) CCR4⁺ CD8⁺ T lymphocytes (CD45⁺CD3⁺CD8⁺CCR4⁺ cells) were quantified on BALF by flow cytometry. Additionally, the flow cytometric analysis was performed on lung tissue: percentage (E) and MFI (F) of CCR4⁺ CD4⁺ T lymphocytes (CD45⁺CD3⁺CD4⁺CCR4⁺ cells); and (G and H) CCR4⁺ CD8⁺ T lymphocytes (CD45⁺CD3⁺CD8⁺CCR4⁺ cells) were quantified on lungs by flow cytometry. Graphs representative of two experiments. Data are shown as mean ± SEM. Each symbol represents data of an individual mouse. *p< 0.05 when compared with the healthy, unchallenged control group. #p<0.05 when

comparing different time points with day 2. ANOVA test followed by Bonferroni correction was used in the graphs with normal distribution. Otherwise, Kruskal-Wallis test was used. n=4

The last receptor that we evaluated, CCR5, is commonly linked with Th1 or activated T lymphocytes, as CXCR3 (261,276,279). As observed in Figure 18, there was some fluctuation in the percentages and MFI of $CD4^+$ $CCR5^+$ T cells, but no important differences were observed between the control and the challenged groups (Figure 19A, B, E, F). Regarding the $CD8^+$ T cells, CCR5 is important for the activation, response to cytokines, and migration of these cells (280). In our model, $CCR5^+$ $CD8^+$ T cells were almost absent in BALF and the CCR5 expression level was reduced in all the challenged groups (Figure 19C, D). In contrast, the number of $CCR5^+$ $CD8^+$ T cells almost doubled in lung tissue on day 2 but returned to basal levels at the later time points (Figure 19G, H).

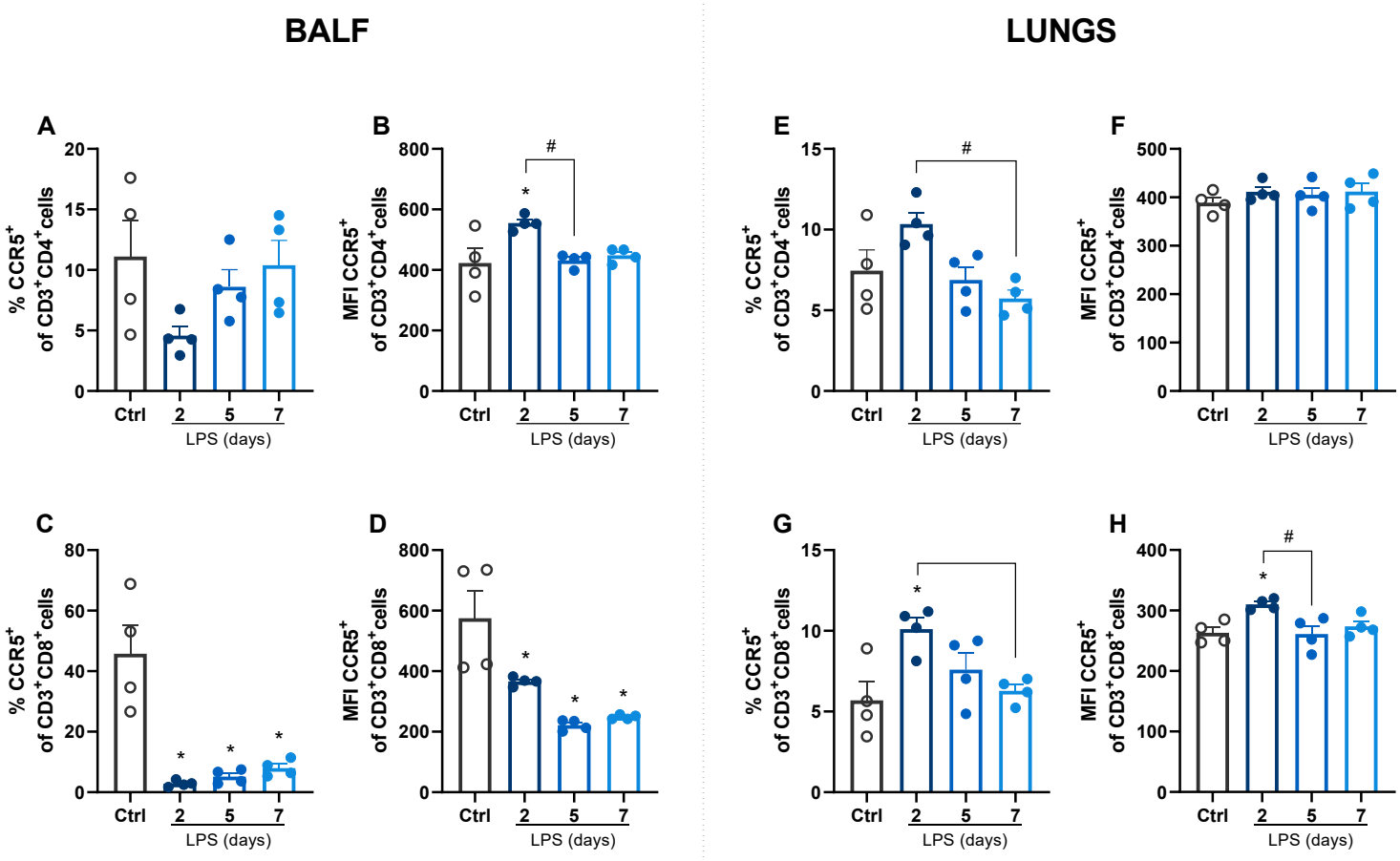

Figure 19 – Percentages and MFI of CCR5 expression in lymphocytes in BALF and lungs in ARDS. C57BL/6 mice were challenged with LPS (12.5 µg/mouse) or PBS (Ctrl group) intranasally and dissected at the indicated days. Percentage (A) and MFI (B) of $CCR5^+$ $CD4^+$ T lymphocytes ($CD45^+CD3^+CD4^+CCR5^+$ cells); and (C and D) $CCR5^+$ $CD8^+$ T lymphocytes ($CD45^+CD3^+CD8^+CCR5^+$ cells) were quantified on BALF by flow cytometry. Additionally, the flow cytometric analysis was performed on lung tissue: percentage (E) and MFI (F) of $CCR5^+$ $CD4^+$ T lymphocytes ($CD45^+CD3^+CD4^+CCR5^+$ cells); and (G and H) $CCR5^+$ $CD8^+$ T lymphocytes ($CD45^+CD3^+CD8^+CCR5^+$ cells). Graphs representative of two experiments. Data are shown as mean ± SEM. Each symbol represents data of an individual mouse. *$p< 0.05$ when compared with the healthy, unchallenged control group. #$p<0.05$ when comparing different time points with day 2. ANOVA test followed by Bonferroni correction was used in the graphs with normal distribution. Otherwise, Kruskal-Wallis test was used. n=4

3.2. PART II: ABSENCE OF CCR2 PROMOTES PROLIFERATION OF ALVEOLAR MACROPHAGES THAT CONTROL LUNG INFLAMMATION IN ACUTE RESPIRATORY DISTRESS SYNDROME IN MICE

3.2.1. *LACK OF CCR2 MODIFIES THE RECRUITMENT PROFILE OF MONOCYTES AND NEUTROPHILS IN EARLY TIME POINTS AFTER LPS INSTILLATION*

Before studying the role of CCR2 in the model of LPS-induced ARDS, we evaluated the levels of its ligand, CCL2, in the BALF of $CCR2^{+/+}$ and $CCR2^{-/-}$ mice and observed increased levels of this chemokine mainly on days 2 and 3 after the insult, but at remarkedly higher levels in $CCR2^{-/-}$ mice when compared to $CCR2^{+/+}$ mice (Figure 20A). Next, we analyzed the differences in inflammatory profile in lungs in both mice upon intranasal LPS challenge. Regarding cell accumulation, leukocyte numbers increased on days 1 to 3 after the LPS challenge, with higher total cell numbers in $CCR2^{-/-}$ mice, mostly neutrophils (Figure 20B, C). In contrast, $CCR2^{+/+}$ presented with a higher accumulation of macrophages derived from monocytes in the first two time points as compared to CCR2-deficient mice (Figure 20D). Interestingly, despite differences in the profile of cells accumulated in the lung at days 1 to 3, both strains had comparable numbers of cells at later time points, when the cell counts returned to the basal levels (from day four onwards). In order to evaluate the impact of those differences in cell influx on lung pathology, we analyzed the total protein concentration in the bronchoalveolar fluid to quantify pulmonary edema and the changes in body weight. However, there were no differences in those parameters between $CCR2^{+/+}$ and $CCR2^{-/-}$ mice during the whole period evaluated (Figure 20E, F), despite being clear that on the first 3 days after the challenge, both $CCR2^{+/+}$ and $CCR2^{-/-}$ mice had protein leakage into the alveolar space. Thus, we investigated other parameters to understand the impact of the differing leukocyte profile in the lungs on tissue inflammation.

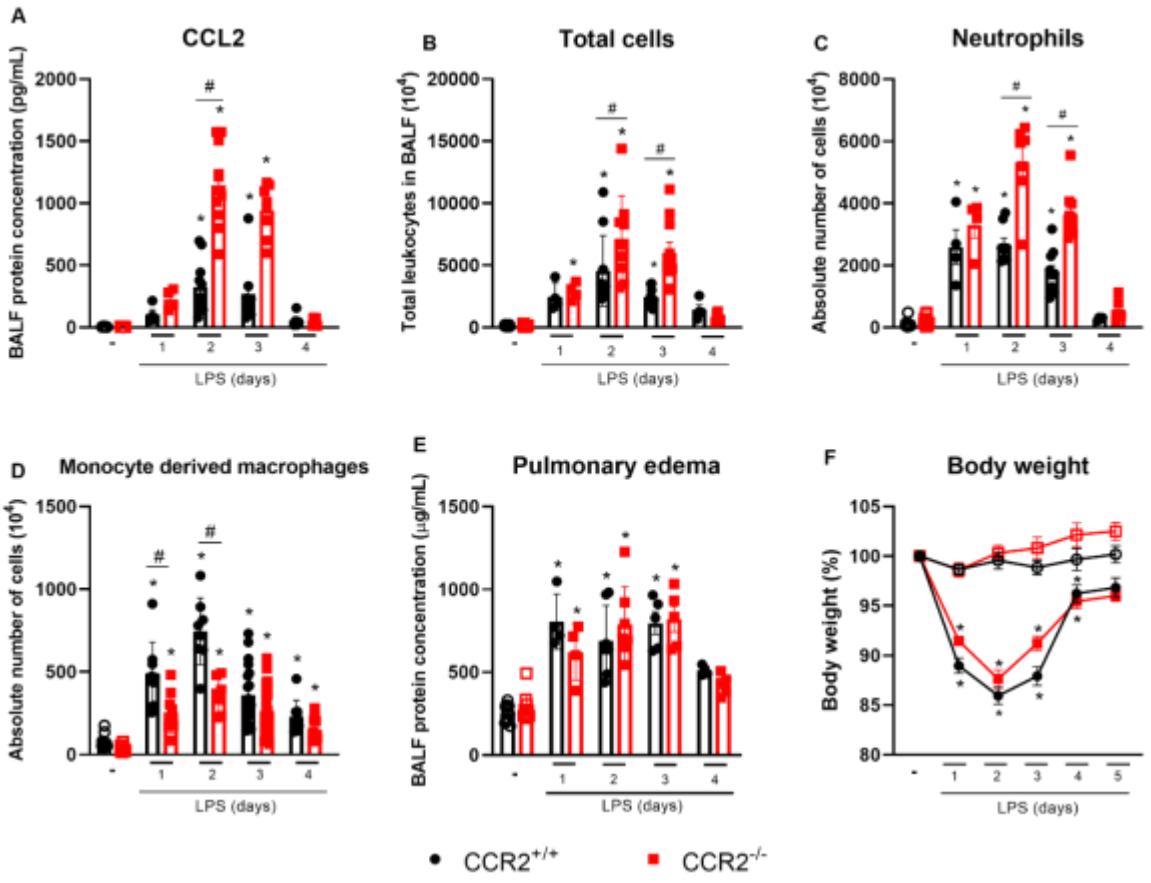

Figure 20 – CCR2 absence results in increased accumulation of neutrophils and decreased macrophage numbers in the lungs without affecting changes in inflammation, pulmonary edema, or weight loss. $CCR2^{+/+}$ (black symbols) and $CCR2^{-/-}$ (red symbols) C57BL/6 mice were challenged with LPS (12.5 µg/mouse) or PBS (ctrl group; -) and dissected at the indicated days. Levels of CCL2 (A) were measured in the BALF by ELISA. Absolute numbers of leukocytes in BALF (B) were counted in Bürker chamber. Absolute numbers of neutrophils ($CD45^+Ly6G^+CD11b^+$) (C) or macrophages ($CD45^+CD11b^+Ly6G^-CD3^-CD19^-$ $NKp46^-CD103^-$ $SiglecF^-MHCII^+CD11c^-$ cells) (D) isolated from the lungs and BALF were quantified by flow cytometry. Pulmonary edema was quantified based on the protein concentration in the BALF (E). Changes in body weight (F) were calculated with the weight before challenge (day 0) as a reference. Compilation of three experiments. Data are shown as mean ± SEM. Each symbol in panels A to E represents data of an individual mouse. *p< 0.05 when compared with the healthy, unchallenged control group. #p<0.05 when comparing wild type and knockout groups at the same time point. ANOVA test followed by Bonferroni correction was used in the graphs with normal distribution. Otherwise, Kruskal-Wallis test was used. n=6-12.

3.2.2. CYTOKINE PRODUCTION IN THE INITIAL PHASES OF INFLAMMATION IS ALTERED IN THE ABSENCE OF CCR2 BUT DOES NOT IMPACT THE TISSUE DAMAGE

Cytokines and chemokines were measured in BALF to better determine the inflammatory profile of this ARDS model in $CCR2^{+/+}$ and $CCR2^{-/-}$ mice. IFN-γ and TNF-α are important cytokines associated with tissue inflammation and damage caused by LPS. Both cytokines are increased in $CCR2^{+/+}$ mice, on day 2 after LPS insult for both and on day 3 only for IFN-γ (Figure 21A, B).

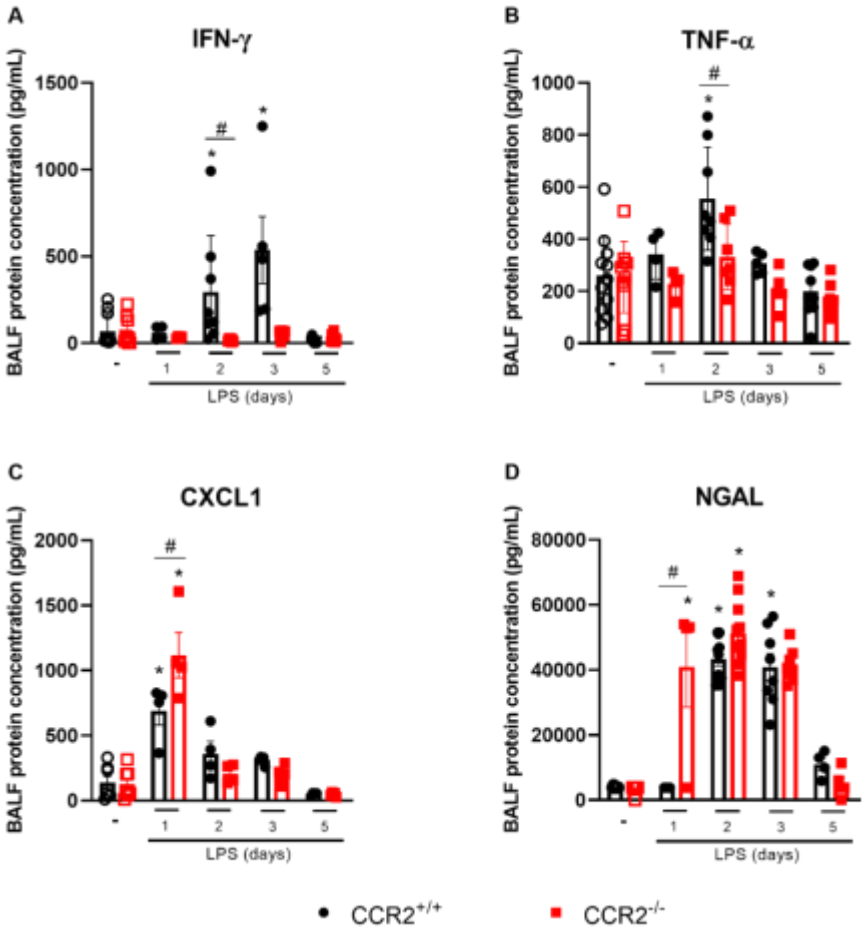

Figure 21 – CCR2 deficiency affects cytokine levels in the pro-inflammatory phase of the inflammation. $CCR2^{+/+}$ (black symbols) and $CCR2^{-/-}$ (red symbols) C57BL/6 mice were challenged with LPS (12.5 µg/mouse) or PBS (ctrl group; -) intranasally and dissected at the indicated days. Levels of IFN-γ (A), TNF-α (B), CXCL1 (C), and NGAL (D) were measured in the BALF by ELISA. Compilation of three experiments. Data are shown as mean ± SEM. Each symbol

represents data of an individual mouse. *p<0.05 when compared with the healthy, unchallenged control group. #p<0.05 when comparing wild type and knockout groups at the same time point. ANOVA test followed by Bonferroni correction was used in the graphs with normal distribution. Otherwise, Kruskal-Wallis test was used. n=4-12.

Of note, no increase in those cytokines was measured in CCR2-deficient mice at any of the time points evaluated. However, the level of CXCL1, an important chemokine related with neutrophil recruitment was increased in $CCR2^{-/-}$ mice already at day 1 (Figure 21C), which can explain the more pronounced accumulation of neutrophils in $CCR2^{-/-}$ mice (Figure 20C) when compared to $CCR2^{+/+}$ mice. Consequently, more neutrophil gelatinase-associated lipocalin (NGAL), a protein released specifically by activated neutrophils, was observed already very early in the absence of CCR2 (Figure 21D).

Despite the outspoken difference in cell accumulation and cytokine production, no significant alterations were detected in histology. Compared to healthy mice, both $CCR2^{+/+}$ and $CCR2^{-/-}$ mice presented higher histopathological scores on day 2 after LPS instillation, as observed in Figure 22. On day 5 after the challenge, the histopathological score is reduced for both mice, being comparable with the healthy control groups. Interestingly, $CCR2^{+/+}$ and $CCR2^{-/-}$ have similar results at every time point evaluated, suggesting that, despite the differences previously demonstrated at the peak of inflammation, the inflammatory response is resolved within the same time frame in both strains.

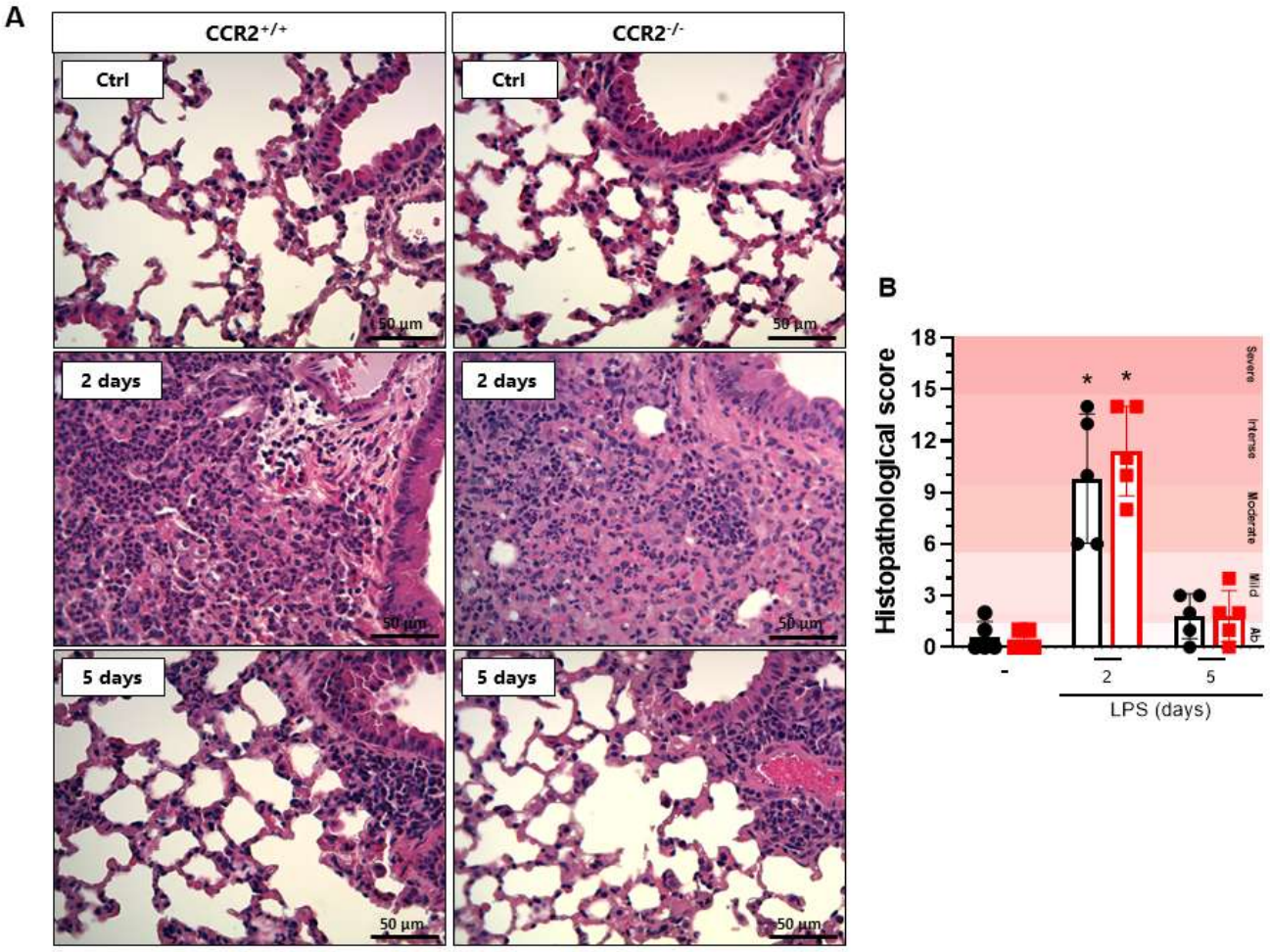

Figure 22 – CCR2-deficiency does not influence the histopathological score in CCR2$^{-/-}$ compared to CCR2$^{+/+}$ mice. CCR2$^{+/+}$ (black symbols) and CCR2$^{-/-}$ (red symbols) C57BL/6 mice were challenged with LPS (12.5 µg/mouse) or PBS (ctrl group; -) and dissected after 2 or 5 days. (A) Representative hematoxylin and eosin-stained preparations of lung tissue from mice. Scale bar: 50 µm, as reported in the figure. (B) Histopathological score with ranges of tissue damage (severe, intense, moderate, mild, or absent). Data are shown as mean ± SEM from one representative out of two independent experiments. Each symbol represents data of an individual mouse. *p<0.05 when compared with the healthy, unchallenged control group (Kruskal-Wallis with Dunn's multiple comparisons test). n=5.

3.2.3. THE PROFILE OF MONOCYTES/MACROPHAGES VARIES BETWEEN CCR2$^{+/+}$ AND CCR2$^{-/-}$ MICE

CCR2 is an important receptor for monocyte recruitment in the early stages of tissue inflammation. The accumulation of these cells in lung tissue directly contributes to increased inflammation, but the recruited cells also contribute to the end stages of inflammation, with crucial participation in the resolution of inflammation and tissue repair (246). Thus, we evaluated the profile of monocytes and macrophages at different time points after LPS-induced ARDS.

As expected, the absence of CCR2 prevented the vast accumulation of macrophages ($CD45^+CD11b^+Ly6G^-CD3^-CD19^-NKp46^-CD103^-SiglecF^-MHCII^+$ $CD11c^-$), inflammatory monocytes ($CD45^+CD11b^+SiglecF^-Ly6G^-CD3^-NKp46^-CD19^-CD103^-CD64^+Ly6C^+$), and IM ($CD45^+CD11b^+SiglecF^-Ly6G^-CD3^-NKp46^-CD19^-CD103^-CD64^+MHCII^+$) in CCR2$^{-/-}$ mice when compared to CCR2$^{+/+}$ mice at days 1 to 3 after the challenge (Figure 19D and Figure 23A, B). In contrast, the number of AM ($CD45^+SiglecF^+CD11c^+$) was significantly higher on days 3 and 4 in the CCR2-deficient mice compared to the CCR2$^{+/+}$ mice, which largely maintained the same AM counts along the whole duration of the experiment (Figure 23C).

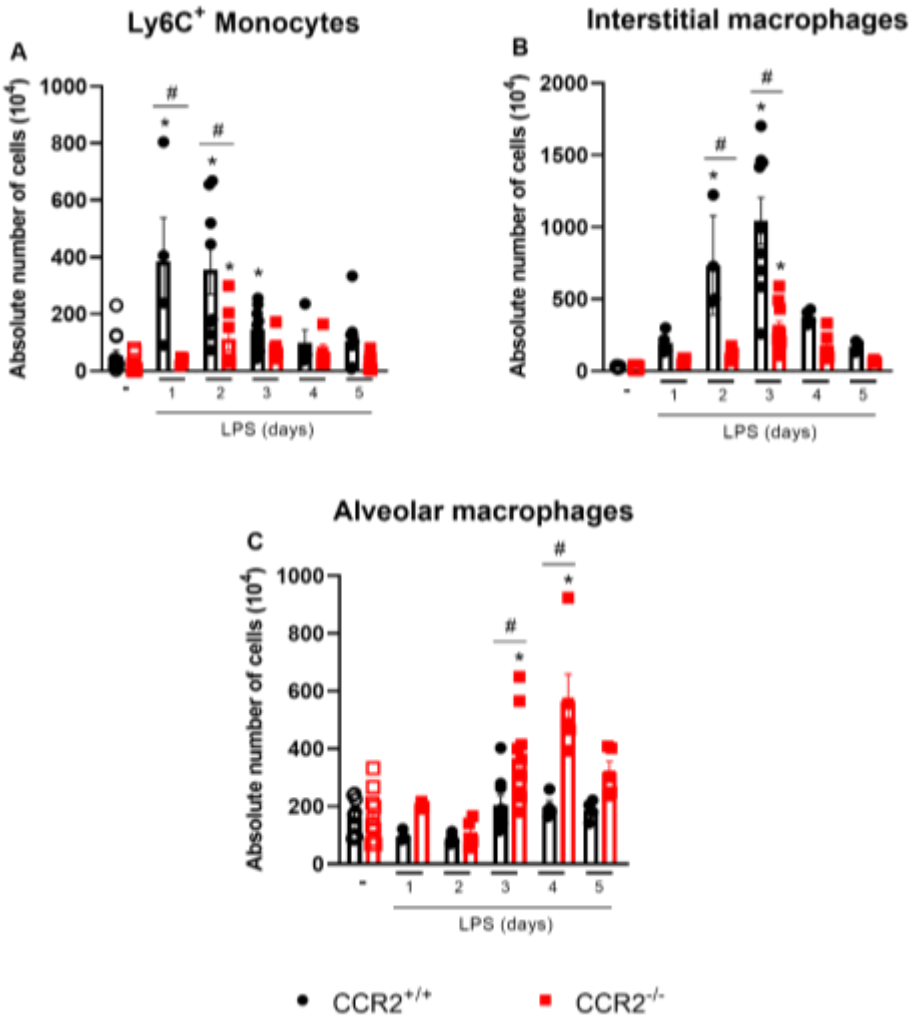

Figure 23 – Largely reduced numbers of Ly6C$^+$ monocytes and interstitial macrophages but increased alveolar macrophage counts are observed in CCR2$^{-/-}$ compared to CCR2$^{+/+}$ mice. CCR2$^{+/+}$ (black symbols) and CCR2$^{-/-}$ (red symbols) C57BL/6 mice were challenged with LPS (12.5 µg/mouse) or PBS (ctrl group; -) and dissected at the indicated days. Absolute numbers of Ly6C$^+$ monocytes (CD45$^+$CD11b$^+$SiglecF$^-$Ly6G$^-$Dump$^-$CD103$^-$MHCII$^-$Ly6C$^+$ cells) (A) IM (CD45$^+$CD11b$^+$SiglecF$^-$Ly6G$^-$Dump$^-$CD103$^-$MHCII$^+$ cells) (B) and AM (CD45$^+$SiglecF$^+$CD11c$^+$ cells) (C) were quantified by flow cytometry. Compilation of four experiments for graph A and three experiments for graphs B-C. Data are shown as mean ± SEM. Each symbol represents data of an individual mouse. *p<0.05 when compared with the healthy, unchallenged control group. #p<0.05 when comparing wild type and knockout groups at the same time point. ANOVA test followed by Bonferroni correction was used in the graphs with normal distribution. Otherwise, Kruskal-Wallis test was used. n=4-12.

Since there was a significant increase in the number of AM in the CCR2-deficient mice, the proliferation of these cells was evaluated. Two different assays were performed: the analysis of Ki-67 expression (Fig 24A, B) and the assessment of BrdU incorporation in the DNA (Fig 24C, D). Interestingly, the expression of Ki-67 in the AM was enhanced, and more AM expressed Ki-67 3 days after the LPS challenge. This effect was even more pronounced in the CCR2-deficient mice. In the $CCR2^{-/-}$ group, more BrdU had been incorporated at 3 and 4 days after the LPS challenge in the AM. These results indicate that the lack of CCR2 is linked to the increase in AM proliferation on days 3 and 4, time points associated with the reduction of neutrophils, and most likely the beginning of the resolution of inflammation.

To better elucidate the increase in cell proliferation, the most important growth factors for macrophages, granulocyte-macrophage colony-stimulating factor (GM-CSF) and macrophage colony-stimulating factor (M-CSF) (324), were measured in BALF (Figure 25). Interestingly, we only observed an increase of M-CSF level in BALF in $CCR2^{-/-}$ on day 3 (Figure 25B).

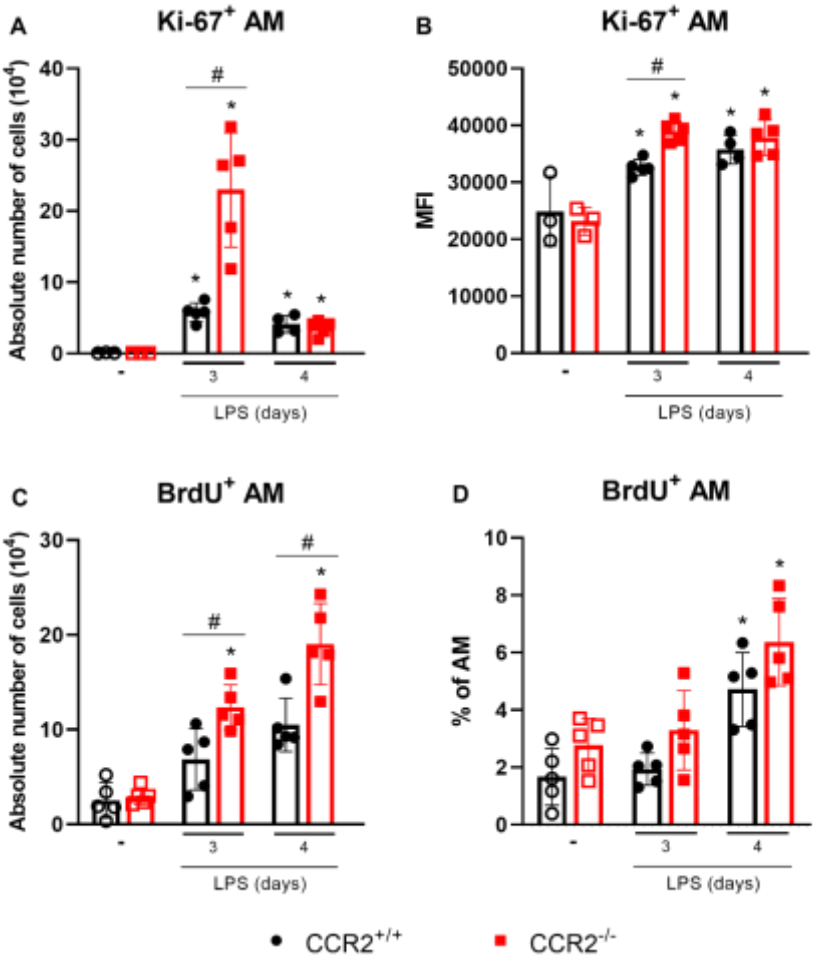

Figure 24 – CCR2$^{-/-}$ mice show increased proliferation of AM. CCR2$^{+/+}$ (black symbols) and CCR2$^{-/-}$ (red symbols) C57BL/6 mice were challenged with LPS (12.5 µg/mouse) or PBS (ctrl group; -) and dissected at the indicated days. (A) Absolute number of AM expressing Ki-67 was quantified by flow cytometry using the following markers: CD45^{+}CD11c^{+}SiglecF^{+}Ki-67^{+}. (B) Mean fluorescence intensity (MFI) of Ki-67 in AM. (C) Absolute number of BrdU^{+} AM was quantified by flow cytometry using the following markers: CD45^{+}CD11c^{+}SiglecF^{+}BrdU^{+}. (D) Percentage of BrdU^{+} AM. Data are shown as mean ± SEM from one representative out of two independent experiments. Each symbol represents data of an individual mouse. *p<0.05 when compared with the healthy, unchallenged control group (ANOVA test followed by Bonferroni correction). #p<0.05 when comparing wild type and knockout group at the same time point (ANOVA test followed by Bonferroni correction). n= 3-5.

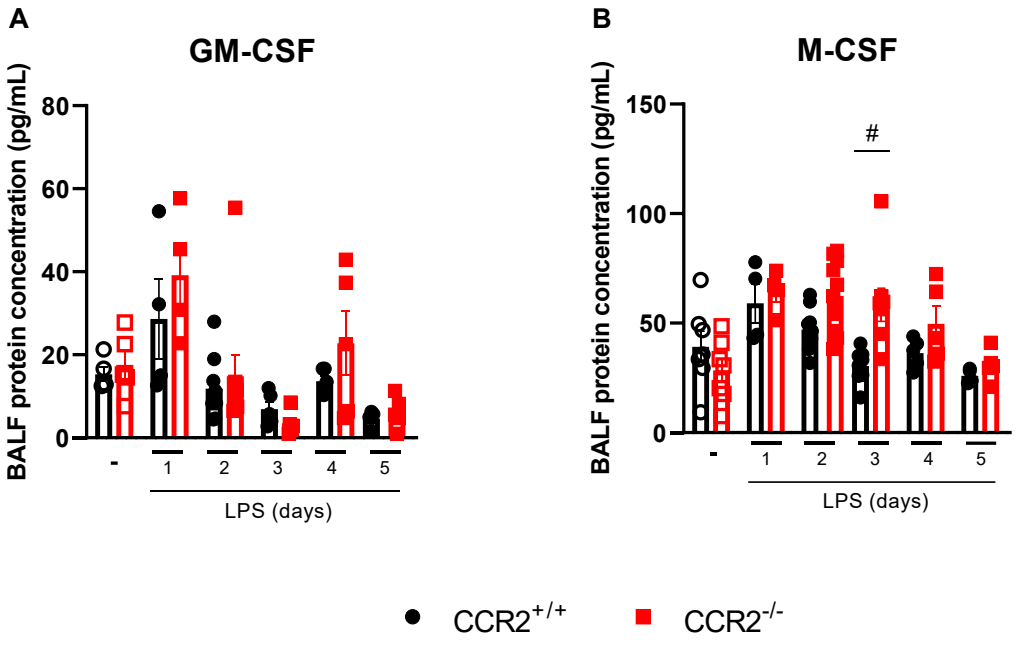

Figure 25 – Levels of GM-CSF and M-CSF in CCR2$^{+/+}$ and CCR2$^{-/-}$ mice. CCR2$^{+/+}$ and CCR2$^{-/-}$ C57BL/6 mice were challenged with LPS (12.5 µg/mouse) or PBS (ctrl group; -) intranasally and dissected at the indicated days. Levels of GM-CSF (A), and M-CSF (B) were measured in the BALF by ELISA. Data are shown as mean ± SEM. #p<0.05 when comparing wild type and knockout groups at the same time point. ANOVA test followed by Bonferroni correction was used in the graphs with normal distribution. Otherwise, Kruskal-Wallis test was used. n=4-12.

3.2.4. AM CAN BE ASSOCIATED WITH THE FINAL EVENTS OF TISSUE INFLAMMATION AND ITS RESOLUTION IN THE ABSENCE OF CCR2

Different parameters are associated with the resolving phase of acute inflammation, such as the polarization of macrophages to an M2 profile and the production of pro-resolving mediators. Analysis of the expression of CD206, a marker indicative of M2-polarization in macrophages, showed that the numbers of AM were enhanced after 3 days in CCR2$^{+/+}$ and CCR2$^{-/-}$ mice. Mice deficient for CCR2 had even more AM expressing CD206 at day 4 after the LPS stimulation compared to CCR2$^{+/+}$ mice (Figure 26A). In contrast, AM expressing NOS2, a marker for M1 polarization of macrophages, were decreased in the absence of CCR2 (Figure 26B). Confirming these results, the ratio of

NOS2 over Arg1 mRNA expression was significantly reduced in the lungs of mice deficient for CCR2 (Figure 26C). At day 3, the deficiency of CCR2 also led to increased protein levels of TGF-β and CCL22 compared to the wild-type mice (Figure 26D, E). TGF-β is an important cytokine related with the resolution of inflammation that is able to induce apoptosis of leukocytes (325). Both TGF-β and CCL22 are differentially produced by M2 macrophages (326,327).

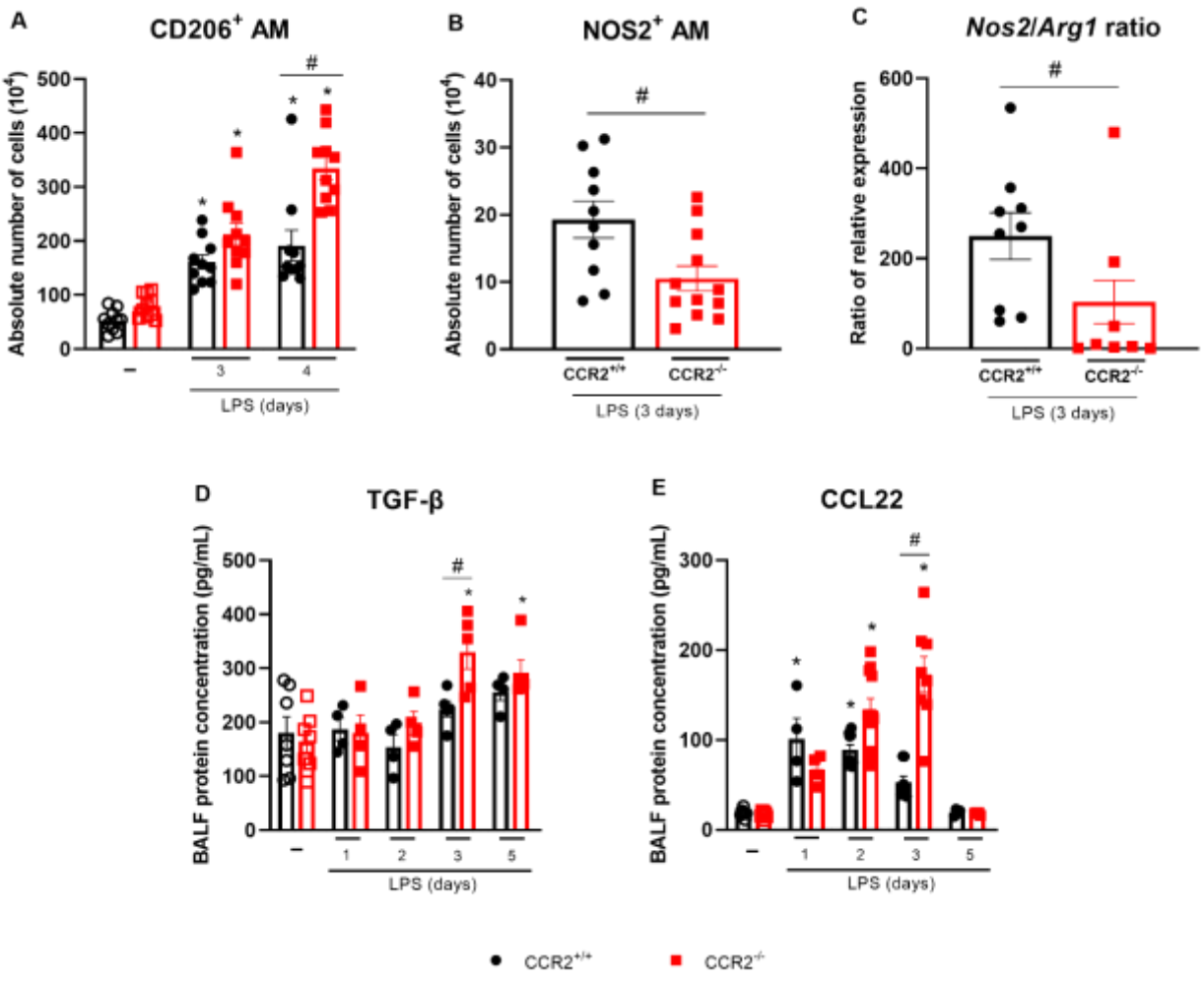

Figure 26 – CCR2 deficiency is associated with the increase of molecules related with M2 macrophages. $CCR2^{+/+}$ (black symbols) and $CCR2^{-/-}$ (red symbols) C57BL/6 mice were challenged with LPS (12.5 µg/mouse) or PBS (ctrl group; -) and dissected at the indicated days. Absolute numbers of $CD206^{+}$ AM ($CD45^{+}CD11c^{+}SiglecF^{+}CD206^{+}$ cells) (A) and $iNOS^{+}$ AM ($CD45^{+}CD11c^{+}SiglecF^{+}iNOS^{+}$ cells) (B) quantified by flow cytometry. (C) Ratio of NOS2 and Arginase mRNA expression relative to the endogenous control. Levels of TGF-β (D) and CCL22

(E) in BALF quantified by ELISA. Compilation of three experiments in panels A, D, and E; and two experiments in panels B and C. Data are shown as mean ± SEM. Each symbol represents data of an individual mouse. *p<0.05 when compared with the healthy, unchallenged control group. #p<0.05 when comparing wild type and knockout groups at the same time point. ANOVA test followed by Bonferroni correction was used in the graphs with normal distribution. Otherwise, Kruskal-Wallis test was used. Mann-Whitney U test was used in panels B and C. n=4-12.

Three days after the LPS challenge, CCR2$^{-/-}$ mice expressed more Siglec5 and Mrc1, i.e., mRNAs associated with AM and M2 macrophages, respectively (Figure 27A, B). In contrast, these mice had fewer IL-1b and IL-12b mRNA transcripts on the third day, suggesting that they contained reduced M1 macrophage numbers (Figure 27C, D). Therefore, the absence of CCR2 is associated with the increase of AM expressing CD206, the increase of other M2 markers in the lungs/BALF (Mrc1, CCL22, and TGF- β), and a reduction of M1 markers (NOS2, IL-1b, IL-12b).

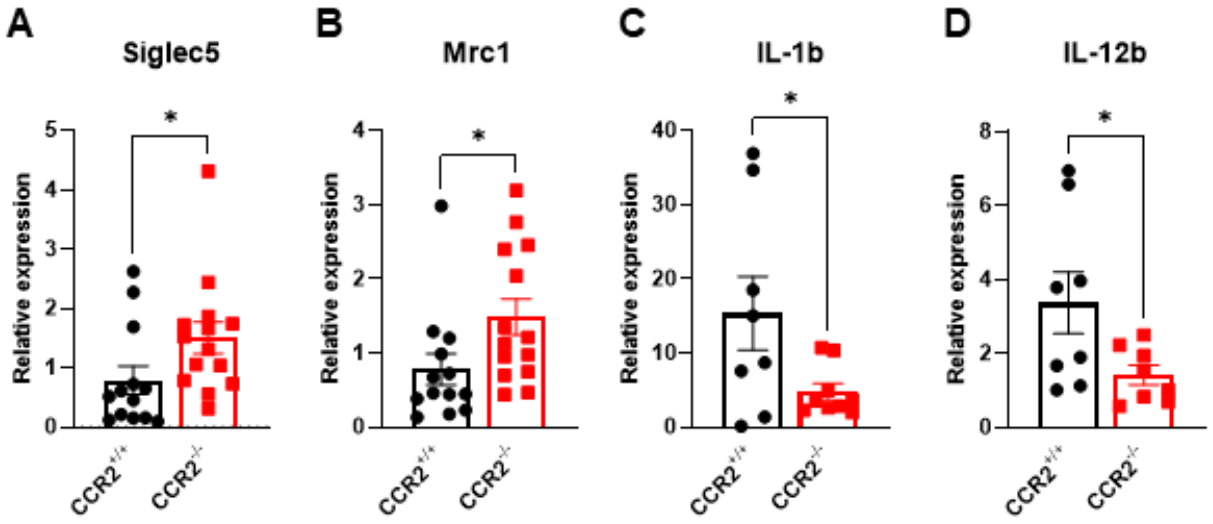

Figure 27 – Expression of macrophage-associated genes in the lungs of CCR2$^{+/+}$ and CCR2$^{-/-}$ mice. CCR2$^{+/+}$ and CCR2$^{-/-}$ C57BL/6 mice were challenged with LPS (12.5 µg/mouse). 3 days post-instillation, the lungs were removed, and the expression of (A) Siglec5, (B) Mrc1, (C) IL-1b, and (D) IL-12b was determined using qPCR. Results are represented as gene expression relative to lungs that were not instilled with LPS. Statistical differences were determined using Mann-Whitney U tests (A-C) or unpaired t-test (D) (*p <0.05).

3.2.5. DEPLETION OF AM BEFORE THE LPS CHALLENGE LEADS TO UNCONTROLLED INFLAMMATION WHICH IS WORSENED IN THE ABSENCE OF CCR2

To further demonstrate the role of AM in the absence of CCR2, $CCR2^{+/+}$ and $CCR2^{-/-}$ mice were treated with clodronate-loaded liposomes. As observed in Figures 28A and B, the depletion of AM was successful since the percentage and absolute numbers of this specific cell population were reduced. Depletion triggered an increase in the number of total leukocytes and neutrophils in the alveolar space in both $CCR2^{+/+}$ and $CCR2^{-/-}$ mice at 4 days after the LPS challenge (Figure 28C and D). Interestingly, more leukocytes were detected in $CCR2^{-/-}$ compared to $CCR2^{+/+}$ mice. To evaluate the impact of alveolar macrophage depletion on lung pathology, we analyzed the total protein concentration in the bronchoalveolar fluid to quantify pulmonary edema. Figure 28E shows that both $CCR2^{+/+}$ and $CCR2^{-/-}$ mice had more pulmonary edema after the depletion, but that the inflammatory insult had still more impact in $CCR2^{-/-}$ mice on day 4, probably because the resolution of inflammation is delayed in those mice. Lastly, we evaluated the changes in body weight and, while its reduction was observed in all the groups during the course of the inflammation, only the mice treated with clodronate-loaded liposomes were not able to recover and still weighed significantly less on day 4 (Figure 28F).

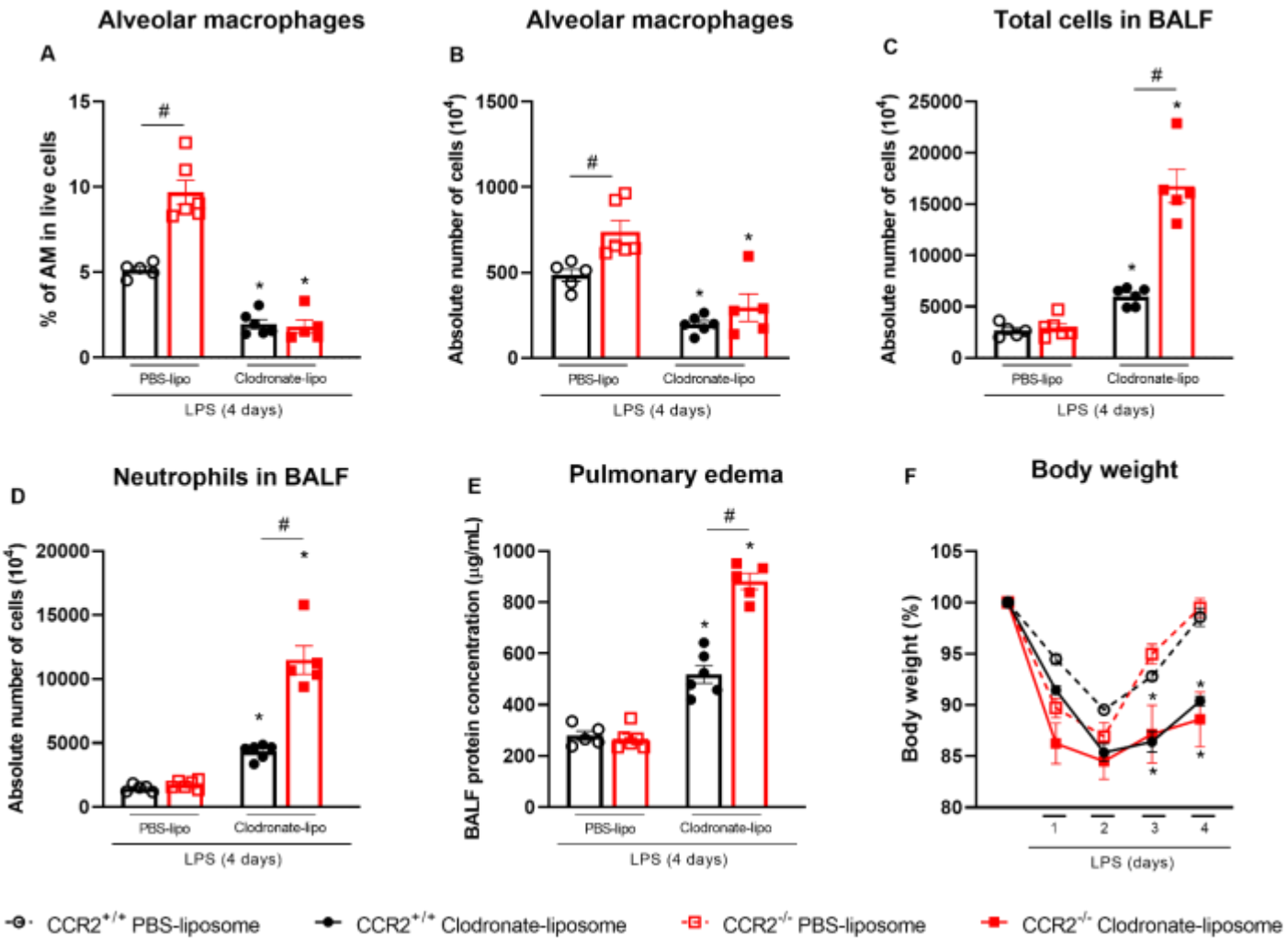

Figure 28 – Depletion of AM leads to worsened inflammation especially in CCR2$^{-/-}$ mice. CCR2$^{+/+}$ (black symbols) and CCR2$^{-/-}$ (red symbols) C57BL/6 mice were treated intranasally with liposomes loaded with clodronate or PBS. One day later, they were challenged with LPS (12.5 µg/mouse) and dissected after 4 days. Percentage (A) and absolute numbers (B) of AM (CD45^{+}CD11c^{+}SiglecF^{+} cells) isolated from the lungs and BALF were quantified by flow cytometry. Absolute numbers of leukocytes (C) and neutrophils (D) in BALF were measured by microscope count. Pulmonary edema was quantified based on the protein concentration in the BALF (E). Changes in body weight (C) were calculated with the weight before challenge (day 0) as reference. Data are shown as mean ± SEM. Each symbol represents data of an individual mouse. *p<0.05 when compared with the respective group treated with PBS-loaded liposomes. #p<0.05 when comparing wild type and knockout group treated with Clodronate-loaded liposomes. Mann-Whitney U test was used. n=5-6.

3.3. PART III: EFFECT OF TREATMENT WITH THE GAG-BINDING CHEMOKINE FRAGMENT CXCL9(74–103) IN MURINE MODELS OF PNEUMONIA

3.3.1. TIME-COURSE OF S. AUREUS-INDUCED PNEUMONIA MICE MODEL

S. aureus-induced pneumonia is characterized by a massive influx of cells, mainly neutrophils, into the lungs, which is essential to control the bacterial load, but may cause severe tissue damage (187). Blocking chemokine binding to GAGs can be used as a strategy to reduce the cell migration to control tissue inflammation. In this sense, the treatment with CXCL9(74-103) is able to reduce the recruitment of neutrophils in different models of acute inflammation (131,371,372). It is therefore interesting to study this peptide in our bacterial infection model because it has great potential to reduce the troubles of uncontrolled inflammation. To be able to make a well-considered decision on the best time points for treatment and euthanasia, we first studied the time course of this infection.

In the first time point evaluated, 12 h after the infection, there was a relevant increase in cells, mainly neutrophils but also mononuclear cells, accumulating in the BALF (Figure 29A-C). The numbers of neutrophils were high during the whole period analyzed (Figure 29B). In contrast, mononuclear cells had even higher counts later, at 48 h. In addition to cell accumulation in BALF, we evaluated the changes in body weight (Figure 29D) and the bacterial load in BALF and lungs (Figure 29E, F). Twelve h after the infection, the animals had a major decrease in body weight that was sustained at 24 h, but self-limited and reversed at 48 h. Accordingly, the bacterial load in BALF and lungs was already strongly reduced at 48h after infection. It should be noted that the number of bacteria in the lungs was higher than in the BALF (Figure 29E), which can probably be explained by the high number of adhesion molecules produced by *S. aureus* that ensure its adhesion to the tissue (373). Therefore, we concluded that the peak of inflammation in this model is around 12 to 24 h and that the resolution of inflammation starts after 48 h, based on the increase in mononuclear cells, the body weight, and the bacterial load. Consequently, we decided to stablish the time point of 24 h to investigate the anti-inflammatory effect of CXCL9(74-103) peptide in this model.

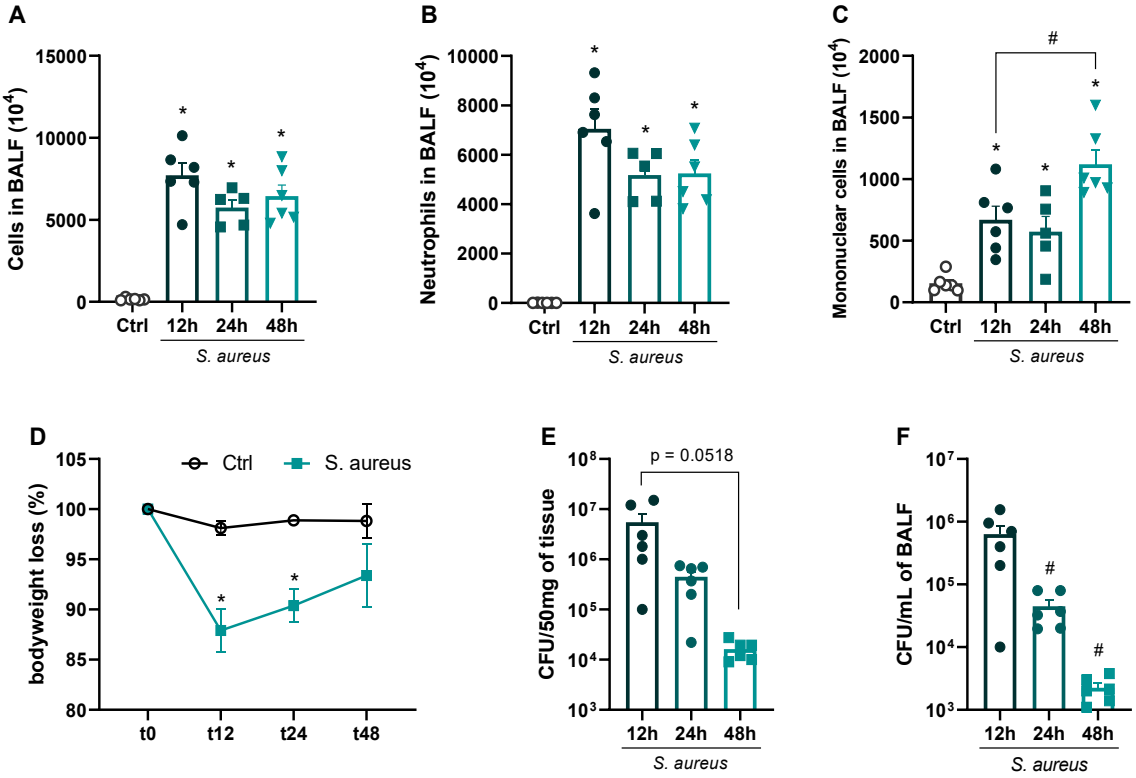

Figure 29 – *S. aureus* infection kinetics. C57BL/6 mice were infected with *S. aureus* (10^8 CFU/mouse) or saline (Ctrl group) and dissected at the indicated time intervals. (A) Numbers of leukocytes in BALF were counted in Bürker chambers. Neutrophils (B) or mononuclear cells (C) in BALF were differentially counted in cytospin slides. Changes in body weight (D) were calculated with the weight before infection (day 0) as reference. Bacterial load was measured in the lungs (E) and BALF (F). Data are shown as mean ± SEM. Each symbol in panels A-C, E, and F represents data of an individual mouse. *p< 0.05 when compared with the healthy, unchallenged control group. #p<0.05 when comparing different time points with 12 h. ANOVA test followed by Bonferroni correction was used in the graphs with normal distribution. Otherwise, Kruskal-Wallis with Dunn's multiple comparisons test was used. n=5-6.

3.3.2. CXCL9(74-103) TREATMENT IMPROVES THE ACCUMULATION OF CELLS IN BALF AND LUNG ELASTICITY BUT DOES NOT AFFECT OTHER INFLAMMATORY PARAMETERS IN THE S. AUREUS-INDUCED PNEUMONIA MICE MODEL

CXCL9(74-103) is a GAG-binding peptide that competes with chemokines for display on the GAGs of the vessel wall, which leads to the reduction in chemokine-directed neutrophil recruitment (129,131). In our experimental bacterial pneumonia model,

CXCL9(74-103) treatment starting at 6 or 12 h after the infection with *S. aureus* reduced the numbers of total cells (Figure 30A) and neutrophils in BALF (Figure 30B) and improved the clinical score (Figure 30D). In contrast, the treatment did not decrease the number of mononuclear cells (Figure 30C), the concentration of protein in BALF (Figure 30E), nor the bacterial load in BALF and lungs (Figure 30F, G). In fact, the bacterial load in BALF was increased in the group treated 6 h after the infection (Figure 30G), but an additional experiment should be performed to confirm this rather surprising finding.

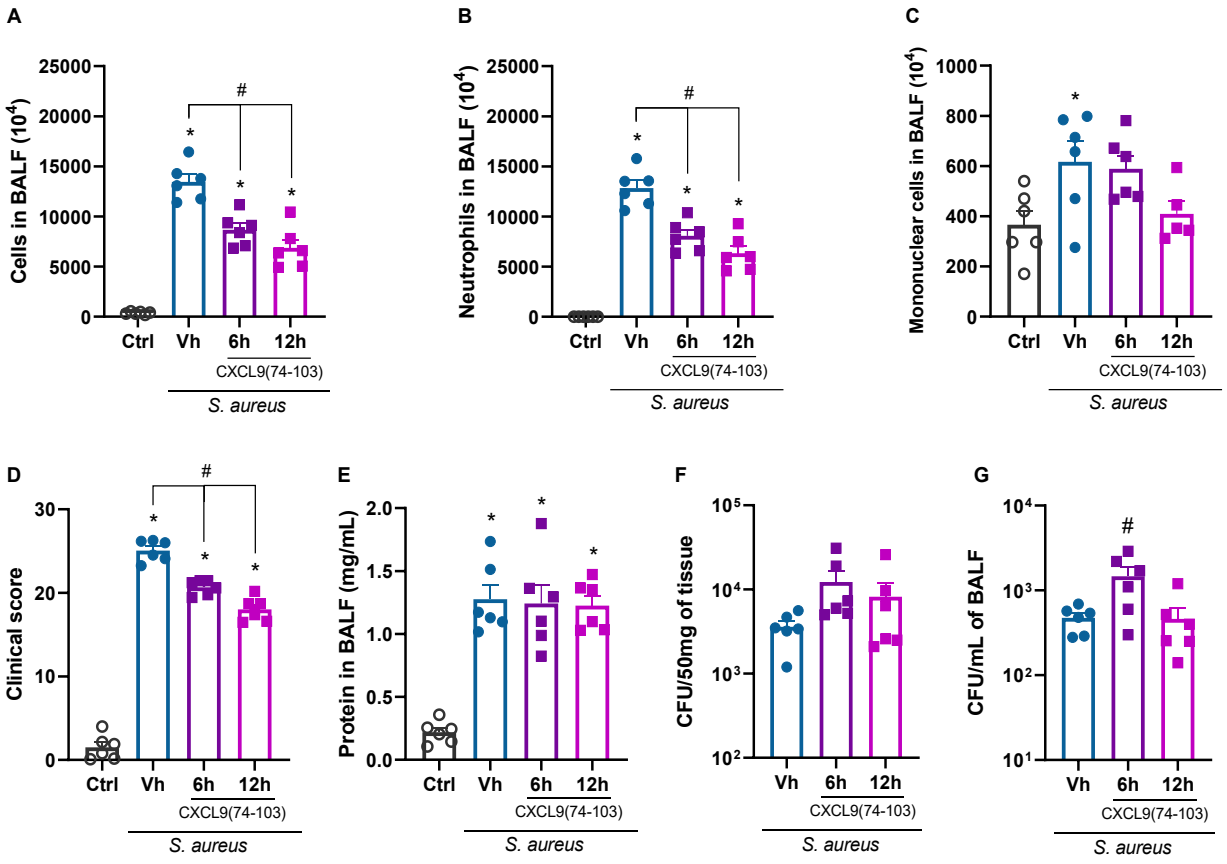

Figure 30 – CXCL9(74-103) treatment reduces several inflammatory parameters in *S. aureus* infection. C57BL/6 mice were infected with *S. aureus* (10^8 CFU/mouse) or saline (Ctrl group) and dissected 24 h later. At the indicated times after the challenge, mice were treated with CXCL9(74-103). (A) Numbers of leukocytes in BALF were differentially counted in Bürker chambers. Neutrophils (B) or mononuclear cells (C) in BALF were counted in cytospin slides. Clinical score (D) was calculated based on observational parameters and changes in body weight. The concentration of protein in BALF was measured to assess pulmonary edema (E). Bacterial load

was measured in the lungs (F) and BALF (G). Data are shown as mean ± SEM. Each symbol represents data of an individual mouse. *p< 0.05 when compared with the healthy, unchallenged control group. #p<0.05 when comparing different time points with the vehicle. ANOVA test followed by Bonferroni correction was used in the graphs with normal distribution. Otherwise, Kruskal-Wallis with Dunn's multiple comparisons test was used. n=6.

The accumulation of neutrophils observed in bacterial infection is usually associated with high levels of pro-inflammatory mediators. Besides the recruitment of additional immune cells, such as neutrophils and macrophages, cytokines and chemokines dictate the pace of inflammation because they are indispensable in the activation of the leukocytes (374). To better understand the inflammation and the mechanisms behind the CXCL9(74-103) effect, we measured some cytokines that are important in *S. aureus* infection (375). Interestingly, the treatment was not able to alter the levels of CXCL1 (Figure 31A), IL-1β (Figure 31B), IL-6 (Figure 31C), and TNF-α (Figure 31D) in BALF and the levels of CXCL1 (Figure 31E), IL-1β (Figure 31F), and TNF-α (Figure 31G) in lungs. Thus, despite the changes in cell accumulation, the cytokines evaluated were not affected by CXCL9(74-103) and are not related with its molecular mechanisms.

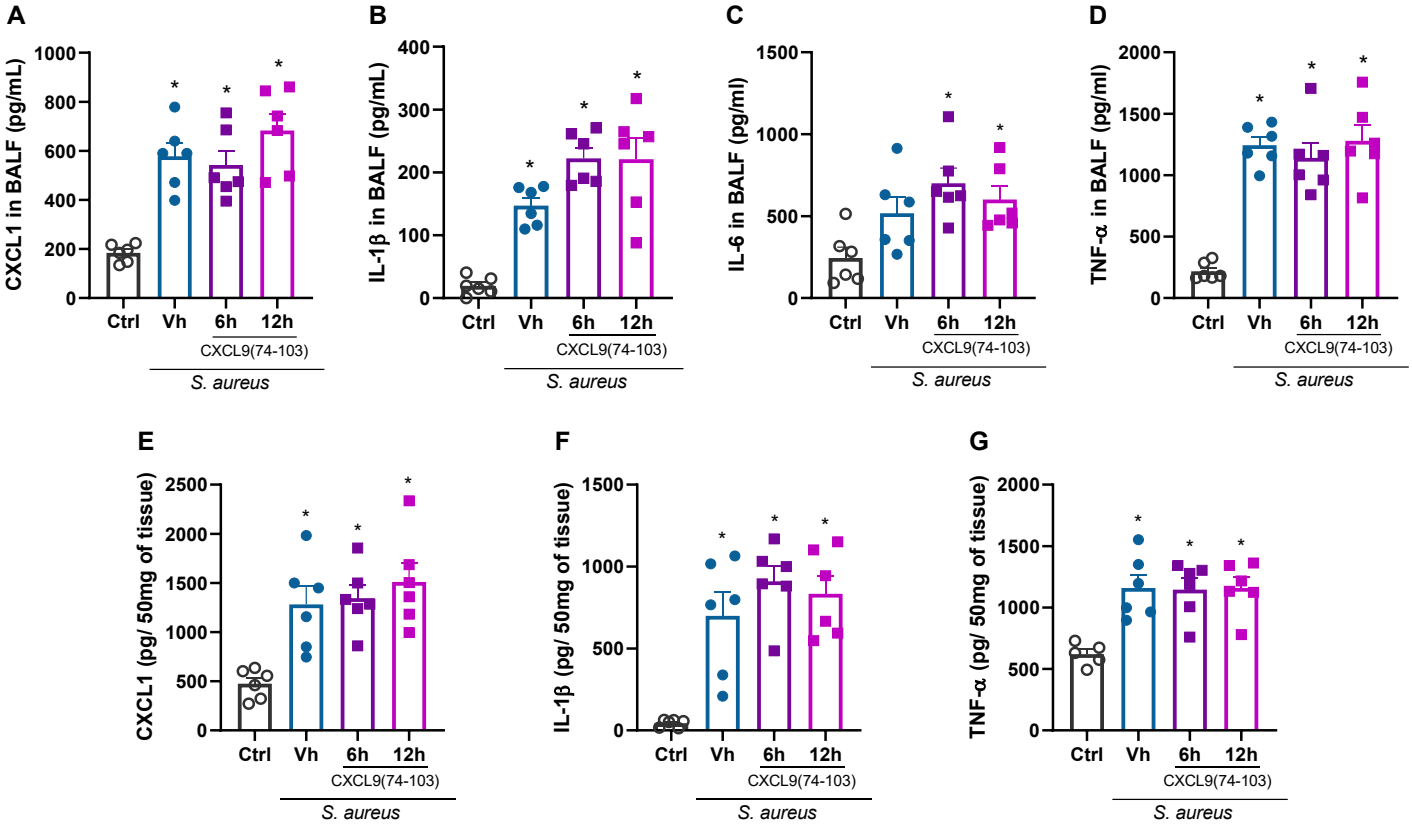

Figure 31 – CXCL9(74-103) treatment does not affect the levels of cytokines in *S. aureus* infection. C57BL/6 mice were infected with *S. aureus* (10^8 CFU/mouse) or saline (Ctrl group) and dissected 24 h later. At the indicated times after the challenge, mice were treated with CXCL9(74-103). Levels of CXCL1 (A), IL-1β (B), IL-6 (C), and TNF-α (D) were measured in BALF by ELISA. Levels of CXCL1 (E), IL-1β (F), and TNF-α (G) were measured in the lungs by ELISA. Data are shown as mean ± SEM. Each symbol represents data of an individual mouse. *p< 0.05 when compared with the healthy, unchallenged control group. ANOVA test followed by Bonferroni correction was used in the graphs with normal distribution. Otherwise, Kruskal-Wallis with Dunn's multiple comparisons test was used. n=6.

Additionally, we assessed the pulmonary mechanic function to evaluate whether CXCL9(74-103) could prevent the loss of elasticity and the reduction in pulmonary volumes and airway flow caused by *S. aureus* infection. As observed in Figure 32, the only parameter that improved by the treatment was the lung elasticity (Figure 32A), while the lung volumes (Figure 32B), and the airway flow (Figure 32C) are not different from the untreated, vehicle group.

It is known that the excess of leukocytes has an important role in lung tissue damage. Even so, despite the obvious reduction in cell recruitment after CXCL9(74-103) treatment, this was not enough to reverse the damage caused by the infection and the initial inflammatory response (Figure 33). In the histology preparations of lung tissue, intense inflammatory infiltrates and the destruction of lung structures can be observed in all infected groups (Figure 33A). Lung inflammation was also quantified and expressed as histopathological score and histopathological damage (Figure 33B, C).

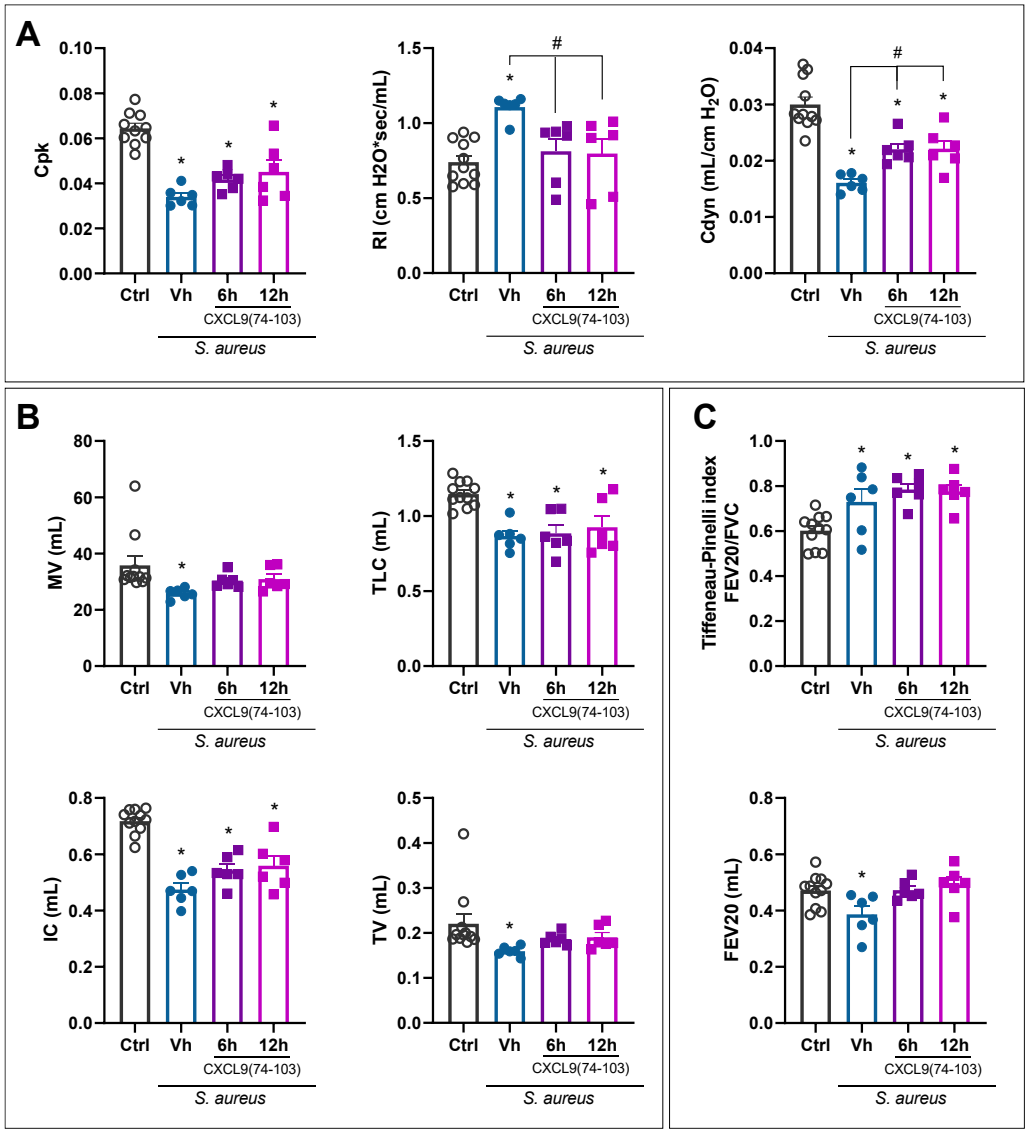

Figure 32 – CXCL9(74-103) treatment only improves the lung elasticity in *S. aureus* infection. C57BL/6 mice were infected with *S. aureus* (10^8 CFU/mouse) or saline (Ctrl group) and dissected 24 h later. Right before euthanasia, pulmonary mechanic functions were assessed. At the indicated times after the challenge, mice were treated with CXCL9(74-103). Invasive forced spirometry was performed to investigate functional modifications in pulmonary mechanics. The assessed parameters were (A) Lung elasticity represented by Peak of Compliance (Cpk), Lung Resistance (RI), and Dynamic Compliance Forced (Cdyn); (B) Lung volumes by Minute Volume (MV), Total Lung Capacity (TLC), Inspiratory Capacity (IC), and Tidal Volume (TV); (C) Airway flow by Tiffeneau-Pinelli index (FEV20/FVC) and Forced Expiratory Volume at 20 ms (FEV20). Data are shown as mean ± SEM. Each symbol represents data of an individual mouse. *p< 0.05 when compared with the healthy, unchallenged control group. #p<0.05 when comparing different

treatment groups with the vehicle. ANOVA test followed by Bonferroni correction was used in the graphs with normal distribution. Otherwise, Kruskal-Wallis with Dunn's multiple comparisons test was used. n=6-12.

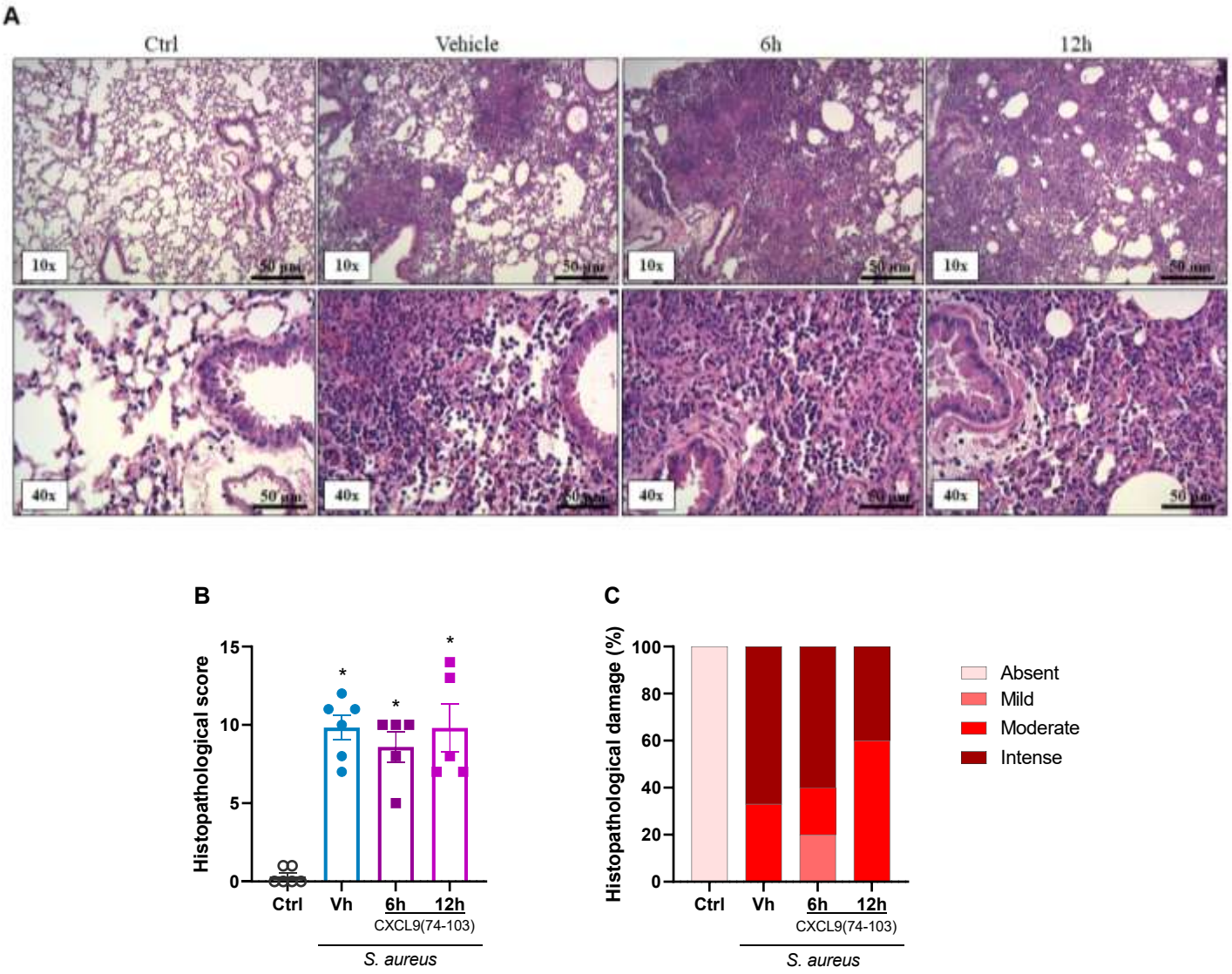

Figure 33 – CXCL9(74-103) does not affect the tissue damage in *S. aureus* infection. C57BL/6 mice were infected with *S. aureus* (10^8 CFU/mouse) or saline (Ctrl group) and dissected 24 h later. At the indicated times after the challenge, mice were treated with CXCL9(74-103). (A) Representative hematoxylin and eosin-stained preparations of lung tissue from mice. Scale bar: 50 µm, as reported in the figure. (B) Histopathological score and (C) Contingency graph according to ranges of tissue damage (severe, intense, moderate, mild, and absent). Data are shown as mean ± SEM in panel B. *p< 0.05 when compared with the healthy, unchallenged control group.

ANOVA test followed by Bonferroni correction was used in the graphs with normal distribution. Otherwise, Kruskal-Wallis with Dunn's multiple comparisons test was used. n=5-6.

3.3.3. CXCL9(74-103) TREATMENT IMPROVES SEVERAL INFLAMMATORY PARAMETERS IN THE MHV-3 INDUCED PNEUMONIA MOUSE MODEL

The murine model using MHV-3 was previously standardized by Andrade et al (77) and, based on the concentration-response and the time course observed in that work, we challenged the mice with 3×10^3 PFU/mouse and they were euthanized 3 days later, at the peak of pulmonary infection. Due to the lack of stability of CXCL9(74-103), the treatment was done twice a day and started immediately before the challenge (0h group) or 12 h after viral instillation (12h group). Additionally, the animals were monitored daily for changes in posture, appearance, and body weight, but only the body weight was affected by the infection. Therefore, it was used as a parameter to evaluate the clinical features of this model.

As observed in Figure 35, compared to control animals, mice infected with MHV-3 and treated with vehicle (Vh) lost body weight, and their BALF contained more neutrophils and proteins than the control group, demonstrating that the virus is able to induce lung inflammation. In addition, we can confirm that the infection was established in the lungs, since it was possible to recover around 10^2 PFU/g of MHV-3 virus in the lung tissue (Figure 34). Regarding the CXCL9(74-103) treatment, we observed that the total number of cells in BALF is reduced in the 12h group (Figure 34A), while neutrophils are decreased in both treated groups (Figure 34B). Mononuclear cells are not affected by the infection nor the treatment, (Figure 34C) indicating the key role of neutrophils in the inflammation. In addition to the recruitment of cells, CXCL9(74-103) treatment starting at 12 h can also decrease the bodyweight loss (Figure 34D) and does not increase the leakage of proteins to the alveolar space when compared to the control group (Figure 34E), as opposed to the untreated group. Lastly, all the changes observed in the treated groups were not reflected in the viral load, as this is not positively or negatively affected by CXCL9(74-103) (Figure 34E).

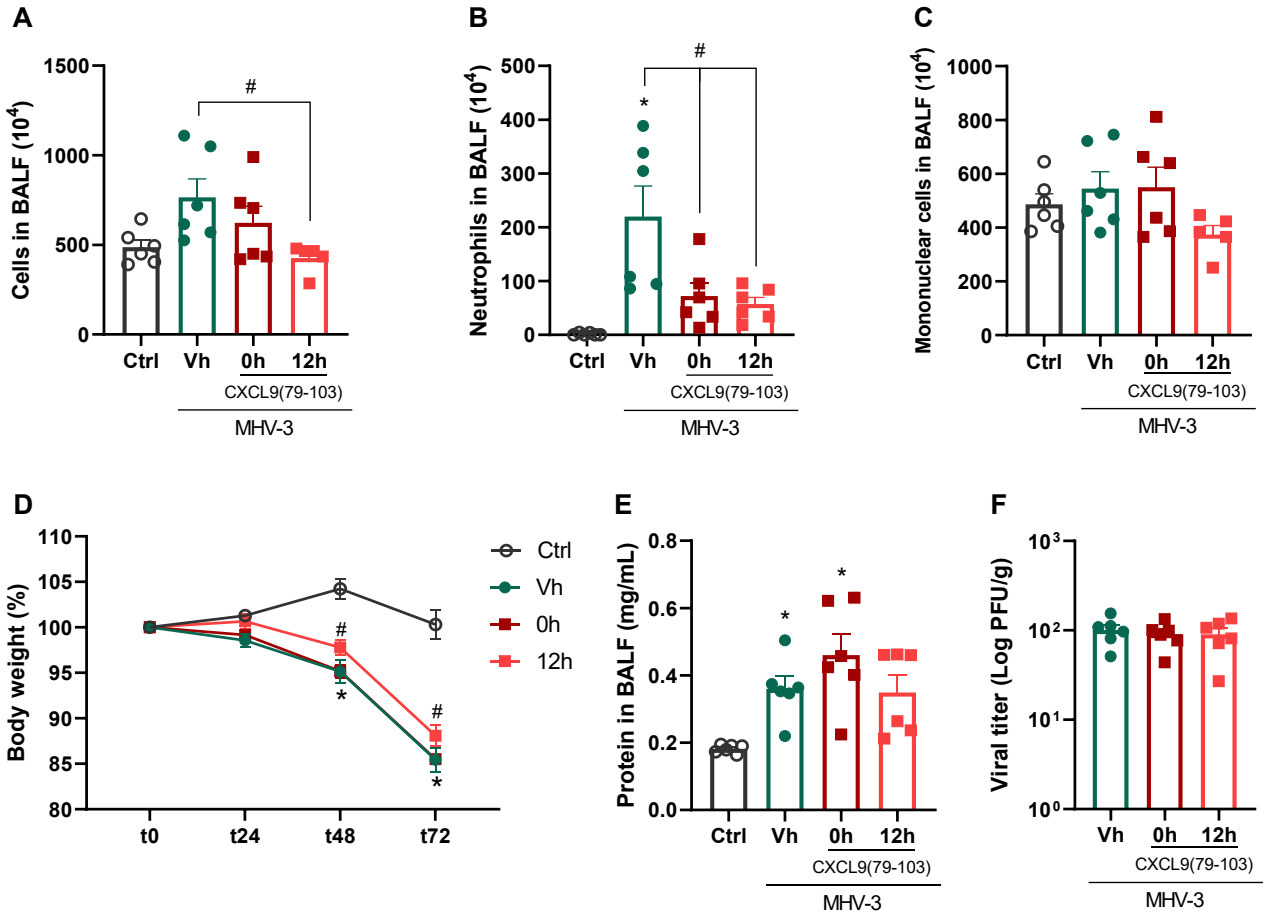

Figure 34 – CXCL9(74-103) treatment reduces several inflammatory parameters in MHV-3 infection. C57BL/6 mice were infected with MHV-3 (3×103 PFU/mouse) or saline (Ctrl group) and dissected 3 days later. At the indicated times after the challenge, mice were treated with CXCL9(74-103). (A) Numbers of leukocytes in BALF were counted in the Bürker chamber. Numbers of neutrophils (B) or mononuclear cells (C) in BALF were counted in cytospin slides. Changes in body weight (D) were calculated with the weight before infection (day 0) as reference. The concentration of protein in BALF was measured to assess pulmonary edema (E). Viral load was determined in the lungs by titration (F). Data are shown as mean ± SEM. Each symbol in panels A-C, E, and F represents data of an individual mouse. *p<0.05 when compared with the healthy, unchallenged control group. #p<0.05 when comparing treatment groups with the vehicle. ANOVA test followed by Bonferroni correction was used in the graphs with normal distribution. Otherwise, Kruskal-Wallis with Dunn's multiple comparisons test was used. n=6.

Similar to what we did for *S. aureus* infection, we measured the cytokines associated with MHV-3 infection in both BALF and lungs. The cytokines/chemokines

selected were also based on the report of Andrade et al (77): IL-6, IL-1β, CXCL1, and CCL3 (Figure 35). Interestingly, the cytokine levels were not significantly elevated in BALF 3 days after the MHV-3 infection, though IL-6 levels tended to be higher in infected mice. Surprisingly, the treatment that started 12 h after the challenge, seemed to induce an increase in IL-6 (Figure 35A) and CXCL10 (Figure 35C), compared to uninfected control animals, and IL-1β (Figure 35C), compared to mice that received vehicle. In contrast, IL-6 (Figure 35E), IL-1β (Figure 35F), and CCL3 (Figure 35H) levels were increased in the lungs when mice were infected with MHV-3, while CXCL10 (Figure 35G) was surprisingly reduced. Pretreatment (0h) with CXCL9(74-103) only attenuated the increase in IL-6 levels (Figure 35E) and both treatments prevented the increase of IL-1β levels in the lungs (Figure 35F).

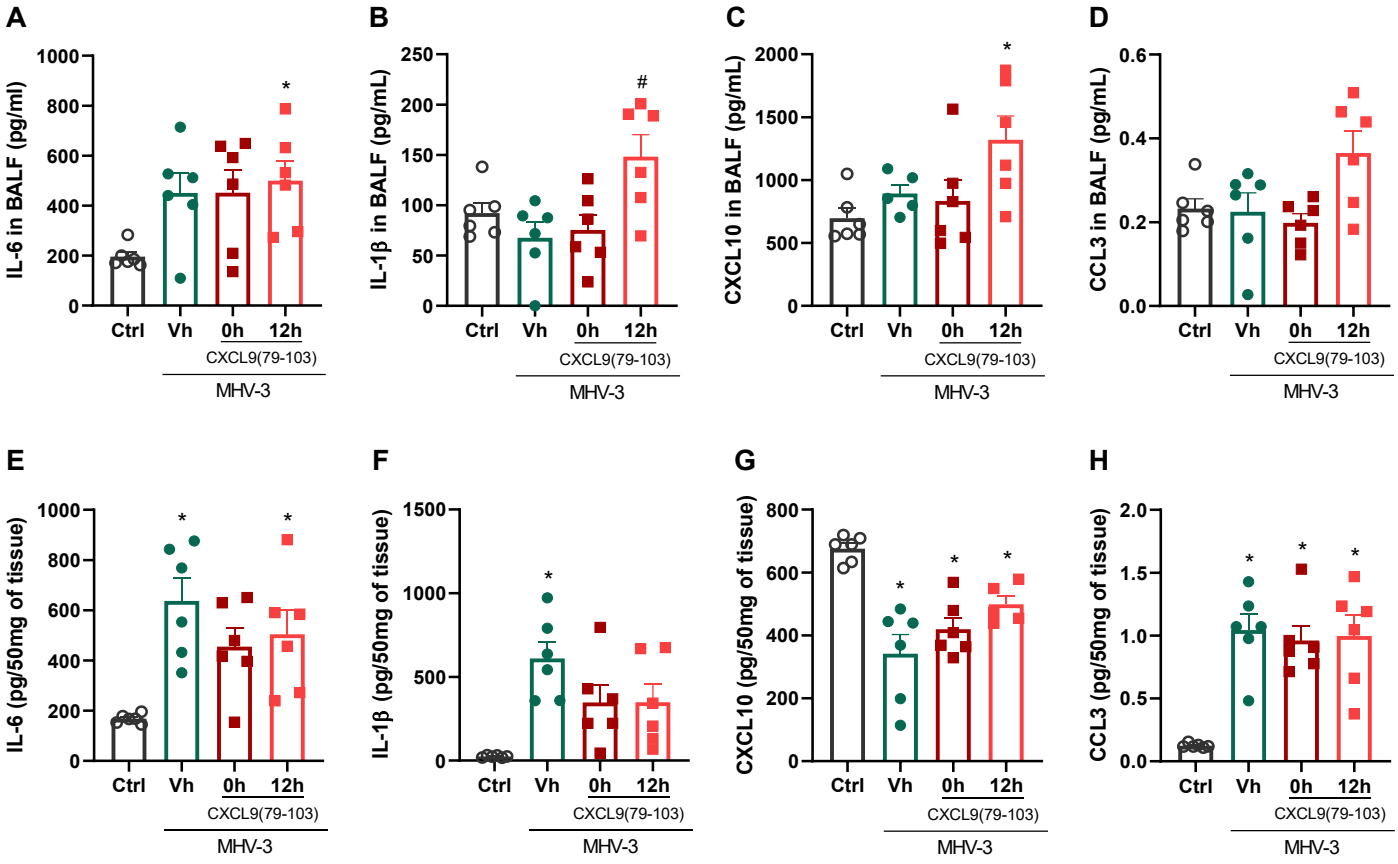

Figure 35 – CXCL9(74-103) treatment does not affect the levels of cytokines in MHV-3 infection. C57BL/6 mice were infected with MHV-3 (3×10^3 PFU/mouse) or saline (Ctrl group) and dissected 3 days later. At the indicated times after the challenge, mice were treated with CXCL9(74-103). Levels of IL-6 (A), IL-1β (B), CXCL10 (C), and CCL3 (D) were measured in BALF by ELISA. Levels of IL-6 (E), IL-1β (F), CXCL10 (G), and CCL3 (H) were measured in the lungs by ELISA. Data are shown as mean ± SEM. Each symbol represents data of an individual mouse. *p< 0.05 when compared with the healthy, unchallenged control group. ANOVA test followed by Bonferroni correction was used in the graphs with normal distribution. Otherwise, Kruskal-Wallis with Dunn's multiple comparisons test was used. n=5-6.

Despite the rather modest cytokine production, the pulmonary mechanic functions were substantially impacted by the MHV-3 infection. All the parameters evaluated – lung elasticity (Figure 36A), lung volumes (Figure 36B), and airway flow (Figure 36C) – by the forced spirometry got significantly worse after the viral challenge. However, the pretreatment (0h) was effective to reverse them all to basal levels and prevent the

pulmonary mechanical distress caused by MHV-3. Here, the treatment starting immediately before the challenge was more effective than starting 12 h after, in contrast with the observed in the other experiments.

Lastly, the tissue damage was evaluated by histopathological analysis. As observed in Figure 37A, the MHV-3 infection caused a massive influx of leukocytes and the destruction of the airway walls, which can be directly related with the forced spirometry results. Nevertheless, in contrast to lung function measurements, the mice treated 12 h after the challenge displayed a significant improvement in the histopathological score and damage (Figure 37B, C), showing that this group has less intense and frequent tissue damage, while the 0h group did not have significant improvement when compared with the Vehicle group.

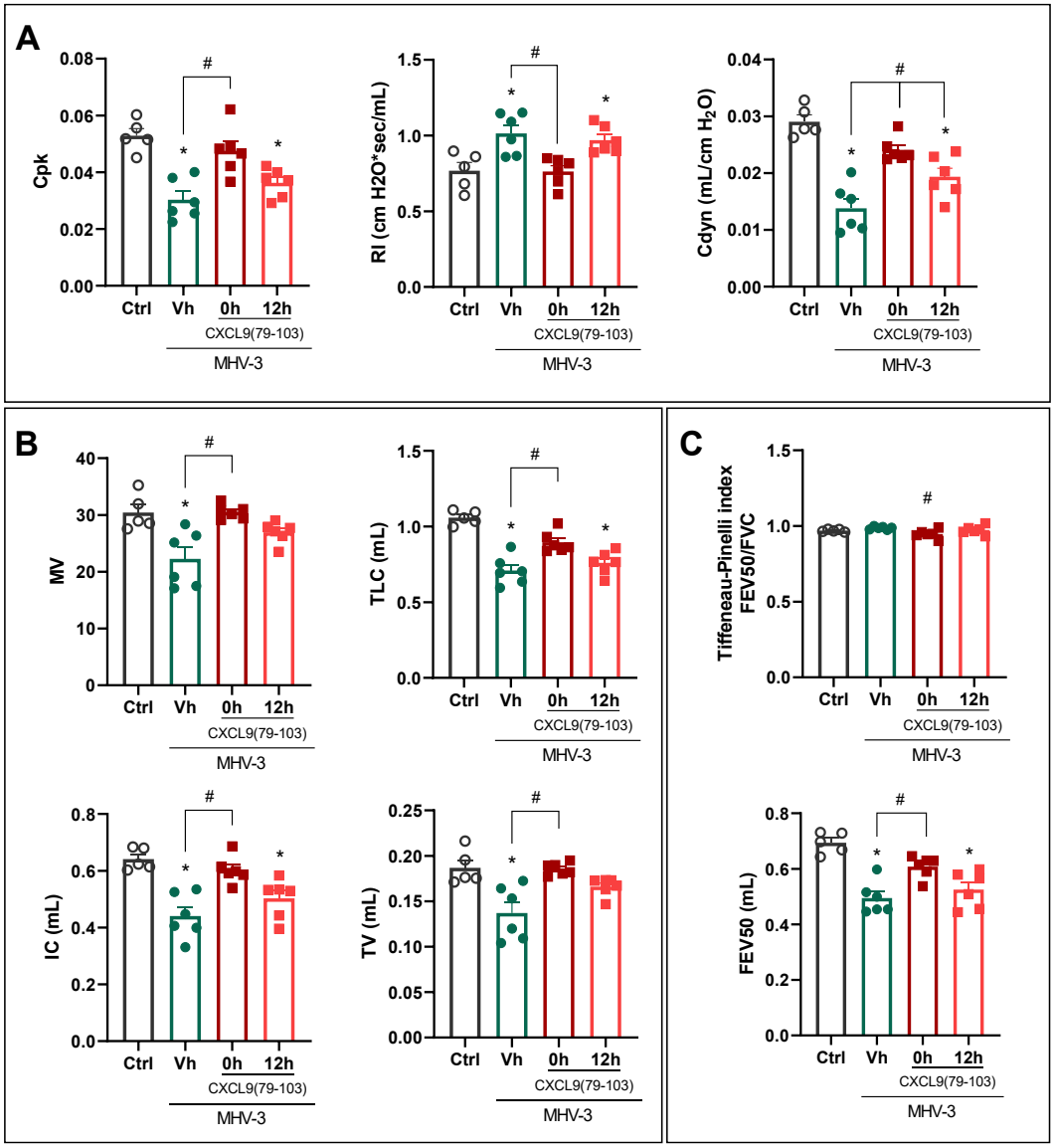

Figure 36 – CXCL9(74-103) treatment improves several parameters of lung function in MHV-3 infection. C57BL/6 mice were infected with MHV-3 (3×10^3 PFU/mouse) or saline (Ctrl group) and dissected 3 days later. Right before euthanasia, pulmonary mechanic functions were assessed. At the indicated times after the challenge, mice were treated with CXCL9(74-103). Invasive forced spirometry was performed to investigate functional modifications in pulmonary mechanics. The assessed parameters were (A) Lung elasticity represented by Peak of Compliance (Cpk), Lung Resistance (RI), and Dynamic Compliance Forced (Cdyn); (B) Lung volumes by Minute Volume (MV), Total Lung Capacity (TLC), Inspiratory Capacity (IC), and Tidal Volume (TV); (C) Airway flow by Tiffeneau-Pinelli index (FEV20/FVC) and Forced Expiratory Volume at 50 ms (FEV20). Data are shown as mean ± SEM. Each symbol represents data of an

individual mouse. *p< 0.05 when compared with the healthy, unchallenged control group. #p<0.05 when comparing different time points with the vehicle. ANOVA test followed by Bonferroni correction was used in the graphs with normal distribution. Otherwise, Kruskal-Wallis with Dunn's multiple comparisons test was used. n=6.

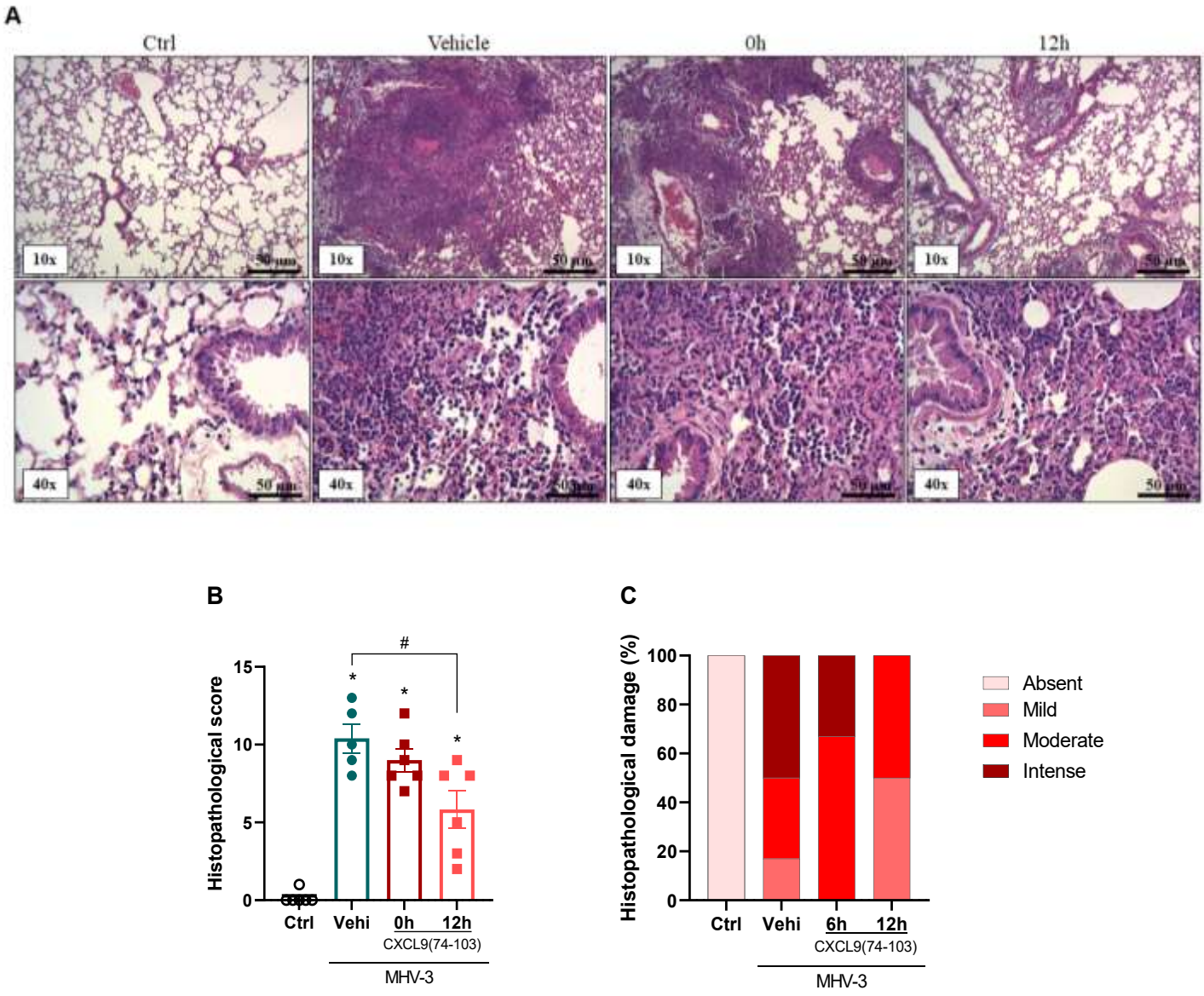

Figure 37 – CXCL9(74-103) does not affect the tissue damage in MHV-3 infection. C57BL/6 mice were infected with MHV-3 (3×10^3 PFU/mouse) or saline (Ctrl group) and dissected 3 days later. At the indicated times after the challenge, mice were treated with CXCL9(74-103). (A) Representative hematoxylin and eosin-stained preparations of lung tissue from mice. Scale bar: 50 μm, as reported in the figure. (B) Histopathological score and (C) Contingency graph according

to ranges of tissue damage (severe, intense, moderate, mild, and absent). Data are shown as mean ± SEM in panel B. *p< 0.05 when compared with the healthy, unchallenged control group. ANOVA test followed by Bonferroni correction was used in the graphs with normal distribution. Otherwise, Kruskal-Wallis with Dunn's multiple comparisons test was used. n=5-6.

4

DISCUSSION

4. DISCUSSION

4.1. PART I: ROLE OF LYMPHOCYTES IN A MURINE MODEL OF ARDS

Resolution of inflammation is an active and complex process that occurs when the inflammatory stimulus is controlled, includes repair of damaged tissue, and ensures reestablishment of homeostasis (240). During the resolution, the production of pro-inflammatory mediators and the recruitment of PMN leukocytes are diminished, and the PMN leukocytes accumulated in the tissue undergo a process of apoptosis and are engulfed by macrophages, leading to the clearance of dead cells and cellular debris. In addition, events related with the resolution of pulmonary inflammation include reduction of edema, repopulation of airway epithelium, and restoration of pulmonary surfactants (281). It is difficult to precisely establish the start of resolution due to its complexity and the lack of specialized tools. In our ARDS model, we suggest that the resolution process begins after the third day of inflammation, forasmuch as we observed a significant decrease of neutrophils and an increase of macrophages, the cell type that is currently considered to be the prime executor of resolution (282,283), from this time point onwards. Together with macrophages, we observed an increase in lymphocytes and we sought to investigate their role throughout this process.

The role of T cells in the resolution of inflammation has become increasingly relevant. Classically, T_{regs} are extremely important in this context because of their ability to secrete IL-10 and amphiregulin (284,285), besides the induction of efferocytosis and, consequently, the promotion of tissue repair (259). However, little is known about the other populations of lymphocytes in resolution, and this is emerging as a critically important topic. For a long time, adaptive immune responses were studied apart from innate immune responses and the relation between them remained vague. Lymphocytes have well-defined roles in the adaptive response which generally takes some time and may coincide with a reduction in the accumulation of neutrophils at the inflammatory site. That time coincidence could be associated with a connection between the different phases of the inflammatory process. For instance, lipoxins and Th2-derived protectin D1 suppress pro-inflammatory cytokines and infiltration of leukocytes into inflammatory sites (286). In addition, T lymphocytes expose phosphatidylserine in their membranes even in non-

apoptotic contexts (287), leading to their efferocytosis and the release of anti-inflammatory and pro-resolving molecules.

Despite not being strictly related with the resolution of inflammation, the ratio of neutrophils and lymphocytes (NLR) is largely used as a prognostic biomarker in different diseases. High NLR in patients with cancer (288), stroke (289), sepsis (290), rheumatoid arthritis (291), COVID-19, and more (292), is associated with worse prognosis and increased rates of complications and mortality. Deficiency in the clearance of neutrophils and the decrease of lymphocytes may represent an impairment of the resolution of inflammation (292). Therefore, high NLR or inadequate resolution is associated with disease severity and lymphocytes may be part of it.

Although lymphocytes have a great potential to participate in resolution, the absence of mature B and T cells in our model did not significantly affect the inflammation or its resolution. Similarly, Verjans et al. (293) induced ARDS by LPS instillation in $RAG2^{-/-}$ mice, and the deterioration and recovery of lung mechanics were not altered by the lack of adaptive lymphocytes. In contrast, D'Alessio et al. (186) and Kearns et al. (250) observed that $RAG1^{-/-}$ mice with acute lung injury induced by LPS have impaired recovery when compared to wild-type mice and concluded that lymphocytes are important for events related with the resolution of inflammation. Therefore, the role of B and T cells in ARDS/ALI is not yet fully explored and may be more complex than just beneficial or harmful. These cells might play a minor role in the initiation, propagation, and resolution of LPS-induced lung inflammation and, maybe their role can be taken over by other immune cells, such as ILCs and alveolar macrophages (293). In addition, it is difficult to evaluate the significance of lymphocytes in general, considering that they represent different subpopulations with distinct effector mechanisms. Hence, we decided to focus on the subsets of $CD4^+$ T cells based on the expression of chemokine receptors. Besides the correlation of these receptors with Th1, Th2, and Th17 classification, the evaluation of their presence will allow us to inhibit the recruitment of specific subsets in follow-up experiments as good neutralizing antibodies or performant antagonists are available for most chemokine receptors. Also, the expression of specific chemokine receptors on $CD8^+$ T cells is an important indicator of their activation status and homing behavior/capacity (294).

Regarding $CD4^+$ T cells classification, it has been proposed that Th1 cells express CXCR3 and CCR5, Th2 cells express CCR4 and CCR8, and Th17 express CCR4, CCR6, and CXCR3 (261). However, this strict relation between Th subtype and chemokine expression pattern is sometimes contested (261) and our results do not show significant co-expression of the receptors as expected. In addition, due to methodological limitations, we were not able to evaluate the expression of all the chemokine receptors used in the $CD4^+$ T cell subdivision. Thus, we decided to focus on the chemokine receptor itself and study two lung compartments to correlate the lymphocyte localization with the chemokine receptors' expression.

Surprisingly, CCR3, CCR4, and CCR5 were not so abundant and their expression in lymphocytes from BALF and lung tissue was comparable. In between them, CCR4 is detected most often and, together with CCR5, may be linked to the early recruitment of $CD8^+$ T cells to the lung tissue, but not to the alveolar space. In contrast, the high expression of CXCR3 and CXCR6 in both $CD4^+$ and $CD8^+$ T cells in the BALF, but not in the lung tissue, indicates a key role for these receptors at later time points of airway inflammation. As observed in other studies, CXCR3 and CXCR6 mediate the recruitment of activated $CD4^+$ and $CD8^+$ T cells and their long-term survival and tissue distribution (295–298). We also observed an increase in CXCR3 ligand levels: CXCL9, and CXCL10. These chemokines are predominantly induced by interferons, including IFN-γ, which is also enhanced at the beginning of the inflammation.

Since CXCR3 and its ligands apparently are important for the recruitment of T cells to the alveolar space at later time points, this receptor seems like a good therapeutic target to inhibit the attraction of specific lymphocytes, allowing evaluation of their involvement in the inflammation and/or resolution phase in the ARDS model. The treatment with CXCR3 antagonists significantly decreased the recruitment, activation, and differentiation of T lymphocytes (299), reducing the inflammation in models of pneumonia (300) and arthritis (301,302), inhibiting lung tumor metastasis (303), and showing therapeutic effects in neurological diseases (304). In contrast, CXCR3 blockade did not prevent allergen-induced airway inflammation in a mouse allergy model (305). Notably, CXCR3 antagonists were not yet used in investigations of inflammation resolution and their role in pro-resolving events remains unclear. Based upon our results, we anticipate

that such treatment would potentially change the resolution timeline in the ARDS model. Therefore, we plan to use the CXCR3 antagonist AMG487 to further explore the role of these cells.

In conclusion, total T and B lymphocytes do not seem to have a major role on the resolution of neutrophilic inflammation in this self-resolving model of LPS-induced acute lung inflammation. On the other hand, the increased presence of innate lymphocytes in later phases after LPS stimulation could counterbalance the lack of T and B lymphocytes in RAG2$^{-/-}$ mice to control lung inflammation. However, targeting chemokine receptors, mainly CXCR3, could give additional information about any role of T cells for the resolution of inflammation.

4.2. PART II: ABSENCE OF CCR2 PROMOTES PROLIFERATION OF ALVEOLAR MACROPHAGES THAT CONTROL LUNG INFLAMMATION IN ACUTE RESPIRATORY DISTRESS SYNDROME IN MICE

The resolution of lung inflammation requires an orchestrated immune response and several control mechanisms to avoid excessive inflammation and chronic disease (185,328). CCR2 is a crucial receptor that regulates tissue inflammation through its fundamental role in monocyte recruitment. The CCL2-CCR2 axis plays an important role in monocyte biology, guiding the compartmentalization of these cells in different tissues during homeostasis and inflammation. CCR2-deficient mice are known to have lower numbers of circulating Ly6C^{Hi} cells since CCR2 is required for the mobilization of monocytes from the bone marrow to the circulation during a systemic inflammatory response (329). It has been demonstrated that CCR2 is important in the development of inflammation in the lungs (asthma (330), tuberculosis (331) and pulmonary fibrosis (332)), liver (333), myocardium (334,335) and others (336) due to its importance in monocyte recruitment.

In this study, we used CCR2-deficient mice to understand the kinetics of lung inflammation using an experimental model of ARDS induced by LPS, which can elicit a powerful pro-inflammatory, though self-resolving immune response (337). The lack of CCR2 generally leads to a decrease in monocytes/macrophages at the site of the

inflammation, which may lead to a milder disease (334,338). In contrast with our findings, Maus et al. (339,340) and Francis et al. (341) showed that the absence or blocking of CCR2 dramatically reduced the recruitment of myeloid cells in general, and not only the monocyte/macrophage population, impacting the disease parameters greatly in models of ARDS induced by LPS and ozone, respectively. Similarly, the depletion of circulating monocytes by intravenous injection of clodronate liposomes 2 days before intratracheal LPS treatment significantly suppressed acute lung injury in mice (342). Adversely, our data show that the reduced monocyte influx does not prevent the development of inflammation in the model of ARDS induced by intranasal low-dose LPS instillation. We found that in the initial phases of the inflammation, the absence of CCR2 led to a dramatic decrease in the accumulation of macrophages in the lungs and an increase in the recruitment of neutrophils, congruous with the higher levels of CXCL1 in the BALF. Contrastingly, at later time points we did not observe major differences in the body weight kinetics, inflammatory parameters, or immunopathological score between the two mouse strains indicating that although lack of CCR2 does not prevent lung inflammation, it does not hamper adequate resolution. We discovered that the absence of CCR2 was compensated by increased proliferation of AM that were more skewed towards an M2 phenotype as we detected an increased expression of the M2 marker CD206 on AM, and higher levels of CCL22 and TGF-β in the BALF. In addition, pulmonary *Nos2*, *IL-1β*, and *IL-12b* expression was reduced, while *Mrc1* was increased in $CCR2^{-/-}$ mice (Figures 25 and 26). Interestingly, the lower expression of *IL-12b* might be connected with the reduced levels of IFN-γ observed in CCR2-deficient mice (Figure 21) (343) and, consequently, the reduction of NOS2 (344). Together, those elements are indicative of efficient resolution of inflammation in the CCR2-deficient mice as the general paradigm states that the resolution of acute inflammation is characterized by the accumulation of pro-resolving macrophages that phagocytose apoptotic cells and produce pro-resolving molecules (345).

The effect of CCR2 absence at later time points of inflammation is indeed ambivalent. Previous reports showed that the lack of CCR2 signaling (a) reduces pro-fibrotic responses in the lungs (333,338); (b) refrains extracellular matrix remodeling (333), (c) delays the resolution of inflammation and the recovery of gastrointestinal

functions (342); (d) improves cardiac remodeling (335), and (e) limits recovery following spinal cord injury (346). In our study, the deficiency of CCR2 did not change the resolution timeline, suggesting that this receptor is not crucial in this acute and self-resolving model of lung inflammation. This is in agreement with the study by Pollenus et al. (347), who observed that CCR2 is dispensable for the resolution of malaria-induced lung pathology. Together, these studies indicate that CCR2 divergently affects the development of different diseases probably depending on the organ involved, and the profile and timing of each aspect of the inflammatory response. According to the mice, the model, and the type of inflammation, monocytes/macrophages may be beneficial for the proper development and resolution of inflammation, and they may impact other leukocytes differentially.

Even though CCR2 is essential for the recruitment of monocytes, in the absence of this receptor, a minor increase in monocyte-derived macrophages, monocytes, and IM at 2 and 3 days after the LPS challenge was observed in the CCR2 knockout mice when compared with the unchallenged group (Figure 22). Other chemokine receptors, such as CCR1, CCR4, and CCR5 and their corresponding ligands, may participate in the accumulation of macrophages in the absence of CCR2 (348,349). Besides recruitment, these ligands have a role in the activation, differentiation, and polarization of macrophages in numerous diseases and contexts (350). In addition to CC chemokines and their receptors, the CX3CL1-CX3CR1 axis is also an important pathway mediating monocyte migration, playing a major, but environment-specific, role in either pro-inflammatory or pro-resolving responses (351) and contributing to the development of inflammatory diseases, such as kidney ischemia-reperfusion injury (352) and pulmonary fibrosis (349).

CCR2 is mainly expressed in circulating peripheral blood monocytes, but not in AM. It is known that AM originate from fetal liver monocytes and are independent of circulating monocytes (353,354); therefore, the deficiency of CCR2 or the inhibition of CCL2 has little or no effect on this cell population (355). Contrastingly, the IM originate from yolk sac progenitors and in adulthood they are replaced by circulating monocytes (204,207), thus being susceptible to CCR2 deficiency. AM are crucial for the recognition and clearance of pathogens from the airways, promoting the initiation of host defense as well as tissue repair (283). This cell population is very important for the resolution of lung injury since

they can clear apoptotic neutrophils and tissue debris through efferocytosis (283), avoiding dying cells from releasing pro-inflammatory and toxic mediators into the surroundings while activating pro-resolving and repair factors (319). Indeed, depletion of AMs by intranasal delivery of clodronate liposomes prolonged the inflammation with a higher number of leukocytes in the BALF, lack of bodyweight recovery, and worse pulmonary edema (Figure 27). Likewise, other studies already showed that depletion of alveolar macrophage in LPS-induced ALI/ARDS leads to an increased influx of polymorphonuclear leukocytes (356) and more severe disease and lung inflammation (342). Interestingly, our results show that these phenomena are more pronounced in the absence of CCR2, supporting our hypothesis that AM are the key cell in the control of inflammation in CCR2-deficient mice.

According to Mahida et al. (357), ARDS in humans may be associated with impaired efferocytosis by AM, demonstrating how important this type of macrophage is. Our findings indeed suggest that increased proliferation of AM can compensate for the lack of macrophages derived from monocytes, promoting proper resolution of ARDS in the absence of CCR2. It is not totally clear what causes the proliferation of AM in our study. GM-CSF and M-CSF are important growth factors for the expansion of AM (324). Although there was no difference in GM-CSF levels between $CCR2^{+/+}$ and $CCR2^{-/-}$ mice at any time point evaluated, we observed a mild increase in M-CSF 3 days after the LPS instillation in the $CCR2^{-/-}$ mice (Figure 24). M-CSF is linked with the homeostasis of macrophage and monocyte populations and is able to prone monocytes towards an M2 profile, as shown by Hamilton et al. (358,359). It must also be noted that in the $CCR2^{-/-}$ mice, relatively more growth factor is available per target cell, as fewer monocytes/macrophages are present in the lungs of those animals.

In conclusion, in our murine model, CCR2 is not essential for the development, nor the resolution of ARDS induced by LPS. We observed different patterns and intensities of cell recruitment, especially in the initial phases of the inflammation, although disease development was not affected. Despite the importance of CCR2 in monocyte recruitment and the crucial role of macrophages in the resolution of inflammation, our data did also not show major effects on resolution when this receptor was absent. We hypothesize that the lack of monocyte recruitment is counterbalanced by the recruitment of neutrophils, in

the first days, and later by the proliferation of AM. More studies are necessary to further elucidate the mechanisms involved in this process and to clarify the mediators responsible for the enhanced proliferation of AM.

4.3. PART III: EFFECT OF TREATMENT WITH THE GAG-BINDING CHEMOKINE FRAGMENT CXCL9(74–103) IN MURINE MODELS OF PNEUMONIA

GAGs function as structural elements, but also as cellular effectors, because they can act as signaling molecules or as regulators that control protein activity. Through interaction with proteins, such as growth factors, chemokines, and adhesion molecules, or their corresponding receptor complexes, GAGs have been shown to modulate a wide range of biological processes, including directional cell migration, regulation of enzymatic activities, extracellular matrix assembly, and receptor binding/signaling (376). These processes are relevant in different (patho)physiological processes, including cardiovascular disease (377), cancer (378), infectious diseases (379), inflammation (380), and wound healing (381). In the diapedesis process, the GAG-chemokine binding is essential, because it ensures the presentation of chemokines on the endothelial layer of blood vessels, creating a concentration gradient, and allowing the chemokine receptors from the recruited cells to bind to their respective chemokine. The latter interaction guides the activated leukocyte to the inflamed site (382). In addition, GAG binding often protects the chemokines from enzymatic degradation, increases their stability, and promotes their multimerization (120).

GAGs have many pharmacological properties such as anti-inflammatory, anti-viral, anti-angiogenesis, anti-neoplastic, and anti-metastatic effects (383). Based on that, several studies have been developed using GAGs or molecules that compete with GAGs for chemokine-binding as therapeutic targets. For instance, Hylan G-F 20 provides significant pain relief in patients with knee osteoarthritis (384) and NOX-A12 releases CXCL12 from stromal cell-surface–bound GAGs, neutralizing this chemokine interfering with cell migration in chronic lymphocytic leukemia (385). Thus, GAG-chemokine binding is a potential therapeutic target for the development of anti-inflammatory strategies, especially in the context of chronic non-resolving inflammation or hyperinflammation and

autoimmune diseases (386). In our study, we used the chemokine-derived peptide CXCL9(74-103), which binds to GAGs, competing with the natural GAG-chemokine binding and, consequently, reducing the chemokine's activity and the recruitment of neutrophils (131).

The timing of the application of neutrophil-targeting drugs is crucial. Hence, we performed kinetics experiments of the *S. aureus* pneumonia model, and we observed that the peak of inflammation in this model is around 12 h after the infection and the bacterial load in lung tissue and BALF is significantly reduced at 48 h (Figure 29). Based on these results, we decided to treat the mice at 6 or 12 h after the bacterial challenge and perform the euthanasia at 24 h. The mice treated at 6 h had a higher bacterial load in BALF, demonstrating that the early recruitment of neutrophils is indispensable for the control of *S. aureus* infection. This is in accordance with Robertson et al, given that the depletion of neutrophils impaired the control of *S. aureus* infection and led to decreased rates of survival in a murine model of pneumonia (387).

The treatment with drugs that inhibit the chemokine activity and the recruitment of neutrophils in infections has a complex timeline since these cells are essential for the clearance of the pathogen but might also be linked with excessive inflammation and tissue damage (366). The main outcome of the CXCL9(74-103) administration was a reduction in neutrophil accumulation in the lungs and in clinical severity score in both treated groups (Figure 30). This is in agreement with previous articles published by our group that showed that a reduction in neutrophil numbers was associated with less inflammation in murine models of gout (372), AIA (129), and *K. pneumoniae*-induced pneumonia (371).

Despite the reduction in the number of neutrophils, CXCL9(74-103) treatment did not decrease levels of inflammatory cytokines, nor prevent tissue damage (quantitated with the histopathological score). In contrast with what was observed by Boff et al. in more than one study (129,371), the treatment with CXCL9(74-103) did not affect the levels of cytokines and chemokines in either BALF or lungs in our model. This fact is probably related with the complexity of the infection and the reminiscent inflammation, considering that the treatment did not deplete neutrophils completely and many inflammatory reactions were still ongoing. The same incoherence was observed in the lung function parameters,

as only the lung elasticity was recovered by the peptide treatment 6 or 12 h after the challenge. Interestingly, neutrophil elastase induces elastic fiber degradation and impair the elastic fiber assembly, resulting in loss of lung elasticity. Thus, the reduction of neutrophils is associated with the observed in the pulmonary function evaluation (388). In summary, CXCL9(74-103) is able to lessen the inflammation in pneumonia induced by S. aureus, but not all the inflammatory parameters are reduced by the peptide and, especially, the tissue damage was not reversed. This indicates that CXCL9(74-103) alone is not effective in the treatment of this model of pneumonia and more studies should be performed to study combinations of this peptide with antibiotics or other anti-inflammatory drugs.

Although neutrophils play a prominent role in bacterial infections, their role in viral infections is not fully explored and varies greatly depending on the virus. In pneumonia caused by the Influenza virus, for instance, neutrophils are extensively recruited and have a major role in pulmonary damage (389). In contrast, in Chikungunya virus infection, neutrophils and specifically NETs can capture and neutralize the virus, being essential for viral load control (390). In the case of SARS-Cov-2 infections, neutrophils are also extensively present and, associated with a low count of lymphocytes, indicative for a poor prognosis in COVID-19 (391). Not much is known about the role of neutrophils in murine models of pneumonia induced by MHV-3. According to Andrade et al. (77), there is an increase in neutrophil accumulation in the lungs 3 days after the infection. Nevertheless, they are not the main accumulating cell type, representing approximately 15% of cells only. The same is observed using a mouse-adapted SARS-Cov model (392). Based on those reports, we euthanized the mice on day 3 and we indeed observed an increase of neutrophils in the vehicle group. Interestingly, the group treated 12 h after the infection had a significant decrease in total cells and neutrophils. This group also did not have increase of pulmonary edema when compared to the Ctrl group, suggesting that the inflammation and tissue damage was reduced after CXCL9(74-103) administration. Nonetheless, no reduction was observed in the cytokine and chemokine levels. Surprisingly, some cytokines in the BALF are even increased after the CXCL9(74-103) treatment, which does not match with available reports (371).

The infection with MHV-3 via nasal instillation causes mild lung inflammation and severe lung dysfunction. Here, we observed that pretreatment with CXCL9(74-103) was able to reduce the loss of elasticity, the disturbance in the lung volumes, and the impairment of airway flow caused by the virus. Likewise, hACE2-transgenic mice infected with SARS-CoV-2 also had a decrease in inspiratory capacity and compliance and an increase in resistance (393). Histopathological analysis confirmed the positive impact of CXCL9(74-103) treatment. The mice treated with the peptide 12 h after the infection showed a partial reduction in the histopathological score and the frequency of intense and moderate tissue damage. The recovery of treated mice may be associated with the reduction in neutrophil recruitment, which has a major role in tissue damage and, consequently, lung dysfunction (394,395). In addition, we observed that for some parameters pretreatment was better, whereas for others the treatment starting at 12 h was more efficient. This fact demonstrates the complexity of this model. It also enlightens the need for more studies to further explore the role of neutrophils, to reveal the specific impact of GAG-binding peptides on cell recruitment and to further establish the relation between cell recruitment and disease outcome.

There are several limitations in the use of MHV-3 to study pneumonia and, especially to study Sars-Cov-2-induced pathology. Due to its preference for the liver, MHV-3 causes a mild infection in the lungs and the infection time-course is very different from the one observed in COVID-19. In addition, despite the similarities shared by these viruses, there are differences between them that need to be addressed (396). Nevertheless, MHV-3 is an important tool to bring insights and elucidate some mechanisms that might be relevant in other contexts as well. Many therapeutic strategies for COVID-19 are being studied with the help of β-coronaviruses, such as the programmed cell death protein 1 and its ligand (PD-1/PD-L1) blockade (397) and the combination of Remdesivir and Ivermectin (398).

In summary, we used two very different models of pneumonia to explore the benefits of the CXCL9(74-103) treatment. Each pathogen infects cells and spreads over time through a distinct mechanism. Neutrophils are essential for bacterial clearance in pneumonia caused by *S. aureus*, but not in MHV-3. In a viral infection, neutrophils are

also relevant, but mainly to propagate inflammation and recruit new cells. There is a significant variance in the time course and clinical manifestations of both infections as well. The effects of the *S. aureus* infection on the lungs manifest rapidly and systemic symptoms were observed in approximately 12 h, while MHV-3 affects the lungs gradually and the peak of inflammation is around 3 days after the challenge. It is important to notice, however, that the amount of virus instilled is way smaller compared to the number of bacteria, since MHV-3 in higher numbers quickly infects the liver and the mice die due to liver failure (77). These differences are reflected in our results and should be taken into consideration when investigating the data.

In general, we can conclude that CXCL9(74-103) has the potential to ameliorate the burden of pneumonia induced by *S. aureus* and MHV-3. However, more studies should be performed to find the ideal time points for the treatment of the inflammation without impairing infection control. Remarkably, MHV-3 induced tissue damage and lung dysfunction were greatly reverted by CXCL9(74-103) treatment and this might help in the search for COVID-19 treatments.

4.4. FINAL DISCUSSION AND CONCLUSION

Leukocyte trafficking is a key factor in immunological responses and is tightly coordinated by chemokine signaling. Recent studies linked dysregulation in the chemokine system to the development of cancer and inflammatory illnesses. Therefore, chemokine receptors are currently being considered potential therapeutic targets. Approximately, 50 chemokine receptor-targeting medicines have been created in the last decades, but only three were fully approved in clinical trials (399): Maraviroc, a CCR5 antagonist with anti-HIV properties (400), Plerixafor, a CXCR4 antagonist for non-Hodgkin's lymphoma and multiple myeloma (401), and Mogamulizumab, an anti-CCR4 monoclonal antibody for treatment of T cell leukemia and lymphoma (402). In addition, other drugs are being developed and might be approved for clinical use in the following years, such as the CXCL12 inhibitor NOX-A12 in the treatment of different types of cancer, such as brain and pancreatic cancer (385). Despite their significant potential, a limited number of drugs associated with chemokines were approved, and they are mostly related

with HIV and cancer. Thus, much of this field is yet to be explored and new approaches should be used to further elucidate the chemokine signaling pathways and allow development of new medicines.

In the present study, we used three different paths to study chemokines and chemokine receptors in the context of lung inflammation. First, we characterized the receptors expressed in lymphocytes in the period of resolution of inflammation induced by LPS, allowing the future application of specific inhibitors to further explore the role of these cells. Then, we focused on the role of a chemokine receptor, CCR2, in the inflammation profile of ARDS. Finally, we evaluated the therapeutic effects of a GAG-binding peptide, CXCL9(74-103), in models of pneumonia induced by *S. aureus* and MHV-3.

The role of the different populations of lymphocytes in the resolution of inflammation is not fully uncovered. Since the general ablation of T and B cells did not affect the resolution of LPS-induced ARDS seen in RAG2-deficient mice, we decided to try and identify subpopulations of lymphocytes based on their chemokine receptor expression pattern. We reasoned that this information would allow us thereafter to block a specific chemokine receptor to evaluate whether the corresponding lymphocyte subpopulation is involved in the resolution of ARDS. As the main receptor expressed by lymphocytes in the resolution phase, CXCR3 is a potential therapeutic target. By its inhibition, CXCR3 has been proven important for the progression of apical periodontitis (403), inflammatory fibrosing diseases (404), autoimmune diseases and graft rejection (405), airway hyperresponsiveness and inflammation (406), to name a few conditions. In general, $CXCR3^+$ lymphocytes are important for the development of inflammation. However, in our model, we observed the enhancement of these cells in later time points but not at the peak of inflammation. Therefore, we still aim to further elucidate the role of $CXCR3^+$ lymphocytes in the resolution of LPS-induced ARDS.

CCR2 is a crucial receptor in monocyte recruitment and activation by the recognition of its high-affinity ligand CCL2 (317,318). Using CCR2-deficient mice, we unraveled that the development and resolution of ARDS driven by LPS do not require CCR2. Even though the development of the disease was not affected, we observed different patterns of cell recruitment, particularly in the early stages of the inflammation in

the absence of CCR2. Similarly, the resolution of inflammation was not impaired by the lack of CCR2, but different populations of macrophages were observed in the lungs. Therefore, the initial neutrophil recruitment and later AM proliferation balance out the absence of monocyte recruitment. The plasticity of AM is very relevant in lung inflammation because they patrol the alveolar epithelium and eliminate pathogens, but also exert different anti-inflammatory and pro-resolving functions (407).

Next, we investigated the effects of the CXCL9(74-103) therapy using two distinct models of pneumonia. In general, the treatment reduced the accumulation of neutrophils in the lungs, leading to different outcomes according to the causative pathogen. In the *S. aureus*-induced pneumonia, the clinical severity score and parameters of lung elasticity were improved after CXCL9(74-103) treatment 6 or 12 h post-infection. However, lung histopathologic damage and other parameters of lung dysfunction were not affected by the peptide. Importantly, the treatment with CXCL9(74-103) 12 h after the infection did not increase the bacterial load, being the most appropriate treatment time evaluated in this study. The ambiguous results observed in this model are probably related to the difficult decision regarding timing the therapy and the balance between the beneficial and harmful roles of neutrophils in bacterial infections. The struggle to find this balance is commonly observed in the literature (366). For instance, the treatment with Kineret, an IL-1 receptor antagonist (IL-1Ra), affects the IL-1/IL-8 signaling cascade but leads to an increase in the bacterial burden in the lungs (408). Another example is the treatment of septic arthritis with DF2156A, a non-competitive antagonist of chemokine receptors important in the recruitment of neutrophils: CXCR1/2. According to Boff et al., the early treatment with DF2156A led to an increase in bacterial load, while the later treatment prevented the increase in bacterial load, and reduced the local nociception, but did not improve tissue damage (409). In contrast, in MHV-3 induced pneumonia, the role of neutrophils is mainly to extent inflammation and induce the recruitment of new cells, instead of actively controlling the virus. Here, besides reducing neutrophil accumulation, CXCL9(74-103) treatment partially prevented weight loss and lung dysfunction and did not increase the viral load in the lungs. Therefore, the reduction in neutrophil recruitment in this model might be beneficial and should be explored. Several studies show that excessive neutrophil numbers or neutrophil products are associated with disease severity and tissue

damage. For instance, neutrophils recruited to the lungs in COVID-19, by producing excessive ROS, might spread a local inflammatory response turning it systemic and more severe (410). In addition, the use of Baricitinib, a JAK1/JAK2 inhibitor, induced a reduction in lung infiltration by inflammatory cells, including neutrophils, and, consequently, controlled lung pathology in a model of COVID-19 (411). Similarly, neutrophil-predominant immune responses are associated with worse outcomes in influenza infections (412). Reparixin, a CXCL8 inhibitor targeting its two receptors CXCR1/2, has been tested in a Phase II clinical trial to improve the outcome of a severe COVID-19 infection. The results of the study were encouraging but should be confirmed in a large Phase III trial (413).

The complexity of lung diseases and the chemokine system implies the necessity of more studies linking the two fields and exploring their particularities. In summary, the present study showed the different roles of chemokines and chemokine receptors and paved the way for the development of new therapeutic options for lung inflammation. As observed in Figure 38, we can conclude that $CXCR3^+$ and $CXCR6^+$ are the most frequent chemokine receptors expressed by lymphocytes in the resolution phase (A), CCR2 is not essential for LPS-induced ARDS but its absence changes the profile of cells recruited to the lungs (B), and CXCL9(74-103) treatment has beneficial effects in pneumonia models, especially on breathing parameters and lung damage inflicted by infection with MHV-3 (C).

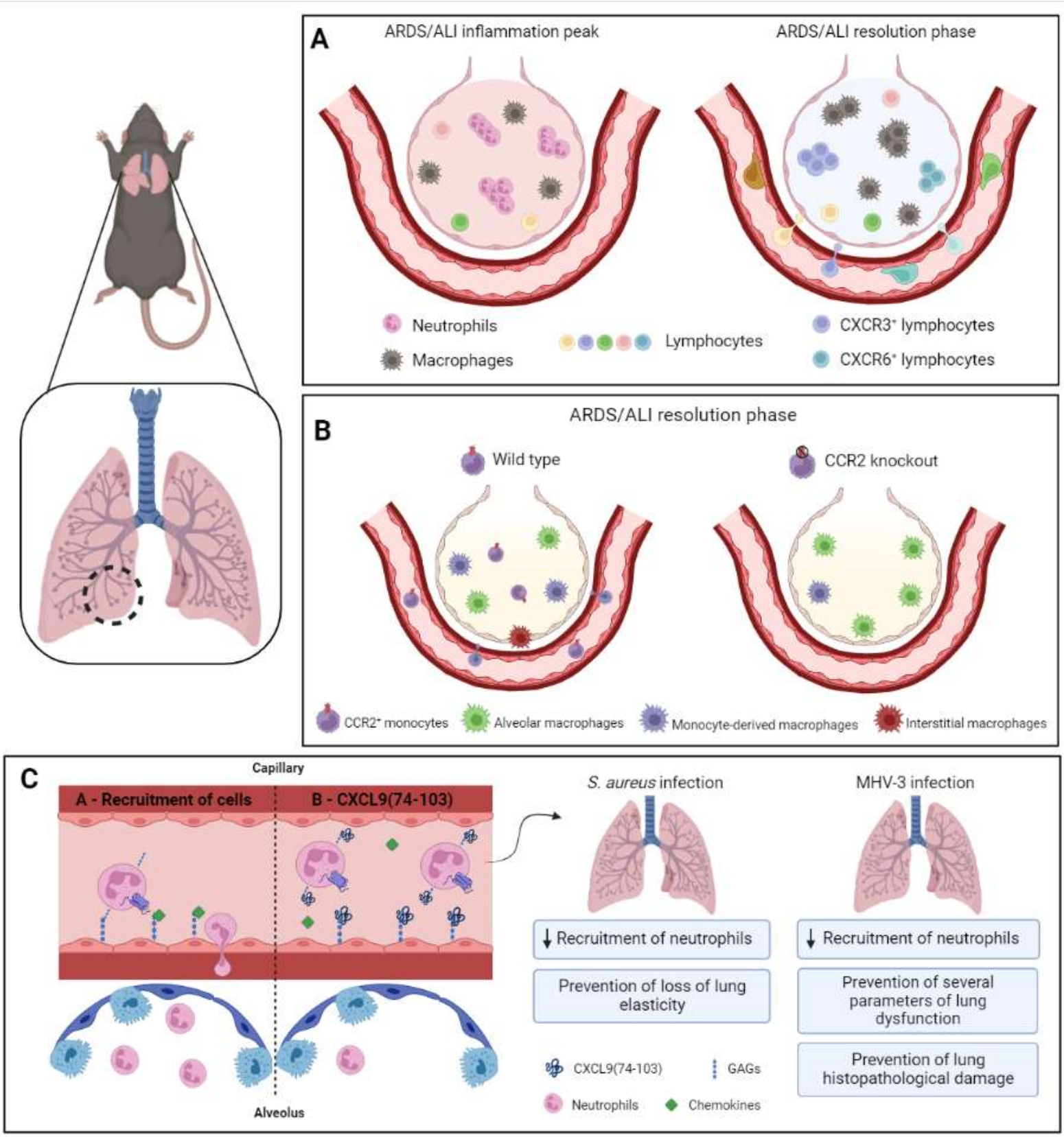

Figure 38 – Conclusion

5. REFERENCES

1. World Health Organization. Global Health Estimates 2016: Deaths by Cause, Age, Sex, by Country and by Region, 2000-2016. Geneva; 2018.

2. Roth GA, Abate D, Abate KH, Abay SM, Abbafati C, Abbasi N, et al. Global, regional, and national age-sex-specific mortality for 282 causes of death in 195 countries and territories, 1980–2017: a systematic analysis for the Global Burden of Disease Study 2017. The Lancet. 2018;392(10159):1736–88.

3. James SL, Abate D, Abate KH, Abay SM, Abbafati C, Abbasi N, et al. Global, regional, and national incidence, prevalence, and years lived with disability for 354 Diseases and Injuries for 195 countries and territories, 1990-2017: A systematic analysis for the Global Burden of Disease Study 2017. The Lancet. 2018;392(10159):1789–858.

4. De Amorim Corrêa R, De São José BP, Malta DC, De Azeredo Passos VM, França EB, Teixeira RA, et al. Carga de doença por infecções do trato respiratório inferior no Brasil, 1990 a 2015: Estimativas do estudo Global Burden of Disease 2015. Revista Brasileira de Epidemiologia. 2017;20:171–81.

5. Lamb AB. Acute Lung Injury. In: Nunn's Applied Respiratory Physiology. 2017. p. 439–49.

6. Ferkol T, Schraufnagel D. The global burden of respiratory disease. Ann Am Thorac Soc. 2014;11(3):404–6.

7. Sweeney R mac, McAuley DF. Acute respiratory distress syndrome. The Lancet [Internet]. 2016;388(10058):2416–30. Available from: http://dx.doi.org/10.1016/S0140-6736(16)00578-X

8. West JB, Luks AM. West's Respiratory Physiology: The Essentials. 10th ed. Wolters Kluwer Health, editor. Philadelphia; 2015. 224 p.

9. Chaudhry R, Bordoni B. Anatomy, Thorax, Lungs. StatPearls. 2020.

10. Amador C, Varacallo M. Anatomy, Thorax, Bronchial. StatPearls. 2020.

11. Khan YS, Lynch DT. Histology, Lung. StatPearls. 2020.

12. Franks TJ, Colby T V., Travis WD, Tuder RM, Reynolds HY, Brody AR, et al. Resident Cellular Components of the Human Lung: Current Knowledge and Goals for Research on Cell Phenotyping and Function. Proc Am Thorac Soc. 2008 Sep 15;5(7):763–6.

13. Dangelo JG, Fattini CC. Anatomia sistêmica e segmentar. 3rd ed. Atheneu, editor. São Paulo; 2007.

14. Kuek LE, Lee RJ. First contact: the role of respiratory cilia in host-pathogen interactions in the airways. American Journal of Physiology-Lung Cellular and Molecular Physiology. 2020 Oct 1;319(4):L603–19.

15. Toczyłowska-Mamińska R, Dołowy K. Ion transporting proteins of human bronchial epithelium. J Cell Biochem. 2012 Feb;113(2):426–32.

16. Sagel SD, Davis SD, Campisi P, Dell SD. Update of respiratory tract disease in children with primary ciliary dyskinesia. Proc Am Thorac Soc. 2011 Sep;8(5):438–43.

17. Riches DWH, Martin TR. Overview of Innate Lung Immunity and Inflammation. In: Humana Press, editor. Lung Innate Immunity and Inflammation. New York; 2018. p. 17–30.

18. World Health Organization. Pneumonia [Internet]. 2019. Available from: https://www.who.int/news-room/fact-sheets/detail/pneumonia

19. Mackenzie G. The definition and classification of pneumonia. Pneumonia. 2016;8(1):1–5.

20. Lanks CW, Musani AI, Hsia DW. Community-acquired Pneumonia and Hospital-acquired Pneumonia. Medical Clinics of North America. 2019;103(3):487–501.

21. Cillóniz C, Polverino E, Ewig S, Aliberti S, Gabarrús A, Menéndez R, et al. Impact of age and comorbidity on cause and outcome in community-acquired pneumonia. Chest. 2013;144(3):999–1007.

22. Torres A, Peetermans WE, Viegi G, Blasi F. Risk factors for community-acquired pneumonia in adults in Europe: A literature review. Thorax. 2013;68(11):1057–65.

23. Corrêa RDA, Costa AN, Lundgren F, Michelim L, Figueiredo MR, Holanda M. 2018_44_5_16_Portugues. 2018;44(5):405–23.

24. Troeger CE, Blacker BF, Khalil IA, Zimsen SRM, Albertson SB, Abate D, et al. Mortality, morbidity, and hospitalisations due to influenza lower respiratory tract infections, 2017: an analysis for the Global Burden of Disease Study 2017. Lancet Respir Med. 2019;7(1):69–89.

25. Musher DM, Abers MS, Bartlett JG. Evolving Understanding of the Causes of Pneumonia in Adults, with Special Attention to the Role of Pneumococcus. Clinical Infectious Diseases. 2017;65(10):1736–44.

26. Teng F, Liu X, Guo S Bin, Li Z, Ji WQ, Zhang F, et al. Community-acquired bacterial co-infection predicts severity and mortality in influenza-associated pneumonia admitted patients. Journal of Infection and Chemotherapy. 2019;25(2):129–36.

27. MacIntyre CR, Chughtai AA, Barnes M, Ridda I, Seale H, Toms R, et al. The role of pneumonia and secondary bacterial infection in fatal and serious outcomes of pandemic influenza a(H1N1)pdm09 11 Medical and Health Sciences 1103 Clinical Sciences 11 Medical and Health Sciences 1117 Public Health and Health Services. BMC Infect Dis. 2018;18(1):1–20.

28. Kalil AC, Metersky ML, Klompas M, Muscedere J, Sweeney DA, Palmer LB, et al. Executive Summary: Management of Adults With Hospital-acquired and Ventilator-associated Pneumonia: 2016 Clinical Practice Guidelines by the Infectious Diseases Society of America and the American Thoracic Society. Clinical Infectious Diseases. 2016;63(5):575–82.

29. Torres A, Niederman MS, Chastre J, Ewig S, Fernandez-Vandellos P, Hanberger H, et al. International ERS/ESICM/ESCMID/ALAT guidelines for the management of hospital-acquired pneumonia and ventilator-associated pneumonia. European Respiratory Journal. 2017;50(3).

30. Burgos J, Falcó V, Almirante B. Chemical pharmacotherapy for hospital-acquired pneumonia in the elderly. Expert Opin Pharmacother. 2019;20(4):423–34.

31. Quartin AA, Scerpella EG, Puttagunta S, Kett DH. A comparison of microbiology and demographics among patients with healthcare-associated, hospital-acquired, and ventilator-associated pneumonia: A retrospective analysis of 1184 patients from a large, international study. BMC Infect Dis. 2013;13(1):0–5.

32. Madden GR, Sifri CD. Antimicrobial Resistance to Agents Used for Staphylococcus aureus Decolonization : Is There a Reason for Concern ? 2018;

33. Giuliano KK, Baker D, Quinn B. The epidemiology of nonventilator hospital-acquired pneumonia in the United States. Am J Infect Control. 2018;46(3):322–7.

34. De la Calle C, Morata L, Cobos-Trigueros N, Martinez JA, Cardozo C, Mensa J, et al. Staphylococcus aureus bacteremic pneumonia. European Journal of Clinical Microbiology and Infectious Diseases. 2016;35(3):497–502.

35. Kollef MH, Shorr A, Tabak YP, Gupta V, Liu LZ, Johannes RS. Epidemiology and outcomes of health-care-associated pneumonia: Results from a large US database of culture-positive pneumonia. Chest. 2005;128(6):3854–62.

36. Pletz MW, Rohde GG, Welte T, Kolditz M, Ott S. Advances in the prevention, management, and treatment of community-acquired pneumonia. F1000Res. 2016;5(0):300.

37. Thammavongsa V, Kim HK, Missiakas D, Schneewind O. Staphylococcal manipulation of host immune responses. Nat Rev Microbiol. 2015;13(9):529–43.

38. Gómez MI, Lee A, Reddy B, Muir A, Soong G, Pitt A, et al. Staphylococcus aureus protein A induces airway epithelial inflammatory responses by activating TNFR1. Nat Med. 2004;10(8):842–8.

39. Guo Y, Song G, Sun M, Wang J, Wang Y. Prevalence and Therapies of Antibiotic-Resistance in Staphylococcus aureus. Front Cell Infect Microbiol. 2020 Mar 17;10.

40. Woods C, Colice G. Methicillin-resistant Staphylococcus aureus pneumonia in adults. Expert Rev Respir Med. 2014;8(5):641–51.

41. Cohen TS, Boland ML, Boland BB, Takahashi V, Tovchigrechko A, Lee Y, et al. S. aureus Evades Macrophage Killing through NLRP3-Dependent Effects on Mitochondrial Trafficking. Cell Rep. 2018;22(9):2431–41.

42. Becker REN, Berube BJ, Sampedro GR, Dedent AC, Bubeck Wardenburg J. Tissue-specific patterning of host innate immune responses by staphylococcus aureus α-Toxin. J Innate Immun. 2014;6(5):619–31.

43. Tuffs SW, James DBA, Bestebroer J, Richards AC, Goncheva MI, O'Shea M, et al. The Staphylococcus aureus superantigen SEIX is a bifunctional toxin that inhibits neutrophil function. PLoS Pathog. 2017;13(9):1–28.

44. de Jong NWM, van Kessel KPM, van Strijp JAG. Immune Evasion by Staphylococcus aureus. Microbiol Spectr. 2019 Mar 22;7(2).

45. Opitz B, van Laak V, Eitel J, Suttorp N. Innate immune recognition in infectious and noninfectious diseases of the lung. Am J Respir Crit Care Med. 2010 Jun 15;181(12):1294–309.

46. Balamayooran T, Balamayooran G, Jeyaseelan S. Review: Toll-like receptors and NOD-like receptors in pulmonary antibacterial immunity. Innate Immun. 2010 Jun;16(3):201–10.

47. Takeuchi O, Hoshino K, Akira S. Cutting Edge: TLR2-Deficient and MyD88-Deficient Mice Are Highly Susceptible to Staphylococcus aureus Infection. The Journal of Immunology. 2000 Nov 15;165(10):5392–6.

48. DeLeo FR, Diep BA, Otto M. Host Defense and Pathogenesis in Staphylococcus aureus Infections. Infect Dis Clin North Am. 2009;23(1):17–34.

49. Wang X, Thompson CD, Weidenmaier C, Lee JC. Release of Staphylococcus aureus extracellular vesicles and their application as a vaccine platform. Nat Commun. 2018;9(1):1379.

50. Sharff KA, Richards EP, Townes JM. Clinical management of septic arthritis. Curr Rheumatol Rep. 2013;15(6).

51. Torres A, Niederman MS, Chastre J, Ewig S, Fernandez-Vandellos P, Hanberger H, et al. International ERS/ESICM/ESCMID/ALAT guidelines for the management of hospital-acquired pneumonia and ventilator-associated pneumonia. European Respiratory Journal. 2017;50(3).

52. Pletz MW, Rohde GG, Welte T, Kolditz M, Ott S. Advances in the prevention, management, and treatment of community-acquired pneumonia. F1000Res. 2016;5(0):300.

53. Wu WF, Fang Q, He GJ. Efficacy of corticosteroid treatment for severe community-acquired pneumonia: A meta-analysis. Am J Emerg Med. 2018 Feb;36(2):179–84.

54. Liapikou A, Dimakou K, Toumbis M. Telavancin in the treatment of Staphylococcus aureus hospital-acquired and ventilator-associated pneumonia: Clinical evidence and experience. Ther Adv Respir Dis. 2016;10(4):368–78.

55. Chastre J, Wolff M, Fagon JY, Chevret S, Thomas F, Wermert D, et al. Comparison of 8 vs 15 Days of Antibiotic Therapy for Ventilator-Associated Pneumonia in Adults. JAMA. 2003 Nov 19;290(19):2588.

56. Arshad S, Hartman P, Zervos MJ. A novel treatment option for MRSA pneumonia: ceftaroline fosamil-yielding new hope in the fight against a persistent infection. Expert Rev Anti Infect Ther. 2014 Jul 5;12(7):727–9.

57. Zhou Y, Hou Y, Shen J, Huang Y, Martin W, Cheng F. Network-based drug repurposing for novel coronavirus 2019-nCoV/SARS-CoV-2. Cell Discov. 2020 Dec 16;6(1):14.

58. Körner RW, Majjouti M, Alejandre Alcazar MA, Mahabir E. Of mice and men: The coronavirus mhv and mouse models as a translational approach to understand sars-cov-2. Viruses. 2020;12(8):1–26.

59. Wu F, Zhao S, Yu B, Chen YM, Wang W, Song ZG, et al. A new coronavirus associated with human respiratory disease in China. Nature. 2020 Mar 12;579(7798):265–9.

60. Muralidar S, Ambi SV, Sekaran S, Krishnan UM. The emergence of COVID-19 as a global pandemic: Understanding the epidemiology, immune response and potential therapeutic targets of SARS-CoV-2. Biochimie. 2020;179:85–100.

61. Hannah R, Mathieu E, Rodés-Guirao L, Appel C, Giattino C, Ortiz-Ospina E, et al. COVID-19 Data Explorer [Internet]. Our World in Data. 2022 [cited 2022 May 24]. Available from: https://ourworldindata.org/explorers/coronavirus-data-explorer

62. Harrison AG, Lin T, Wang P. Mechanisms of SARS-CoV-2 Transmission and Pathogenesis. Trends Immunol. 2020;41(12):1100–15.

63. Otter JA, Donskey C, Yezli S, Douthwaite S, Goldenberg SD, Weber DJ. Transmission of SARS and MERS coronaviruses and influenza virus in healthcare settings: The possible role of dry surface contamination. Journal of Hospital Infection. 2016;92(3):235–50.

64. Comber L, O Murchu E, Drummond L, Carty PG, Walsh KA, De Gascun CF, et al. Airborne transmission of SARS-CoV-2 via aerosols. Rev Med Virol. 2021 May 26;31(3):8.

65. Bulfone TC, Malekinejad M, Rutherford GW, Razani N. Outdoor Transmission of SARS-CoV-2 and Other Respiratory Viruses: A Systematic Review. Journal of Infectious Diseases. 2021;223(4):550–61.

66. Huang C, Wang Y, Li X, Ren L, Zhao J, Hu Y, et al. Clinical features of patients infected with 2019 novel coronavirus in Wuhan, China. The Lancet. 2020;395(10223):497–506.

67. Hoffmann M, Kleine-Weber H, Schroeder S, Krüger N, Herrler T, Erichsen S, et al. SARS-CoV-2 Cell Entry Depends on ACE2 and TMPRSS2 and Is Blocked by a Clinically Proven Protease Inhibitor. Cell. 2020;181(2):271-280.e8.

68. Saad N, Moussa S. Immune response to COVID-19 infection: a double-edged sword. Immunol Med. 2021 Jul 3;44(3):187–96.

69. Fara A, Mitrev Z, Rosalia RA, Assas BM. Cytokine storm and COVID-19: a chronicle of pro-inflammatory cytokines. Open Biol. 2020 Sep 23;10(9):200160.

70. Bhaskar S, Sinha A, Banach M, Mittoo S, Weissert R, Kass JS, et al. Cytokine Storm in COVID-19—Immunopathological Mechanisms, Clinical Considerations, and Therapeutic Approaches: The REPROGRAM Consortium Position Paper. Front Immunol. 2020 Jul 10;11.

71. Ragab D, Salah Eldin H, Taeimah M, Khattab R, Salem R. The COVID-19 Cytokine Storm; What We Know So Far. Front Immunol. 2020 Jun 16;11.

72. Gavriatopoulou M, Ntanasis-Stathopoulos I, Korompoki E, Fotiou D, Migkou M, Tzanninis IG, et al. Emerging treatment strategies for COVID-19 infection. Clin Exp Med. 2021 May 30;21(2):167–79.

73. Stasi C, Fallani S, Voller F, Silvestri C. Treatment for COVID-19: An overview. Eur J Pharmacol. 2020;889(October):173644.

74. Fricke-Galindo I, Falfán-Valencia R. Pharmacogenetics approach for the improvement of covid-19 treatment. Vol. 13, Viruses. 2021.

75. Bok K, Sitar S, Graham BS, Mascola JR. Accelerated COVID-19 vaccine development: milestones, lessons, and prospects. Immunity. 2021;54(8):1636–51.

76. Dinnon KH, Leist SR, Schäfer A, Edwards CE, Martinez DR, Montgomery SA, et al. A mouse-adapted model of SARS-CoV-2 to test COVID-19 countermeasures. Nature. 2020;586(7830):560–6.

77. Andrade AC dos SP, Campolina-Silva GH, Queiroz-Junior CM, de Oliveira LC, Lacerda L de SB, Gaggino JCP, et al. A Biosafety Level 2 Mouse Model for Studying Betacoronavirus-Induced Acute Lung Damage and Systemic Manifestations. Schultz-Cherry S, editor. J Virol [Internet]. 2021 Oct 27;95(22):18. Available from: https://journals.asm.org/doi/10.1128/JVI.01276-21

78. Artika IM, Dewantari AK, Wiyatno A. Molecular biology of coronaviruses: current knowledge. Heliyon. 2020 Aug;6(e04743):22.

79. Cheever FS, Daniels JB, Pappenheimer AM, Bailey OT. A MURINE VIRUS (JHM) CAUSING DISSEMINATED ENCEPHALOMYELITIS WITH EXTENSIVE DESTRUCTION OF MYELIN. Journal of Experimental Medicine. 1949 Sep 1;90(3):181–94.

80. Macphee PJ, Dindzans VJ, Fung LS, Levy GA. Acute and chronic changes in the microcirculation of the liver in inbred strains of mice following infection with mouse hepatitis virus type 3. Hepatology. 1985 Jul;5(4):649–60.

81. Singh M, Khan RS, Dine K, Das Sarma J, Shindler KS. Intracranial Inoculation Is More Potent Than Intranasal Inoculation for Inducing Optic Neuritis in the Mouse Hepatitis Virus-Induced Model of Multiple Sclerosis. Front Cell Infect Microbiol. 2018 Sep 4;8.

82. Hartenian E, Nandakumar D, Lari A, Ly M, Tucker JM, Glaunsinger BA. The molecular virology of coronaviruses. Journal of Biological Chemistry. 2020 Sep;295(37):12910–34.

83. Barthold SW, Smith AL. Viremic dissemination of mouse hepatitis virus-JHM following intranasal inoculation of mice. Arch Virol. 1992 Mar;122(1–2):35–44.

84. Butt Y, Kurdowska A, Allen TC. Acute lung injury: A clinical and molecular review. Arch Pathol Lab Med. 2016;140(4):345–50.

85. Meyer NJ, Gattinoni L, Calfee CS. Acute respiratory distress syndrome. The Lancet. 2021 Aug;398(10300):622–37.

86. Matuschak GM, Lechner AJ. Acute lung injury and the acute respiratory distress syndrome. Mo Med. 2010;(August):154–71.

87. Johnson ER, Matthay MA. Acute Lung Injury: Epidemiology, Pathogenesis, and Treatment. J Aerosol Med Pulm Drug Deliv [Internet]. 2010 Aug;23(4):243–52. Available from: http://www.liebertpub.com/doi/10.1089/jamp.2009.0775

88. Huppert L, Matthay M, Ware L. Pathogenesis of Acute Respiratory Distress Syndrome. Semin Respir Crit Care Med. 2019 Feb 6;40(01):031–9.

89. Tu G wei, Shi Y, Zheng Y jun, Ju M jie, He H yu, Ma G guang, et al. Glucocorticoid attenuates acute lung injury through induction of type 2 macrophage. J Transl Med. 2017;15(1):1–11.

90. Fan E, Brodie D, Slutsky AS. Acute Respiratory Distress Syndrome. JAMA. 2018 Feb 20;319(7):698.

91. D'Alessio FR. Mouse models of acute lung injury and ARDS. Methods in Molecular Biology. 2018;1809:341–50.

92. Shen Y, Sun Z, Guo X. Citral inhibits lipopolysaccharide-induced acute lung injury by activating PPAR-γ. Eur J Pharmacol. 2015 Jan;747:45–51.

93. Zhang Z, Luo Z, Bi A, Yang W, An W, Dong X, et al. Compound edaravone alleviates lipopolysaccharide (LPS)-induced acute lung injury in mice. Eur J Pharmacol. 2017;811(May):1–11.

94. Gouwy M, Struyf S, Proost P, Van Damme J. Synergy in cytokine and chemokine networks amplifies the inflammatory response. Cytokine Growth Factor Rev. 2005;16(6):561–80.

95. Parsons PE, Matthay MA, Ware LB, Eisner MD. Elevated plasma levels of soluble TNF receptors are associated with morbidity and mortality in patients with acute lung injury. Am J Physiol Lung Cell Mol Physiol. 2005;288(3 32-3):426–31.

96. Tsai HC, Velichko S, Hung LY, Wu R. IL-17A and Th17 cells in lung inflammation: An update on the role of Th17 cell differentiation and IL-17R signaling in host defense against infection. Clin Dev Immunol. 2013;2013.

97. Gouda MM, Bhandary YP. Acute Lung Injury: IL-17A-Mediated Inflammatory Pathway and Its Regulation by Curcumin. Inflammation. 2019;42(4):1160–9.

98. Patel B V., Wilson MR, O'Dea KP, Takata M. TNF-Induced Death Signaling Triggers Alveolar Epithelial Dysfunction in Acute Lung Injury. The Journal of Immunology. 2013;190(8):4274–82.

99. Proudfoot A, Bayliffe A, O'Kane CM, Wright T, Serone A, Bareille PJ, et al. Novel anti-tumour necrosis factor receptor-1 (TNFR1) domain antibody prevents pulmonary inflammation in experimental acute lung injury. Thorax. 2018;73(8):723–30.

100. Wu CL, Lin LY, Yang JS, Chan MC, Hsueh CM. Attenuation of lipopolysaccharide-induced acute lung injury by treatment with IL-10. Respirology. 2009;14(4):511–21.

101. Inoue G. Effect of interleukin-10 (IL-10) on experimental LPS-induced acute lung injury. Journal of Infection and Chemotherapy. 2000;6(1):51–60.

102. David BA, Kubes P. Exploring the complex role of chemokines and chemoattractants in vivo on leukocyte dynamics. Immunol Rev. 2019;289(1):9–30.

103. Raman D, Sobolik-Delmaire T, Richmond A. Chemokines in health and disease. Exp Cell Res. 2011 Mar;317(5):575–89.

104. Kawaguchi N, Zhang TT, Nakanishi T. Involvement of CXCR4 in Normal and Abnormal Development. Cells. 2019 Feb 20;8(2):185.

105. Vilgelm AE, Richmond A. Chemokins modulate immune surveillance in tumorignesis, metastatsis, and response to immunotherapy. Front Immunol. 2019;10(FEB):6–8.

106. Zlotnik A, Yoshie O. The Chemokine Superfamily Revisited. Immunity. 2012 May;36(5):705–16.

107. Griffith JW, Sokol CL, Luster AD. Chemokines and Chemokine Receptors: Positioning Cells for Host Defense and Immunity. Annu Rev Immunol. 2014 Mar 21;32(1):659–702.

108. Bizzarri C, Beccari AR, Bertini R, Cavicchia MR, Giorgini S, Allegretti M. ELR+ CXC chemokines and their receptors (CXC chemokine receptor 1 and CXC chemokine receptor 2) as new therapeutic targets. Pharmacol Ther. 2006 Oct;112(1):139–49.

109. Hughes CE, Nibbs RJB. A guide to chemokines and their receptors. FEBS Journal. 2018;285(16):2944–71.

110. Steen A, Larsen O, Thiele S, Rosenkilde MM. Biased and G Protein-Independent Signaling of Chemokine Receptors. Front Immunol. 2014 Jun 23;5.

111. Zweemer AJM, Toraskar J, Heitman LH, IJzerman AP. Bias in chemokine receptor signalling. Trends Immunol. 2014 Jun;35(6):243–52.

112. Hilger D, Masureel M, Kobilka BK. Structure and dynamics of GPCR signaling complexes. Nat Struct Mol Biol. 2018 Jan 8;25(1):4–12.

113. Allen SJ, Crown SE, Handel TM. Chemokine:Receptor Structure, Interactions, and Antagonism. Annu Rev Immunol. 2007;25(1):787–820.

114. White GE, Iqbal AJ, Greaves DR. CC Chemokine Receptors and Chronic Inflammation—Therapeutic Opportunities and Pharmacological Challenges. Garland CJ, editor. Pharmacol Rev. 2013 Jan 8;65(1):47–89.

115. Hughes CE, Nibbs RJB. A guide to chemokines and their receptors. FEBS Journal. 2018;285(16):2944–71.

116. Dyer DP, Medina-Ruiz L, Bartolini R, Schuette F, Hughes CE, Pallas K, et al. Chemokine Receptor Redundancy and Specificity Are Context Dependent. Immunity. 2019;50(2):378-389.e5.

117. Yamada S, Sugahara K, Özbek S. Evolution of glycosaminoglycans. Commun Integr Biol. 2011 Mar 27;4(2):150–8.

118. Shi D, Sheng A, Chi L. Glycosaminoglycan-Protein Interactions and Their Roles in Human Disease. Front Mol Biosci. 2021 Mar 9;8.

119. Monneau Y, Arenzana-Seisdedos F, Lortat-Jacob H. The sweet spot: how GAGs help chemokines guide migrating cells. J Leukoc Biol. 2016 Jun;99(6):935–53.

120. Crijns H, Vanheule V, Proost P. Targeting Chemokine—Glycosaminoglycan Interactions to Inhibit Inflammation. Front Immunol [Internet]. 2020 Mar 31;11. Available from: https://www.frontiersin.org/article/10.3389/fimmu.2020.00483/full

121. Dyer DP, Salanga CL, Volkman BF, Kawamura T, Handel TM. The dependence of chemokine–glycosaminoglycan interactions on chemokine oligomerization. Glycobiology. 2015 Nov 17;26(3):312–326.

122. Ospelt C, Kurowska-Stolarska M, Neidhart M, Michel BA, Gay RE, Laufer S, et al. The dual inhibitor of lipoxygenase and cyclooxygenase ML3000 decreases the expression of CXCR3 ligands. Ann Rheum Dis. 2008 Apr;67(4):524–9.

123. Gao W, Topham PS, King JA, Smiley ST, Csizmadia V, Lu B, et al. Targeting of the chemokine receptor CCR1 suppresses development of acute and chronic cardiac allograft rejection. Journal of Clinical Investigation. 2000 Jan 1;105(1):35–44.

124. Andres PG, Beck PL, Mizoguchi E, Mizoguchi A, Bhan AK, Dawson T, et al. Mice with a Selective Deletion of the CC Chemokine Receptors 5 or 2 Are Protected from Dextran Sodium Sulfate-Mediated Colitis: Lack of CC Chemokine Receptor 5 Expression Results in a NK1.1 + Lymphocyte-Associated Th2-Type Immune Response in the Intestine. The Journal of Immunology. 2000 Jun 15;164(12):6303–12.

125. Tokuyama H, Ueha S, Kurachi M, Matsushima K, Moriyasu F, Blumberg RS, et al. The simultaneous blockade of chemokine receptors CCR2, CCR5 and CXCR3 by a non-peptide chemokine receptor antagonist protects mice from dextran sodium sulfate-mediated colitis. Int Immunol. 2005 Aug 1;17(8):1023–34.

126. Gong JH, Clark-Lewis I. Antagonists of monocyte chemoattractant protein 1 identified by modification of functionally critical NH2-terminal residues. Journal of Experimental Medicine. 1995 Feb 1;181(2):631–40.

127. Proudfoot AEI. Chemokine receptors: multifaceted therapeutic targets. Nat Rev Immunol. 2002 Feb;2(2):106–15.

128. Struyf S, Noppen S, Loos T, Mortier A, Gouwy M, Verbeke H, et al. Citrullination of CXCL12 Differentially Reduces CXCR4 and CXCR7 Binding with Loss of Inflammatory and Anti-HIV-1 Activity via CXCR4. The Journal of Immunology. 2009;182(1):666–74.

129. Boff D, Crijns H, Janssens R, Vanheule V, Menezes GB, Macari S, et al. The chemokine fragment CXCL9(74-103) diminishes neutrophil recruitment and joint inflammation in antigen-induced arthritis. J Leukoc Biol [Internet]. 2018 Aug;104(2):413–22. Available from: https://onlinelibrary.wiley.com/doi/10.1002/JLB.3MA1217-502R

130. Vanheule V, Crijns H, Poosti F, Ruytinx P, Berghmans N, Gerlza T, et al. Anti-inflammatory effects of the GAG-binding CXCL9(74-103) peptide in dinitrofluorobenzene-induced contact hypersensitivity in mice. Clinical & Experimental Allergy [Internet]. 2018 Oct;48(10):1333–44. Available from: https://onlinelibrary.wiley.com/doi/10.1111/cea.13227

131. Vanheule V, Boff D, Mortier A, Janssens R, Petri B, Kolaczkowska E, et al. CXCL9-Derived Peptides Differentially Inhibit Neutrophil Migration In Vivo through Interference with Glycosaminoglycan Interactions. Front Immunol [Internet]. 2017 May 10;8. Available from: http://journal.frontiersin.org/article/10.3389/fimmu.2017.00530/full

132. van Raemdonck K, van den Steen PE, Liekens S, van Damme J, Struyf S. CXCR3 ligands in disease and therapy. Cytokine Growth Factor Rev [Internet]. 2015 Jun;26(3):311–27. Available from: https://linkinghub.elsevier.com/retrieve/pii/S1359610114001634

133. Vestweber D. How leukocytes cross the vascular endothelium. Nat Rev Immunol. 2015;15(11):692–704.

134. Kolaczkowska E, Kubes P. Neutrophil recruitment and function in health and inflammation. Nat Rev Immunol. 2013;13(3):159–75.

135. Williams MR, Azcutia V, Newton G, Alcaide P, Luscinskas FW. Emerging mechanisms of neutrophil recruitment across endothelium. Trends Immunol. 2011 Oct;32(10):461–9.

136. Kirsebom FCM, Kausar F, Nuriev R, Makris S, Johansson C. Neutrophil recruitment and activation are differentially dependent on MyD88/TRIF and MAVS signaling during RSV infection. Mucosal Immunol. 2019 Sep 29;12(5):1244–55.

137. Zarbock A, Ley K. Neutrophil Adhesion and Activation under Flow. Microcirculation. 2009 Jan;16(1):31–42.

138. de Oliveira S, Rosowski EE, Huttenlocher A. Neutrophil migration in infection and wound repair: going forward in reverse. Nat Rev Immunol. 2016 Jun 27;16(6):378–91.

139. Filippi MD. Neutrophil transendothelial migration: updates and new perspectives. Blood. 2019 May 16;133(20):2149–58.

140. Daniel AE, van Buul JD. Endothelial Junction Regulation: A Prerequisite for Leukocytes Crossing the Vessel Wall. J Innate Immun. 2013;5(4):324–35.

141. Woodfin A, Voisin MB, Beyrau M, Colom B, Caille D, Diapouli FM, et al. The junctional adhesion molecule JAM-C regulates polarized transendothelial migration of neutrophils in vivo. Nat Immunol. 2011 Aug 26;12(8):761–9.

142. Basu S, Hodgson G, Katz M, Dunn AR. Evaluation of role of G-CSF in the production, survival, and release of neutrophils from bone marrow into circulation. Blood. 2002 Aug 1;100(3):854–61.

143. Galli SJ, Borregaard N, Wynn TA. Phenotypic and functional plasticity of cells of innate immunity: Macrophages, mast cells and neutrophils. Nat Immunol. 2011;12(11):1035–44.

144. Pillay J, den Braber I, Vrisekoop N, Kwast LM, de Boer RJ, Borghans JAM, et al. In vivo labeling with 2H2O reveals a human neutrophil lifespan of 5.4 days. Blood. 2010 Jul 29;116(4):625–7.

145. Li KW, Turner SM, Emson CL, Hellerstein MK, Dale DC. Deuterium and neutrophil kinetics. Blood. 2011 Jun 2;117(22):6052–3.

146. Tofts PS, Chevassut T, Cutajar M, Dowell NG, Peters AM. Doubts concerning the recently reported human neutrophil lifespan of 5.4 days. Blood. 2011 Jun 2;117(22):6050–2.

147. Dorward DA, Lucas CD, Chapman GB, Haslett C, Dhaliwal K, Rossi AG. The Role of Formylated Peptides and Formyl Peptide Receptor 1 in Governing Neutrophil Function during Acute Inflammation. Am J Pathol. 2015 May;185(5):1172–84.

148. Miyabe Y, Miyabe C, Murooka TT, Kim EY, Newton GA, Kim ND, et al. Complement C5a receptor is the key initiator of neutrophil adhesion igniting immune complex–induced arthritis. Sci Immunol. 2017 Jan 13;2(7).

149. ADAIRKIRK T, SENIOR R. Fragments of extracellular matrix as mediators of inflammation. Int J Biochem Cell Biol. 2008 Jun;40(6–7):1101–10.

150. Majumdar R, Tavakoli Tameh A, Arya SB, Parent CA. Exosomes mediate LTB4 release during neutrophil chemotaxis. Marrack P, editor. PLoS Biol. 2021 Jul 7;19(e3001271).

151. Brinkmann V, Reichard U, Goosmann C, Fauler B, Uhlemann Y, Weiss DS, et al. Neutrophil Extracellular Traps Kill Bacteria. Science (1979). 2004 Mar 5;303(5663):1532–5.

152. Borregaard N. Neutrophils, from Marrow to Microbes. Immunity. 2010 Nov;33(5):657–70.

153. Mortaz E, Alipoor SD, Adcock IM, Mumby S, Koenderman L. Update on neutrophil function in severe inflammation. Front Immunol. 2018;9(OCT):1–14.

154. Kobayashi SD, Malachowa N, DeLeo FR. Neutrophils and Bacterial Immune Evasion. J Innate Immun. 2018;10(5–6):432–41.

155. Flannagan RS, Jaumouillé V, Grinstein S. The Cell Biology of Phagocytosis. Annual Review of Pathology: Mechanisms of Disease. 2012 Feb 28;7(1):61–98.

156. Nordenfelt P, Tapper H. Phagosome dynamics during phagocytosis by neutrophils. J Leukoc Biol. 2011 Aug;90(2):271–84.

157. Lawrence SM, Corriden R, Nizet V. The Ontogeny of a Neutrophil: Mechanisms of Granulopoiesis and Homeostasis. Microbiology and Molecular Biology Reviews. 2018 Mar;82(1).

158. Borregaard N, Cowland JB. Granules of the Human Neutrophilic Polymorphonuclear Leukocyte. Blood. 1997 May 15;89(10):3503–21.

159. Rørvig S, Østergaard O, Heegaard NHH, Borregaard N. Proteome profiling of human neutrophil granule subsets, secretory vesicles, and cell membrane: correlation with transcriptome profiling of neutrophil precursors. J Leukoc Biol. 2013 Oct;94(4):711–21.

160. van Kessel KPM, Bestebroer J, van Strijp JAG. Neutrophil-Mediated Phagocytosis of Staphylococcus aureus. Front Immunol. 2014 Sep 26;5.

161. Naumenko V, Turk M, Jenne CN, Kim SJ. Neutrophils in viral infection. Cell Tissue Res. 2018 Mar 11;371(3):505–16.

162. Feigin RD, Shackelford PG. Value of Repeat Lumbar Puncture in the Differential Diagnosis of Meningitis. New England Journal of Medicine. 1973 Sep 13;289(11):571–4.

163. Stevens DA, Ferrington RA, Jordan GW, Merigan TC. Cellular Events in Zoster Vesicles: Relation to Clinical Course and Immune Parameters. Journal of Infectious Diseases. 1975 May 1;131(5):509–15.

164. Smith P, Wang SZ, Dowling K, Forsyth K. Leucocyte populations in respiratory syncytial virus-induced bronchiolitis. J Paediatr Child Health. 2001 Apr 10;37(2):146–51.

165. Perrone LA, Plowden JK, García-Sastre A, Katz JM, Tumpey TM. H5N1 and 1918 Pandemic Influenza Virus Infection Results in Early and Excessive Infiltration of Macrophages and Neutrophils in the Lungs of Mice. Baric RS, editor. PLoS Pathog. 2008 Aug 1;4(e1000115).

166. Reading PC, Bozza S, Gilbertson B, Tate M, Moretti S, Job ER, et al. Antiviral Activity of the Long Chain Pentraxin PTX3 against Influenza Viruses. The Journal of Immunology. 2008 Mar 1;180(5):3391–8.

167. Costa S, Bevilacqua D, Cassatella MA, Scapini P. Recent advances on the crosstalk between neutrophils and B or T lymphocytes. Immunology. 2019 Jan;156(1):23–32.

168. Barr FD, Ochsenbauer C, Wira CR, Rodriguez-Garcia M. Neutrophil extracellular traps prevent HIV infection in the female genital tract. Mucosal Immunol. 2018 Sep 6;11(5):1420–8.

169. Borges L, Pithon-Curi TC, Curi R, Hatanaka E. COVID-19 and Neutrophils: The Relationship between Hyperinflammation and Neutrophil Extracellular Traps. Vago J, editor. Mediators Inflamm. 2020 Dec 2;2020:1–7.

170. Galani IE, Andreakos E. Neutrophils in viral infections: Current concepts and caveats. J Leukoc Biol. 2015 Oct 1;98(4):557–64.

171. Kruger P, Saffarzadeh M, Weber ANRR, Rieber N, Radsak M, von Bernuth H, et al. Neutrophils: Between Host Defence, Immune Modulation, and Tissue Injury. Dehio C, editor. PLoS Pathog [Internet]. 2015 Mar 12;11(e1004651). Available from: https://dx.plos.org/10.1371/journal.ppat.1004651

172. Narasaraju T, Yang E, Samy RP, Ng HH, Poh WP, Liew AA, et al. Excessive Neutrophils and Neutrophil Extracellular Traps Contribute to Acute Lung Injury of Influenza Pneumonitis. Am J Pathol. 2011 Jul;179(1):199–210.

173. Fox S, Leitch AE, Duffin R, Haslett C, Rossi AG. Neutrophil apoptosis: Relevance to the innate immune response and inflammatory disease. J Innate Immun. 2010;2(3):216–27.

174. Greenlee-Wacker MC. Clearance of apoptotic neutrophils and resolution of inflammation. Immunol Rev. 2016;273(1):357–70.

175. Hillion S, Arleevskaya MI, Blanco P, Bordron A, Brooks WH, Cesbron JY, et al. The Innate Part of the Adaptive Immune System. Clin Rev Allergy Immunol. 2020 Apr 1;58(2):151–4.

176. Bonilla FA, Oettgen HC. Adaptive immunity. Journal of Allergy and Clinical Immunology. 2010 Feb;125(2):S33–40.

177. Stein J V., Nombela-Arrieta C. Chemokine control of lymphocyte trafficking: A general overview. Immunology. 2005;116(1):1–12.

178. Laufer JM, Legler DF. Beyond migration—Chemokines in lymphocyte priming, differentiation, and modulating effector functions. J Leukoc Biol. 2018;104(2):301–12.

179. Karauzum H, Datta SK. Adaptive immunity against Staphylococcus aureus. Curr Top Microbiol Immunol. 2017;5(3):629–34.

180. Guillén C, McInnes IB, Vaughan DM, Kommajosyula S, Van Berkel PHC, Leung BP, et al. Enhanced Th1 response to Staphylococcus aureus infection in human lactoferrin-transgenic mice. J Immunol. 2002 Apr 15;168(8):3950–7.

181. Diep BA, Le VTM, Badiou C, Le HN, Pinheiro MG, Duong AH, et al. IVIG-mediated protection against necrotizing pneumonia caused by MRSA. Sci Transl Med. 2016 Sep 21;8(357).

182. Tomioka H, Tatano Y, Shimizu T, Sano C. Immunoadjunctive Therapy against Bacterial Infections Using Herbal Medicines Based on Th17 Cell-mediated Protective Immunity. Curr Pharm Des. 2021 Oct 25;27(38):3949–62.

183. Schmaler M, Jann NJ, Ferracin F, Landmann R. T and B Cells Are Not Required for Clearing Staphylococcus aureus in Systemic Infection Despite a Strong TLR2–MyD88-Dependent T Cell Activation . The Journal of Immunology. 2011;186(1):443–52.

184. Sun J, Madan R, Karp CL, Braciale TJ. Effector T cells control lung inflammation during acute influenza virus infection by producing IL-10. Nat Med. 2009;15(3):277–84.

185. Wang L, Wang X, Tong L, Wang J, Dou M, Ji S, et al. Recovery from acute lung injury can be regulated via modulation of regulatory T cells and Th17 cells. Scand J Immunol [Internet]. 2018 Nov;88(5):1–13. Available from: https://onlinelibrary.wiley.com/doi/10.1111/sji.12715

186. D'Alessio FR, Tsushima K, Aggarwal NR, West EE, Willett MH, Britos MF, et al. CD4+CD25+Foxp3+ Tregs resolve experimental lung injury in mice and are present in humans with acute lung injury. Journal of Clinical Investigation. 2009;119(10):2898–913.

187. Holt PG, Strickland DH, Wikström ME, Jahnsen FL. Regulation of immunological homeostasis in the respiratory tract. Nat Rev Immunol. 2008 Feb;8(2):142–52.

188. Cheng P, Li S, Chen H. Macrophages in Lung Injury, Repair, and Fibrosis. Cells. 2021;10(2):1–17.

189. Byrne AJ, Mathie SA, Gregory LG, Lloyd CM. Pulmonary macrophages: Key players in the innate defence of the airways. Vol. 70, Thorax. 2015. p. 1189–96.

190. Laskin DL, Malaviya R, Laskin JD. Role of Macrophages in Acute Lung Injury and Chronic Fibrosis Induced by Pulmonary Toxicants. Vol. 168, Toxicological Sciences. 2019. p. 287–301.

191. Hamilton RF, Thakur SA, Mayfair JK, Holian A. MARCO Mediates Silica Uptake and Toxicity in Alveolar Macrophages from C57BL/6 Mice. 2006;

192. Song L, Weng D, Dai W, Tang W, Chen S, Li C, et al. Th17 can regulate silica-induced lung inflammation through an IL-1β-dependent mechanism. J Cell Mol Med. 2014;18(9):1773–84.

193. Liu H, Fang S, Wang W, Cheng Y, Zhang Y, Liao H, et al. Macrophage-derived MCPIP1 mediates silica-induced pulmonary fibrosis via autophagy. 2016;

194. Wang L, Scabilloni JF, Antonini JM, Rojanasakul Y, Castranova V, Mercer RR. Induction of secondary apoptosis, inflammation, and lung fibrosis after intratracheal instillation of apoptotic cells in rats. Am J Physiol Lung Cell Mol Physiol. 2006;290:695–702.

195. Liu H, Cheng Y, Yang J, Wang W, Fang S, Zhang W, et al. BBC3 in macrophages promoted pulmonary fibrosis development through inducing autophagy during silicosis. Cell Death Dis. 2017;8(3).

196. Tan S, Chen S. Macrophage Autophagy and Silicosis: Current Perspective and Latest Insights. Int J Mol Sci. 2021 Jan 5;22(1):453.

197. Lech M, Anders HJ. Macrophages and fibrosis: How resident and infiltrating mononuclear phagocytes orchestrate all phases of tissue injury and repair. Biochimica et Biophysica Acta (BBA) - Molecular Basis of Disease. 2013 Jul;1832(7):989–97.

198. Wallace AM, Sandford AJ, English JC, Burkett KM, Li H, Finley RJ, et al. COPD: Journal of Chronic Obstructive Pulmonary Disease Matrix Metalloproteinase Expression by Human Alveolar Macrophages in Relation to Emphysema. 2009;

199. Iizuka T, Ishii Y, Itoh K, Kiwamoto T, Kimura T, Matsuno Y, et al. Nrf2-deficient mice are highly susceptible to cigarette smoke-induced emphysema. Genes to Cells. 2005;10(12):1113–25.

200. Grumelli S, Corry DB, Song LZ, Song L, Green L, Huh J, et al. An Immune Basis for Lung Parenchymal Destruction in Chronic Obstructive Pulmonary Disease and Emphysema. 2004;

201. Houghton AMG, Quintero PA, Perkins DL, Kobayashi DK, Kelley DG, Marconcini LA, et al. Elastin fragments drive disease progression in a murine model of emphysema. Journal of Clinical Investigation. 2006;116(3):753–9.

202. Rønnow SR, Langholm LL, Sand JMB, Thorlacius-Ussing J, Leeming DJ, Manon-Jensen T, et al. Specific elastin degradation products are associated with poor outcome in the ECLIPSE COPD cohort. Sci Rep. 2019;9(1).

203. Zhou J Sen, Li ZY, Xu XC, Zhao Y, Wang Y, Chen HP, et al. Cigarette smoke-initiated autoimmunity facilitates sensitisation to elastin-induced COPD-like pathologies in mice. European Respiratory Journal. 2020;56(3).

204. Liegeois M, Legrand C, Desmet CJ, Marichal T, Bureau F. The interstitial macrophage: A long-neglected piece in the puzzle of lung immunity. Cell Immunol [Internet]. 2018 Aug [cited 2021 Jun 20];330:91–6. Available from: www.elsevier.com/locate/ycimm

205. Bedoret D, Wallemacq H, Marichal T, Desmet C, Calvo FQ, Henry E, et al. Lung interstitial macrophages alter dendritic cell functions to prevent airway allergy in mice. J Clin Invest. 2009;119:3723.

206. Toussaint M, Fievez L, Drion P v, Cataldo D, Bureau F, Lekeux P, et al. Myeloid hypoxia-inducible factor 1α prevents airway allergy in mice through macrophage-mediated immunoregulation. Mucosal Immunol. 2013 May 12;6(3):485–97.

207. Schyns J, Bureau F, Marichal T. Lung Interstitial Macrophages: Past, Present, and Future. J Immunol Res [Internet]. 2018;2018(1):1–10. Available from: https://doi.org/10.1155/2018/5160794

208. Locati M, Mantovani A, Sica A. Macrophage Activation and Polarization as an Adaptive Component of Innate Immunity. 1st ed. Vol. 120, Advances in Immunology. Elsevier Inc.; 2013. 163–184 p.

209. Murray PJ. Macrophage Polarization. Annu Rev Physiol. 2017;79:541–66.

210. Wang N, Liang H, Zen K. Molecular mechanisms that influence the macrophage M1-M2 polarization balance. Vol. 5, Frontiers in Immunology. 2014.

211. Fubini B, Hubbard A. Reactive oxygen species (ROS) and reactive nitrogen species (RNS) generation by silica in inflammation and fibrosis. Free Radic Biol Med. 2003 Jun;34(12):1507–16.

212. Castranova V. Signaling Pathways Controlling The Production Of Inflammatory Mediators in Response To Crystalline Silica Exposure: Role Of Reactive Oxygen/Nitrogen Species. Free Radic Biol Med. 2004 Oct;37(7):916–25.

213. Li H, Yang T, Ning Q, Li F, Chen T, Yao Y, et al. Cigarette smoke extract-treated mast cells promote alveolar macrophage infiltration and polarization in experimental chronic obstructive pulmonary disease. Inhal Toxicol. 2015;27(14):822–31.

214. Kaku Y, Imaoka H, Morimatsu Y, Komohara Y, Ohnishi K, Oda H, et al. Overexpression of CD163, CD204 and CD206 on alveolar macrophages in the lungs of patients with severe chronic obstructive pulmonary disease. PLoS One. 2014;9(1):87400.

215. Eapen MS, Hansbro PM, McAlinden K, Kim RY, Ward C, Hackett TL, et al. Abnormal M1/M2 macrophage phenotype profiles in the small airway wall and lumen in smokers and chronic obstructive pulmonary disease (COPD). Sci Rep. 2017 Dec 17;7(1):13392.

216. Athari SS. Targeting cell signaling in allergic asthma. Vol. 4, Signal Transduction and Targeted Therapy. 2019.

217. Makita N, Hizukuri Y, Yamashiro K, Murakawa M, Hayashi Y. IL-10 enhances the phenotype of M2 macrophages induced by IL-4 and confers the ability to increase eosinophil migration. Int Immunol. 2015;27(3):131–41.

218. Draijer C, Boorsma CE, Robbe P, Timens W, Hylkema MN, Ten Hacken NH, et al. Human asthma is characterized by more IRF5+ M1 and CD206+ M2 macrophages and less IL-10+ M2-like macrophages around airways compared with healthy airways. Journal of Allergy and Clinical Immunology. 2017 Jul;140(1):280-283.e3.

219. Vance RE, Isberg RR, Portnoy DA. Patterns of Pathogenesis: Discrimination of Pathogenic and Nonpathogenic Microbes by the Innate Immune System. Cell Host Microbe. 2009;6(1):10–21.

220. Rehwinkel J, Tan CP, Goubau D, Schulz O, Pichlmair A, Bier K, et al. RIG-I Detects Viral Genomic RNA during Negative-Strand RNA Virus Infection. Cell. 2010;140(3):397–408.

221. Wang JP, Bowen GN, Padden C, Cerny A, Finberg RW, Newburger PE, et al. Toll-like receptor-mediated activation of neutrophils by influenza A virus. Blood. 2008;112(5):2028–34.

222. Kirby AC, Raynes JG, Kaye PM. The role played by tumor necrosis factor during localized and systemic infection with Streptococcus pneumoniae. Journal of Infectious Diseases. 2005;191(9):1538–47.

223. Julkunen I, Sareneva T, Pirhonen J, Ronni T, Melén K, Matikainen S. Molecular pathogenesis of influenza A virus infection and virus-induced regulation of cytokine gene expression. Cytokine Growth Factor Rev. 2001;12(2–3):171–80.

224. Divangahi M, King IL, Pernet E. Alveolar macrophages and type I IFN in airway homeostasis and immunity. Trends Immunol. 2015;36(5):307–14.

225. Pidwill GR, Gibson JF, Cole J, Renshaw SA, Foster SJ. The Role of Macrophages in Staphylococcus aureus Infection. Front Immunol. 2021;11(January):1–30.

226. Gonzalez-Ferrer S, Peñaloza HF, Budnick JA, Bain WG, Nordstrom HR, Lee JS, et al. Finding order in the chaos: Outstanding questions in Klebsiella pneumoniae Pathogenesis. Infect Immun. 2021;89(4).

227. Corleis B, Dorhoi A. Early dynamics of innate immunity during pulmonary tuberculosis. Immunol Lett. 2020;221(November 2019):56–60.

228. Kelly AM, McLoughlin RM. Target the Host, Kill the Bug; Targeting Host Respiratory Immunosuppressive Responses as a Novel Strategy to Improve Bacterial Clearance During Lung Infection. Front Immunol. 2020;11(April).

229. Wang J, Nikrad MP, Travanty EA, Zhou B, Phang T, Gao B, et al. Innate immune response of human alveolar macrophages during influenza a infection. PLoS One. 2012;7(3).

230. Dalskov L, Møhlenberg M, Thyrsted J, Blay-Cadanet J, Poulsen ET, Folkersen BH, et al. SARS-CoV-2 evades immune detection in alveolar macrophages. EMBO Rep. 2020;21(12):1–10.

231. Gracia-Hernandez M, Sotomayor EM, Villagra A. Targeting Macrophages as a Therapeutic Option in Coronavirus Disease 2019. Front Pharmacol. 2020;11(October):1–16.

232. Wager CML, Wormley FL. Classical versus alternative macrophage activation: The Ying and the Yang in host defense against pulmonary fungal infections. Mucosal Immunol. 2014;7(5):1023–35.

233. Williams PB, Barnes CS, Portnoy JM, Baxi S, Grimes C, Horner WE, et al. Innate and Adaptive Immune Response to Fungal Products and Allergens. Journal of Allergy and Clinical Immunology: In Practice. 2016;4(3):386–95.

234. Morais EA, Chame DF, Melo EM, de Carvalho Oliveira JA, de Paula ACC, Peixoto AC, et al. TLR 9 involvement in early protection induced by immunization with rPb27 against Paracoccidioidomycosis. Microbes Infect. 2016;18(2):137–47.

235. Bartemes KR, Kita H. Innate and adaptive immune responses to fungi in the airway. Journal of Allergy and Clinical Immunology. 2018;142(2):353–63.

236. Gilbert AS, Wheeler RT, May RC. Fungal pathogens: Survival and replication within macrophages. Cold Spring Harb Perspect Med. 2015;5(7):1–14.

237. Leseigneur C, Lê-Bury P, Pizarro-Cerdá J, Dussurget O. Emerging Evasion Mechanisms of Macrophage Defenses by Pathogenic Bacteria. Front Cell Infect Microbiol. 2020;10(September):1–9.

238. Thakur A, Mikkelsen H, Jungersen G. Intracellular pathogens: Host immunity and microbial persistence strategies. J Immunol Res. 2019;2019.

239. Netea MG, Domínguez-Andrés J, Barreiro LB, Chavakis T, Divangahi M, Fuchs E, et al. Defining trained immunity and its role in health and disease. Nat Rev Immunol. 2020 Jun 4;20(6):375–88.

240. Buckley CD, Gilroy DW, Serhan CN, Stockinger B, Tak PP. The resolution of inflammation. Nat Rev Immunol [Internet]. 2013;13(1):59–66. Available from: http://dx.doi.org/10.1038/nri3362

241. Lucas CD, Dorward DA, Tait MA, Fox S, Marwick JA, Allen KC, et al. Downregulation of Mcl-1 has anti-inflammatory pro-resolution effects and enhances bacterial clearance from the lung. Mucosal Immunol [Internet]. 2014;7(4):857–68. Available from: http://dx.doi.org/10.1038/mi.2013.102

242. Fullerton JN, Gilroy DW. Resolution of inflammation: A new therapeutic frontier. Nat Rev Drug Discov [Internet]. 2016;15(8):551–67. Available from: http://dx.doi.org/10.1038/nrd.2016.39

243. Schett G, Neurath MF. Resolution of chronic inflammatory disease: universal and tissue-specific concepts. Nat Commun [Internet]. 2018;9(1). Available from: http://dx.doi.org/10.1038/s41467-018-05800-6

244. Levy BD, Serhan CN. Resolution of Acute Inflammation in the Lung. Annu Rev Physiol [Internet]. 2014;76(1):467–92. Available from: http://www.annualreviews.org/doi/10.1146/annurev-physiol-021113-170408

245. Sugimoto MA, Ribeiro ALC, Costa BRC, Vago JP, Lima KM, Carneiro FS, et al. Phagocytes, granulocytes, & myelopoiesis: Plasmin & plasminogen induce macrophage

reprogramming & regulate key steps of inflammation resolution via annexin A1. Blood. 2017;129(21):2896–907.

246. Kaur M, Bell T, Salek-Ardakani S, Hussell T. Macrophage adaptation in airway inflammatory resolution. European Respiratory Review [Internet]. 2015;24(137):510–5. Available from: http://dx.doi.org/10.1183/16000617.0030-2015

247. Otsuka K, Yamada K, Taquahashi Y, Arakaki R, Ushio A, Saito M, et al. Long-Term polarization of alveolar macrophages to a profibrotic phenotype after inhalation exposure to multi-wall carbon nanotubes. PLoS One. 2018;13(10):1–18.

248. Lichtnekert J, Kawakami T, Parks WC, Duffield JS. Changes in macrophage phenotype as the immune response evolves. Curr Opin Pharmacol [Internet]. 2013;13(4):555–64. Available from: http://dx.doi.org/10.1016/j.coph.2013.05.013

249. Dalli J, Serhan CN. Specific lipid mediator signatures of human phagocytes : microparticles stimulate macrophage efferocytosis and pro-resolving mediators. 2012;120(15):60–72.

250. Kearns MT, Barthel L, Bednarek JM, Yunt ZX, Henson PM, Janssen WJ. Fas ligand-expressing lymphocytes enhance alveolar macrophage apoptosis in the resolution of acute pulmonary inflammation. Am J Physiol Lung Cell Mol Physiol. 2014;307(1):62–70.

251. Malyshkina A, Littwitz-salomon E, Sutter K, Zelinskyy G, Windmann S, Schimmer S, et al. Fas Ligand-mediated cytotoxicity of CD4 + T cells during chronic retrovirus infection. Sci Rep [Internet]. 2017;(July):1–10. Available from: http://dx.doi.org/10.1038/s41598-017-08578-7

252. Gagliani N, Amezcua Vesely MC, Iseppon A, Brockmann L, Xu H, Palm NW, et al. TH17 cells transdifferentiate into regulatory T cells uring resolution of inflammation. Nature. 2015;523(7559):221–5.

253. Alessio FRD, Mcdyer JF, King LS, Alessio FRD, Tsushima K, Aggarwal NR, et al. lung injury in mice and are present in humans with acute lung injury Find the latest version : experimental lung injury in mice and are present in humans with acute lung injury. 2009;119(10):2898–913.

254. Weirather J, Hofmann UDW, Beyersdorf N, Ramos GC, Vogel B, Frey A, et al. Foxp3+ CD4+ T cells improve healing after myocardial infarction by modulating monocyte/macrophage differentiation. Circ Res. 2014;115(1):55–67.

255. Newson J, Stables M, Karra E, Arce-Vargas F, Quezada S, Motwani M, et al. Resolution of acute inflammation bridges the gap between innate and adaptive immunity. Blood. 2014;124(11):1748–64.

256. Rajakariar R, Lawrence T, Bystrom J, Hilliard M, Colville-Nash P, Bellingan G, et al. Novel biphasic role for lymphocytes revealed during resolving inflammation. Blood. 2008;111(8):4184–92.

257. LAROSA D, ORANGE J. Lymphocytes. Journal of Allergy and Clinical Immunology. 2008 Feb;121(2):S364–9.

258. Sanaei MJ, Nahid-Samiei M, Abadi MSS, Arjmand MH, Ferns GA, Bashash D, et al. New insights into regulatory B cells biology in viral, bacterial, and parasitic infections. Infection, Genetics and Evolution. 2021 Apr;89:104753.

259. Proto JD, Doran AC, Gusarova G, Yurdagul A, Sozen E, Subramanian M, et al. Regulatory T Cells Promote Macrophage Efferocytosis during Inflammation Resolution. Immunity [Internet]. 2018;49(4):666-677.e6. Available from: https://linkinghub.elsevier.com/retrieve/pii/S1074761318303352

260. Oo YH, Shetty S, Adams DH. The Role of Chemokines in the Recruitment of Lymphocytes to the Liver. Digestive Diseases. 2010;28(1):31–44.

261. Andalib A, Doulabi H, Hasheminia S, Maracy M, Rezaei A. CCR3, CCR4, CCR5, and CXCR3 receptor expression in peripheral blood CD4 $^{+}$ lymphocytes in patients with gastric cancer. Adv Biomed Res. 2013;2(1):31.

262. Sato T, Thorlacius H, Johnston B, Staton TL, Xiang W, Littman DR, et al. Role for CXCR6 in Recruitment of Activated CD8 $^{+}$ Lymphocytes to Inflamed Liver. The Journal of Immunology. 2005 Jan 1;174(1):277–83.

263. Hu JK, Kagari T, Clingan JM, Matloubian M. Expression of chemokine receptor CXCR3 on T cells affects the balance between effector and memory CD8 T-cell generation. Proceedings of the National Academy of Sciences. 2011 May 24;108(21).

264. Matute-Bello G, Frevert CW, Martin TR. Animal models of acute lung injury. American Journal of Physiology-Lung Cellular and Molecular Physiology. 2008 Sep;295(3):L379–99.

265. Williams AE, Chambers RC. The mercurial nature of neutrophils: Still an enigma in ARDS? Am J Physiol Lung Cell Mol Physiol. 2014;306(3).

266. Huang X, Xiu H, Zhang S, Zhang G. The Role of Macrophages in the Pathogenesis of ALI/ARDS. Mediators Inflamm [Internet]. 2018 May 13;2018(12):1–8. Available from: https://www.hindawi.com/journals/mi/2018/1264913/

267. Lukacs NW, Strieter RM, Chensue SW, Widmer M, Kunkel SL. TNF-alpha mediates recruitment of neutrophils and eosinophils during airway inflammation. The Journal of Immunology. 1995;154(10).

268. McAleer JP, Kolls JK. Mechanisms controlling Th17 cytokine expression and host defense. J Leukoc Biol [Internet]. 2011 Aug [cited 2022 Oct 28];90(2):263–70. Available from: https://pubmed.ncbi.nlm.nih.gov/21486905/

269. Kawano H, Kayama H, Nakama T, Hashimoto T, Umemoto E, Takeda K. IL-10-producing lung interstitial macrophages prevent neutrophilic asthma. Int Immunol [Internet]. 2016 Oct [cited 2021 Jun 21];28(10):489–501. Available from: https://academic.oup.com/intimm/article/28/10/489/2614107

270. Huynh MLN, Fadok VA, Henson PM. Phosphatidylserine-dependent ingestion of apoptotic cells promotes TGF-β1 secretion and the resolution of inflammation. Journal of Clinical Investigation. 2002;109(1):41–50.

271. Bhatia M, Zemans RL, Jeyaseelan S. Role of chemokines in the pathogenesis of acute lung injury. Am J Respir Cell Mol Biol [Internet]. 2012 May [cited 2022 Oct 30];46(5):566–72. Available from: www.atsjournals.org

272. Marques RE, Guabiraba R. Remo Castro Russo & Mauro Martins Teixeira (2013) Targeting CCL5 in inflammation. Expert Opin Ther Targets [Internet]. 2013 [cited 2022 Oct 30];17:1439–60. Available from: https://www.tandfonline.com/action/journalInformation?journalCode=iett20

273. Sato T, Thorlacius H, Johnston B, Staton TL, Xiang W, Littman DR, et al. Role for CXCR6 in Recruitment of Activated CD8 $^{+}$ Lymphocytes to Inflamed Liver. The Journal of Immunology. 2005 Jan 1;174(1):277–83.

274. Ashhurst AS, Flórido M, Lin LCW, Quan D, Armitage E, Stifter SA, et al. CXCR6-Deficiency Improves the Control of Pulmonary Mycobacterium tuberculosis and Influenza Infection Independent of T-Lymphocyte Recruitment to the Lungs. Front Immunol. 2019 Mar 7;10.

275. Bocchino V, Bertorelli G, Bertrand CP, Ponath PD, Newman W, Franco C, et al. Eotaxin and CCR3 are up-regulated in exacerbations of chronic bronchitis. Allergy. 2002 Jan;57(1):17–22.

276. Sallusto F, Lenig D, Mackay CR, Lanzavecchia A. Flexible Programs of Chemokine Receptor Expression on Human Polarized T Helper 1 and 2 Lymphocytes. Journal of Experimental Medicine. 1998 Mar 16;187(6):875–83.

277. von Andrian UH, Mackay CR. T-Cell Function and Migration — Two Sides of the Same Coin. New England Journal of Medicine. 2000 Oct 5;343(14):1020–34.

278. Karni A, Balashov K, Hancock WW, Bharanidharan P, Abraham M, Khoury SJ, et al. Cyclophosphamide modulates CD4+ T cells into a T helper type 2 phenotype and reverses increased IFN-γ production of CD8+ T cells in secondary progressive multiple sclerosis. J Neuroimmunol. 2004 Jan;146(1–2):189–98.

279. Santucci MB. Expansion of CCR5+ CD4+ T-lymphocytes in the course of active pulmonary tuberculosis. European Respiratory Journal. 2004 Oct 1;24(4):638–43.

280. Wang X, Russell-Lodrigue KE, Ratterree MS, Veazey RS, Xu H. Chemokine receptor CCR5 correlates with functional CD8 $^{+}$ T cells in SIV-infected macaques and the

potential effects of maraviroc on T-cell activation. The FASEB Journal. 2019 Aug 29;33(8):8905–12.

281. Levy BD, Vachier I, Serhan CN. Resolution of Inflammation in Asthma. Clin Chest Med [Internet]. 2012;33(3):559–70. Available from: http://dx.doi.org/10.1016/j.ccm.2012.06.006

282. Martin KR, Ohayon D, Witko-Sarsat V. Promoting apoptosis of neutrophils and phagocytosis by macrophages: Novel strategies in the resolution of inflammation. Swiss Med Wkly. 2015;145(February):1–10.

283. Herold S, Mayer K, Lohmeyer J. Acute Lung Injury: How Macrophages Orchestrate Resolution of Inflammation and Tissue Repair. Front Immunol [Internet]. 2011;2(65):1–13. Available from: http://journal.frontiersin.org/article/10.3389/fimmu.2011.00065/abstract

284. D'Alessio FR, Tsushima K, Aggarwal NR, West EE, Willett MH, Britos MF, et al. CD4+CD25+Foxp3+ Tregs resolve experimental lung injury in mice and are present in humans with acute lung injury. Journal of Clinical Investigation. 2009 Oct 1;119(10):2898–913.

285. Arpaia N, Green JA, Moltedo B, Arvey A, Hemmers S, Yuan S, et al. A Distinct Function of Regulatory T Cells in Tissue Protection. Cell [Internet]. 2015;162(5):1078–89. Available from: http://dx.doi.org/10.1016/j.cell.2015.08.021

286. Buckley CD, Gilroy DW, Serhan CN. Proresolving Lipid Mediators and Mechanisms in the Resolution of Acute Inflammation. Immunity. 2014 Mar;40(3):315–27.

287. Elliott JI, Surprenant A, Marelli-Berg FM, Cooper JC, Cassady-Cain RL, Wooding C, et al. Membrane phosphatidylserine distribution as a non-apoptotic signalling mechanism in lymphocytes. Nat Cell Biol. 2005 Aug 17;7(8):808–16.

288. Templeton AJ, McNamara MG, Šeruga B, Vera-Badillo FE, Aneja P, Ocaña A, et al. Prognostic Role of Neutrophil-to-Lymphocyte Ratio in Solid Tumors: A Systematic Review and Meta-Analysis. JNCI: Journal of the National Cancer Institute. 2014 Jun;106(6).

289. Ferro D, Matias M, Neto J, Dias R, Moreira G, Petersen N, et al. Neutrophil-to-Lymphocyte Ratio Predicts Cerebral Edema and Clinical Worsening Early After Reperfusion Therapy in Stroke. Stroke. 2021 Mar;52(3):859–67.

290. Huang Z, Fu Z, Huang W, Huang K. Prognostic value of neutrophil-to-lymphocyte ratio in sepsis: A meta-analysis. Am J Emerg Med. 2020 Mar;38(3):641–7.

291. Erre GL, Paliogiannis P, Castagna F, Mangoni AA, Carru C, Passiu G, et al. Meta-analysis of neutrophil-to-lymphocyte and platelet-to-lymphocyte ratio in rheumatoid arthritis. Eur J Clin Invest. 2019 Jan;49(1):e13037.

292. Buonacera A, Stancanelli B, Colaci M, Malatino L. Neutrophil to Lymphocyte Ratio: An Emerging Marker of the Relationships between the Immune System and Diseases. Int J Mol Sci. 2022 Mar 26;23(7):3636.

293. Verjans E, Kanzler S, Ohl K, Rieg AD, Ruske N, Schippers A, et al. Initiation of LPS-induced pulmonary dysfunction and its recovery occur independent of T cells. BMC Pulm Med. 2018 Dec 22;18(1):174.

294. Nolz JC. Molecular mechanisms of CD8+ T cell trafficking and localization. Cellular and Molecular Life Sciences. 2015 Jul 11;72(13):2461–73.

295. Groom JR, Luster AD. CXCR3 in T cell function. Exp Cell Res. 2011 Mar;317(5):620–31.

296. Hu JK, Kagari T, Clingan JM, Matloubian M. Expression of chemokine receptor CXCR3 on T cells affects the balance between effector and memory CD8 T-cell generation. Proceedings of the National Academy of Sciences. 2011 May 24;108(21).

297. Pontes Ferreira C, Moro Cariste L de, Henrique Noronha I, Fernandes Durso D, Lannes-Vieira J, Ramalho Bortoluci K, et al. CXCR3 chemokine receptor contributes to specific CD8+ T cell activation by pDC during infection with intracellular pathogens. PLoS Negl Trop Dis. 2020 Jun 23;14(6):e0008414.

298. Heesch K, Raczkowski F, Schumacher V, Hünemörder S, Panzer U, Mittrücker HW. The Function of the Chemokine Receptor CXCR6 in the T Cell Response of Mice against Listeria monocytogenes. PLoS One. 2014 May 15;9(5):e97701.

299. Hua X, Zhang J, Ge S, Liu H, Du H, Niu Q, et al. *CXCR3* antagonist AMG487 ameliorates experimental autoimmune prostatitis by diminishing Th1 cell differentiation and inhibiting macrophage M1 phenotypic activation. Prostate. 2022 Sep 14;82(13):1223–36.

300. Vidal A, Wikell C, Dainty I. Effects of a highly selective CXCR3 antagonist in two murine models of lung inflammation. European Respiratory Society. 2014.

301. Bakheet SA, Alrwashied BS, Ansari MA, Nadeem A, Attia SM, Assiri MA, et al. CXCR3 antagonist AMG487 inhibits glucocorticoid-induced tumor necrosis factor-receptor-related protein and inflammatory mediators in CD45 expressing cells in collagen-induced arthritis mouse model. Int Immunopharmacol. 2020 Jul;84:106494.

302. Bakheet SA, Ansari MA, Nadeem A, Attia SM, Alhoshani AR, Gul G, et al. CXCR3 antagonist AMG487 suppresses rheumatoid arthritis pathogenesis and progression by shifting the Th17/Treg cell balance. Cell Signal. 2019 Dec;64:109395.

303. Walser TC, Rifat S, Ma X, Kundu N, Ward C, Goloubeva O, et al. Antagonism of CXCR3 Inhibits Lung Metastasis in a Murine Model of Metastatic Breast Cancer. Cancer Res. 2006 Aug 1;66(15):7701–7.

304. Zhou YQ, Liu DQ, Chen SP, Sun J, Zhou XR, Xing C, et al. The Role of CXCR3 in Neurological Diseases. Curr Neuropharmacol. 2019 Jan 7;17(2):142–50.

305. Shin YS, Takeda K, Ohnishi H, Jia Y, Shiraishi Y, Cox ML, et al. Targeting CXCR3 reduces ligand-induced T-Cell activation but not development of lung allergic responses. Annals of Allergy, Asthma & Immunology. 2011 Aug;107(2):145–53.

306. Ashbaugh DavidG, Boyd Bigelow D, Petty ThomasL, Levine BernardE. ACUTE RESPIRATORY DISTRESS IN ADULTS. The Lancet [Internet]. 1967 Aug;290(7511):319–23. Available from: https://linkinghub.elsevier.com/retrieve/pii/S0140673667901687

307. Zemans RL, Colgan SP, Downey GP. Transepithelial Migration of Neutrophils. Am J Respir Cell Mol Biol [Internet]. 2009 May;40(5):519–35. Available from: http://www.atsjournals.org/doi/abs/10.1165/rcmb.2008-0348TR

308. Calfee CS, Eisner MD, Parsons PE, Thompson BT, Conner ER, Matthay MA, et al. Soluble intercellular adhesion molecule-1 and clinical outcomes in patients with acute lung injury. Intensive Care Med [Internet]. 2009 Feb 1;35(2):248–57. Available from: http://link.springer.com/10.1007/s00134-008-1235-0

309. Matthay MA, Zemans RL, Zimmerman GA, Arabi YM, Beitler JR, Mercat A, et al. Acute respiratory distress syndrome. Nat Rev Dis Primers [Internet]. 2019 Dec 14;5(1):1–18. Available from: http://dx.doi.org/10.1038/s41572-019-0069-0

310. Sadikot RT, Rubinstein I. Long-Acting, Multi-Targeted Nanomedicine: Addressing Unmet Medical Need in Acute Lung Injury. J Biomed Nanotechnol [Internet]. 2009 Dec 1;5(6):614–9. Available from: http://openurl.ingenta.com/content/xref?genre=article&issn=1550-7033&volume=5&issue=6&spage=614

311. Zoulikha M, Xiao Q, Boafo GF, Sallam MA, Chen Z, He W. Pulmonary delivery of siRNA against acute lung injury/acute respiratory distress syndrome. Acta Pharm Sin B [Internet]. 2022 Feb;12(2):600–20. Available from: https://linkinghub.elsevier.com/retrieve/pii/S2211383521002999

312. Dowdy DW, Eid MP, Dennison CR, Mendez-Tellez PA, Herridge MS, Guallar E, et al. Quality of life after acute respiratory distress syndrome: a meta-analysis. Intensive Care Med [Internet]. 2006 Aug 17;32(8):1115–24. Available from: http://link.springer.com/10.1007/s00134-006-0217-3

313. Choi H ran, Song IA, Oh TK. Quality of life and mortality among survivors of acute respiratory distress syndrome in South Korea: a nationwide cohort study. J Anesth [Internet]. 2022 Apr 21;36(2):230–8. Available from: https://link.springer.com/10.1007/s00540-022-03036-9

314. Thepen T, McMenamin C, Oliver J, Kraal G, Holt PG. Regulation of immune response to inhaled antigen by alveolar macrophages: differential effects ofin vivo alveolar

macrophage elimination on the induction of tolerancevs. immunity. Eur J Immunol [Internet]. 1991 Nov;21(11):2845–50. Available from: http://doi.wiley.com/10.1002/eji.1830211128

315. Melo EM, Oliveira VLS, Boff D, Galvão I. Pulmonary macrophages and their different roles in health and disease. International Journal of Biochemistry and Cell Biology [Internet]. 2021 Dec;141(October):1060–95. Available from: https://linkinghub.elsevier.com/retrieve/pii/S135727252100176X

316. Machado-Aranda D, v. Suresh M, Yu B, Dolgachev V, Hemmila MR, Raghavendran K. Alveolar macrophage depletion increases the severity of acute inflammation following nonlethal unilateral lung contusion in mice. Journal of Trauma and Acute Care Surgery [Internet]. 2014 Apr;76(4):982–90. Available from: https://journals.lww.com/01586154-201404000-00011

317. Petermann M, Orfanos Z, Sellau J, Gharaibeh M, Lotter H, Fleischer B, et al. CCR2 Deficiency Impairs Ly6Clo and Ly6Chi Monocyte Responses in Orientia tsutsugamushi Infection. Front Immunol. 2021;12(July):1–15.

318. Rose CE, Sung SSJ, Fu SM. Significant involvement of CCL2 (MCP-1) in inflammatory disorders of the lung. Microcirculation. 2003;10(3–4):273–88.

319. Buckley CD, Gilroy DW, Serhan CN, Stockinger B, Tak PP. The resolution of inflammation. Nat Rev Immunol [Internet]. 2012;13(1):59–66. Available from: http://dx.doi.org/10.1038/nri3362

320. Basil MC, Levy BD. Specialized pro-resolving mediators: Endogenous regulators of infection and inflammation. Nat Rev Immunol. 2016;16(1):51–67.

321. Rittirsch D, Flierl MA, Day DE, Nadeau BA, McGuire SR, Hoesel LM, et al. Acute Lung Injury Induced by Lipopolysaccharide Is Independent of Complement Activation. The Journal of Immunology [Internet]. 2008 Jun 1;180(11):7664–72. Available from: http://www.jimmunol.org/lookup/doi/10.4049/jimmunol.180.11.7664

322. Horvat JC, Beagley KW, Wade MA, Preston JA, Hansbro NG, Hickey DK, et al. Neonatal Chlamydial Infection Induces Mixed T-Cell Responses That Drive Allergic Airway

Disease. Am J Respir Crit Care Med [Internet]. 2007 Sep 15;176(6):556–64. Available from: http://www.atsjournals.org/doi/abs/10.1164/rccm.200607-1005OC

323. Sencio V, Barthelemy A, Tavares LP, Machado MG, Soulard D, Cuinat C, et al. Gut Dysbiosis during Influenza Contributes to Pulmonary Pneumococcal Superinfection through Altered Short-Chain Fatty Acid Production. Cell Rep [Internet]. 2020 Mar;30(9):2934-2947.e6. Available from: https://linkinghub.elsevier.com/retrieve/pii/S2211124720301674

324. Ushach I, Zlotnik A. Biological role of granulocyte macrophage colony-stimulating factor (GM-CSF) and macrophage colony-stimulating factor (M-CSF) on cells of the myeloid lineage. J Leukoc Biol [Internet]. 2016 Sep;100(3):481–9. Available from: http://doi.wiley.com/10.1189/jlb.3RU0316-144R

325. Bakhshayesh M, Zaker F, Hashemi M, Katebi M, Solaimani M. TGF- β1–mediated Apoptosis Associated With SMAD-dependent MitochondrialBcl-2 Expression. Clin Lymphoma Myeloma Leuk [Internet]. 2012 Apr;12(2):138–43. Available from: https://linkinghub.elsevier.com/retrieve/pii/S2152265011006069

326. Atri C, Guerfali FZ, Laouini D. Role of human macrophage polarization in inflammation during infectious diseases. Int J Mol Sci. 2018;19(6):1–15.

327. Arabpour M, Saghazadeh A, Rezaei N. Anti-inflammatory and M2 macrophage polarization-promoting effect of mesenchymal stem cell-derived exosomes. Int Immunopharmacol [Internet]. 2021 Aug;97(107823):1–8. Available from: https://linkinghub.elsevier.com/retrieve/pii/S1567576921004598

328. Feehan KT, Gilroy DW. Is Resolution the End of Inflammation? Trends Mol Med [Internet]. 2019 Mar;25(3):198–214. Available from: https://linkinghub.elsevier.com/retrieve/pii/S1471491419300176

329. Tsou CL, Peters W, Si Y, Slaymaker S, Aslanian AM, Weisberg SP, et al. Critical roles for CCR2 and MCP-3 in monocyte mobilization from bone marrow and recruitment to inflammatory sites. Journal of Clinical Investigation. 2007 Apr 2;117(4):902–9.

330. Ip WK, Wong CK, Lam CWK. Interleukin (IL)-4 and IL-13 up-regulate monocyte chemoattractant protein-1 expression in human bronchial epithelial cells: Involvement of p38 mitogen-activated protein kinase, extracellular signal-regulated kinase 1/2 and Janus kinase-2 but not c-Jun NH2. Clin Exp Immunol. 2006;145(1):162–72.

331. Flores-Villanueva PO, Ruiz-Morales JA, Song CH, Flores LM, Jo EK, Montaño M, et al. A functional promoter polymorphism in monocyte chemoattractant protein-1 is associated with increased susceptibility to pulmonary tuberculosis. Journal of Experimental Medicine. 2005;202(12):1649–58.

332. Venosa A, Cowman S, Katzen J, Tomer Y, Armstrong BS, Mulugeta S, et al. Role of CCR2+ Myeloid Cells in Inflammation Responses Driven by Expression of a Surfactant Protein-C Mutant in the Alveolar Epithelium. Front Immunol. 2021;12(April):1–14.

333. Dal-Secco D, Wang J, Zeng Z, Kolaczkowska E, Wong CHY, Petri B, et al. A dynamic spectrum of monocytes arising from the in situ reprogramming of CCR2+ monocytes at a site of sterile injury. Journal of Experimental Medicine. 2015;212(4):447–56.

334. Lavine KJ, Epelman S, Uchida K, Weber KJ, Nichols CG, Schilling JD, et al. Distinct macrophage lineages contribute to disparate patterns of cardiac recovery and remodeling in the neonatal and adult heart. Proceedings of the National Academy of Sciences [Internet]. 2014 Nov 11;111(45):16029–34. Available from: www.pnas.org/cgi/doi/10.1073/pnas.1406508111

335. Epelman S, Lavine KJ, Beaudin AE, Sojka DK, Carrero JA, Calderon B, et al. Embryonic and adult-derived resident cardiac macrophages are maintained through distinct mechanisms at steady state and during inflammation. Immunity [Internet]. 2014;40(1):91–104. Available from: http://dx.doi.org/10.1016/j.immuni.2013.11.019

336. Deshmane SL, Kremlev S, Amini S, Sawaya BE. Monocyte chemoattractant protein-1 (MCP-1): An overview. Journal of Interferon and Cytokine Research. 2009;29(6):313–25.

337. Juskewitch JE, Knudsen BE, Platt JL, Nath KA, Knutson KL, Brunn GJ, et al. LPS-Induced Murine Systemic Inflammation Is Driven by Parenchymal Cell Activation and Exclusively

Predicted by Early MCP-1 Plasma Levels. Am J Pathol [Internet]. 2012 Jan;180(1):32–40. Available from: https://linkinghub.elsevier.com/retrieve/pii/S0002944011009187

338. Cui TX, Brady AE, Fulton CT, Zhang YJ, Rosenbloom LM, Goldsmith AM, et al. CCR2 Mediates Chronic LPS-Induced Pulmonary Inflammation and Hypoalveolarization in a Murine Model of Bronchopulmonary Dysplasia. Front Immunol. 2020;11(October):1–16.

339. Maus U, von Grote K, Kuziel WA, Mack M, Miller EJ, Cihak J, et al. The Role of CC Chemokine Receptor 2 in Alveolar Monocyte and Neutrophil Immigration in Intact Mice. Am J Respir Crit Care Med [Internet]. 2002 Aug 1;166(3):268–73. Available from: https://www.atsjournals.org/doi/10.1164/rccm.2112012

340. Maus UA, Waelsch K, Kuziel WA, Delbeck T, Mack M, Blackwell TS, et al. Monocytes Are Potent Facilitators of Alveolar Neutrophil Emigration During Lung Inflammation: Role of the CCL2-CCR2 Axis. The Journal of Immunology. 2003;170(6):3273–8.

341. Francis M, Groves AM, Sun R, Cervelli JA, Choi H, Laskin JD, et al. CCR2 Regulates Inflammatory Cell Accumulation in the Lung and Tissue Injury following Ozone Exposure. Toxicological Sciences [Internet]. 2017 Feb;155(2):474–84. Available from: https://academic.oup.com/toxsci/article-lookup/doi/10.1093/toxsci/kfw226

342. Jiang Z, Zhou Q, Gu C, Li D, Zhu L. Depletion of circulating monocytes suppresses IL-17 and HMGB1 expression in mice with LPS-induced acute lung injury. Am J Physiol Lung Cell Mol Physiol. 2017;312(2):L231–42.

343. Trinchieri G. Interleukin-12 and the regulation of innate resistance and adaptive immunity. Nat Rev Immunol. 2003 Feb;3(2):133–46.

344. Tötemeyer S, Sheppard M, Lloyd A, Roper D, Dowson C, Underhill D, et al. IFN-γ Enhances Production of Nitric Oxide from Macrophages via a Mechanism That Depends on Nucleotide Oligomerization Domain-2. The Journal of Immunology. 2006 Apr 15;176(8):4804–10.

345. Sugimoto MA, Sousa LP, Pinho V, Perretti M, Teixeira MM. Resolution of inflammation: What controls its onset? Front Immunol. 2016;7(160):1–18.

346. Shechter R, London A, Varol C, Raposo C, Cusimano M, Yovel G, et al. Infiltrating Blood-Derived Macrophages Are Vital Cells Playing an Anti-inflammatory Role in Recovery from Spinal Cord Injury in Mice. Graeber MB, editor. PLoS Med [Internet]. 2009 Jul 28;6(7):1–17. Available from: https://dx.plos.org/10.1371/journal.pmed.1000113

347. Pollenus E, Pham TT, Vandermosten L, Possemiers H, Knoops S, Opdenakker G, et al. CCR2 Is Dispensable for Disease Resolution but Required for the Restoration of Leukocyte Homeostasis Upon Experimental Malaria-Associated Acute Respiratory Distress Syndrome. Front Immunol [Internet]. 2021 Feb 16;11(628643):1–17. Available from: https://www.frontiersin.org/articles/10.3389/fimmu.2020.628643/full

348. Ruytinx P, Proost P, van Damme J, Struyf S. Chemokine-Induced Macrophage Polarization in Inflammatory Conditions. Front Immunol [Internet]. 2018 Sep 7;9(1930):1–12. Available from: https://www.frontiersin.org/article/10.3389/fimmu.2018.01930/full

349. Ishida Y, Kimura A, Nosaka M, Kuninaka Y, Hemmi H, Sasaki I, et al. Essential involvement of the CX3CL1-CX3CR1 axis in bleomycin-induced pulmonary fibrosis via regulation of fibrocyte and M2 macrophage migration. Sci Rep [Internet]. 2017 Dec 4;7(16833):1–12. Available from: http://www.nature.com/articles/s41598-017-17007-8

350. Mantovani A, Sica A, Sozzani S, Allavena P, Vecchi A, Locati M. The chemokine system in diverse forms of macrophage activation and polarization. Trends Immunol. 2004;25(12):677–86.

351. Lee M, Lee Y, Song J, Lee J, Chang SY. Tissue-specific Role of CX3CR1 Expressing Immune Cells and Their Relationships with Human Disease. Immune Netw [Internet]. 2018;18(1):1–15. Available from: https://immunenetwork.org/DOIx.php?id=10.4110/in.2018.18.e5

352. Li L, Huang L, Sung SSJ, Vergis AL, Rosin DL, Rose CE, et al. The chemokine receptors CCR2 and CX3CR1 mediate monocyte/macrophage trafficking in kidney ischemia-reperfusion injury. Kidney Int. 2008;74(12):1526–37.

353. Evren E, Ringqvist E, Willinger T. Origin and ontogeny of lung macrophages: from mice to humans. Immunology [Internet]. 2020 Jun 4;160(2):126–38. Available from: https://onlinelibrary.wiley.com/doi/10.1111/imm.13154

354. Guilliams M, de Kleer I, Henri S, Post S, Vanhoutte L, de Prijck S, et al. Alveolar macrophages develop from fetal monocytes that differentiate into long-lived cells in the first week of life via GM-CSF. Journal of Experimental Medicine [Internet]. 2013 Sep 23;210(10):1977–92. Available from: https://rupress.org/jem/article/210/10/1977/41425/Alveolar-macrophages-develop-from-fetal-monocytes

355. Opalek JM, Ali NA, Lobb JM, Hunter MG, Marsh CB. Alveolar macrophages lack CCR2 expression and do not migrate to CCL2. J Inflamm. 2007;4:1–10.

356. Beck-Schimmer B, Schwendener R, Pasch T, Reyes L, Booy C, Schimmer RC. Alveolar macrophages regulate neutrophil recruitment in endotoxin-induced lung injury. Respir Res [Internet]. 2005 Dec 22;6(1):61. Available from: http://respiratory-research.biomedcentral.com/articles/10.1186/1465-9921-6-61

357. Mahida RY, Scott A, Parekh D, Lugg ST, Hardy RS, Lavery GG, et al. Acute respiratory distress syndrome is associated with impaired alveolar macrophage efferocytosis. European Respiratory Journal [Internet]. 2021 Sep;58(2100829):1–5. Available from: http://erj.ersjournals.com/lookup/doi/10.1183/13993003.00829-2021

358. Hamilton TA, Zhao C, Pavicic PG, Datta S. Myeloid Colony-Stimulating Factors as Regulators of Macrophage Polarization. Front Immunol [Internet]. 2014 Nov 21;5(554):1–6. Available from: http://journal.frontiersin.org/article/10.3389/fimmu.2014.00554/abstract

359. Lukic A, Larssen P, Fauland A, Samuelsson B, Wheelock CE, Gabrielsson S, et al. GM-CSF– and M-CSF–primed macrophages present similar resolving but distinct inflammatory lipid mediator signatures. The FASEB Journal [Internet]. 2017 Oct 19;31(10):4370–81. Available from: https://onlinelibrary.wiley.com/doi/abs/10.1096/fj.201700319R

360. Chambers HF, DeLeo FR. Waves of resistance: Staphylococcus aureus in the antibiotic era. 2009 [cited 2022 Nov 5]; Available from: www.nature.com/reviews/micro

361. Guerra FE, Borgogna TR, Patel DM, Sward EW, Voyich JM. Epic immune battles of history: Neutrophils vs. Staphylococcus aureus. Vol. 7, Frontiers in Cellular and Infection Microbiology. Frontiers Media S.A.; 2017.

362. Guerra FE, Borgogna TR, Patel DM, Sward EW, Voyich JM. Epic Immune Battles of History: Neutrophils vs. Staphylococcus aureus. Front Cell Infect Microbiol. 2017 Jun 30;7.

363. Poosti F, Soebadi MA, Crijns H, de Zutter A, Metzemaekers M, Berghmans N, et al. Inhibition of renal fibrosis with a human CXCL9-derived glycosaminoglycan-binding peptide. Clin Transl Immunology. 2022;11(2):1–18.

364. Boff D, Russo RC, Crijns H, de Oliveira VLS, Mattos MS, Marques PE, et al. The Therapeutic Treatment with the GAG-Binding Chemokine Fragment CXCL9(74–103) Attenuates Neutrophilic Inflammation and Lung Dysfunction during Klebsiella pneumoniae Infection in Mice. Int J Mol Sci. 2022;23(11):6246.

365. Németh T, Sperandio M, Mócsai A. Neutrophils as emerging therapeutic targets. Nat Rev Drug Discov [Internet]. 2020;19(4):253–75. Available from: http://dx.doi.org/10.1038/s41573-019-0054-z

366. Boff D, Crijns H, Teixeira MM, Amaral FA, Proost P. Neutrophils: Beneficial and harmful cells in septic arthritis. Int J Mol Sci. 2018;19(2):1–28.

367. Loos T, Mortier A, Proost P. Isolation, Identification, and Production of Posttranslationally Modified Chemokines. In: Methods in Enzymology. 2009. p. 3–29.

368. Boff D, Oliveira VLS, Queiroz Junior CM, Galvão I, Batista NV, Gouwy M, et al. Lipoxin A4 impairs effective bacterial control and potentiates joint inflammation and damage caused by Staphylococcus aureus infection. FASEB Journal. 2020;34(9):11498–510.

369. Blättner S, Das S, Paprotka K, Eilers U, Krischke M, Kretschmer D, et al. Staphylococcus aureus Exploits a Non-ribosomal Cyclic Dipeptide to Modulate Survival within Epithelial Cells and Phagocytes. PLoS Pathog. 2016 Sep 15;12(9):e1005857.

370. Russo RC, Savino B, Mirolo M, Buracchi C, Germano G, Anselmo A, et al. The atypical chemokine receptor ACKR2 drives pulmonary fibrosis by tuning influx of CCR2 $^{+}$ and CCR5 $^{+}$ IFNγ-producing γδT cells in mice. American Journal of Physiology-Lung Cellular and Molecular Physiology. 2018 Jun 1;314(6):L1010–25.

371. Boff D, Russo RC, Crijns H, de Oliveira VLS, Mattos MS, Marques PE, et al. The Therapeutic Treatment with the GAG-Binding Chemokine Fragment CXCL9(74–103) Attenuates Neutrophilic Inflammation and Lung Dysfunction during Klebsiella pneumoniae Infection in Mice. Int J Mol Sci [Internet]. 2022 Jun 2;23(11):6246. Available from: https://www.mdpi.com/1422-0067/23/11/6246

372. Vanheule V, Janssens R, Boff D, Kitic N, Berghmans N, Ronsse I, et al. The Positively Charged COOH-terminal Glycosaminoglycan-binding CXCL9(74–103) Peptide Inhibits CXCL8-induced Neutrophil Extravasation and Monosodium Urate Crystal-induced Gout in Mice. Journal of Biological Chemistry. 2015 Aug;290(35):21292–304.

373. Foster TJ, Geoghegan JA, Ganesh VK, Höök M. Adhesion, invasion and evasion: the many functions of the surface proteins of Staphylococcus aureus. Nat Rev Microbiol. 2014 Jan 16;12(1):49–62.

374. Capucetti A, Albano F, Bonecchi R. Multiple Roles for Chemokines in Neutrophil Biology. Front Immunol. 2020 Jul 9;11.

375. Teng TS, Ji AL, Ji XY, Li YZ. Neutrophils and immunity: From bactericidal action to being conquered. J Immunol Res. 2017;2017.

376. Vallet SD, Clerc O, Ricard-Blum S. Glycosaminoglycan–Protein Interactions: The First Draft of the Glycosaminoglycan Interactome. Journal of Histochemistry & Cytochemistry. 2021 Feb 6;69(2):93–104.

377. Wight TN, Merrilees MJ. Proteoglycans in Atherosclerosis and Restenosis. Circ Res. 2004 May 14;94(9):1158–67.

378. Ma SN, Mao ZX, Wu Y, Liang MX, Wang DD, Chen X, et al. The anti-cancer properties of heparin and its derivatives: a review and prospect. Cell Adh Migr. 2020 Jan 1;14(1):118–28.

379. Kamhi E, Joo EJ, Dordick JS, Linhardt RJ. Glycosaminoglycans in infectious disease. Biological Reviews. 2013 Nov;88(4):928–43.

380. Morla S, Sankaranarayanan NV, Afosah DK, Kumar M, Kummarapurugu AB, Voynow JA, et al. On the Process of Discovering Leads That Target the Heparin-Binding Site of Neutrophil Elastase in the Sputum of Cystic Fibrosis Patients. J Med Chem. 2019 Jun 13;62(11):5501–11.

381. Salbach J, Rachner TD, Rauner M, Hempel U, Anderegg U, Franz S, et al. Regenerative potential of glycosaminoglycans for skin and bone. J Mol Med. 2012 Jun 21;90(6):625–35.

382. Shi D, Sheng A, Chi L. Glycosaminoglycan-Protein Interactions and Their Roles in Human Disease. Front Mol Biosci. 2021 Mar 9;8.

383. Hao C, Xu H, Yu L, Zhang L. Heparin: An essential drug for modern medicine. In 2019. p. 1–19.

384. Chevalier X, Jerosch J, Goupille P, van Dijk N, Luyten FP, Scott DL, et al. Single, intra-articular treatment with 6 ml hylan G-F 20 in patients with symptomatic primary osteoarthritis of the knee: a randomised, multicentre, double-blind, placebo controlled trial. 2009 [cited 2022 Nov 10]; Available from: http://ard.bmj.com/content/vol69/issue1http://ard.bmj.com/info/unlocked.dtl

385. Hoellenriegel J, Zboralski D, Maasch C, Rosin NY, Wierda WG, Keating MJ, et al. The Spiegelmer NOX-A12, a novel CXCL12 inhibitor, interferes with chronic lymphocytic leukemia cell motility and causes chemosensitization. Blood. 2014 Feb 13;123(7):1032–9.

386. Rek A, Krenn E, Kungl A. Therapeutically targeting protein-glycan interactions. Br J Pharmacol. 2009 Jul;157(5):686–94.

387. Robertson CM, Perrone EE, McConnell KW, Dunne WM, Boody B, Brahmbhatt T, et al. Neutrophil depletion causes a fatal defect in murine pulmonary Staphylococcus aureus clearance. J Surg Res. 2008 Dec;150(2):278–85.

388. Benjamin JT, Plosa EJ, Sucre JMS, van der Meer R, Dave S, Gutor S, et al. Neutrophilic inflammation during lung development disrupts elastin assembly and predisposes adult mice to COPD. Journal of Clinical Investigation. 2021 Jan 4;131(1).

389. Zhu B, Zhang R, Li C, Jiang L, Xiang M, Ye Z, et al. BCL6 modulates tissue neutrophil survival and exacerbates pulmonary inflammation following influenza virus infection. Proc Natl Acad Sci U S A [Internet]. 2019 Jun 11 [cited 2022 Nov 5];116(24):11888–93. Available from: https://pubmed.ncbi.nlm.nih.gov/31138703/

390. Hiroki CH, Toller-Kawahisa JE, Fumagalli MJ, Colon DF, Figueiredo LTM, Fonseca BALD, et al. Neutrophil Extracellular Traps Effectively Control Acute Chikungunya Virus Infection. Front Immunol [Internet]. 2020 Jan 31 [cited 2022 Nov 5];10. Available from: https://pubmed.ncbi.nlm.nih.gov/32082301/

391. Borges L, Pithon-Curi TC, Curi R, Hatanaka E. COVID-19 and Neutrophils: The relationship between hyperinflammation and neutrophil extracellular traps. Mediators Inflamm. 2020;2020.

392. Roberts A, Deming D, Paddock CD, Cheng A, Yount B, Vogel L, et al. A Mouse-Adapted SARS-Coronavirus Causes Disease and Mortality in BALB/c Mice. PLoS Pathog. 2007;3(1):e5.

393. Winkler ES, Bailey AL, Kafai NM, Nair S, McCune BT, Yu J, et al. SARS-CoV-2 infection of human ACE2-transgenic mice causes severe lung inflammation and impaired function. Nat Immunol. 2020 Nov 24;21(11):1327–35.

394. Cortjens B, de Boer OJ, de Jong R, Antonis AF, Sabogal Piñeros YS, Lutter R, et al. Neutrophil extracellular traps cause airway obstruction during respiratory syncytial virus disease. J Pathol. 2016 Feb;238(3):401–11.

395. Galani IE, Andreakos E. Neutrophils in viral infections: Current concepts and caveats. J Leukoc Biol. 2015 Oct 1;98(4):557–64.

396. Körner RW, Majjouti M, Alejandre Alcazar MA, Mahabir E. Of Mice and Men: The Coronavirus MHV and Mouse Models as a Translational Approach to Understand SARS-CoV-2. Viruses 2020, Vol 12, Page 880 [Internet]. 2020 Aug 12 [cited 2022 Nov 5];12(8):880. Available from: https://www.mdpi.com/1999-4915/12/8/880/htm

397. Duhalde Vega M, Olivera D, Gastão Davanzo G, Bertullo M, Noya V, Fabiano de Souza G, et al. PD-1/PD-L1 blockade abrogates a dysfunctional innate-adaptive immune axis in critical β-coronavirus disease. Sci Adv. 2022 Sep 23;8(38).

398. Tan YL, Tan KSW, Chu JJH, Chow VT. Combination Treatment With Remdesivir and Ivermectin Exerts Highly Synergistic and Potent Antiviral Activity Against Murine Coronavirus Infection. Front Cell Infect Microbiol. 2021 Jul 30;11:699.

399. Lai WY, Mueller A. Latest update on chemokine receptors as therapeutic targets. Biochem Soc Trans. 2021 Jun 30;49(3):1385–95.

400. Dorr P, Westby M, Dobbs S, Griffin P, Irvine B, Macartney M, et al. Maraviroc (UK-427,857), a Potent, Orally Bioavailable, and Selective Small-Molecule Inhibitor of Chemokine Receptor CCR5 with Broad-Spectrum Anti-Human Immunodeficiency Virus Type 1 Activity. Antimicrob Agents Chemother. 2005 Nov;49(11):4721–32.

401. de Clercq E. Mozobil® (Plerixafor, AMD3100), 10 years after its approval by the US Food and Drug Administration. Antivir Chem Chemother. 2019 Jan 18;27:204020661982938.

402. Ollila TA, Sahin I, Olszewski AJ. Mogamulizumab: a new tool for management of cutaneous T-cell lymphoma . Onco Targets Ther. 2019 Feb;Volume 12:1085–94.

403. Hasegawa T, Venkata Suresh V, Yahata Y, Nakano M, Suzuki S, Suzuki S, et al. Inhibition of the CXCL9-CXCR3 axis suppresses the progression of experimental apical periodontitis by blocking macrophage migration and activation. Sci Rep. 2021 Dec 28;11(1):2613.

404. Groover MK, Richmond JM. Potential therapeutic manipulations of the CXCR3 chemokine axis for the treatment of inflammatory fibrosing diseases. F1000Res. 2020 Oct 5;9:1197.

405. Jenh CH, Cox MA, Cui L, Reich EP, Sullivan L, Chen SC, et al. A selective and potent CXCR3 antagonist SCH 546738 attenuates the development of autoimmune diseases and delays graft rejection. BMC Immunol. 2012;13(1):2.

406. Suzaki Y, Hamada K, Nomi T, Ito T, Sho M, Kai Y, et al. A small-molecule compound targeting CCR5 and CXCR3 prevents airway hyperresponsiveness and inflammation. European Respiratory Journal. 2008 Apr 1;31(4):783–9.

407. Allard B, Panariti A, Martin JG. Alveolar Macrophages in the Resolution of Inflammation, Tissue Repair, and Tolerance to Infection. Front Immunol. 2018 Jul 31;9.

408. Labrousse D, Perret M, Hayez D, da Silva S, Badiou C, Couzon F, et al. Kineret®/IL-1ra Blocks the IL-1/IL-8 Inflammatory Cascade during Recombinant Panton Valentine Leukocidin-Triggered Pneumonia but Not during S. aureus Infection. PLoS One. 2014 Jun 6;9(6):e97546.

409. Boff D, Oliveira VLS, Queiroz Junior CM, Silva TA, Allegretti M, Verri WA, et al. CXCR2 is critical for bacterial control and development of joint damage and pain in Staphylococcus aureus-induced septic arthritis in mouse. Eur J Immunol. 2018;48(3):454–63.

410. Laforge M, Elbim C, Frère C, Hémadi M, Massaad C, Nuss P, et al. Tissue damage from neutrophil-induced oxidative stress in COVID-19. Vol. 20, Nature Reviews Immunology. Nature Research; 2020. p. 515–6.

411. Hoang TN, Pino M, Boddapati AK, Viox EG, Starke CE, Upadhyay AA, et al. Baricitinib treatment resolves lower-airway macrophage inflammation and neutrophil recruitment in SARS-CoV-2-infected rhesus macaques. Cell. 2021 Jan;184(2):460-475.e21.

412. Tang BM, Shojaei M, Teoh S, Meyers A, Ho J, Ball TB, et al. Neutrophils-related host factors associated with severe disease and fatality in patients with influenza infection. Nat Commun. 2019 Dec 1;10(1).

413. Landoni G, Piemonti L, Monforte A d'Arminio, Grossi P, Zangrillo A, Bucci E, et al. A Multicenter Phase 2 Randomized Controlled Study on the Efficacy and Safety of Reparixin in the Treatment of Hospitalized Patients with COVID-19 Pneumonia. Infect Dis Ther. 2022 May 26;

Supplementary materials

Table S1 – Antibodies used in the flow cytometry experiments

Panel	Laser	Fluorochrome	Marker	Antibody clone	Company
Lymphoid panel (PART II)	BLUE	FITC	CD3	145-2C11	eBioscience
	BLUE	PerCP-Cy5.5	CD8	53-6.7	eBioscience
	YG	PE	CXCR3	CXCR3-173	Biolegend
	RED	APC-eFluor780	CD4	RM4-5	eBioscience
	RED	APC	CD49b	DX5	eBioscience
	VIOLET	BV786	B220	RA3-6B2	BD Biosciences
	UV	eFluor 450	CD45	30-F11	eBioscience
	VIOLET	Zombie Aqua	Live/dead	-	Biolegend
ILC panel (PART 2)	BLUE	Alexa fluor 488	GATA-3	TWAJ	eBioscience
	YG	PE	T-bet	4B10	eBioscience
	RED	APC	Mouse lineage cocktail	-	BD Biosciences
	RED	APC-e780	CD4	RM4-5	eBioscience
	VIOLET	BV786	ROR-γt	Q31-378	BD Biosciences
	VIOLET	BV650	CD90.2	30-H12	BD Biosciences
	UV	BUV395	CD3	145-2C11	BD Biosciences
	VIOLET	Zombie Aqua	Live dead	-	Biolegend
Chemokine receptors (PART 2)	BLUE	FITC	CD3	145-2C11	eBioscience
	BLUE	PerCP-Cy5.5	CD8	53-6.7	eBioscience
	YG	PE	CD194 (CCR4)	2G12	Biolegend
	YG	PE-Cy7	CD195 (CCR5)	HM-CCR5	Biolegend
	RED	APC-eFluor780	CD4	RM4-5	eBioscience
	VIOLET	BV421	CD193 (CCR3)	J073E5	Biolegend
	VIOLET	BV711	CD186 (CXCR6)	SA051D1	Biolegend
	UV	BUV395	CD45	30-F11	BD Biosciences
	VIOLET	Zombie Aqua	Live/dead	-	Biolegend

Myeloid panel (PART 3)	BLUE	FITC	CD45	30-F11	Biolegend
	BLUE	PerCP-eFluor 710	CD103	2E7	eBioscience
	YG	PE-Cy7	CD11c	N418	Biolegend
	YG	PE	CD64	X54-5/7.1	Biolegend
	YG	PE-CF594	SiglecF	E50-2440	BD Biosciences
	RED	Alexa Fluor 647	CD206	MMR	Biolegend
	RED	Alexa Fluor 700	Ly6G	1A8	BD Biosciences
	RED	APC-Cy7	Ly6C	AL-21	BD Biosciences
	VIOLET	eFluor 450	CD11b	M1/70	eBioscience
	VIOLET	Horizon v500	MHCII	M5/114.15.2	BD Biosciences
	VIOLET	BV650	CD3	17A2	Biolegend
	VIOLET	BV650	CD19	6D5	Biolegend
	VIOLET	BV650	NKp46	29A1.1	Biolegend
	UV	Zombie UV	Live/dead	-	Biolegend
iNOS panel (PART 3)	BLUE	FITC	CD45	30-F11	Biolegend
	YG	PerCP-Cy5.5	CD11c	N418	eBioscience
	YG	PE-Cy7	iNOS	CXNFT	eBioscience
	YG	PE-CF594	SiglecF	E50-2440	BD Biosciences
	VIOLET	eFluor 450	CD11b	M1/70	eBioscience
	UV	Zombie UV	Live/dead	-	Biolegend
Proliferation panels (PART 3)	BLUE	FITC	CD45	30-F11	Biolegend
	YG	PE-Cy7	CD11c	N418	Biolegend
	YG	PE-CF594	SiglecF	E50-2440	BD Biosciences
	VIOLET	eFluor 450	CD11b	M1/70	eBioscience
	RED	Alexa Fluor 647	Ki-67	16A8	Biolegend
	YG	PE	BrdU or Isotype control	-	BD Biosciences
	UV	Zombie UV	Live/dead	-	Biolegend

Figure S1. Gating Strategies

Samples were analyzed in the Flow Jo V10 software and gated as follows.

a. Lymphoid panel

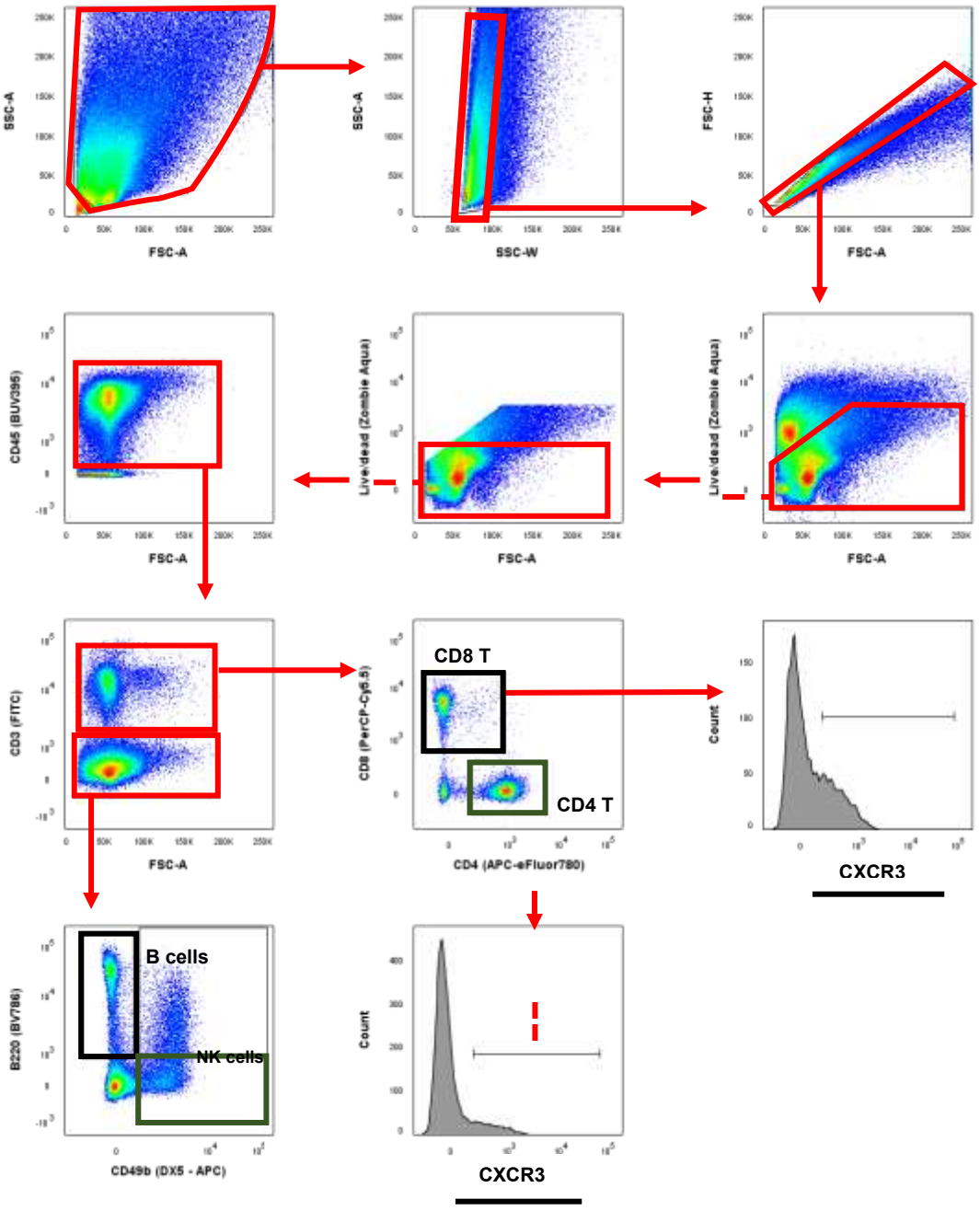

b. ILC panel

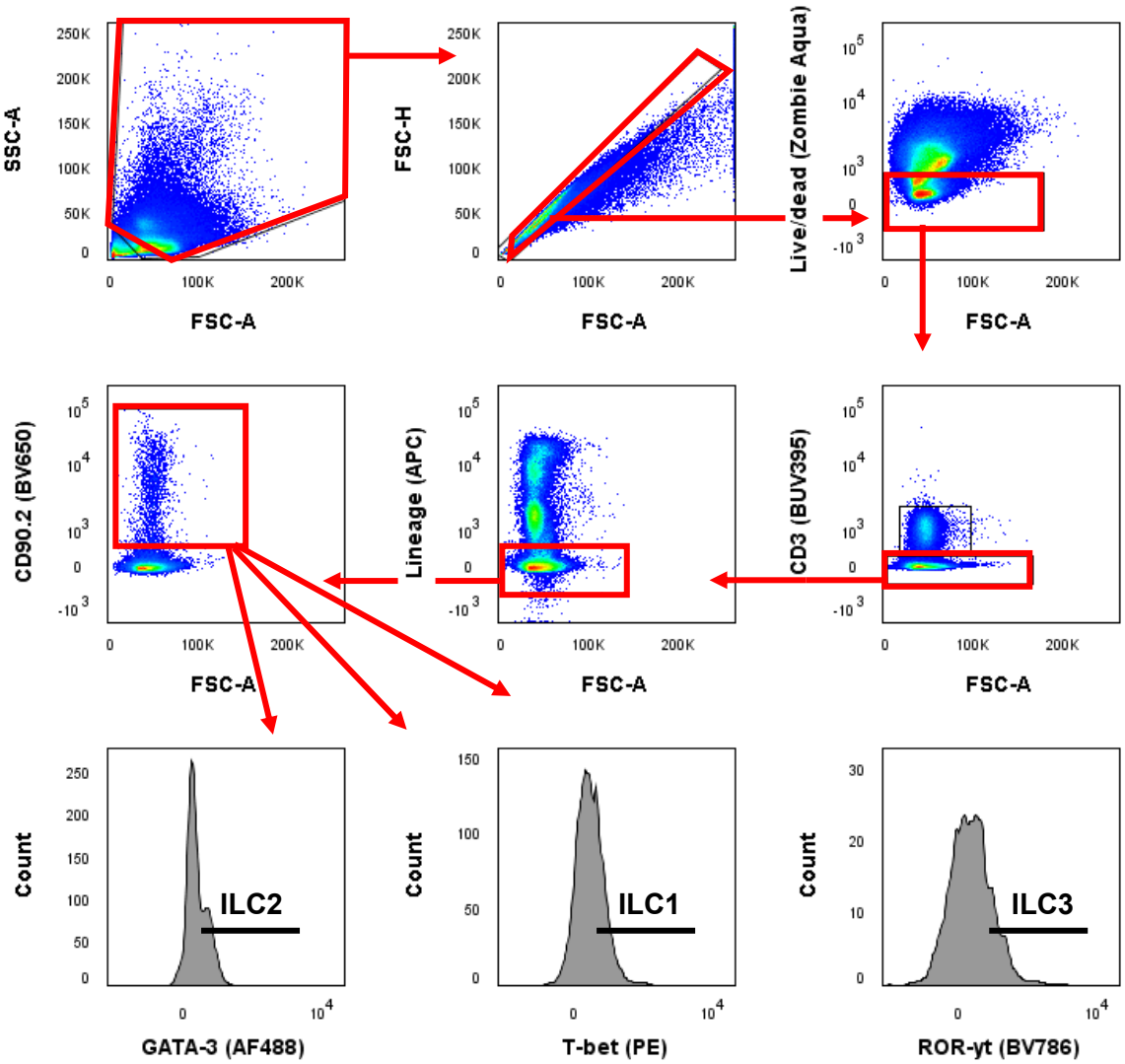
SSC-A
FSC-A
FSC-H
FSC-A
Live/dead (Zombie Aqua)
FSC-A
CD90.2 (BV650)
FSC-A
Lineage (APC)
FSC-A
CD3 (BUV395)
FSC-A
Count
ILC2
GATA-3 (AF488)
Count
ILC1
T-bet (PE)
Count
ILC3
ROR-γt (BV786)

c. Chemokine receptors panel

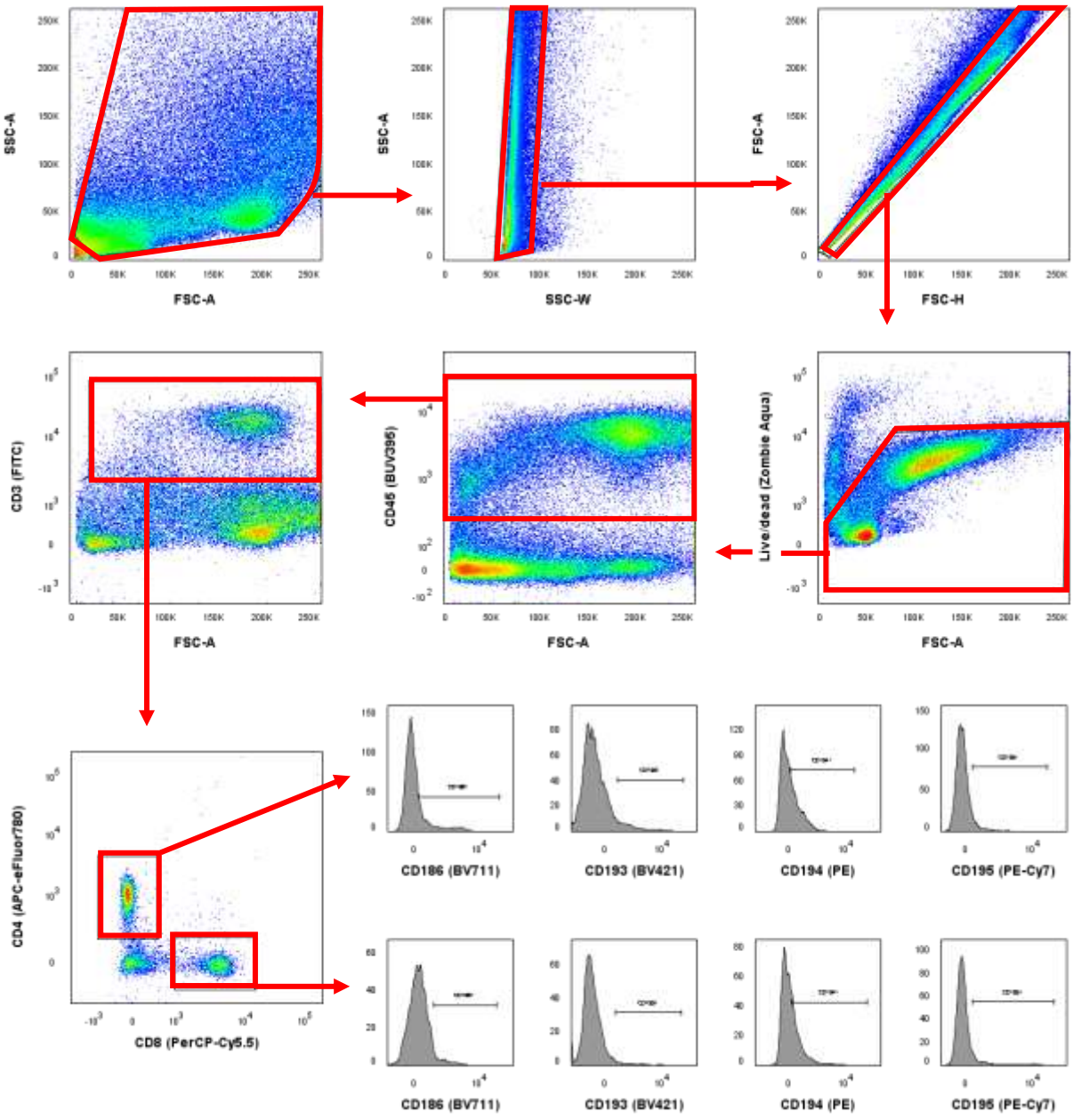

d. Myeloid panel

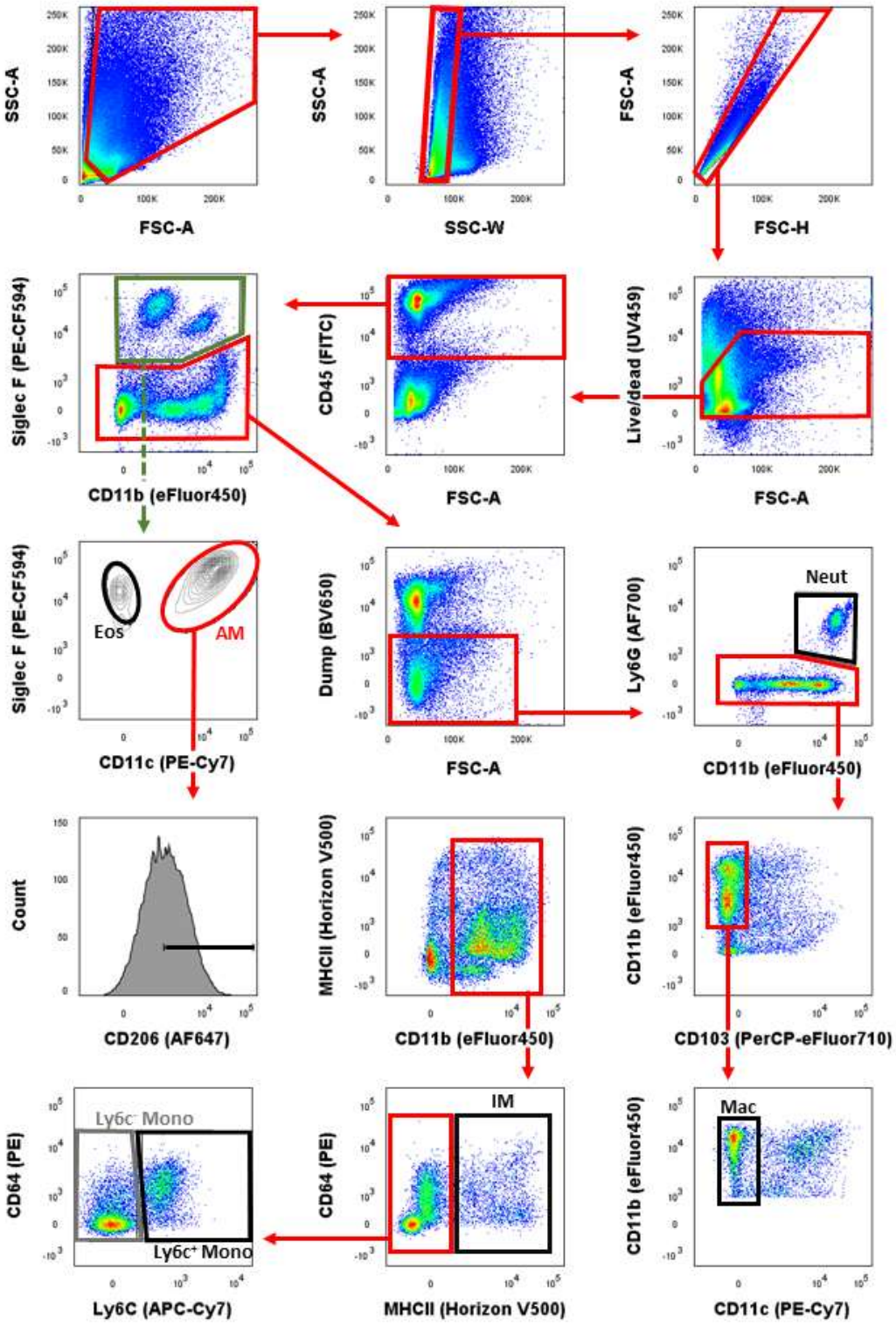

e. iNOS panel

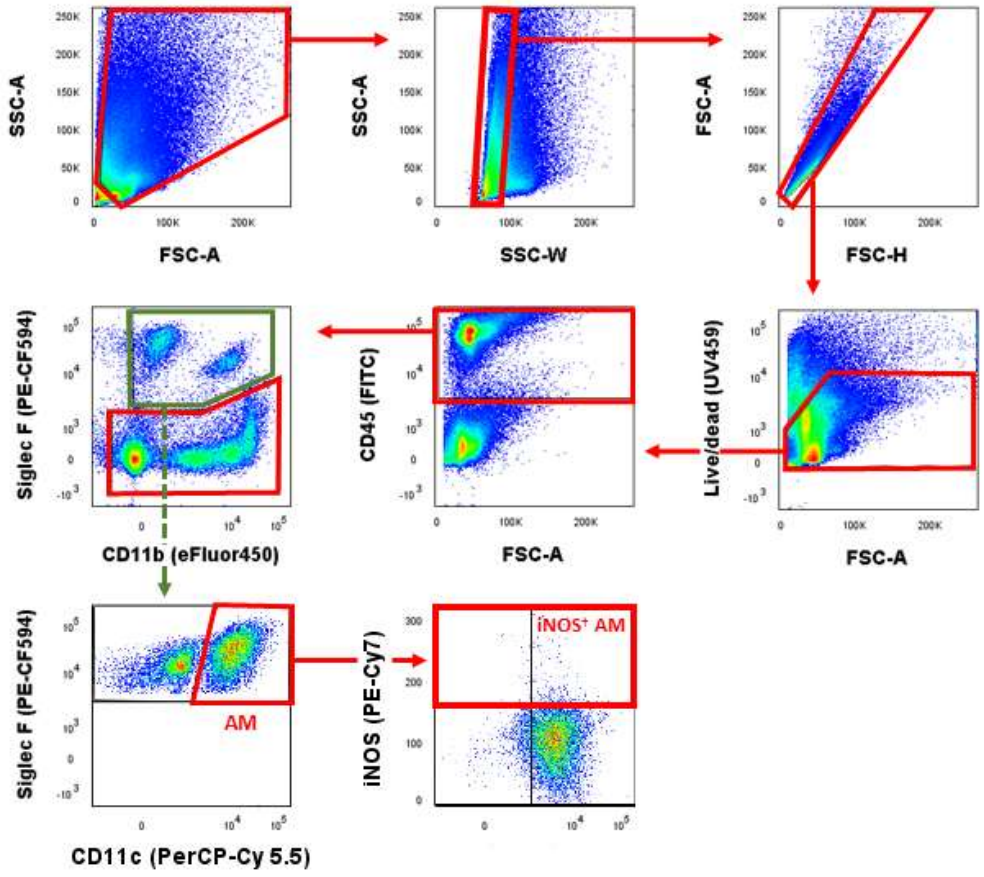
SSC-A
FSC-A
SSC-A
SSC-W
FSC-A
FSC-H
Live/dead (UV459)
FSC-A
CD45 (FITC)
FSC-A
Siglec F (PE-CF594)
CD11b (eFluor450)
Siglec F (PE-CF594)
AM
CD11c (PerCP-Cy 5.5)
iNOS (PE-Cy7)
iNOS+ AM

f. BrdU panel

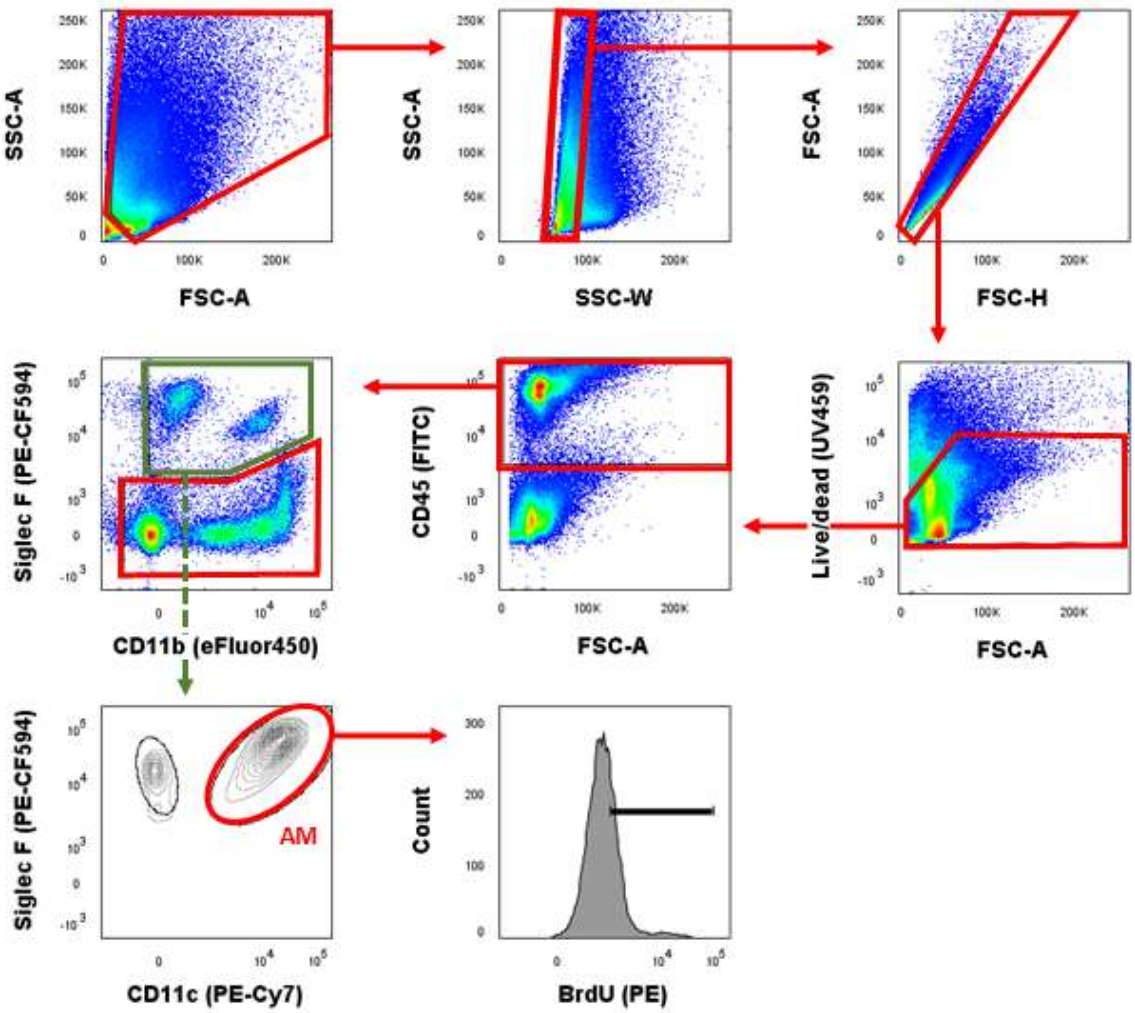
SSC-A
FSC-A
SSC-A
SSC-W
FSC-A
FSC-H
Live/dead (UV459)
FSC-A
CD45 (FITC)
FSC-A
Siglec F (PE-CF594)
CD11b (eFluor450)
Siglec F (PE-CF594)
AM
CD11c (PE-Cy7)
Count
BrdU (PE)

g. Ki-67 panel

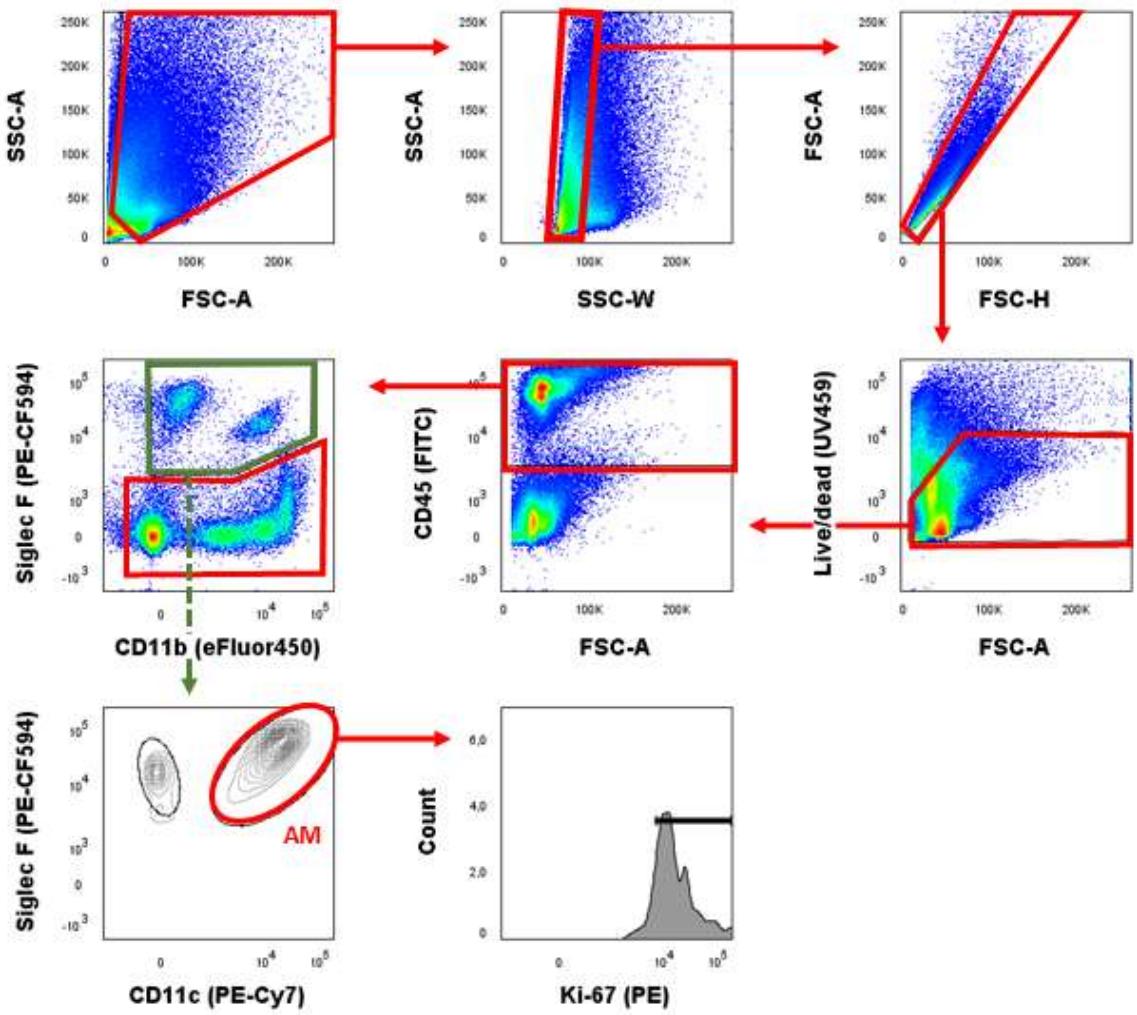
SSC-A
FSC-A
SSC-A
SSC-W
FSC-A
FSC-H
Live/dead (UV459)
FSC-A
CD45 (FITC)
FSC-A
Siglec F (PE-CF594)
CD11b (eFluor450)
Siglec F (PE-CF594)
AM
CD11c (PE-Cy7)
Count
Ki-67 (PE)

Table S2. Clinical Score parameters (369)

Observation	Score points
I Body weight	
- No change	0
- Loss of body weight in % = score points; e.g. loss of body weight 8% = 8 points	1-20
- Loss of body weight ≥20%	20
II General conditions	
Fur	
- Shining	0
- Matte	2
- Ruffled	4
Eyes	
- Clear and clean	0
- Unclean and sticky, closed or semi-closed	3
Posture	
- Normal	0
- Hunched	10
- Massively hunched	20
Clinical complications	
- Tension, paralysis, tremor	20
- Breath noises	20
- Animal feels cold to the touch	20
III Motility	
- Spontaneous (normal behavior, social contacts)	0
- Spontaneous but reduced	1
- Moderately reduced activity	2
- Motility only after stimulation	5
- Isolation, lethargy, coordination disorders	10
- Self-mutilation, aggression	20
IV Respiration	
- Breathing normal	0
- Breathing slightly changed	1
- Accelerated breathing + 30% (tachypnoea)	10
- Strongly accelerated breathing + 50%	20

Annexes I and II (papers published by the PhD candidate)

I – Melo, E. M., Oliveira, V. L. S., Boff, D., & Galvão, I. (2021). Pulmonary macrophages and their different roles in health and disease. *International Journal of Biochemistry and Cell Biology*, *141*(October), 1060–1095. https://doi.org/10.1016/j.biocel.2021.106095 (co-first author)

II – Oliveira, V. L. S. de, Pollenus, E., Berghmans, N., Queiroz-Junior, C. M., Blanter, M., Mattos, M. S., Teixeira, M. M., Proost, P., van den Steen, P. E., Amaral, F. A., & Struyf, S. (2022). Absence of CCR2 Promotes Proliferation of Alveolar Macrophages That Control Lung Inflammation in Acute Respiratory Distress Syndrome in Mice. *International Journal of Molecular Sciences*, *23*(21), 12920. https://doi.org/10.3390/ijms232112920